

Exploiting Novel Antibodies for the Early Detection of Cardiac Disease

Paul Conroy B.Sc. (Hons.)

Ph.D. Thesis

Based on research carried out

for

Biomedical Diagnostics Institute (BDI) in the School of Biotechnology,

Dublin City University,

Dublin 9,

Ireland.

September, 2011.

Under the supervision of Professor Richard O’Kennedy.

Declaration

I hereby certify that this material, which I now submit for assessment on the programme of study leading to the award of Ph.D. is entirely my own work, that I have exercised reasonable care to ensure that the work is original, and does not to the best of my knowledge breach any law of copyright, and has not been taken from the work of others save and to the extent that such work has been cited and acknowledged within the text of my work.

Signed: _____

ID No.: 53556191

Date: _____

Table of Contents

Declaration	ii
Table of Contents	iii
Dedication	xi
Acknowledgements	xii
List of Figures	xiii
List of Tables.....	xix
List of Equations	xxi
Abbreviations	xxii
Units	xxvi
Publications	xxvii
Abstract	xxx
Chapter 1: Introduction	1-1
1.1 The immune system.....	1-2
1.1.1 Innate immunity	1-2
1.1.2 Acquired immunity	1-3
1.1.3 Antibody structure.....	1-3
1.1.4 Antibody diversity.....	1-6
1.2 Biosensors	1-8
1.2.1 Introduction	1-8
1.2.2 Antibodies and their significance in biosensor development.....	1-9
1.3 Cardiovascular disease	1-13
1.3.1 Overview	1-13
1.3.2 Pathophysiology.....	1-14
1.3.3 Biomarkers of cardiovascular disease.....	1-17

1.3.3.1	Overview.....	1–17
1.3.3.2	The ‘golden’ biomarker	1–17
1.3.3.3	Clinical considerations.....	1–19
1.3.3.4	Current and emerging biomarkers	1–20
1.4	Thesis aims and objectives	1–25
Chapter 2:	Materials and Methods	2–1
2.1	Materials	2–2
2.1.1	Equipment	2–2
2.1.2	Chemicals.....	2–4
2.1.3	Cells	2–5
2.1.4	Media and buffers	2–6
2.1.4.1	Media used for the growth of mammalian cells	2–6
2.1.4.2	Media used for the growth of bacterial cells.....	2–7
2.1.4.3	Media additives used for the growth of bacterial cells	2–7
2.1.4.4	Buffers	2–9
2.1.4.5	Sodium dodecyl sulfate polyacrylamide gel electrophoresis (SDS-PAGE) and Western blotting (WB)	2–10
2.1.4.6	Protein purification	2–11
2.1.5	Commercially sourced kits and solutions	2–13
2.1.6	Commercially sourced antibodies	2–14
2.1.7	Commercially sourced proteins.....	2–15
2.1.8	Vectors	2–16
2.2	Licencing	2–16
2.3	Methods	2–17
2.3.1	General molecular methods.....	2–17
2.3.1.1	Ethanol precipitation of DNA.....	2–17
2.3.1.2	Plasmid propagation and purification	2–17

2.3.1.3	Agarose electrophoresis	2–18
2.3.1.4	Ligation of DNA into a vector	2–18
2.3.1.5	Preparation of competent cells	2–19
2.3.1.6	Preparation of bacterial cell stocks	2–20
2.3.1.7	Lysis of E. coli cells for small-scale analysis and purification	2–21
2.3.1.8	Optimisation of recombinant protein expression	2–21
2.3.1.9	Purification of produced recombinant proteins	2–22
2.3.1.10	Preparation of helper-phage	2–23
2.3.1.11	SDS-PAGE	2–24
2.3.1.12	Western blotting	2–24
2.3.2	Cardiac Troponin I antigen	2–26
2.3.2.1	Quality of commercially sourced antigen	2–26
2.3.2.2	Evaluation of protein-based immunisation regimes	2–26
2.3.2.3	Recombinant Troponin I	2–27
2.3.2.4	Fusion of epitopes 1 and 2 to fatty acid binding protein	2–29
2.3.3	Monoclonal antibody generation	2–31
2.3.3.1	Immunisation of Balb/c mice with synthetic epitope conjugate	2–31
2.3.3.2	Anti-serum titre analysis of immune response to epitope-2 of cTnI ..	2–31
2.3.3.3	Fusion of splenocytes and myeloma	2–32
2.3.3.4	Analysis of fused hybridoma progeny	2–33
2.3.3.5	Scale-up and cloning by limiting dilution of screened progeny	2–36
2.3.3.6	General mammalian cell culture methods	2–37
2.3.3.7	Purification of anti-epitope-2 monoclonal antibody	2–39
2.3.3.8	Kinetic analysis of monoclonal antibody on Biacore™ 3000	2–40
2.3.4	Recombinant antibody generation	2–41
2.3.4.1	Immunisation of chickens	2–41

2.3.4.2	Extraction of RNA and cDNA synthesis from chicken	2-41
2.3.4.3	pComb3xSS vector preparation	2-42
2.3.4.4	Antibody (scFv) library construction	2-43
2.3.4.5	Bio-panning of phage displayed libraries	2-50
2.3.4.6	Polyclonal-phage ELISA for specific antibody-displaying phage	2-54
2.3.4.7	Soluble scFv expression and lysis	2-55
2.3.5	Screening for anti-epitope-1-specific scFv from bio-panned libraries	2-56
2.3.5.1	Wild-type scFv screening approach	2-56
2.3.5.2	Mutant scFv screening approach	2-59
2.3.6	Inhibition ELISA comparison of wild-type and mutant scFv	2-62
2.3.6.1	Titre	2-62
2.3.6.2	Inhibition	2-62
2.3.7	Full kinetic profiling using fatty acid binding protein fusion	2-63
2.3.7.1	Determination of fatty acid binding protein fusion concentration	2-63
2.3.7.2	Kinetic evaluation of wild-type and mutant scFv	2-64
2.3.8	Sequence analysis and protein modelling of scFv	2-64
2.3.8.1	Sequence analysis of two selected scFv clones	2-64
2.3.8.2	Protein modelling of two scFv clones	2-64
2.3.9	Thermal challenge assay for assessment of improved stability	2-65
2.3.10	Determination of crystal structure	2-65
2.3.10.1	Gel filtration of purified scFv	2-65
2.3.10.2	Coarse screening for optimal crystal formation conditions	2-66
2.3.10.3	Fine screening to refine optimal crystal formation conditions	2-67
2.3.10.4	X-ray diffraction of scFv 180 crystals	2-68
2.3.11	Evaluation of selected scFvs and the industry standard	2-68
2.3.12	Conversion of scFv to scAb format	2-68

2.3.12.1	Genetic manipulation of scFv construct	2-68
2.3.12.2	scAb expression analysis	2-70
2.3.13	Purification of generated recombinant antibodies.....	2-71
Chapter 3:	Cardiac Troponin I antigen	3-1
3.1	Introduction	3-2
3.1.1	Cardiac Troponin I (cTnI).....	3-2
3.1.2	Design of cTnI peptides	3-4
3.1.3	Recombinant antigen expression.....	3-6
3.2	Results	3-10
3.2.1	cTnI antigen quality	3-10
3.2.2	Initial immunisations with whole cTnI	3-11
3.2.3	Recombinant Troponin I	3-13
3.2.3.1	Cloning strategy for recombinant Troponin I.....	3-13
3.2.3.2	Results.....	3-14
3.2.3.3	Conclusion and adaption of the cloning strategy	3-17
3.2.4	Expression of epitope 1 and 2 regions as a fusion to the fatty acid binding protein (FABP).....	3-18
3.2.4.1	Cloning strategy for the FABP fusion construct.....	3-18
3.2.4.2	Screening, expression and purification	3-20
3.3	Chapter conclusions	3-26
Chapter 4:	Monoclonal Antibodies	4-1
4.1	Introduction	4-2
4.1.1	Hybridoma technology.....	4-2
4.1.2	Surface plasmon resonance (SPR)	4-6
4.2	Results of the generation and isolation of a monoclonal antibody against epitope-2 of cTnI.....	4-9
4.2.1	Immunisation of Balb/c mice with synthetic-epitope-2 conjugate	4-9

4.2.2	Clone selection by data-rich screening	4–10
4.2.2.1	Epitope and protein-specificity screening.....	4–11
4.2.2.2	Capture ranking of Hybridoma clones on Biacore™ 3000	4–18
4.2.2.3	Additional screening of the hybridoma progeny	4–22
4.2.3	Purification of the monoclonal antibody 20B3	4–28
4.2.4	Determination of antibody affinity on Biacore™ 3000	4–32
4.3	Chapter conclusions	4–35
Chapter 5: Recombinant Antibodies		5–1
5.1	Introduction to recombinant antibodies for diagnostic-based applications.....	5–2
5.1.1	Applications and potential.....	5–2
5.1.2	Emergence of recombinant antibody technology.....	5–3
5.1.3	Antibody fragments and formats.....	5–3
5.1.4	Antibody libraries.....	5–5
5.1.5	Advantages of display technology	5–5
5.1.6	Phage display	5–8
5.1.6.1	Introduction.....	5–8
5.1.6.2	The principle of phage display.....	5–8
5.1.6.3	Selection considerations for successful phage display	5–11
5.1.7	Ribosome display	5–14
5.1.7.1	Introduction.....	5–14
5.1.7.2	The principle of ribosome display	5–14
5.1.7.3	Considerations for successful ribosome display	5–17
5.1.8	Mutagenesis strategies for evolution of antibody affinity.....	5–18
5.1.9	Genetically coded-tags for biosensor development	5–20
5.1.10	High-throughput screening of antibody libraries	5–21
5.1.11	Avian and mammalian repertoires as sources of antibody libraries	5–23

5.2	Results of the generation and isolation of recombinant antibodies against epitope-1 of cTnI	5–27
5.2.1	Anti-epitope-1 wild-type scFv development.....	5–28
5.2.1.1	Immunisation	5–28
5.2.1.2	Library construction by PCR	5–30
5.2.1.3	Phage display of the anti-epitope-1 scFv library	5–36
5.2.1.4	Screening of anti-peptide-1 scFv library post selection.....	5–40
5.2.1.5	Sequence analysis of four selected scFvs	5–52
5.2.2	Mutagenesis of anti-epitope-1 scFv	5–54
5.2.2.1	Overview of the mutagenesis strategy	5–54
5.2.2.2	Library construction by PCR	5–58
5.2.2.3	Bio-panning of the anti-epitope-1 mutant library	5–59
5.2.2.4	Mutant screening for improved affinity clones.....	5–61
5.2.2.5	Comparison of wild-type and mutant clones	5–67
5.2.3	Investigation of crystal structure of recombinant proteins.....	5–83
5.2.3.1	Crystal structure determination by X-ray crystallography	5–84
5.2.3.2	Results.....	5–86
5.2.3.3	Future work to determine the crystal structure of scFv	5–94
5.3	Isolation of recombinant antibodies against epitope-3 of cTnI	5–95
5.3.1	Identification of anti-epitope 3 scFv from the screened library	5–95
5.3.2	Purification of anti-epitope-3 scFv from bacterial culture.....	5–99
5.4	Chapter conclusions	5–100
Chapter 6: Recombinant antibodies – assay development: benefits and pitfalls		6–1
6.1	Foreword	6–2
6.2	Results	6–3
6.2.1	Comparison of wild-type, mutant and Hytest antibodies.....	6–3
6.2.2	Reformatting recombinant antibodies	6–4

6.2.3	Initial development of plate-based assays	6–9
6.2.4	Assays compromised by antigen variability	6–11
6.3	Chapter conclusions	6–13
Chapter 7:	Concluding remarks and discussion.....	7–1
Chapter 8:	Appendices	8–1
8.1	Supporting material	8–2
Chapter 9:	References	9–1

Dedication

I dedicate this thesis to my parents, family and all those whose unwavering support I have been lucky to have.....

"I never did anything worth doing by accident, nor did any of my inventions come by accident: they came by work." Thomas Edison

Acknowledgements

Firstly, I would like to extend a sincere word of thanks to Professor Richard O’Kennedy. Since my undergraduate days Richard has provided inspiration, promoting my interest in science and a research career. I also appreciate his constant encouragement and endless support for me in every endeavour, application and idea throughout my Ph.D.

I also wish to acknowledge the support, guidance, encouragement and direction provided to me for the last number of years by Dr. Stephen Hearty. Stephen is a truly talented scientist and a very good friend. It has been my pleasure to work with and learn from Stephen, who has taught me a great deal.

A word of thanks to the student and staff members of the School of Biotechnology, the National Centre for Sensor Research and the Biomedical Diagnostics Institute, both past and present, for their friendship. For blindly supporting everything from feeble attempts to grow a ‘MO’ during MOvember to BRS table quizzes and Bio-TAG-nology. Many thanks for the aliquots of something desperately needed or the equally desperately needed glass (or bottle) of wine!

Joey, thanks for the laughs and the 1000’s of kilometres that must have gone into this thesis.

I owe an immense debt of gratitude to my parents and family, for whom this thesis is dedicated, for their support and encouragement. Without their unwavering commitment to my education (over many years!) I could never have achieved so much.

Finally, I would like to say a special word of thanks to Louise for the constant support and companionship over the years. For the numerous cups of coffee over the last few weeks, the enumerable words of support, the constant encouragement and total belief. Thank you.

This research is supported by Science Foundation Ireland under CSET Grant no. 05/CE3/B754 and by the Irish Research Council for Science, Engineering and Technology (IRCSET) Embark Scholarship. I also gratefully acknowledge the support of the Orla Benson Postgraduate Scholarship (2010-2011), the Benson Family and DCU Educational Trust.

List of Figures

Figure 1.1-1: Overview of the basic immunoglobulin structure	1–5
Figure 1.1-2: Ribbon structure of IgG molecule	1–5
Figure 1.1-3: Genes encoding for human antibodies	1–7
Figure 1.2-1: Components of a biosensor	1–8
Figure 1.2-2: Overview of the routes to antibody generation	1–12
Figure 1.3-1: Atherogenesis leading to thrombosis formation.....	1–15
Figure 1.3-2: Route to the classification of acute coronary syndrome by electrocardiography pattern.....	1–16
Figure 1.3-3: The release kinetics of biomarkers during acute coronary syndrome	1–20
Figure 1.3-4: Biochemical markers released during acute coronary syndrome.....	1–21
Figure 1.3-5: Actin-Tropomyosin-Troponin complex	1–24
Figure 2.3-1: Generic time course experiment for expression of recombinant proteins..	2–22
Figure 2.3-2: Flow diagram of scale-up and cloning by limiting dilution of generated hybridomas	2–37
Figure 3.1-1: Illustration of the sources of assay interference in the detection of cTnI	3–3
Figure 3.1-2: Cardiac Troponin I amino acid sequence and model	3–5
Figure 3.1-3: Control and production of recombinant protein expression by <i>T7lac</i>	3–9
Figure 3.2-1: 12.5 (w/v) SDS-PAGE and Western blot of commercially available cTnI	3–10
Figure 3.2-2: Evaluation of immune response to the synthesised peptides from a chicken immunised with cTnI	3–12
Figure 3.2-3: Design and amino acid composition of the rTnI gene	3–14
Figure 3.2-4: rTnI gene cloning from the maintenance vector into an expression vector	3–14
Figure 3.2-5: Western blot detection of rTnI secreting clones.....	3–16
Figure 3.2-6: Expression of rTnI as an inclusion body in the pET28b vector	3–16
Figure 3.2-7: Schematic overview of FABP peptide 1 and 2 fusion construct.....	3–19
Figure 3.2-8: Initial screening of FABP-P1&2-expressing clones	3–21
Figure 3.2-9: SDS and WB analysis of antibody reactivity with expressed FABP-P1&2 fusion.....	3–21
Figure 3.2-10: Optimisation of expression of the selected FABP-P1&2 clone	3–22

Figure 3.2-11: Optimisation of salt and imidazole concentration for purification of FABP-P1&2 fusion	3-24
Figure 3.2-12: Large-scale, optimised purification of recombinant FABP-P1&2 protein by IMAC	3-25
Figure 3.2-13: Gel filtration elution profile of recombinant FABP-P1&2 protein	3-25
Figure 4.1-1: Schematic overview of mouse monoclonal antibody production	4-4
Figure 4.1-2: HAT selection for B-cell-myeloma fusions	4-4
Figure 4.1-3: Schematic overview of identification and isolation of stable hybridomas... ..	4-5
Figure 4.1-4: Overview of the surface plasmon resonance biosensor configuration	4-7
Figure 4.2-1: Anti-serum response in KLH-peptide-2-sensitised mouse	4-10
Figure 4.2-2: First screen of antibody-secreting hybridomas by a direct binding ELISA	4-11
Figure 4.2-3: Biacore™ 4000 flow cell setup for epitope-specificity mapping of generated hybrids	4-12
Figure 4.2-4: Epitope-specificity screening for anti-cTnI epitope-specific antibodies on Biacore™ 4000	4-13
Figure 4.2-5: Direct binding ELISA to confirm retention of positivity at 48-well plate scale of hybridoma expansion	4-14
Figure 4.2-6: Epitope-specificity of expanded clones at the 48-well plate stage of hybridoma scale-up	4-14
Figure 4.2-7: Competitive ELISA comparison of twenty-four selected hybridomas	4-16
Figure 4.2-8: Biacore™ 4000 high-throughput percentage left ranking of anti-peptide-2 hybridomas	4-18
Figure 4.2-9: Biacore™ 3000 'off-rate' ranking flow cell setup	4-19
Figure 4.2-10: Biacore™ 3000 'off-rate' analysis of four selected hybridomas for the cTnI protein	4-20
Figure 4.2-11: Biacore™ 3000 percentage left ranking of twenty clones for cTnI protein binding	4-21
Figure 4.2-12: Direct binding ELISA-based analysis of hybridoma antibody expression levels	4-22
Figure 4.2-13: Sandwich ELISA for cTnI using hybridoma supernatant	4-23
Figure 4.2-14: Isotype determination of monoclonal antibody 20B3	4-23
Figure 4.2-15: Analysis of the expression levels of individual hybridomas by direct binding ELISA	4-24

Figure 4.2-16: Titre and competitive analysis of selected monoclonal antibody 20B3...	4-26
Figure 4.2-17: Route to the selection of lead monoclonal antibodies from the analysis strategy employed	4-27
Figure 4.2-18: Elution profiles for protein G and PD10 columns used in the purification of 20B3	4-29
Figure 4.2-19: SDS-PAGE and WB analysis of the purification steps for monoclonal antibody, 20B3	4-29
Figure 4.2-20: SEC-HPLC analysis of the 20B3 monoclonal antibody following purification	4-30
Figure 4.2-21: Titrations of purified the 20B3 and Hytest 228 antibodies	4-31
Figure 4.2-22: Sandwich ELISA using the 20B3 antibody and equivalent control antibody for cTnI.....	4-31
Figure 4.2-23: Immobilisation of monoclonal antibody 20B3 onto the surface of a Biacore™ 3000 chip	4-33
Figure 4.2-24: Kinetic analysis of the 20B3 antibody-immobilised surface	4-34
Figure 5.1-1: Recombinant antibody formats	5-4
Figure 5.1-2: Phage display of a single chain fragment variable antibody.....	5-9
Figure 5.1-3: Overview of phage selection strategies.....	5-13
Figure 5.1-4: Overview of the principle of ribosome display.....	5-16
Figure 5.1-5: Overview of mutagenesis strategies for the evolution of antibody affinity	5-19
Figure 5.1-6: Illustration of the structural differences between IgG and IgY.....	5-24
Figure 5.1-7: Overview of the process of gene conversion in chicken Ig genes	5-25
Figure 5.2-1: Alignment of human, mouse and chicken cardiac Troponin I	5-28
Figure 5.2-2: Avian antiserum titration for a chicken sensitised with the peptide-1-KLH conjugate	5-29
Figure 5.2-3: Optimisation of spleen and bone marrow V _L and V _H amplification from cDNA	5-31
Figure 5.2-4: Large-scale V _H and V _L amplification from cDNA.....	5-31
Figure 5.2-5: Splice-by-overlap extension (SOE) PCR of avian bone marrow and spleen V _H and V _L	5-32
Figure 5.2-6: pComb3xSS vector map.....	5-33
Figure 5.2-7: Test digestion of pComb3xSS vector.....	5-34
Figure 5.2-8: Large-scale triple digestion of pComb3xSS vector	5-35

Figure 5.2-9: Purified triple digested pComb3xSS vector	5–35
Figure 5.2-10: SfiI digestion of avian anti-peptide-1 scFv SOE-PCR inserts	5–36
Figure 5.2-11: Antigen presentation strategy and optimisation for bio-panning of the anti-epitope-1 library	5–38
Figure 5.2-12: Polyclonal-phage ELISA after four rounds of stringent bio-panning	5–40
Figure 5.2-13: Genetic fingerprint analysis of eighteen clones after four rounds of bio-panning	5–42
Figure 5.2-14: Initial screening of one anti-epitope-1 scFv bio-panned library output plate	5–43
Figure 5.2-15: Sandwich ELISA screening for positive clones selected during anti-epitope-1 scFv bio-panning	5–44
Figure 5.2-16: Ranking of anti-epitope-1 scFv based upon their binding ratio in a sandwich assay	5–45
Figure 5.2-17: High-throughput screening by capture format on Biacore™ 4000 used for scFv analysis	5–48
Figure 5.2-18: High-throughput stability early versus stability late ranking of anti-epitope-1 scFv	5–49
Figure 5.2-19: High-throughput scFv capture level plot for anti-epitope-1 scFv	5–49
Figure 5.2-20: High-throughput percentage left plot for anti-epitope-1 scFv	5–50
Figure 5.2-21: Alignment of four selected wild-type scFv for sequence comparison	5–53
Figure 5.2-22: Overview of light chain shuffling mutagenesis strategy for the wild-type scFv library	5–55
Figure 5.2-23: Solution-phase bio-panning for anti-epitope-1 mutant scFv	5–56
Figure 5.2-24: Pre-panning optimisation of peptide concentrations for in-solution bio-panning	5–57
Figure 5.2-25: V _H amplification from wild-type gene	5–58
Figure 5.2-26: Mutant library SOE-PCR	5–59
Figure 5.2-27: Polyclonal-phage ELISA for the light chain shuffled library	5–60
Figure 5.2-28: Functional assay screening of mutant scFv for immobilised and captured cTnI protein	5–62
Figure 5.2-29: High-throughput (HT) screening of the mutant scFv on the Biacore™ 4000	5–63
Figure 5.2-30: 'On/off-rate' map of phage selected scFv mutants for anti-epitope-1	5–64

Figure 5.2-31: HT ‘percentage-left’ ranking of scFv mutants in comparison to the wild-type clone	5–64
Figure 5.2-32: Flow cell setup for ‘2 over 2’ kinetic experiment	5–65
Figure 5.2-33: ‘2 over 2’ kinetic curves for wild-type and one selected mutant	5–66
Figure 5.2-34: Plot of k_a and k_d from the ‘2 over 2’ experiment for anti-epitope-1 mutant selection.....	5–66
Figure 5.2-35: Full kinetic evaluation of selected scFv mutants on Biacore™ 4000	5–68
Figure 5.2-36: Kinetic comparison of wild-type and mutant scFv 2B12.....	5–69
Figure 5.2-37: Titre and competitive analysis of wild-type and mutant scFvs for cTnI and free peptide.....	5–71
Figure 5.2-38: Purification of 2B12 scFv (mutant) by immobilised metal affinity chromatography (IMAC)	5–73
Figure 5.2-39: Purification of scFv 180 (wild-type) by IMAC.....	5–73
Figure 5.2-40: Full kinetic evaluation of wild-type and mutant scFv with the FABP-peptide fusion.....	5–75
Figure 5.2-41: Comparison of the stability of the scFvs 180 and 2B12 by thermal challenge	5–77
Figure 5.2-42: Sequence alignment of mutant and wild-type antibodies.....	5–78
Figure 5.2-43: Predicted hypothetical model of 180 and 2B12 scFvs	5–80
Figure 5.2-44: Modelled mutations for the wild-type and mutant scFvs with displayed side chains.....	5–81
Figure 5.2-45: Instrument setup for collection of X-ray diffraction patterns	5–85
Figure 5.2-46: Gel filtration chromatogram for IMAC-purified scFv 180	5–87
Figure 5.2-47: Mass and purity determination for scFv 180 by MALDI-TOF MS.....	5–87
Figure 5.2-48: Drop methods for crystal screening	5–89
Figure 5.2-49: Formation of a crystal of scFv 180 in a manually prepared screen.....	5–91
Figure 5.2-50: X-ray diffraction pattern of scFv 180 crystal from the manual tray	5–91
Figure 5.2-51: Formation of a crystal of scFv 180 in position B10 of PEG/ION screen	5–93
Figure 5.2-52: X-ray diffraction pattern of scFv 180 crystal from condition B10 of PEG/ION screen.....	5–93
Figure 5.3-1: Customised macro for anti-epitope-3 scFv ranking experiments.....	5–96
Figure 5.3-2: Epitope-specificity mapping of the scFv isolated from a cTnI protein-based avian library	5–98

Figure 5.3-3: Inhibition analysis of identified anti-epitope-3-specific clone 4G5	5–98
Figure 6.2-1: Comparison of wild-type and mutant scFv to Hytest anti-epitope-1 antibody	6–4
Figure 6.2-2: Reformatting scFv to include chicken constant light domains	6–5
Figure 6.2-3: PCR modification of SfiI sites in 2B12 and 4G5 scFv	6–6
Figure 6.2-4: SDS-PAGE and Western blotting of scAb purification steps	6–8
Figure 6.2-5: SDS-PAGE and Western blotting of 2B12_scAb-cys purification steps.....	6–8
Figure 6.2-6: Optimisation of capture and reporter reagent combinations for a cTnI sandwich assay	6–10
Figure 6.2-7: Demonstration FLISA for a cTnI sandwich assay	6–10
Figure 6.2-8: Test of capture reagents including the positive control mAb 228 with the new batch of cTnI	6–12
Figure 6.2-9: Test of new cTnI batch by SDS-PAGE and WB	6–12
Figure 8.1-1: DNA and amino acid sequence of hFABP (Val ² to Ala ¹³³)	8–2
Figure 8.1-2: DNA and amino acid sequence of rTnI (Asp ²⁵ to Ser ²¹⁰)	8–3
Figure 8.1-3: pET26a-c(+)	8–4
Figure 8.1-4: pET28a-c(+)	8–5
Figure 8.1-5: pET32a-c(+)	8–5
Figure 8.1-6: pUC57	8–6
Figure 8.1-7: pMoPac vector.....	8–6
Figure 8.1-8: Properties of antibody binding proteins A, G and L	8–7
Figure 8.1-9: 1kb plus ladder from Invitrogen.....	8–8
Figure 8.1-10: Fermentas Page-Ruler Plus MW maker.....	8–8
Figure 8.1-11: N-end rule for protein degradation in <i>E. coli</i>	8–9
Figure 8.1-12: Venn diagram of amino acid properties	8–9
Figure 8.1-13: Amino acid structure and properties	8–10
Figure 8.1-14: Amino acid sequence of the avian-derived scFv 4G5.....	8–11
Figure 8.1-15: Gel filtration profiles for the scFvs purified by IMAC from periplasmic extraction.....	8–11

List of Tables

Table 1.1-1: Cellular elements of the internal innate immune system.....	1–2
Table 1.1-2: Summary of the properties and function of antibody isotypes.....	1–4
Table 1.2-1: Examples of antibody-based biosensors.....	1–10
Table 1.2-2: Characteristics of poly-, mono- and recombinant antibodies.....	1–11
Table 1.3-1: Definition of myocardial infarction (MI). Criteria for acute, evolving or recent MI.....	1–14
Table 1.3-2: The characteristics of an ideal biochemical marker.....	1–18
Table 1.3-3: Current cardiovascular biomarkers and their associated properties.....	1–22
Table 1.3-4: Creatine kinase characteristics.....	1–23
Table 1.3-5: Circulating cTn forms.....	1–24
Table 2.1-1: Mammalian cell lines.....	2–5
Table 2.1-2: <i>E. coli</i> cells and genotypes.....	2–5
Table 2.3-1: General ligation reaction components.....	2–18
Table 2.3-2: components of the digestion reaction for rTnI and vectors.....	2–27
Table 2.3-3: pComb3xSS vector digestion components.....	2–43
Table 2.3-4: Avian scFv library PCR primer list.....	2–44
Table 2.3-5: Amplification of avian variable domains from cDNA.....	2–44
Table 2.3-6: Variable domain amplification PCR cycle parameters.....	2–45
Table 2.3-7: Splice-by-overlap extension PCR.....	2–46
Table 2.3-8: SOE amplification PCR cycle parameters.....	2–46
Table 2.3-9: Large-scale <i>SfiI</i> digestion of scFv library and insert.....	2–47
Table 2.3-10: Triple digestion and Antarctic phosphatase treatment of vector.....	2–47
Table 2.3-11: scFv library ligation reaction components.....	2–48
Table 2.3-12: Bio-panning conditions employed for isolating the wild-type anti-epitope-1 scFv.....	2–53
Table 2.3-13: Solution-phase bio-panning conditions for mutant anti-epitope-1 scFv selection.....	2–54
Table 2.3-14: Colony pick PCR master mix.....	2–57
Table 2.3-15: <i>AluI</i> and <i>BstNI</i> digestion tube setup.....	2–57
Table 2.3-16: Layout of the fine screening conditions for scFv 180 crystal formation...	2–67

Table 2.3-17: Preparation of mother liquor for fine screening of crystal conditions.....	2-67
Table 2.3-18: Primer sequence to transfer pComb3x-based scFv to pMopacC _λ	2-69
Table 2.3-19: Amplification and modification of scFv from pComb3x vector	2-69
Table 2.3-20: Modified scFv amplification PCR cycle parameters.....	2-69
Table 2.3-21: Large-scale SfiI digests of pMopacC _λ vector and modified scFv inserts..	2-70
Table 3.1-1: Cardiac Troponin I peptides	3-6
Table 3.2-1: Biochemical properties of FABP-P1&2 fusion protein.....	3-19
Table 4.1-1: Definitions of biophysical determinants for bio-molecular interactions	4-8
Table 4.2-1: Ranking of hybridomas by percentage left.....	4-17
Table 4.2-2: Percentage left values for nineteen hybridomas from Biacore™ 3000-based experiment.....	4-21
Table 4.2-3: Kinetic constants derived for monoclonal antibody 20B3	4-33
Table 5.1-1: Examples of recombinant antibody-based biosensors for important applications	5-2
Table 5.1-2: Phage and ribosome display compared	5-6
Table 5.1-3: Examples of recombinant antibodies generated to specific targets	5-7
Table 5.1-4: Phage and phagemid systems compared for antibody production	5-10
Table 5.1-5: Factors affecting translational efficiency in ribosome display.....	5-17
Table 5.1-6: Properties of IgG and IgY	5-23
Table 5.1-7: Advantages of exploiting the avian immune system for diagnostic antibody generation.....	5-26
Table 5.2-1: Bio-panning input and output titres for anti-epitope-1 scFv	5-39
Table 5.2-2: Genetic fingerprint identification of eighteen selected clones	5-41
Table 5.2-3: Rationalised selection of anti-epitope-1 scFvs	5-51
Table 5.2-4: Mutant clones selected for further characterisation.....	5-67
Table 5.2-5: Purified scFv protein determination	5-72
Table 5.2-6: Derived kinetic constants for wild-type and mutant scFv using FABP-peptide fusion.....	5-75
Table 5.2-7: Biochemical properties of wild-type and mutant scFv	5-77
Table 5.2-8: Relationship between resolution of X-ray diffraction and the structural features obtained.....	5-85
Table 5.3-1: Biochemical properties of the anti-epitope-3 scFv	5-99
Table 8.1-1: Restriction enzymes and recognition sequences	8-2

Table 8.1-2: Protein crystallisation screening kits	8–10
---	------

List of Equations

Equation 2.3-1: 1:1 molar ratio of vector and insert for ligation reactions	2–18
Equation 4.1-1: 1:1 binding interaction for analytes A and B forming the complex AB ..	4–7
Equation 4.2-1: Calculation of percentage (%) left values in Biacore™ ‘off-rate’ experiments	4–19

Abbreviations

A&E	Accident and emergency
Ab	Antibody
ACCF	American College of Cardiology Foundation
ACS	Acute coronary syndrome
ADCC	Antibody-dependent cell-mediated cytotoxicity
AFM	Atomic force microscopy
Ag	Antigen
AHA	American Heart Association
AMI	Acute myocardial infarction
ARM	Antibody-ribosome-mRNA
BM	Bone marrow
BNP	Brain natriuretic peptide
BW	Bulk wave
cDNA	Complementary deoxyribonucleic acid
CDR	Complementarity determining region
C _H	Constant heavy chain of antibody
CK	Creatine kinase
C _L	Constant light chain of antibody
CRP	C-reactive protein
cTn	Cardiac Troponin
TnC	Troponin C
cTnI	Cardiac Troponin I
cTnT	Cardiac Troponin T
CV	Column volume
CVD	Cardiovascular disease
DMEM	Dulbecco's modified Eagle's medium
DNA	Deoxyribonucleic acid
ECG	Electrocardiogram
EDC	1-Ethyl-3-[3-dimethylaminopropyl] carbodiimide hydrochloride
EDTA	Ethylenediaminetetraacetic acid
ELISA	Enzyme-linked immunosorbent assay
ESC	European Society of Cardiology
Fab	Antigen binding fragment of antibody

FABP	Fatty acid binding protein
Fc	Fragment crystallisable
FC	Flow cell
FCA	Freund's complete adjuvant
FCS	Foetal calf serum
FET	Field effect transistor
FFAu	Unbound free fatty acid
FICA	Freund's incomplete adjuvant
FLISA	Fluorescent-linked immunosorbent assay
FPLC	Fast protein liquid chromatography
FO	Fibre optic
Fv	Variable fragment of antibody
FW	Framework
FWR	Framework region
GP	Glycogen phosphorylase
HAMA	Human anti-mouse antibodies
HAT	Hypoxanthine-aminopterin-thymidine medium
HEPES	4-(2-hydroxyethyl)-1-piperazineethanesulfonic acid
HGPRT	Hypoxanthine-guanine phosphoribosyltransferase
HRP	Horseradish peroxidase
HT	High-throughput
HT Medium	Hypoxanthine-thymidine medium
Ig	Immunoglobulin
IgG	Immunoglobulin G
IMA	Ischemia-modified albumin
IMAC	Immobilised-metal affinity chromatography
IP	Intraperitoneal
IPA	Isopropyl alcohol
IPTG	Isopropyl- β -D-1-thiogalactopyranoside
KLH	Keyhole limpet haemocyanin
LB	Luria broth
LIMS	Laboratory information management system
LN ₂	Liquid Nitrogen
LOD	Limit of detection
LOQ	Limit of quantitation

mAb	Monoclonal antibody
MgCl ₂	Magnesium chloride
MI	Myocardial infarction
MMP-9	Matrix metalloproteinase 9
MOPS	3-(N-morpholino) propanesulfonic acid
Mol. G. H ₂ O	Molecular grade water
MPO	Myeloperoxidase
mRNA	Messenger ribonucleic acid
MTA	Material transfer agreement
NACB	National Academy of Clinical Biochemistry
NEAA	Non-essential amino acids
NHS	N-hydroxysuccinimide
NPV	Negative predictive value
NSTEMI	Non-ST-elevation myocardial infarction
OmpD	Outer membrane protein D
O/N	Overnight
ORF	Open reading frame
OWLS	Optical waveguide light mode spectroscopy
PAPP-A	Pregnancy-associated plasma protein A
PBS	Phosphate buffered saline
PBSM	PBS-Milk
PBST	PBS-Tween
PBSTM	PBST-Milk
PCR	Polymerase chain reaction
PDB	Protein Data Bank
PDI	Protein disulphide isomerase
PEG	Polyethylene glycol
pH	Log of the hydrogen ion concentration
pI	Isoelectric point
PlGF	Placental growth factor
pNPP	p-nitrophenyl phosphate
POC	Point-of-care
p-polarised	Plane polarised
PR ⁺	Page ruler plus
PRM	Protein-ribosome-mRNA

QCM	Quartz crystal microbalance
rAb	Recombinant antibody
RI	Refractive index
RIFS	Reflectometric interference spectroscopy
R _{max}	Maximal binding response
RNA	Ribonucleic acid
RSS	Recombination signal sequence
rTnI	Recombinant Troponin I
RT	Room temperature
RT-PCR	Reverse transcriptase PCR
RU	Response unit
SAF	Supercritical angle fluorescence
SB	Super broth
SBP	Streptavidin binding peptide
sCD40L	Soluble CD40 ligand
SDS-PAGE	Sodium dodecyl sulphate polyacrylamide gel electrophoresis
SHM	Somatic hypermutation
SOC	Super optimal catabolite
SP	Spleen
SPR	Surface plasmon resonance
ssDNA	Single strand DNA
STEMI	ST-elevation myocardial infarction
sTnI	Skeletal Troponin I
sTnT	Skeletal Troponin T
Taq	<i>Thermus aquaticus</i>
TIR	Total internal reflection
TIRF	Total internal reflection fluorescence
TMB	3, 3', 5, 5'-tetramethylbenzidine
UV	Ultra violet
V _H	Variable heavy chain of antibody
V _L	Variable light chain of antibody
WHF	World Heart Foundation
w/o	Without
WHO	World Health Organisation
$\Delta\theta_{\text{SPR}}$	Change in SPR angle

θ_c	Critical angle
θ_{SPR}	SPR angle

Units

%	Percentage
χ^2	Chi ² or ‘goodness of fit’
Å	Angstrom
AU	Absorbance units
bp	Base pair
Da	Dalton
g	Grams
Hz	Hertz
K	Kelvin
L	Litre
M	Molar
mAU	Milliabsorbance units
mg	Milligram
mL	Millilitre
mM	Millimolar
mV	Millivolts
nM	Nanomolar
°C	Degrees Celsius
pg	Picogram
pM	Picomolar
rpm	Revolutions per minute
RU	Response units
v/v	Volume per unit volume
w/v	Weight per unit volume
µg	Microgram
µL	Microlitre
µM	Micromolar

Publications

Peer-Reviewed Research Publications:

“Generation and in vitro evolution of recombinant antibodies for improved cTnI diagnostics”. **Conroy, P.J.**, Hearty, S., O’Kennedy R.J. In preparation, (2011).

Peer-Reviewed Literary Review Publications:

“Surface plasmon resonance for vaccine design and efficacy studies: recent applications and future trends”. Hearty, S., **Conroy, P.J.**, Ayyar, V., Byrne, B., O’Kennedy R. Expert Reviews in Vaccines (Impact Factor: 4.214), 9, (2010), 645-664.

“Antibody production, design and use for biosensor-based applications.” **Conroy, P.J.**, Hearty, S., Leonard, P., O’Kennedy R.J. Seminars in Cell & Developmental Biology (Impact Factor: 6.482), 20, (2009), 10–26 (article artwork featured on front cover).

Book Chapter:

“Technologies and methodologies used in the development and optimisation of immunoassays and immunoassay surfaces” **Conroy, P.J.**, Dixit, C. in Immunoassays – development and applications, and future trends. Murphy, C.S., O’Kennedy, R.J. (Eds.). In preparation for publication in 2012.

Poster Presentations:

Conroy, P.J., Hearty S., and O’Kennedy R.J. (2010). ***Improving detection of cardiac troponin I with rationally selected antibody pairings.*** IBC Antibody Engineering and Antibody Therapeutics, San Diego, California, USA. 4– 9th December, 2010.

Conroy, P.J., Hearty S., and O’Kennedy R.J. (2009). ***Screening for epitope-specific anti-cardiac Troponin I monoclonal antibodies using a High-Throughput (HT) surface plasmon resonance (SPR)-based method.*** CHI PEGS European Summit, Hannover, Germany, 5th – 9th October 2009 and NCSR 10th Year Anniversary Symposium. 22nd October, 2009.

Conroy, P.J., Hearty S., and O’Kennedy R.J. (2009). ***Screening for epitope-specific anti-cardiac Troponin I monoclonal antibodies.*** IRCSET Symposium, RDS, Dublin. 25th September, 2009.

Hearty, S., McDonnell, B., Leonard, P., Ayyar, V., Gilmartin, N., Conroy, P.J., Desmonts, L.B., Hill, D., MacCraith, B.D., and O’Kennedy R.J. (2008) ***Optimised isolation of recombinant antibodies for biosensor development.*** Europtrode IX Conference, Dublin, Ireland. 30th March – 2nd April, 2008.

Oral Presentations:

“Antibodies for CVD Diagnostics”. P.J. Conroy, S. Hearty and R. O’Kennedy. Monash University: Orla Benson Funded Laboratory Visit, Melbourne, Australia. 9th May 2011.

“Developing a cardiac assay”. P.J. Conroy, S. Hearty and R. O’Kennedy. BDI Retreat, Castleknock Hotel, Dublin, Ireland. 1st April 2011.

“Developing a cardiac assay by intelligent (?) design”. P.J. Conroy, S. Hearty and R. O’Kennedy. DCU School of Biotechnology Research Day, Dublin City University, Ireland. 27th January 2011.

“Pimp my Antibody: Antibody-based diagnostics”. P.J. Conroy, S. Hearty and R. O’Kennedy. CSET Thesis in 3: Innovation Week, The Sugar Club, Dublin, Ireland. 17th November, 2010.

(Awarded runner up prize in commercialisation category)

“Exploiting novel recombinant antibodies for early detection of cardiac disease” P.J. Conroy, S. Hearty and R. O’Kennedy. Ph.D Thesis Transfer Meeting Presentation, DCU. 19th February, 2010.

“Targeting defined epitopes for detection of cardiac troponin I”. P.J. Conroy, S. Hearty and R. O’Kennedy. School of Biotechnology: Research Day, DCU. 29th January, 2010.

“Pimp my Antibody”. P.J. Conroy, S. Hearty and R. O’Kennedy. NCSR 10th Anniversary Symposium. DCU, Dublin. 22nd October, 2009.

“Antibodies: Diagnostic Reagents for CVD” P.J. Conroy, S. Hearty and R. O’Kennedy. Cold Spring Harbour, New York, USA. 6th-19th November, 2008.

Abstract

Cardiovascular disease, the single greatest killer in the western world, is credited with causing 48% of all deaths worldwide and is of huge economic importance in healthcare provision. The cardiac troponins are definitive indicators of cardiovascular disease and elevated levels of cardiac troponin I (cTnI) are highly-specific for cardiovascular damage.

Using a specific targeting strategy, a panel of novel antibodies were successfully generated against key epitopes in cTnI that are of paramount importance for specific cardiovascular disease detection. Panels of both monoclonal and recombinant antibodies were generated and fully characterised. This approach required a combination of high-throughput assay screening with ‘state-of-the-art’ multiplexed surface-plasmon resonance-based instrumentation. The selected antibodies were demonstrated to outperform current commercially available reagents.

In addition, inherent difficulties associated with the use and expression of cardiac troponin I, the key target analyte, were investigated in detail and alternative recombinant constructs developed and evaluated.

The antibodies ultimately selected were chosen for their applicability for integration on to a point-of-care risk-chip for cardiovascular disease determination due to their specificity, high affinity and genetic tailoring for deployment on a microfluidic device. This stage involved close collaboration with clinical and industrial partners and the commercial feasibility and performance of the antibodies are now under evaluation.

Chapter 1: Introduction

1.1 The immune system

The immune system functions as a surveillance mechanism against infectious organisms and/or their toxic products. It can be characterised by two mechanisms; non-adaptive (innate) and adaptive (acquired) immunity [1]. Non-adaptive immunity is a general non-specific response to foreign molecules and includes systems such as phagocytosis (macrophages), cell lysis (natural killer cells) and a host of chemical and physical elements [1, 2]. The key difference between the two mechanisms is the adaptive immunity's ability to improve and refine its response following exposure to antigens. Adaptive immunity is mediated mainly by the B-lymphocytes, a sub-group of white blood cells, which are responsible for the secretion of immunoglobulins. Terminally differentiated B-cells give rise to memory B-cells that immediately recognise an antigen post primary exposure and plasma cells, which are responsible for the secretion of antigen-specific antibodies [2-4].

1.1.1 Innate immunity

Innate immunity is the body's first line of defence and consists of anatomic barriers and physiological barriers. Anatomic barriers, such as the skin and mucous membranes, prevent passive transfer of organisms. Physiological barriers including enzymes present in saliva and tears and the acidic nature of the stomach offer resistance to infection. Should these initial defences be overwhelmed a number of elements of the internal innate immune system become activated, such as those outlined in Table 1.1-1.

Table 1.1-1: Cellular elements of the internal innate immune system

Cell	Action
Mast	Pathogen defence, wound healing and recruitment of macrophages/neutrophils.
Natural killer	Function to kill 'non-self' cells.
Phagocytes	Engulf invading matter and recruitment of chemokines.
Neutrophils	Inhibit growth of bacteria and fungi.
Dendritic	Antigen presentation to the adaptive immune system.

Table adapted from [2].

1.1.2 Acquired immunity

The adaptive immune system is an antigen-specific system capable of mounting a cell-mediated and humoral immune response. The adaptive immune system is only found in gnathostomata and confers immunological memory. T- and B-cells are the two major lymphocyte sub-groups associated with the adaptive immune system and are derived from hematopoietic cells within the bone marrow. T-cells play a role in cell-mediated responses and can be further categorised into helper and killer T-cells. Helper T-cells direct cells of the immune system whereas in contrast killer T-cells directly interact and destroy marked cells. B-cells function in the humoral response and recognise specific antigens via receptors on their surface (antibodies). One category of activated B-cells, called plasma cells, functions to secrete antigen-specific antibodies into the circulatory system.

1.1.3 Antibody structure

The terms immunoglobulin and antibody are used widely and interchangeably. The term “antibody” refers to a molecule that binds a known antigen while the term “immunoglobulin” describes this group of proteins irrespective of whether their antigen is known or not [1]. Immunoglobulins circulate freely in an individual’s serum and control the humoral clearance of invading antigens. Antibodies are a family of glycoproteins that share structural and functional properties. There are five classes of immunoglobulin which are distinguished by their heavy chains; IgA, IgG, IgM, IgD and IgE and the properties of each are summarised in Table 1.1-2.

Table 1.1-2: Summary of the properties and function of antibody isotypes

Isotype	Form	Action
IgA	Mono-, di-, trimer	Found in mucosal secretions.
IgG	Monomer	Activates complement and involved in opsonisation and antibody-dependent cell-mediated cytotoxicity (ADCC).
IgM	Pentamer	Activates complement and is first isotype released in response to antigen.
IgD	Monomer	B-cell receptor.
IgE	Monomer	Allergic response by binding to mast cell surfaces.

Table adapted from [1].

Class-switching of the heavy chains during gene rearrangement dictates the isotype of the immunoglobulin. There are two types of light chains, κ and λ , which combine with the heavy chain to form the complete antibody molecule [5]. IgG is the predominant class of antibody produced during the matured immune response (approximately 70% of the polyclonal antibody serum pool). However, IgM is the first antibody secreted in response to primary exposure (approximately 10% of the polyclonal serum pool). The basic structure of an immunoglobulin is outlined in Figure 1.1-1 and the more detailed ribbon structure is illustrated by Figure 1.1-2. The antibody molecule consists of four polypeptide chains, two heavy (H) chains each with a molecular weight of 50kDa and two light (L) chains of 25kDa each linked by disulphide bridges at the ‘hinge’ region. The chains have both constant (C) and variable (V) regions. The heavy chain has one variable region (V_H) and three constant regions (C_{H1} , C_{H2} and C_{H3}). The light chain has one variable region (V_L) and one constant region (C_L) [5]. The antibody molecule has several distinct regions. The Fc region consists of three domains; C_{H1} , C_{H2} and C_{H3} that confer effector functions, such as complement activation, on the antibody. The Fab region is separated from the Fc by the flexible ‘hinge’ region and Fv consists of the variable domains (V_L and V_H) that bring together the hyper-variable regions of the antibody, known as the complementarity determining regions (CDRs). The antibody constant domains are conserved with only small differences in sequence found across the various antibody classes. The CDRs however, exhibit a high level of sequence diversity [6].

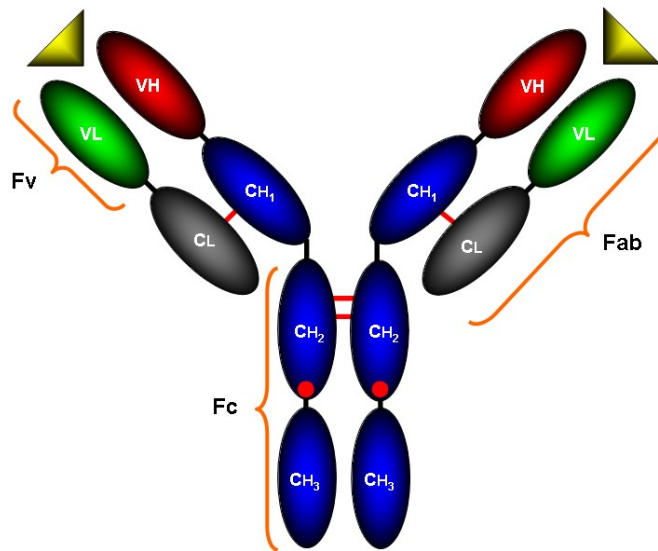


Figure 1.1-1: Overview of the basic immunoglobulin structure

A typical IgG antibody molecule (~150kDa). The immunoglobulin is composed of two identical heavy chains consisting of constant (C_{H1} , C_{H2} , and C_{H3}) and variable (V_H) domains, associated by a disulphide bond (double red lines) at the 'hinge' region of the molecule. The light chain consist of a constant (C_L) and a variable (V_L) domain that are linked with the heavy chain via a disulphide bond (single red lines). The molecule has three distinct regions. The variable fragment (Fv) determines the antigen-binding specificity of the antibody molecule and the antigen binding sites are indicated by the yellow triangles. Specificity is dictated by the complementarity determining regions (CDRs). The antigen binding fragment (Fab) contains the Fv and is separated by the hinge region from the crystallisable fragment (Fc). The Fc domain incorporates the carbohydrate element of the molecule (red dots) and confers effector functions on the antibody.

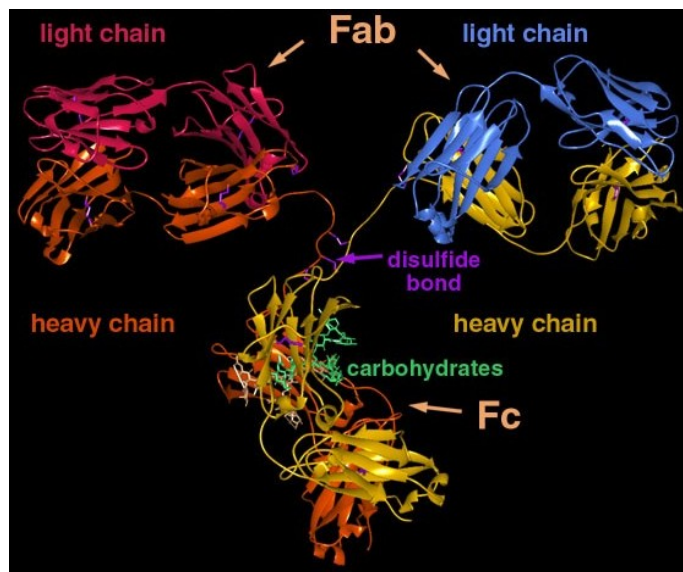


Figure 1.1-2: Ribbon structure of IgG molecule

Here the arrangement of the antiparallel- β strands is clearly illustrated and the stabilisation of the molecule via intra-strand hydrogen bonding is indicated. This image was downloaded online from [7].

1.1.4 Antibody diversity

At any point in time a huge number of different antibodies circulate within the serum of an individual. The human species is capable of generating 10^{11} different antibody molecules in response to multiple antigens. The diversity of antibodies in the immune system is achieved by gene recombination and somatic hyper-mutation (SHM) of the encoding genes [8]. An example of the encoding gene segments is outlined in Figure 1.1-3. In vertebrate genomes, there are 11 constant (C_H), 123-129 variable (V_H), 27 diverse (D_H) and 9 joining (J_H) gene segments that combine to encode the heavy chains. During B-cell development, the immunoglobulin loci undergo rearrangements [9]. Within the heavy chain locus, the V_H - D_H - J_H rearrange and this exon becomes linked to a combination of C_H segments during transcription. Subsequently, the mRNA is translated into the immunoglobulin isotype specific to the lymphocyte. A similar chain of events occurs for the κ and λ loci, with the absence of D segments.

The diversity introduced into the antibody population by these rearrangements is increased further by SHM, a process that introduces errors into the genes encoding the variable regions of the individual B-cells [10]. During a very narrow time frame of B-cell proliferation the locus undergoes an extremely high rate of mutation, predominantly base substitution [10], approximately one million times higher than the spontaneous rate of mutation across the genome [11, 12]. The introduction of random mutations results in antibodies that lose their affinity for the antigen and undergo cell death, or generates advantageous antibodies, where there is an affinity increase and subsequent proliferation of the associated antibody-producing clone of lymphocytes.

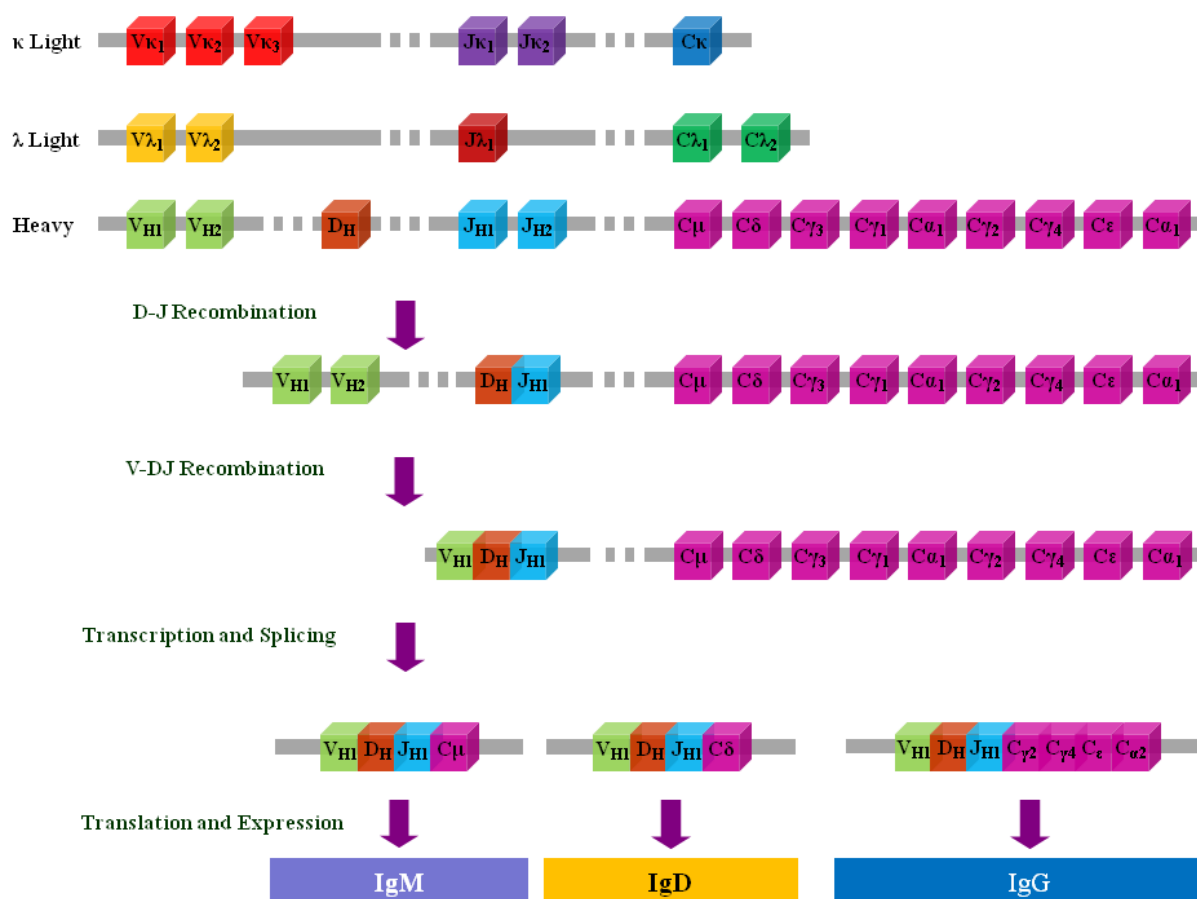


Figure 1.1-3: Genes encoding for human antibodies

Immunoglobulin loci: Heavy chain (chromosome 14), κ light chain (chromosome 2) and λ light chain (chromosome 22). Variable (V), constant I, joining (J) and diverse (D) segments are shown. In the heavy chain locus the V-D-J segments are recombined in immature B-cells and linked by splicing to C μ to produce mRNA encoding for IgM or C δ to give mRNA encoding for IgD. mRNA encoding IgG is produced by splicing leading to recombination of C γ 2, C γ 4, C ϵ and C α 2 by deletion of the other five C_H segments. This figure was adapted from [5, 9].

Exquisite specificity combined with the ability to refine and tailor antibody bio-physical properties has immense applications in therapeutics and diagnostics. Gargantuan advances in molecular biology and novel applications of antibody technologies have propelled antibody-based diagnostics forward. Biosensors is an area experiencing intense research to improve both patient diagnosis and prognosis and also areas such as environmental monitoring, counterterrorism, water monitoring, illicit drugs and food protection to name but a few.

1.2 Biosensors

1.2.1 Introduction

A biosensor can be described as a transducer that incorporates a biological recognition component as the key functional element. It consists of three main components as illustrated in Figure 1.2-1: the biorecognition element, the transducer and the signal display or readout [13]. The transduction system converts the interaction of the analyte with the biorecognition element to a measurable signal which is then visualised on a readout or display. Biosensors are powerful tools for the analysis of biomolecular interactions in clinical, biochemical and environmental analyses [14]. In the context of a medical setting, biosensors have the potential to provide rapid, real-time and accurate results in accident and emergency departments or at the physician's office. A typical example of this is the *in vitro* measurement of glucose (near patient) in diabetic patients [15]. The area of antibody-based sensors, with emphasis on improvements in antibody production and tailoring for the design of biosensors, is crucial for the next generation of useful sensor devices.

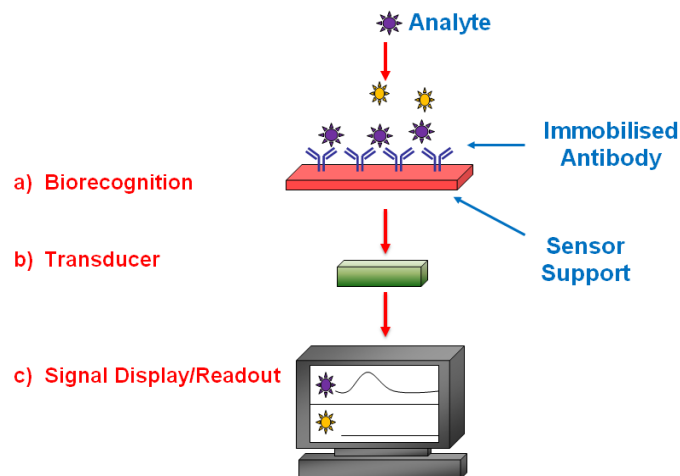


Figure 1.2-1: Components of a biosensor

- Analyte interaction with the biorecognition element: this is facilitated by the specificity of the immobilised antibody for its cognate antigen (purple). Other biorecognition elements include enzymes, lectins, receptors and microbial cells.
- Signal transduction: converts the interaction of the analyte with the immobilised antibody into a quantifiable signal.
- Readout: shows the specific signal generated (yellow = non-specific analyte).

1.2.2 Antibodies and their significance in biosensor development

The “*enzyme electrode*”, demonstrated by Clark and Lyons in 1962, was the first biosensor. This device coupled glucose oxidase to an amperometric electrode for monitoring oxygen levels in blood [16]. In 1987, Vo-Dinh and co-workers showed that antibodies could be utilised *in situ* for the detection of a chemical carcinogen in a fibre optic-based immunosensor [17]. Antibodies have since proven their worth as powerful tools for diagnostic applications, as illustrated by Table 1.2-1. Essentially, the specificity of the biosensor depends on the biorecognition element, which is capable of ‘sensing’ the presence of an analyte [13, 14]. Immunosensors utilising antibody-based recognition elements, have been developed on a wide range of transduction platforms for a multitude of analytes. The transducer element translates the selective recognition of the analyte into a quantifiable signal and thus, has a major influence on sensitivity [18]. Transduction approaches include electrochemical, piezoelectric and optical systems [19].

Table 1.2-1: Examples of antibody-based biosensors

Transducer	Analyte detected	Antibody form	Ref.
Electrochemical			
<i>Potentiometric</i>	Terbuthylazine	Monoclonal	[20]
	Hepatitis B surface antigen	Not specified	[21]
<i>Amperometric</i>	Diphtherotoxin	Monoclonal	[22]
	<i>E. coli</i> O157:H7	Polyclonal	[23]
	Carcinoembryonic antigen (CEA)	Not specified	[24]
	Aflatoxin M1	Monoclonal	[25]
<i>Impedance</i>	Progesterone	Monoclonal	[26]
	<i>Listeria monocytogenes</i> (Internalin B)	Polyclonal	[27]
Piezoelectric			
	<i>E. coli</i> O157:H7	Polyclonal	[28]
	Canine IgG isoforms	Monoclonal	[29]
	Cocaine derivative (BZE-DADOO)	Polyclonal	[30]
	Atrazine	Monoclonal	[31]
	<i>Bacillus anthracis</i>	Polyclonal	[32]
	<i>Francisella tularensis</i>	Polyclonal	[33]
Optical			
<i>SPR</i>	Urediniospores	Monoclonal	[34]
	Polychlorinated biphenyls	Monoclonal	[35]
	Vitellogenin (Carp)	Monoclonal	[36]
	<i>Campylobacter jejuni</i>	Polyclonal	[37]
	<i>Listeria monocytogenes</i>	Monoclonal	[38]
	Okadaic acid	Polyclonal	[39]
<i>Resonant Mirror</i>	<i>Listeria monocytogenes</i>	Monoclonal	[40]
<i>TIRF</i>	Testosterone (also RIIS)	Monoclonal	[41]
	Carbohydrates (maltose and panose)	Monoclonal	[42]
<i>RIIS</i>	Estrone	Polyclonal	[43]
	Tuberculosis (also interferometry)	Monoclonal	[44]
	Cell adhesion	Monoclonal	[45]
<i>OWLS</i>	Trifluralin	Polyclonal	[46]
	Sulfamethazine	Not specified	[47]
<i>Interferometry</i>	Atrazine	Monoclonal	[48]
	Hepatitis B virus surface antigen	Not Specified	[49]
<i>Ellipsometry</i>	Mycotoxin T-2 (TIRE also QCM)	Mono-and polyclonal	[50]
	<i>Salmonella typhimurium</i>	Monoclonal	[51]
<i>Fibre Optic</i>	<i>Listeria monocytogenes</i> (Imaging)	Polyclonal	[52]
	<i>Bacillus anthracis</i> (evanescent wave FO)	Not Specified	[53]
	Raptor™ - biothreat (e.g. <i>B. anthracis</i>)	Various monoclonal Abs	[54]

Antibodies are ideal biorecognition elements due to their exquisite specificities and strong affinities for cognate antigens. Figure 1.2-2 presents an overview of the generation of polyclonal [55, 56], monoclonal [56, 57] and recombinant antibodies [58, 59] from immunised repertoires. Antibodies have had numerous successful applications in the area of diagnostics with monoclonal and polyclonal antibodies exploited in many biosensors, as illustrated by Table 1.2-1. Polyclonal antibodies are derived from multiple plasma cells and monoclonal antibodies are derived from a single clonal hybridoma, all of which have terminally differentiated in response to an antigen [4, 55]. Recombinant antibodies, discussed at length in section 5.1, are the product of genetic manipulation of antibody genes. The specific characteristics of polyclonal, monoclonal and recombinant antibodies are outlined in Table 1.2-2. While each have relative advantages the modular nature of recombinant antibodies make them highly attractive for tailored antibody development.

Table 1.2-2: Characteristics of poly-, mono- and recombinant antibodies

	Polyclonal	Monoclonal	Recombinant
Ease of production	++++	+++	+++
Low Cost	++++	++	+++
Stability¹	+++	++	++
Commercial availability	++++	+++	+
Ease of immobilisation	++++	++++	+++++
Sensitivity (affinity)	+++	++++	+++++
Potential to engineer affinity	-	- (unless convert to rAb)	+++++

¹ Stability of the recombinant antibody is dependent on the format

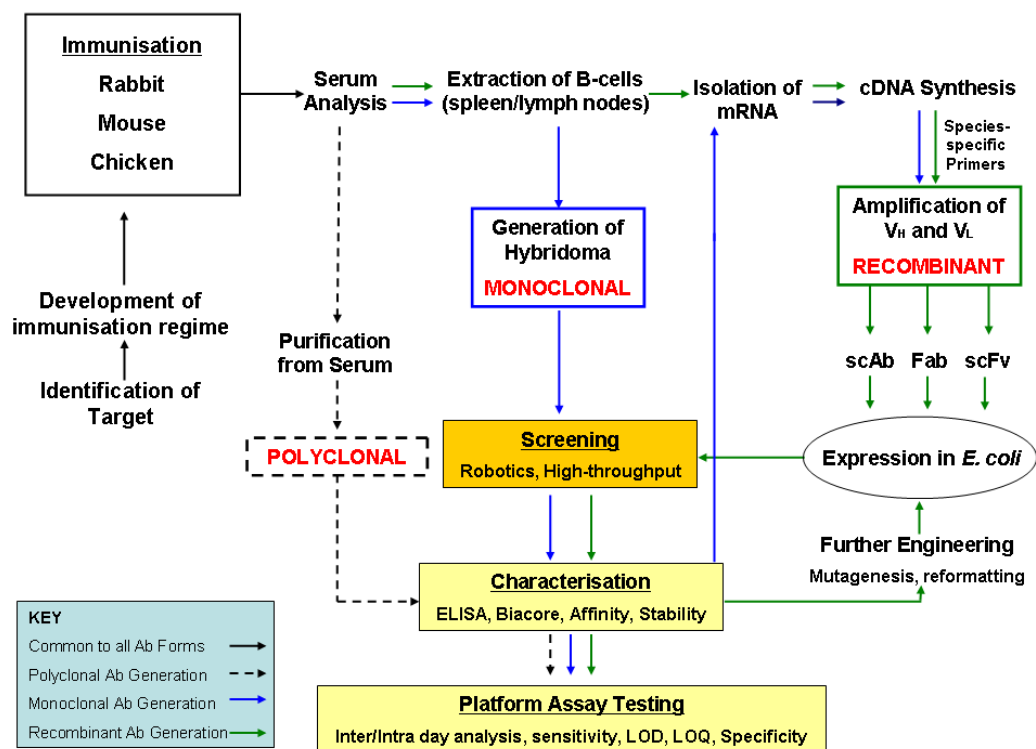


Figure 1.2-2: Overview of the routes to antibody generation

This image illustrates the basic route to antibody generation including poly-, mono-, and recombinant pathways. LOD; limit of detection, LOQ; limit of quantitation.

Key parameters exist for the successful exploitation of antibodies in sensor-based analysis and recombinant antibody technology represents a viable avenue for molecular evolution and specific-tailoring to address these key parameters (discussed in detail in sections 5.1 and 6.1). The ability to generate and tailor highly-specific antibodies for diagnostic applications has huge potential to meet the current challenges facing high-sensitivity rapid cardiovascular disease diagnosis in accident and emergency rooms.

1.3 Cardiovascular disease

1.3.1 Overview

Cardiovascular disease (CVD) is the biggest single killer in the western world [60, 61]. In Europe, CVD is responsible for over 4.3 million deaths, a staggering 48% of all deaths. The healthcare and associated costs of the disease are estimated at €192 billion per year, an average of €233 per EU resident [62]. CVD is also reported as the most frequent cause for hospitalisation in developed countries [63]. Improvements in the diagnosis, prognosis and treatment of cardiac disease can have an impact on patient outcome alleviating hospital congestion and reducing the costs of the disease on the health services [60, 61, 64].

Acute coronary syndrome (ACS) refers to disease of the coronary arteries and is discussed in detail in section 1.3.2. The diagnosis of ACS is one of the most difficult challenges that medical practitioners face [65]. The ability to diagnose a patient presenting with acute chest pain is imperative to the patient's outcome. In fact, a large number of malpractice payments for emergency department physicians are due to failure in diagnosis of acute myocardial infarction (AMI) which can be also referred to as myocardial infarction (MI) and is commonly known as heart attack [66, 67]. A major problem which currently faces the use of conventional biomarkers is that they are often not useful for diagnosis at the time of the patient's arrival to the accident and emergency department [65]. The world health organisation (WHO) developed a definition of AMI in 1997. This definition required two of the three following criteria to be satisfied; chest pain (myocardial ischemia), electrocardiography (ECG) irregularities and detectable laboratory changes [65]. In 2000, the definition of AMI was re-defined by the European Society of Cardiology and the American College of Cardiology joint committee to place greater emphasis on the role of biomarkers in the diagnosis of MI and AMI (Table 1.3-1). In 2007, a joint consensus document from the European Society of Cardiology (ESC), the American College of Cardiology Foundation (ACCF), the American Heart Association (AHA) and the World Heart Foundation (WHF) further revised the definition. This revision added the weight of additional scientific and clinical experiences to the 2000 definition [68, 69].

Table 1.3-1: Definition of myocardial infarction (MI). Criteria for acute, evolving or recent MI

Any of the following criteria:	
a)	Typical rise and gradual fall (troponin) or more rapid rise and fall (CK-MB) of biochemical markers of myocardial necrosis with at least one of the following; <ul style="list-style-type: none">i. Ischemic symptoms.ii. Development of pathological Q-waves in the ECG.iii. ECG changes indicative of ischemia (ST segment elevation).iv. Coronary artery intervention (angioplasty).
b)	Pathological findings of MI.

Table adapted from [70].

1.3.2 Pathophysiology

“Almost all MI’s are as a result of coronary atherosclerosis and generally with superimposed coronary thrombosis” [71].

Numerous clinical symptoms become evident after the disruption of a coronary plaque and are collectively referred to as ACS [66]. Atherosclerotic plaque rupture, the underlying basis for ACS [64], is illustrated in Figure 1.3-1. Atherogenesis causes the development of atheromatous coronary artery plaques, a process which begins quite early in life [67], characterised by the remodelling of the arteries and the accumulation of fatty acid substances [64, 72]. There are several genetic and lifestyle factors which lead to increased risk; sex (especially male), advanced age, diabetic conditions, smoking and a family history of coronary disease [67, 72]. Intra-coronary thrombosis has long been associated with AMI [73] and the importance of stabilising the plaque to prevent rupture has become increasingly pivotal to ACS treatment [64, 74]. Lesions which tend to rupture have a large lipid core overlaid by a fibrous cap. Owing to the ongoing inflammatory response, matrix degradation and cell death destabilises the plaque and subsequent rupture occurs at the shoulder where the fibrous cap is thin [74, 75]. The rupture of this lipid rich structure exposes blood to procoagulants triggering thrombosis (Figure 1.3-1) [64, 74].

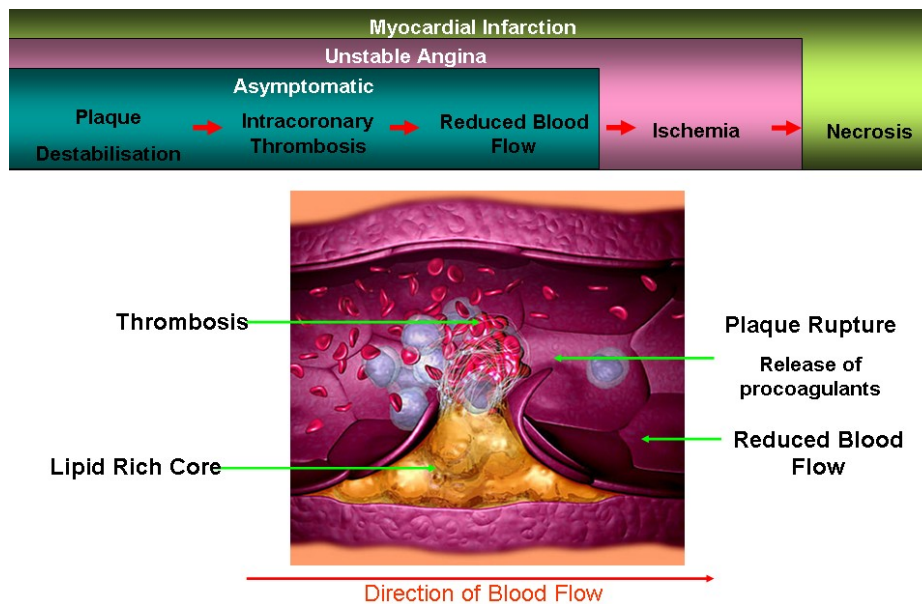


Figure 1.3-1: Atherogenesis leading to thrombosis formation

Plaque rupture leads to intracoronary thrombosis, where the thrombus restricts blood flow and this restriction is often asymptomatic. During ischemia the resulting restriction in the supply of oxygen to the myocardium can lead to unstable angina and subsequently a necrotic state, causing irreversible damage. This image was taken from [76] and adapted from [67].

Clinicians divide patients presenting with AMI into those with Q-wave and those with non-Q-wave infarct, which is based on the ECG pattern. Q-waves indicate the loss of electrically functioning cells and refers to a transmural infarction while a non-Q-wave ECG refers to a subendocardial infarction. The classification of ACS by ECG pattern is shown in Figure 1.3-2 and outlines the difficulties in diagnosing AMI on the basis of ECG alone. This asserts the absolute requirement for biochemical markers to differentiate between patients exhibiting Q-wave or non-Q-wave infarct and unstable angina. The treatment for non-ST-elevation-myocardial infarction (NSTEMI) and ST-elevation-myocardial infarction (STEMI) varies dramatically and the correct categorisation is imperative [66]. Medically, the ST segment refers to the period from the end of ventricular depolarisation to the beginning of ventricular repolarisation on the ECG. The ischemic discomfort felt during NSTEMI can be unstable angina, but may also become much more serious and cause irreversible myocardial damage (non-Q-wave-MI) [70].

After the initial myocardial infarction there is a reduction in cardiac output and the increased pressure on the heart results in heart failure. The body attempts to maintain cardiac output and blood flow to the extremities using several mechanisms. These include

the adrenergic nervous system, the angiotensin (rennin-aldosterone) system, inflammatory cytokines and growth factors [77]. These mechanisms cause a difference in gene expression resulting in disadvantageous functional and structural changes, a process known as left ventricular remodelling [77]. This structural and functional change of the myocytes leads to systolic and diastolic dysfunction. Changes in the myocardium (dilated and ischemic cardiomyopathy) result in hypertrophy and a heart chamber with reduced contractility due to dilation [77]. These events and those leading to myocardial infarction give rise to new strategies for biochemical marker development [63, 65-67, 70, 72, 77, 78] and highlights the necessity for biochemical markers to help guide intervention and positively impact prognosis.

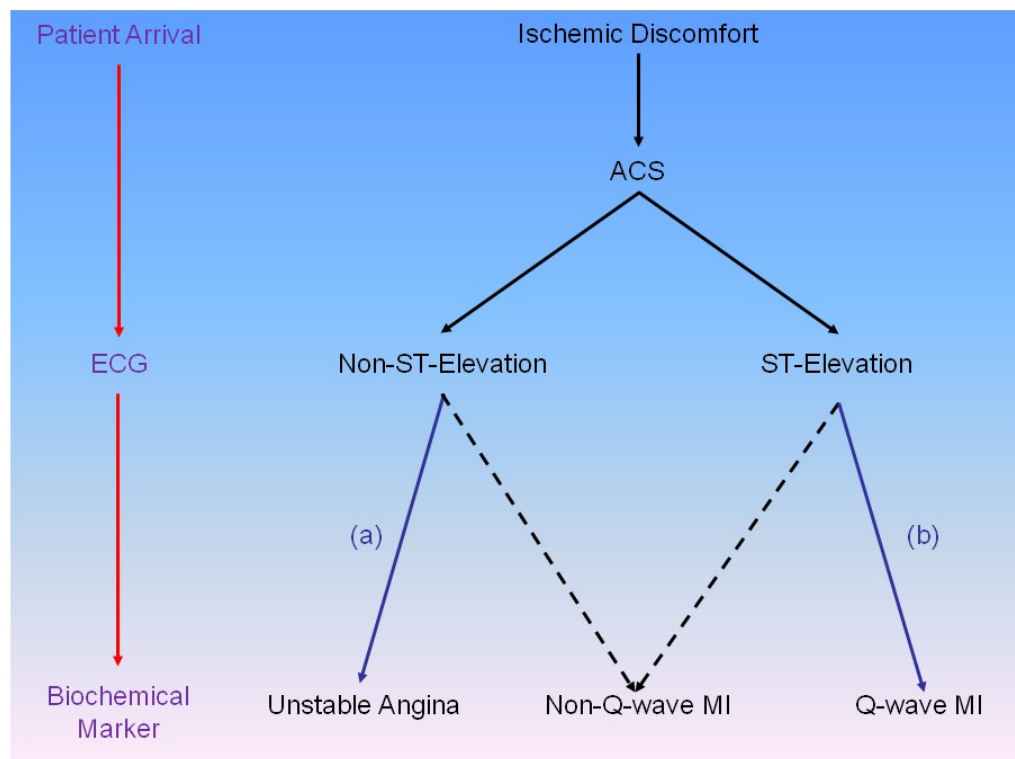


Figure 1.3-2: Route to the classification of acute coronary syndrome by electrocardiography pattern

- The majority of patients presenting with ischemic discomfort where there is no ST elevation in the ECG are experiencing unstable angina or non-ST-elevation-myocardial infarction (NSTEMI), which does not evolve Q-waves in ECG.
- Patients presenting with ST-elevation (STEMI) ultimately go on to develop Q-wave myocardial infarction, but a minority may develop non-Q-wave myocardial infarction.

This figure was adapted from [70, 71].

1.3.3 Biomarkers of cardiovascular disease

1.3.3.1 Overview

In 1954, La Due *et al.* demonstrated use of the first biochemical marker, serum glutamic oxalaoacetic transaminase, to investigate transmural myocardial injury [79]. Since then an explosion of interest and research in both the clinical and analytical development of more suitable biomarkers of ACS has ensued [80, 81]. Combined with a better understanding of the pathophysiology of ACS, advances in proteomics and genomics are providing new biomarkers for exploitation as analytical tools in diagnosis and treatment of patients [81].

Biochemical markers of cardiac injury have a pivotal role in a clinical setting for the effective diagnosis, treatment, prognosis and risk stratification of patients presenting with symptoms of AMI [67]. Accordingly, widespread research aimed to indentify unique biochemical markers and also to integrate those markers into detection systems for use in point-of-care devices (POC). This has reduced the need for laboratory testing and provides rapid, accurate and precise results [67].

1.3.3.2 The ‘golden’ biomarker

The specificity of the marker for the target organ, the heart, is of crucial importance for clinical diagnosis. Other key attributes of an ideal marker are summarised in Table 1.3-2. The size of a prospective biomarker is important as it controls the rate of release during a cardiovascular event and the kinetics of that release has an impact on the speed of diagnosis [78, 80]. The location of the biomarker determines its rate of release with structural proteins appearing in the blood slower than cytoplasmic ones [80]. Prolonged persistence of a biomarker in circulation is of diagnostic value for patients presenting late, after the early markers return to normal levels [60, 80]. To ensure cardiovascular specificity, the concentration of the biomarker must be high in cardiac tissue with relatively low concentrations in non-cardiac related tissues [66, 80]. The distribution of the biomarker within the body under normal physiological and in pathological conditions is of considerable importance. The use of biomarkers for infarction sizing is beneficial for

prognosis as the extent of biomarker release may be correlated to the degree of necrosis, indicating its severity [66, 80]. The necessity to differentiate between reversible (ischemia) and irreversible damage (necrosis), combined with positive outcomes from the physicians intervention and defining a risk score, are paramount [66]. Ultimately, any new biomarkers require thorough evaluation within a large, statistically relevant cohort of clinical studies before being accepted into clinical practice [66]. Unfortunately, no one biochemical marker identified to date meets all the criteria outlined in Table 1.3-2 [60, 80]. Therefore, it is necessary to examine multiple markers of cardiovascular injury to aid current standard practices in accident and emergency departments. This movement towards multiplexed assays is currently under enthusiastic investigation [81, 82].

Table 1.3-2: The characteristics of an ideal biochemical marker

Characteristic	Notes
<i>Size</i> [67]	Small markers are released faster from injured tissue and undergo rapid clearance.
<i>Localisation</i> [67]	Soluble cytoplasmic markers are desirable as they appear in the blood stream more rapidly than structural markers.
<i>High sensitivity</i> [83]	Early diagnosis due to early release of the marker. Prolonged presence in the serum for late diagnosis (longer half-life).
<i>High specificity</i> [83]	Present only in myocardial tissues. Not present in non-afflicted individuals. Allow differentiation between ischemia and necrosis [67].
<i>Analytical characteristics</i> [83]	Detectable and measurable by a low cost assay. Ease of test procedure. Rapid analysis. Sufficient sensitivity and precision.
<i>Clinical characteristics</i>	Release of marker directly proportional to the size of the injury. Peak levels reached soon after injury to provide diagnosis time [67]. Results that can dictate/influence intervention. Results that can improve patient outcome.

Adapted from [60, 65, 67, 83].

1.3.3.3 *Clinical considerations*

Before discussing the current and emerging biomarkers, clinical considerations must be taken into account. Biomarkers need to provide useful, reliable and accurate information for clinicians and physicians alike.

The necessity for serial sampling in the diagnosis of ischemia and/or necrosis is vital due to the rapid changes in biomarker concentration with respect to time and extent of injury which is currently recommended by established guidelines [61, 63, 67, 78, 81, 84]. Single sampling gives low sensitivity for AMI diagnosis due to the differing release kinetics of each biomarker [67], implying that a single measurement may be early or late for AMI detection leading to misdiagnosis [60]. By monitoring the serum levels over time the biomarker concentration profile can indicate the extent of cardiac damage or if the therapeutic intervention was effective. Any rapid change in the concentration of a biomarker is in response to some cardiac event or is indicative of the potential onset of a cardiovascular event and may improve the speed at which medical intervention is taken for a patient presenting with suspected AMI (measurement time from symptom onset) [63]. The development of point-of-care devices would have a huge impact on the serial measurement of biomarkers allowing physicians to analyse the patients' sera without the need for complete laboratory testing hence, greatly improving the intervention decision process taken.

The development of multi-marker detection systems is necessary [82, 85] due to the complex series of events leading up to, during and after AMI combined with the variance between symptom onset and presentation at A&E from patient to patient [66]. The National Academy of Clinical Biochemistry (NACB) Standards of Laboratory Practice recommends that at least two biochemical markers be utilised for the diagnosis of AMI (one early marker and one definitive marker) [60, 86] and these sentiments are reflected in the ACCF/AHA guidelines [84]. As demonstrated in Figure 1.3-3, the Academy recommends that; (a) an early marker which appears in the blood stream ≤ 6 hours after symptom onset and, (b) a definitive marker appearing 6-9 hours after symptom onset which is both a definitive indicator of AMI and provides a large diagnostic window to be used to effectively diagnose AMI [86].

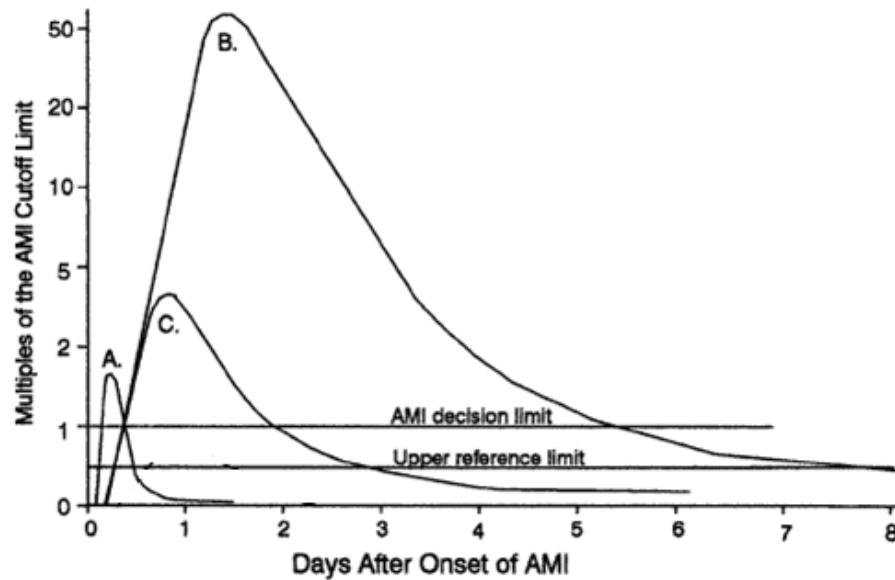


Figure 1.3-3: The release kinetics of biomarkers during acute coronary syndrome

Biomarker appearance versus time after symptom onset. Graph taken from [86].

Legend:

Peak A: Myoglobin release after AMI,

Peak B: Cardiac troponin release after AMI.

Peak C: Creatine kinase myocardium specific isoform (CK-MB) release after AMI.

1.3.3.4 *Current and emerging biomarkers*

Ultimately, the goal of employing biochemical markers is in the prevention of a minor infarction and a reduction in the associated mortality rate [66]. Key factors influencing this are the information available to physicians, the speed at which the injury is detected and the intervention taken [78]. Presently, conventional biomarkers are commonly non-diagnostic at the time of patient presentation [65]. Figure 1.3-4 indicates the stages of AMI and the markers released. The biomarkers that are upstream of cardiac tissue necrosis are of particular interest to prevent AMI developing. However, due to their relatively new status as biomarkers the necessity to definitively identify the occurrence of AMI remains (accepted definitive markers are the troponins).

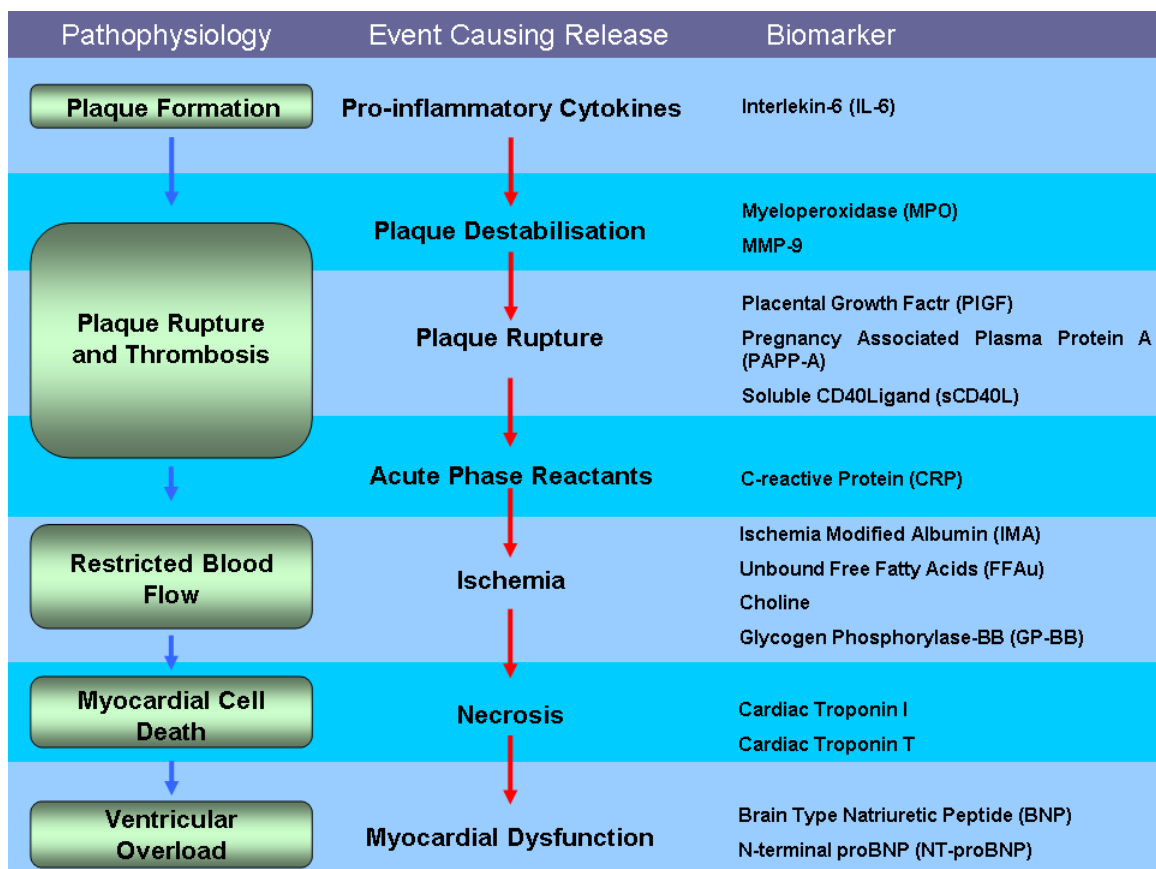


Figure 1.3-4: Biochemical markers released during acute coronary syndrome

Various stages of AMI from the initial formation of the plaque, its destabilisation, subsequent rupture and thrombosis leading to ischemia culminating in myocardial cell death and ventricular overload. Each stage of the AMI releases biological entities which have potential as biochemical markers for diagnosis. Adapted from [78, 83, 87].

To date, assays detecting the established biomarkers primarily indicate myocardial necrosis [78]. The clinically accepted biomarkers of AMI are; the troponins (which are the preferred [69]), CK-MB (Mass assay [69]) and myoglobin (potentially outdated [81]) [60, 78, 84]. The properties of these biomarkers are summarised in Table 1.3-3.

Table 1.3-3: Current cardiovascular biomarkers and their associated properties

Biomarker	Size kDa	Cardio- Specificity	Role in ACS	Value	Elevation Period*	POC-test ^[78]
Myoglobin	17.8	Low	Early MI, Re-infarction	NPV ¹	1-48 hrs	Cardiac STATus, Cardiac M-Test, RAMP Reader, Life Lite, Stratus CS.
CK-MB	85	Yes	Re-infarction	Rule in	24-36 hrs	Cardiac STATus, Stratus CS, RAMP Reader, Life Lite.
Troponin I	23.9	Very High	Necrosis	Definitive, Risk Stratification	2-4 hrs up to 4-7 days	i-STAT, RAMP Reader, AlphaDx, Life Lite, Stratus CS, Architect TnI, Vitrous TnI-ES, Access Accu TnI.
Troponin T	37	High	Necrosis	Definitive, Risk Stratification	2-4hrs up to 10-14 days	CARDIAC T-Test.

This table was prepared from [66, 67, 78]. * Initial elevation to return to normal. ¹NPV: Negative predictive value.

Myoglobin, a haemeprotein, is located in the cytoplasm of both cardiac and skeletal muscle cells [80]. Myoglobin is released rapidly into circulation as early as one hour from the onset of symptoms (Table 1.3-3) and has a high negative predictive value (NPV) for AMI due to its low molecular weight and location within the cell [60, 78, 80]. NPV represents accurate determination of the number of patients with a negative result who are diagnosed correctly and myoglobin has value as a ‘rule out’ biomarker. Myoglobin’s specificity is compromised by its identical amino acid composition in both cardiac and skeletal tissues and its appearance in patients with renal insufficiency [80]. However, myoglobin is still recognised as a useful early marker of myocardial damage as a negative predictive

biomarker [70, 81, 86]. Myoglobin may also identify low grade ACS patients at additional risk, for example detection of a non-cardiovascular disease [81].

Cytoplasmic creatine kinase (CK) is a dimer composed of M (muscle) or B (brain) subunits that associate to form CK-MM (striated muscle), CK-MB (predominantly myocardium) and CK-BB (brain, stomach and liver) [80]. The normal function of CK is to provide high energy phosphate molecules, from creatine, which is used in contractile tissues. Early successful assays included CK-MB-specific mass and CK-MB subtype measurement. The characteristics of each is summarised in Table 1.3-4.

CK-MB isoform was considered the gold standard in AMI diagnosis until 1995, however, its specificity is limited, like myoglobin, due to its role in skeletal muscle damage [60, 67, 78]. CK-MB remains a useful tool, especially in multi-marker analysis, for the assessment of re-infarction [60].

Table 1.3-4: Creatine kinase characteristics

Marker	Cardiac Specific	Initial Elevation (Hours)	Duration of Elevation (Hours)
Total CK	No	4-8	36-48
CK-MB mass	Yes	3-4	24-36
CK-MB subtypes	Yes	2-4	16-24

The troponin complex (Figure 1.3-5) consists of three proteins that function in the regulation of striated muscle contraction. In the complex, calcium mediates the interaction between actin and myosin in the thin filament [80]. The TnI and TnT subunits have both skeletal (sTnI, sTnT) and cardiac isoforms (cTnI, cTnT) that have differing amino acid sequences and immunological activities while TnC has no cardiac specific isoform [80]. Cardiac Troponin I and T which are proteins of the sarcomeric pool are widely recognised as the gold standard biomarkers for AMI diagnosis which also impact the patient prognosis, risk stratification and guide therapeutic intervention [60, 65, 66, 68, 69]. The cardiac troponins (cTn) are markers of myocyte necrosis and take several hours to reach peak elevation after the onset of ischemia (Table 1.3-3) [67]. As indicated by Figure 1.3-3, cTn has a prolonged elevation period providing a large temporal diagnostic window and the

peak concentration can be closely correlated to the size of the infarction [60]. The elevation of cTn occurs 2 to 4 hours after onset of symptoms (Table 1.3-3) and this initial release can be attributed to their cytosolic pool with the prolonged elevation due to the structural release of the regulatory proteins [81, 82]. The circulating forms of cardiac troponin found are listed in Table 1.3-5. The variance in circulating forms of the structural cTn complex and its constituents gives rise to complications in the rational design of an antibody targeting strategy due to the inaccessibility or cloaking of epitopes, the formation of complexes and interference from other serum proteins to exposed regions of the protein. Currently, cTnI is credited with greater discriminatory value compared to cTnT. The detection limits for assays detecting cTnI in patient samples is sub-40pg/mL and so represents a significant challenge in terms of the design of the assay and its components [66].

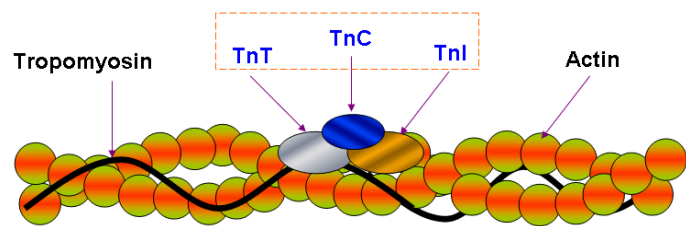


Figure 1.3-5: Actin-Tropomyosin-Troponin complex

The complex regulates calcium-mediated muscle contraction. The Troponin T (TnT) subunit anchors the troponin complex to tropomyosin. The TnI subunit inhibits actomyosin ATPase activity and thus modulates the interaction of actin with myosin. The TnC subunit, common to both striated and cardiac muscle, binds calcium [67, 80].

Table 1.3-5: Circulating cTn forms

cTnT	cTnI*
Free cTnT (major form)	TnI/TnC (major form)
TnT/TnI/TnC complex	
TnT fragments	Free TnI (minor form)
TnT/TnI complex (minor form)	

This table was adapted from [80]. *cTnI exists in these forms in phosphorylated, oxidised and reduced states.

1.4 Thesis aims and objectives

The principal aim of this research is the production, characterisation and development of antibodies for the early detection of cardiac disease by addressing the issues surrounding the *ultra-sensitive* detection of cardiac Troponin I (cTnI).

To achieve these outcomes several key objectives need to be realised:

1. Development of antibodies based on synthetic-epitope targeting immunisation regimes developed by rational, knowledge-based antigen design strategies.
2. Use of this approach to investigate the generation of antibodies by the exploitation of monoclonal and recombinant antibody technologies for targeting key epitopes of interest, underpinned by rigorous selection and screening methodologies incorporating high-throughput surface plasmon resonance-based instrumentation.
3. Efficient characterisation of the generated epitope-specific antibodies by the development and use of modified forms of the antigen.
4. Tailoring, modifying and refining the generated antibodies for highly-specific roles in novel point-of-care platforms.

In addition, work was undertaken to elucidate the three dimensional structure of avian scFvs using advanced crystallographic studies including large-scale production and purification of scFvs, high-throughput screening and systematic optimisation of conditions for crystal formation.

Ultimately, the overall requirement is to generate high-affinity, high-sensitivity anti-cTnI epitope-specific antibodies to facilitate the development of a novel next generation *ultra-sensitive* point-of-care-device capable of detecting cTnI at less than 40pg/mL in whole blood samples.

Chapter 2: Materials and Methods

2.1 Materials

2.1.1 Equipment

Instrument	Manufacturer
Nanodrop™ ND-1000	NanoDrop Technologies, Inc., 3411 Silverside Rd 100BC, Wilmington, DE19810-4803, USA.
Gene Pulser Xcell™ Trans-Blot® Semi-dry transfer cell Bio-Rad PowerPac HC: 250V/3.0A/300W	Bio-Rad Laboratories, Inc., 2000 Alfred Nobel Drive, Hercules, California 94547, USA.
Tecan® Safire 2™ plate reader Tecan® Sunrise™ plate reader	Tecan Group Ltd., Seestrasse 103, CH-8708 Männedorf, Switzerland.
PX2 thermal cycler	Thermo Electron Corporation, 81 Wyman Street, Waltham, MA 02454, USA.
G-Storm™ PCR machine	GRI Ltd., Gene House, Queenborough Lane, Rayne, Braintree, Essex CM77 6TZ, United Kingdom.
Biacore™ 3000 and 4000 AKTA Explorer FPLC System	GE Healthcare Bio-Sciences AB, SE-751 84 Uppsala, Sweden.

Clifton stirred water bath	Nickel – Electro Ltd., Oldmixon Crescent, Weston-super-Mare, North Somerset BS24 9BL, United Kingdom.
Ohaus Explorer balance	Ohaus Europe GmbH, Heuwinkelstrasse 3, CH-8606 Nänikon, Switzerland.
Heraeus Biofuge Pico	Kendro Laboratory Products International Sales, Hanau, Germany.
Stuart Scientific See-saw rocker SSL4	Lennox Laboratory Supplies Ltd., John F Kennedy Drive, Naas Road, Dublin 12, Ireland.
Priorclave tactrol 2 autoclave	Priorclave Ltd., 129/131 Nathan Way, West Thamesmead Business Park, London SE28 0AB, United Kingdom.
Eppendorf refrigerated centrifuge Model 5810R Rotors: F45-30-11 (14,000rpm) A-4-62 (4,000rpm) New Brunswick Scientific U725 (-80°C)	Eppendorf UK Limited Endurance House, Vision Park Histon, Cambridge CB24 9ZR, United Kingdom.
Orbi-Safe TS Netwise orbital shaker 37°C static incubator	Sanyo Europe Ltd., 18 Colonial Way, Watford WD24 4PT, United Kingdom.

Inverted Microscope Leica BMIL	Laboratory Instruments & Supplies (I) Ltd. Pamaron House, Ballybin Road, Ashbourne, Ireland.
Thermo Steri-cycle CO₂ incubator Hearaeus Hera-safe Laminar flow cabinet Thermo Orion pH meter: Model 420A+	Thermo Scientific, 12-16 Sedgeway Business Park, Witchford, Cambridgeshire CB6 2HY, United Kingdom.
Liquid Nitrogen (LN₂) Cryogenic storage LS750	Jencons Scientific, 800 Bursca Dr., Suite 801Bridgeville, PA 15017, USA.
Plate Washer ELx405	BioTek U.S. - World Headquarters, 100 Tigan Street, Winooski, VT 05404, USA.

2.1.2 Chemicals

All chemicals were of the highest possible quality and sourced from Sigma-Aldrich (Sigma-Aldrich Ireland Limited, Vale Road, Arklow, Wicklow, Ireland.) or Fisher Scientific (Fisher Scientific Ireland, Suite 3, Plaza 212, Blanchardstown Corporate Park 2 Ballycoolin, Dublin 15, Ireland.) unless stated otherwise.

2.1.3 Cells

Table 2.1-1 details the mammalian cell lines and Table 2.1-2 outlines the *E. coli* cell types and their genotypes that were utilised in the course of this thesis.

Table 2.1-1: Mammalian cell lines

Cell Line	Description	Catalogue	Supplier
Sp2/0-Ag14	Mouse myeloma, lymphoblast	CRL-1581	ATCC

Table 2.1-2: *E. coli* cells and genotypes

Cell Line	Genotype	Catalogue	Brand
XL1 Blue	<i>recA1 endA1 gyrA96 thi-1 hsdR17 supE44 relA1 lac [F' proAB lacIqZΔM15 Tn10 (Tetr)].</i>	200249	Stratagene
Top10F'	<i>F'[lacIq Tn10 (TetR)] mcrA Δ(mrr-hsdRMS-mcrBC) Φ80lacZΔM15 ΔlacX74 recA1 araD139 Δ(ara-leu)7697 galU galK rpsL endA1 nupG.</i>	C3030-03	Invitrogen
dcm⁻/dam⁻	<i>(dam13::Tn9 (Cam^R), dcm-6)(endA) (hsdR2) (mcrA, mcrB1) (fhuA31)</i>	C2925H	NEB
Top10	<i>F- mcrA Δ(mrr-hsdRMS-mcrBC) φ80lacZΔM15 ΔlacX74 recA1 araD139 Δ(ara-leu) 7697 galU galK rpsL (Str^R) endA1 nupG</i>	C4040-10	Invitrogen
BL21 (DE3)	<i>F- ompT hsdSB(rB⁻, mB⁻) gal dcm (DE3)</i>	70235-3	Novagen
BL21 (DE3) pLysS	<i>F- ompT hsdSB(rB⁻, mB⁻) gal dcm (DE3) pLysS (Cam^R)</i>	70236-3	Novagen
Origami 2 (DE3)	<i>Δ(ara-leu)7697 ΔlacX74 ΔphoA PvuII phoR araD139 ahpC galE galK rpsL F'[lac⁺ lacI^q pro] (DE3) gor522::Tn10 trxB (Str^R, Tet^R)</i>	71408-3	Novagen
Tuner (DE3)	<i>F- ompT hsdS_B(rB⁻ mB⁻) gal dcm lacYI(DE3)</i>	70726-3	Novagen
Rosetta2	<i>F- ompT hsdS_B(rB⁻ mB⁻) gal dcm pRARE2 (Cam^R)</i>	71402-3	Novagen

2.1.4 Media and buffers

2.1.4.1 Media used for the growth of mammalian cells

All cell culture reagents were of the highest possible quality, tested for cell culture and sourced from Sigma-Aldrich (Sigma-Aldrich Ireland Limited, Vale Road, Arklow, Wicklow, Ireland.) or Fisher Scientific (Fisher Scientific Ireland, Suite 3, Plaza 212, Blanchardstown Corporate Park 2 Ballycoolin, Dublin 15, Ireland.) unless stated otherwise.

Media	Component	Composition
SP2/0 Ag14 Growth	DMEM (- L-Glutamine)	500mL
	Foetal Calf Serum (FCS)	10% (v/v)
	L-Glutamine (200mM)	2mM
DMEM w/o FCS	DMEM (- L-Glutamine)	500mL
	L-Glutamine (200mM)	2mM
	Sodium Pyruvate (100mM)	1mM
	NEAA (100X)	1(X)
	25µg/ml Gentamicin	25µg/mL
DMEM + FCS	DMEM (- L-Glutamine)	500mL
	FCS	10% (v/v)
	L-Glutamine (200mM)	2mM
	Sodium Pyruvate (100mM)	1mM
	NEAA (100X)	1(X)
	25µg/ml Gentamicin	25µg/mL
Selection Media (HAT)	DMEM + FCS	500mL
	HAT Medium (100X)	1X
	Briclone (Archport) ²	5% (v/v)
Cloning Media (HT)	DMEM + FCS	500mL
	HT Medium (100X)	1X
	Briclone (Archport)	5% (v/v)

² Briclone is a media additive for use in the fusion stages of hybridoma development promoting the outgrowth of new hybrids. The IL-6 rich conditioned media is collected from a human cell line and Briclone is a registered product of Archport, DCU.

2.1.4.2 *Media used for the growth of bacterial cells*

Media	Component	Composition
Luria Broth (LB)	Tryptone	10g/L
	Yeast extract	5g/L
	NaCl	10g/L
Super Broth (SB)	MOPS	10g/L
	Tryptone	30g/L
	Yeast extract	20g/L
Terrific Broth (TB) (Completed with 100mL TB salts*)	Tryptone	12g/900mL
	Yeast extract	24g/900mL
	Glycerol	4mL/900mL
TB Salts*	KH ₂ PO ₄	2.31g/100mL
	K ₂ HPO ₄	12.54g/100mL
Super Optimal Catabolite (SOC)	Tryptone	20g/L
	Yeast extract	5g/L
	KCl	2.5mM
	NaCl	0.5g/L
	MgCl ₂	20mM
	Glucose	20mM

2.1.4.3 *Media additives used for the growth of bacterial cells*

2.1.4.3.1 Antibiotics

Antibiotics used for bacterial cell culture were prepared as described below and sterile filtered (0.2µm) before use. Antibiotic stocks were retained in aliquots to reduce the instances of contamination.

Antibiotic	Component	Composition
100mg/mL (w/v) Carbenicillin	Carbenicillin salt	500mg
	Molecular grade water	5mL
70 mg/mL (w/v) Kanamycin	Kanamycin	700mg
	Molecular grade water	10mL
5mg/mL (w/v) Tetracycline	Tetracycline	50mg
	Molecular grade ethanol	10mL

2.1.4.3.2 Additives

Additives were prepared with autoclaved dH₂O as described below and, where possible sterile filtered through a 0.2µm syringe filter.

Media Additive	Component	Composition
100X 505	Glycerol	50% (v/v)
	Glucose	5% (w/v)
	dH ₂ O (autoclaved)	to 50mL
30% (w/v) Glucose	Glucose	30% (w/v)
	dH ₂ O (autoclaved)	to 50mL

2.1.4.4 Buffers

Buffer	Component	Composition
Phosphate Buffered Saline (PBS)	NaCl	0.15M
	KCl	2.5mM
	Na ₂ PO ₄	10mM
	KH ₂ PO ₄	18mM
		pH 7.4
5% (w/v) PBS-Milk (PBSM)	PBS	1X
	Milk marvel	5% (w/v)
0.05% (v/v) PBS-Tween (PBST)	PBS	1X
	Tween 20	0.05% (v/v)
1% (w/v) PBST-Milk (PBSTM)	PBST	1X
	Milk marvel	1% (w/v)
10X HBS-EP⁺ (1L)	0.1M HEPES	23.831g
	1.5M NaCl	87.66g
	30mM EDTA	11.17g
	0.5% (v/v) P20/Tween®20	5mL
	MilliQ H ₂ O	to 1L
Tris Buffered Saline (TBS)	Tris	50mM
	NaCl	150mM
		pH 8.0

2.1.4.5 Sodium dodecyl sulfate polyacrylamide gel electrophoresis (SDS-PAGE) and Western blotting (WB)

12.5% (w/v) Separation gel (1 gel: 6mL)	1M TrisHCl, pH 8.8	1.5mL
	30% (w/v) acrylamide (Acrylagel)	2.5mL
	2% (w/v) methylamine bisacrylamide (Bis-Acrylagel)	1.0mL
	dH ₂ O	934μL
	10% (w/v) sodium dodecyl sulphate (SDS)	30μL
	10% (w/v) Ammonium persulfate (APS)	30μL
	TEMED	6μL
4.5% (w/v) Stacking gel (1 gel: 2.5mL)	1M TrisHCl, pH 6.8	300μL
	30% (w/v) acrylamide (Acrylagel)	375μL
	2% (w/v) methylamine bisacrylamide (Bis-Acrylagel)	150μL
	dH ₂ O	1.74mL
	10% (w/v) sodium dodecyl sulphate (SDS)	24μL
	10% (w/v) APS	24μL
	TEMED	2.5μL
10X electrophoresis buffer	50mM Tris, pH 8.3	30g
	196mM Glycine	144g
	0.1% (w/v) SDS	10g
	dH ₂ O	to 1L
Loading buffer (4 X)	0.5M Tris, pH 6.8	2.5mL
	Glycerol	2.0mL
	1-mercaptoethanol	0.5mL
	20% (w/v) SDS	2.5mL
	Bromophenol blue	20ppm
	dH ₂ O	1.25mL
Coomassie stain (500mL)	Coomassie blue R-250	1g
	Methanol	225mL
	Acetic Acid	50mL
	dH ₂ O	225mL
Coomassie destain (1L)	Acetic Acid	150mL
	Methanol	200mL
	dH ₂ O	650mL

Transfer Buffer (500mL)	Trizma Base	2.4g
	Glycine	7.2g
	Methanol	100mL
	dH ₂ O	400mL

2.1.4.6 *Protein purification*

Note: Buffers were prepared in 18.2mΩ water and 0.2µm sterile filtered before use.

2.1.4.6.1 Monoclonal antibody purification buffers

Equilibration Buffer	1X PBS
Wash Buffer	0.05% (v/v) PBST
Elution Buffer	0.1M Glycine HCl, pH 2.5
Neutralisation Buffer	1M Tris-HCl, pH 8.5

2.1.4.6.2 Recombinant protein purification buffers

PBS-based buffers

Equilibration Buffer	1X PBS + 150mM NaCl + 10mM Imidazole, pH 8.0
Wash Buffer	Equilibration buffer + 0.5% (w/v) Tween®20, pH 8.0
Elution Buffer	100mM NaOAc, pH 4.2
Neutralisation Buffer	10X PBS and 100mM NaOH (1:1)

NaH₂PO₄-based buffers

Equilibration Buffer	50mM NaH ₂ PO ₄ + 100-300mM NaCl, pH 8.0
Wash Buffer # 1	Equilibration buffer + 10mM Imidazole, pH 8.0
Wash Buffer # 2	Equilibration buffer + 20mM Imidazole, pH 8.0
Elution Buffer	100mM NaOAc, pH 4.2
Neutralisation Buffer	10X PBS and 100mM NaOH (1:1)

Cation exchange buffers

Equilibration Buffer	50mM NaH ₂ PO ₄ + 100-300mM NaCl, pH 8.0
Elution Buffer	100mM NaOAc, pH 4.2
Neutralisation Buffer	10X PBS and 100mM NaOH (1:1)

Gel filtration buffers for Fast protein liquid chromatography (FPLC)

Gel filtration buffers were composed of 1X PBS or 1X TBS (depending on the intended application of the purified protein) supplemented with 0.02% (w/v) NaN₃. The buffers were prepared and sterile filtered through 0.2µm filter and degassed before use.

2.1.5 Commercially sourced kits and solutions

Kit	Supplier
Superscript III® Reverse Transcriptase Kit (18080-051) Platinum® Taq DNA Polymerase High Fidelity (11304011)	Invitrogen Corporation, 5791 Van Allen Way, PO Box 6482, Carlsbad, California 92008, USA.
NucleoTrap® Gel Extraction Kit (636018) NucleoBond® Xtra Midi (740410.100)	MACHEREY-NAGEL GmbH, Postfach 10 13 52, Neumann Neander Str. 6-8, D-52355 Düren, Germany.
BugBuster™ Protein Extraction Reagent (70923) His•Bind® Resin, Ni²⁺-charged (71035-25ml)	Novagen, Merck KGaA, Darmstadt, Germany.
GoTaq® Flexi DNA Polymerase (Promega - M8301)	Promega Corporation, 2800 Woods Hollow Road, Madison, WI 53711, USA.
Amine Coupling Kit (BR-1000-50)	GE Healthcare Ltd., Amersham Place, Little Chalfont, Buckinghamshire, HP7 9NA, United Kingdom.
Pierce™ Rapid Isotyping Kit plus κ and λ (26179)	Pierce, 3747 N Meridian Rd, Rockford, IL 61101, USA.

2.1.6 Commercially sourced antibodies

Antibody	Species	Supplier
Anti-Mouse (whole molecule) HRP Anti-polyhistidine (HIS) HRP Anti-Mouse-Fc-specific HRP	Goat Mouse Goat	Sigma-Aldrich Ireland Ltd., Vale Road, Arklow, Wicklow, Ireland.
Anti-chicken-IgY-Fc-specific HRP Anti-chicken-IgY-Fab HRP Anti-chicken-IgY-Fc-specific Anti-chicken-IgY-Fab Anti-mouse-IgG-Fc-specific	Goat Goat Donkey Goat Chicken	Gallus Immunotech, 6570 1st Line West Garafraxa, Fergus, ON N1M 2W4, Canada.
Anti-TnI-19C7 Anti-TnI-228 Anti-TnI-16A11	Mouse Mouse Mouse	Hytect, Intelligate 6th floor, Joukahaisenkatu 6, 20520, Turku, Finland.
Anti-Hemagglutinin (HA) HRP	Rat	Roche Diagnostics Ltd., Charles Avenue, Burgess Hill, West Sussex, RH15 9RY, United Kingdom.
Anti-HA epitope pAb <i>(for Biacore™ 4000)</i>	Rabbit	Thermo Fisher Scientific Inc., 3747 N Meridian Rd, Rockford, IL 61101, USA.
Anti-HA-649 Dylight™	Rabbit	Rockland Immunochemicals Inc., Gilbertsville, PA 19525, USA.

2.1.7 Commercially sourced proteins

Protein	Species	Cat.	Supplier
cTnI	Human	1210	Life Diagnostics Inc., P.O. Box 5205, West Chester, PA 19380, USA.
Protein G	Recombinant	P3296	Sigma-Aldrich Ireland Ltd., Vale Road, Arklow, Wicklow, Ireland.
Keyhole limpet Haemocyanin (KLH)	Animal derived	H7017	
NeutrAvidin	Deglycosylated avidin	31000	Pierce Protein Research Products, 3747 N Meridian Rd, Rockford IL 61101 , USA.
Bovine serum albumin (BSA)	Animal derived	BPE1600	Fisher Scientific Ireland, Blanchardstown Corporate Park 2, Ballycoolin, Dublin 15, Ireland.

2.1.8 Vectors

Vector	Resistance	Catalogue	Supplier
pET 26b(+)	Kanamycin	69862	Novagen, Merck KGaA, Darmstadt, Germany.
pET 28b(+)	Kanamycin	69865	
pET 32b(+)	Ampicillin	69016	
pComb3xSS	Ampicillin	N/A	Prof. C. Barbas III, The Scripps Institute, La Jolla, San Diego, California, USA.
pMopac16	Ampicillin	N/A	Andrew Hayhurst, University of Texas at Austin, Austin, TX 78712-1095, USA.
pUC57rTnI FABP-P1&2	Ampicillin	Custom	GenScript USA Inc. 860 Centennial Ave. Piscataway, NJ 08854, USA.

2.2 Licencing

All animal procedures were ethically approved and carried out in accordance with the Department of Health and Children licence number B100/3816 under the direction of trained animal handlers minimising animal distress. PJC has completed Laboratory Animal Science and Training program (LAST) qualifying to handle rodent and avian subjects. All animals were handled and treated humanely in the dedicated Bio-Resource Unit (BRU).

2.3 Methods

2.3.1 General molecular methods

2.3.1.1 *Ethanol precipitation of DNA*

Ethanol precipitation was carried out at -20°C overnight (O/N) or at -80°C for two hours depending on the time requirement. To the 1.5mL tube containing the DNA to be precipitated the following was added:

0.1X the volume of sodium acetate, pH5.2

2X the volume of 100% (v/v) molecular grade ethanol (ice-cold)

1µL glycogen (5mg/mL)

Tubes were agitated and placed at the relevant temperature for the desired length of time. The DNA was then pelleted by centrifugation at 14,000rpm for 30 minutes at 4°C, washed with 70% (v/v) ice-cold ethanol as above, air dried and resuspended in an appropriate volume of molecular grade water (mol. G. H₂O).

2.3.1.2 *Plasmid propagation and purification*

An overnight culture (10mL super broth (SB) supplemented with relevant antibiotic) was prepared from a single transformed colony, or glycerol stock, and incubated at 37°C, while shaking at 210rpm. This culture was then used to inoculate 100mL SB (with antibiotic) and grown overnight at 37°C, while shaking at 210rpm. Bacterial cells were collected by centrifugation at 4000rpm at 4°C for 30 minutes. The plasmid was then purified using NucleoBond® Xtra Midi, as per the manufacturer's guidelines. Purified plasmid was resuspended in a final volume of 250µL mol. G. H₂O and quantified on Nanodrop ND™ 1000 nucleic acid DNA-50 setting.

2.3.1.3 *Agarose electrophoresis*

Various percentage gels (w/v) were prepared by weighing out the desired amount to give the required percentage in grams of agarose. The weighed agarose was added to 1X Tris-acetate-EDTA (TAE) buffer and heated in a microwave (2-3 minutes) until dissolved, allowed to cool, before adding 1X SYBR™ safe DNA gel stain. The gel was then allowed to set in the appropriate gel box with the inserted comb. Gel electrophoresis was carried out using Bio-Rad PowerPac™ HC in 1X TAE-buffer at 90V for between 20 and 40 minutes.

2.3.1.4 *Ligation of DNA into a vector*

Ligations were carried out with a number of vector and inserts using the general ligation reaction conditions (Table 2.3-1). The weight of vector (X) and insert (Y) to obtain a 1:1 ratio was determined using Equation 2.3-1.

Equation 2.3-1: 1:1 molar ratio of vector and insert for ligation reactions

$$\frac{\text{Insert Size (kb)}}{\text{Vector Size (kb)}} \times \text{ng of vector} = \text{ng of insert in a 1:1 molar ratio}$$

The ligations were incubated overnight at room temperature (RT) followed by inactivation at 65°C for 20 minutes and precipitation as described in section 2.3.1.1. The ligations were resuspended in 10-20µL pre-heated mol. G. H₂O (~60°C) post precipitation.

Table 2.3-1: General ligation reaction components

Component	Ligation	Control
Vector DNA	Xµg	Xµg
Insert DNA	Yµg	-
Ligase Buffer (10X)	1X	1X
Mol. G. H ₂ O	to 100µL	to 100µL
T4 Ligase [400U/µL]	10U/µg	10U/µg

2.3.1.5 *Preparation of competent cells*

Electro-competent cells were prepared freshly when required so as to prevent losses in efficiency associated with storage. Prior to preparation cells were streaked onto selective agar and additionally assayed on Kanamycin and Carbenicillin plates to ensure no contamination due to rogue phage.

2.3.1.5.1 Electro-competent cell preparation

A single colony (*E. coli* XL1 Blue) was inoculated into 5ml of SB (5µg/mL tetracycline) and grown O/N at 37°C while shaking at 230rpm. Prior to carrying out any work all surfaces and equipment were bleached as thoroughly as possible. Sterile Pasteur pipettes, dH₂O (autoclaved), 10% (v/v) glycerol (autoclaved) and centrifuge tubes were placed on ice at 4°C O/N. 500mls of LB media with 0.01M MgCl₂ was inoculated with the 5mL O/N culture and grown at 37°C, while shaking at 230rpm until an OD₆₀₀ of 0.5 (max) was reached (in approx. 2-3 hours or so). The culture vessel was then placed on ice at 4°C for 30 minutes and swirling occasionally. The 500mL culture was divided into 10 x 50mL tubes and centrifuged at 3000rpm at 4°C for 20 minutes (Eppendorf 5810R). The supernatant was discarded and the pellets resuspended in 10mL of ice-cold water using a Pasteur pipette and combined into 2 pre-chilled 50mL tubes (100mL). The cultures were centrifuged as before and the volume of water used to resuspend the pellets halved (25mL/50mL tube). The cells were collected by centrifugation as before, the pellets resuspended in 2 x 10mL ice-cold water volumes and combined into one tube. After centrifugation the pellet was re-suspended in 10mL 10% (v/v) ice-cold glycerol. The cells were again collected by centrifugation and re-suspended in 5mL 10% (v/v) ice cold glycerol. The cells were centrifuged a final time and re-suspended in 1.5-2.0mL 10% (v/v) glycerol. The cells are then ready for electroporation.

2.3.1.5.2 Chemically-competent cell preparation

E. coli were treated for the preparation of electro-competent cells (as described section 2.3.1.5.1). However, all washes were carried out with 0.1M CaCl₂ in place of water and 0.1M CaCl₂ with 10% (v/v) glycerol. The cells were dispensed into 50μL aliquots and snap frozen using LN₂ and stored at -80°C.

For transformation, the cells were removed from -80°C storage and placed immediately on ice. The vector/ligation to be transformed was also placed on ice and once the cells had thawed 1μL of DNA was added to the cells and mixed with gentle agitation. The cells and DNA were allowed to stand for one minute before being placed at 42°C for 30 seconds. The tube was then put on ice for 2 minutes and 150μL pre-warmed super optimal broth (SOC) added. The cells were allowed to outgrow for 1 hour at 37°C, while shaking at 230rpm before both 10μL and 100μL volumes were plated out on LB-selective agar (the antibiotic included was dependent on the vector used) and grown O/N, while inverted, at 37°C.

2.3.1.6 *Preparation of bacterial cell stocks*

Cell stocks were prepared in either 1.5mL tubes or 96-well culture plates dependent on the numbers required.

1.5mL tubes: overnight cultures (2mL SB with relevant antibiotic and 1% (v/v) glucose) were grown at 37°C while shaking at 230rpm and the cells were then collected by centrifugation at 4,000rpm at 4°C for 20 minutes. The supernatant was then discarded and the cells re-suspended in SB media containing 10% (v/v) glycerol and 100μL transferred to a number of 1.5mL (screw thread) tubes which were snap frozen in LN₂. Cells were then stored long term at -80°C.

96 well plates: overnight cultures (150μL SB with relevant antibiotic and 1% (v/v) glycerol) were grown at 37°C while shaking at 230rpm. The following day 25μL was removed for expression in 96-deep well plates and replaced with 25μL 80% (v/v) glycerol and placed at -80°C for long term storage.

2.3.1.7 *Lysis of *E. coli* cells for small-scale analysis and purification*

Cells were lysed by a combined Bug Buster™, lysozyme and freeze-thaw treatment regime. The cell pellet was resuspended with 1/10 the culture volume (small-scale) or 2.5mL per 1g cell paste (large-scale) phosphate buffered saline (PBS) and transferred to the relevant number of 2mL tubes (0.75mL/tube). A volume of 0.75mL of 1X Bug Buster™ with 1mg/mL of lysozyme was then added to each tube and the tubes placed on the platform rocker for 20 minutes at room temperature (RT). Post incubation the cells were alternated from -80°C to 37°C for a minimum of three times. Cellular debris was collected by centrifugation at 14,000rpm at 4°C for 30 minutes and the supernatant separated. The supernatant could then be used for sodium dodecyl sulphate polyacrylamide gel electrophoresis (SDS-PAGE) by addition of 10µL 4X dye/30µL lysate or the insoluble matter tested by resuspension in 4X SDS-PAGE loading dye. To enable purification of soluble protein the lysates were pooled together and the volume brought to ~50mL with the relevant equilibration buffer (50mL buffer /400mL large-scale induced culture).

2.3.1.8 *Optimisation of recombinant protein expression*

Optimisation of the expression of various recombinant proteins was undertaken at numerous stages throughout this work. Various lengths of induction time and Isopropyl-β-D-thiogalactoside (IPTG) concentrations were evaluated with a number of different constructs, media types and temperatures. All these expression studies can be described by the generic flow contained in Figure 2.3-1 with refinements or modifications to the protocol noted in the relevant sections. The samples taken were centrifuged and the pellet retained at -80°C until required. The cell pellets were treated similarly during lysis and loading onto SDS-PAGE gels for side-by-side comparison with an un-induced cell control (0mM IPTG).

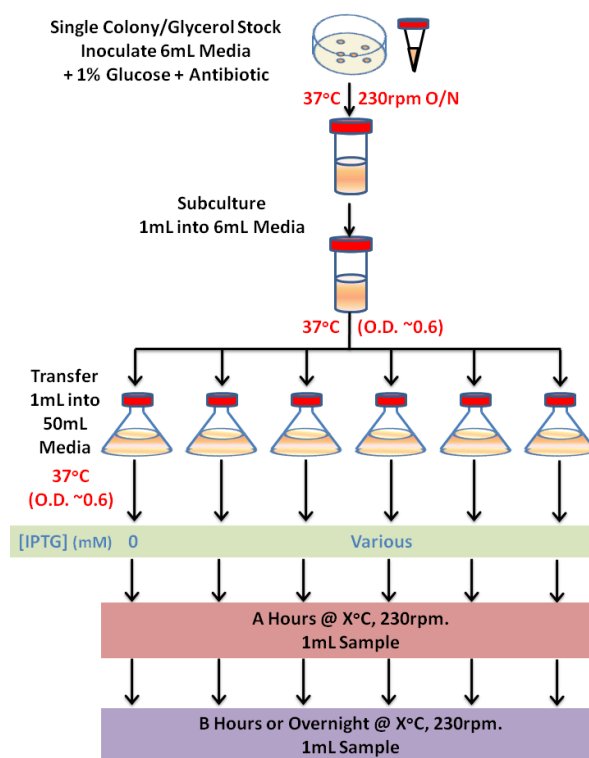


Figure 2.3-1: Generic time course experiment for expression of recombinant proteins

A single colony or glycerol stock was inoculated in 6mL of medium containing antibiotic and 1% (v/v) glucose and grown O/N at 37°C, while shaking at 230rpm. It was then sub-cultured into fresh media containing antibiotic only and grown until an OD₆₀₀ ~0.6 was reached. This starter culture was then employed to inoculate 50mL of media (with antibiotics) into a 250mL flask which was subsequently grown until the OD₆₀₀ reached ~ 0.6. At this stage the cultures were induced with various concentrations of IPTG at a defined temperature (X) and 1mL samples taken at two time points (A and B).

2.3.1.9 Purification of produced recombinant proteins

Numerous purification strategies were undertaken for the recombinant proteins generated. The cells were grown and expressed as described in the relevant section and lysed, as described in 2.3.1.7. The choice of buffers also varied and specific buffers for particular purifications are contained within the relevant section. The buffer recipes for recombinant protein purification can be found in section 2.1.4.6.2.

His• Bind® Ni²⁺ charged resin (Novagen) slurry (1-2mL) was added to a 10mL chromatography column and allowed to settle, corresponding to a 0.5-1mL resin bed. The resin was washed thoroughly with 10-15 column volumes (CV) equilibration buffer. The

lysate volume was adjusted to ~50mL with equilibration buffer (while 30µL sample was taken and retained for analysis – unfiltered lysate) and was then passed through 0.45µm and 0.20µm syringe filters (a 30µL sample was taken and retained for analysis – filtered lysate). The cleared lysate was then applied to the column and a sample of the ‘flow-through’ was retained for SDS-PAGE and Western blotting (WB) analysis. The column was then washed with 10CV wash buffer (or combination of wash buffers depending on the buffer table) and samples retained for analysis (W1 up to W3). The retained protein was then eluted with 4mL elution buffer into 1mL neutralisation buffer or 10 x 150µL neutralisation buffer in 1.5mL tubes. The 5mL eluted sample, or protein-containing samples, were then buffer exchanged against PBS (with 0.02% (w/v) NaN₃) using a Vivaspin 6 column with an appropriate molecular weight cut-off. The protein content of the purified sample was determined and the protein stored at -20°C in several aliquots. A sample of the pure protein, unfiltered and filtered lysates, ‘flow-through’ and washes were then analysed by SDS-PAGE and WB.

2.3.1.10 *Preparation of helper-phage*

A 5mL overnight culture (SB + 5µg/mL tetracycline) was prepared and grown at 37°C while shaking at 230rpm. The following day the culture was subcultured into 10mL SB containing 5µg/mL tetracycline and grown for 2 hours. The cells were then infected with 10µL VCSM13 (1x10¹¹ pfu/mL – Stratagene) and grown for 2 hours at 37°C with shaking at 230rpm. The phage-infected culture was then transferred to a 2L baffled flask containing 400mL SB (70µg/mL Kanamycin) and shaking continued at 37°C O/N. The culture was decanted into two 250mL centrifuge bottles and centrifuged at 4000rpm at 4°C for 15 minutes. The ‘phage-rich’ supernatant was collected and pasteurised (70°C for 20 minutes) followed by clarification by centrifugation at 4000rpm at 4°C for 15 minutes. The phage was ready to use or was precipitated (by addition 4% (w/v) PEG₈₀₀₀ and 3% (w/v) NaCl) on ice for 1 hour followed by centrifugation at 10,000rpm for 20 minutes at 4°C. The pelleted phage was then resuspended in 1% (w/v) PBS-BSA with 0.02% (w/v) NaN₃ and stored at -80°C until required.

2.3.1.11 SDS-PAGE

Assessment of the commercial antigen quality and protein purifications steps were carried out by SDS-PAGE and Western blot (WB) analysis using the buffers described in section 2.1.4.5.

Proteins were separated using 12.5% (w/v) SDS-PAGE gels to analyse purity and to determine the apparent molecular weight. The gel consisted of a resolving gel (12.5%) and a stacking gel (4.5%). The resolving and stacking gels were prepared as described in section 2.1.4.5. These gels were left to polymerise between two clean glass plates. After the stacking gel was poured, a comb was inserted to make wells in preparation for loading of the protein samples. The samples were prepared by adding appropriate volumes of 4X gel loading buffer and deionised water. A 20µg quantity of each protein sample in a total volume of 10µL or lysate diluted with loading buffer to 1X in a volume of 10µL, were added into each well. The gels were placed in an electrophoresis apparatus (Bio-Rad) and submerged in electrophoresis buffer. The apparatus was attached to a power supply and a voltage of 150V was applied to the gel for 15 minutes followed by 200V for 45 minutes. The gels were allowed to run until the tracker dye had reached the bottom of the gel, taking approximately 1 hour. The gels were then removed and stained using Coomassie stain for 20-60 minutes before destaining using Coomassie destain. The destain solution was changed 2-3 times (until the background non-specific staining was removed).

2.3.1.12 Western blotting

Where a Western blot was required the SDS-PAGE gels were setup and run as described in section 2.3.1.11 with one SDS-PAGE gel being placed in transfer buffer (section 2.1.4.5) in place of the Coomassie blue stain. The gel, absorbent paper and nitrocellulose (cut to the gel dimensions) were all placed in the transfer buffer for 10 minutes.

A four layer sandwich consisting of filter paper, nitrocellulose membrane, SDS-PAGE gel and filter paper was assembled. All air bubbles were removed by carefully rolling each of the layers with a disposable plate spreader. Proteins were transferred from the acrylamide

gel to the nitrocellulose using a Trans-Blot[®] Semi-Dry Transfer cell (Bio-Rad) at 15V for 21 minutes. The nitrocellulose membrane was then carefully transferred into a large weighing boat containing 20mL of 5% (w/v) PBS milk (PBSM) solution and blocked for 2 hours at room temperature or at 4°C overnight with agitation. Any excess blocking solution was removed from the membrane via two washes with PBS. Next, the blocked membrane was incubated with 10mL of 1% (w/v) PBSM solution with 0.05% (v/v) tween20 (PBSTM) containing a 1 in 2,000 dilution of the relevant primary antibody for 1 hour at RT with gentle agitation. The antibody solution was then discarded and the membrane washed in PBST (x3) and PBS (x3). Next, a 1 in 2,000 dilution of a specific secondary antibody was prepared in 10mL of 1% (w/v) PBSTM and again incubated with the membrane at RT for 1 hour with agitation. The antibody solution was then discarded and the membrane washed in PBST (x3) and PBS (x3). Development of the specific complex was achieved via the addition of liquid 3, 3', 5, 5'-tetramethylbenzidine (TMB) substrate and stopped by multiple washes with distilled water.

2.3.2 Cardiac Troponin I antigen

2.3.2.1 *Quality of commercially sourced antigen*

Assessment of the commercial antigen quality was carried out by SDS-PAGE and WB using the buffers as described in section 2.1.4.5, while applying the methodology described in sections 2.3.1.11 and 2.3.1.12. The blot was probed with anti-epitope-1 (19C7), anti-epitope-2 (228) and anti-epitope-3 HRP-labelled (16A11) antibodies from Hytest, all diluted 1 in 2,000 in 1% (w/v) PBSTM. The primary antibodies, with the exception of anti-epitope-3 HRP-labelled, were detected using an anti-mouse-Fc-specific HRP-labelled secondary antibody, diluted as above.

2.3.2.2 *Evaluation of protein-based immunisation regimes*

The serum from a previously immunised chicken was evaluated for epitope-specificity by direct binding enzyme-linked immunosorbent assay (ELISA). The chicken was sensitised to the whole cardiac troponin I molecule. cTnI (0.5µg/mL), neutrAvidin (2.5µg/mL), KLH-peptide-1 (0.5µg/mL) and KLH-peptide-2 (0.5µg/mL) in PBS were coated to a series of wells of an ELISA plate O/N at 4°C. The plate was then blocked with 5% (w/v) PBSM for 1 hour at 37°C. Peptide-1-CT, peptide-2-CT, peptide-1-NT and peptide-2-NT (all biotinylated C or N-terminal) at 1µM in 1% (w/v) PBSTM were applied to neutrAvidin-coated wells and incubated as above. The wells were washed with PBST (x3) and PBS (x3). The serum was diluted serially from 1 in 2,000 to 1 in 2 million in 1% (w/v) PBSTM and applied to the various antigen forms. The plate was incubated and washed, as above, followed by application of a 1 in 2,000 dilution of anti-chicken-Fc-specific HRP-labelled secondary antibody in 1% (w/v) PBSTM. After incubation and washing the plate was incubated with TMB and quenched with 10% (v/v) HCl before determining the absorbance at 450nm on the Tecan Sunrise™.

2.3.2.3 Recombinant Troponin I

2.3.2.3.1 Genetic manipulation of designed construct

The TnI gene construct (rTnI - Figure 8.1-2) was designed ‘in-house’, codon optimised for bacterial expression and commercially synthesised by Genscript (USA). The gene was obtained in pUC57 (Figure 8.1-6) and subsequently propagated in *dam⁻dcm⁻ E. coli*, as described in section 2.3.1.2. The plasmid was purified using the NucleoBond® Xtra Midi kit as per the manufacturer’s guidelines. The rTnI gene was isolated from the pUC57 vector by restriction digest and inserted into pET26b and pET32b to assess the ability to express in a soluble form, and purify the protein under non-denaturing conditions. In addition, the gene was also placed into the pET28b vector for expression in the cytoplasm of the cell which was anticipated to be in an aggregated form. Table 2.3-2 outlines the digestion reaction conditions to isolate the rTnI gene from pUC57 and for digestion of the three vectors. The reactions were carried out at 37°C for 3 hours followed by inactivation of the enzymes at 65°C for 30 minutes. The rTnI gene was then precipitated, as described in section 2.3.1.1 and the vectors further treated by Antarctic phosphatase (addition of 1X buffer and 1U/μg enzyme) for 1 hour at 37°C with inactivation at 65°C for 20 minutes. The vectors were also precipitated as outlined in section 2.3.1.1.

Table 2.3-2: components of the digestion reaction for rTnI and vectors

Component	pUC 57 rTnI	pET26b	pET32b	pET28b
Vector	10μg	10μg	10μg	10μg
Buffer 2 (10X)	1X	1X	1X	1X
Mol. G. H₂O	to 100μL	to 100μL	to 100μL	to 100μL
NcoI [20U/μL]	2U/μg	2U/μg	2U/μg	2U/μg
HindIII [20U/μL]	2U/μg	2U/μg	2U/μg	2U/μg

The precipitated, digested reactions were resolved on a 0.5% (w/v) agarose gel to excise and purify the vector backbones and rTnI gene using the NucleoTrap® Gel Extraction Kit as per the manufacturer’s instructions. The purified components were resuspended in ~30μL heated mol. G. H₂O. The components were then ligated using T4 ligase at a ratio of 1:1 vector to insert (section 2.3.1.4).

2.3.2.3.2 Expression of rTnI in *E. coli*

Each of the ligation reactions were transformed into BL21 (DE3) pLysS cells (Table 2.1-2) using the heat shock transformation protocol (section 2.3.1.5.2). Single colonies were obtained on selective agar (dependent on the vector, see section 2.1.8) and grown up in 2mL SB (with relevant antibiotic) O/N at 37°C with shaking at 230rpm. The cultures were then subcultured into SB (containing antibiotic) at 10mL scale for induction with 0.5mM IPTG or into auto-induction media (non-IPTG) for O/N induction. Post induction cells were lysed using Bug Buster™-lysozyme-freeze-thaw method (section 2.3.1.7) and analysed by 12.5% (w/v) SDS-PAGE and WB (sections 2.3.1.11 and 2.3.1.12). The Western blots were probed with anti-HIS HRP-labelled or anti-cTnI-specific antibodies all diluted 1 in 2,000 with 1% (w/v) PBSTM. Where necessary HRP-labelled secondary antibody diluted as above was utilised to detect bound primary antibodies.

2.3.2.3.3 Purification of rTnI

The purification of rTnI in its soluble form was carried out by immobilised metal affinity (IMAC) (results not shown) and cation exchange chromatography. Soluble protein was extracted from cultures (as described in section 2.3.1.7) and IMAC carried out using the buffers delineated in section 2.1.4.6.2, as described in section 2.3.1.9. Cation exchange chromatography was carried out using the AKTA Explorer FPLC (GE Healthcare) and a HiTrap SP column (GE Healthcare) where 2mL of lysate was injected onto the column at a flow rate of 0.5mL minute. The cation exchange buffers listed in section 2.1.4.6.2 were used and elution of bound protein was carried out in a stepwise gradient method, written using the Unicorn control and evaluation software (GE Healthcare).

2.3.2.4 *Fusion of epitopes 1 and 2 to fatty acid binding protein*

2.3.2.4.1 Genetic manipulation of designed construct

To overcome the issues encountered with use of many fusion partners and vector-cell combinations identified thus far, the epitope 1 and 2 region was expressed as a fusion to the DNA sequence encoding human fatty acid binding protein (Val²-Glu¹³² – see appendix Figure 8.1-1). The gene sequence of heart-type fatty acid binding protein (hFABP) was obtained and a serine-glycine linker plus the epitope regions added as a C-terminal fusion to the protein. This gene construct was designed and codon optimised followed by commercial synthesis in pET28b(+) by Genscript. The vector was then transformed into Tuner™ cells by heat shock transformation for identification of positively secreting clones (section 2.3.1.5.2).

2.3.2.4.2 Identification of FABP-P1&2 expressing clones

Three clones were assessed for expression of the protein construct by SDS-PAGE and WB as described in sections 2.3.1.11 and 2.3.1.12, in parallel to an equivalently treated Tuner™ cell control without plasmid (10mL scale, 0.2mM IPTG for 4 hours at 30°C). The clones were probed initially with anti-HIS HRP-labelled (1 in 2,000 in 1% (w/v) PBSTM) and a single clone (#2) carried forward for analysis with a range of secondary antibodies. For this the SDS-PAGE and subsequent WB were carried out on lanes with the same cell lysate sample. The nitrocellulose was blocked and then probed with a battery of specific antibodies; anti-FABP (scFv), 2B12 (scFv), Hytest 228, Hytest 19C7 HRP-labelled, 20B3 mAb and also anti-HIS HRP-labelled which were all diluted 1 in 2,000 in 1% (w/v) PBSTM. The scFv were detected with a 1 in 2,000 dilution of an anti-HA HRP-labelled secondary antibody and the mAbs with an anti-mouse-Fc-specific HRP-labelled secondary antibody. The blot was washed and developed as described in section 2.3.1.12.

2.3.2.4.3 Optimisation of expression of FABP-P1&2

To assess the impact of culture time and IPTG concentration a time course (2.5 hours and 5 hours) at 30°C with shaking at 230rpm was undertaken with a range of IPTG concentrations (0, 0.01, 0.02, 0.1, 0.2 and 0.5mM) as described in the generic expression optimisation method (section 2.3.1.8) and analysed by SDS-PAGE (section 2.3.1.11) and WB (section 2.3.1.12). For the WB the lysates were probed with an anti-HIS HRP-labelled secondary antibody at a 1 in 2,000 dilution in 1% (w/v) PBSTM.

2.3.2.4.4 Optimisation of the purification of FABP-P1&2

A 5mL O/N culture of FABP-P1&2 fusion protein clone#1 (SB with 50µg/mL Kanamycin and 1% (v/v) glucose) was used to inoculate a 400mL culture which was allowed to grow at 37°C shaking at 230rpm until an OD₆₀₀ of ~0.6 was reached. At this point the culture was induced with 0.2mM IPTG for 2.5 hours at 30°C. The culture was then decanted into 2 x 250mL tubes and centrifuged at 4,000rpm at 4°C for 40 minutes. The collected cell pellet was then lysed as described in section 2.3.1.7. Purification was undertaken using the PBS- and NaH₂PO₄-based buffers as outlined in section 2.1.4.6.2 and the generic purification methodology delineated in section 2.3.1.9. In this case the purification required significant optimisation of the washing strategies as is described in the results section.

2.3.2.4.5 Gel filtration of FABP-P1&2 on an AKTA Explorer FPLC

A S75 (16/60) HiLoad gel filtration column (GE Healthcare) was equilibrated with 1 column volume (CV) of 1XTBS (1CV = 120mL). A 2mL sample of FABP purified by IMAC (1.62mg/mL) applied at a flow rate of 1mL/minute. Fractions were collected after 0.3CV and until 1.2CV was reached. Protein was monitored online by A_{280nm} using the dedicated Unicorn control and evaluation software (GE Healthcare). Protein peaks were evaluated and significant protein-containing fractions concentrated to approximately 200µL (concentration 11mg/mL).

2.3.3 Monoclonal antibody generation

2.3.3.1 *Immunisation of Balb/c mice with synthetic epitope conjugate*

cTnI peptide-2-KLH immunisations (200µL) were administered *via* intraperitoneal (IP) injection. On day one, Balb/c mice were immunised with 50µg of the peptide-conjugate in 500µL PBS emulsified in a 1:1 ratio with 500µL Freund's complete adjuvant (FCA). The first boost was delivered 3 weeks later by administration of 25µg of peptide-conjugate, emulsified 1:1 in Freund's incomplete adjuvant (FICA). Subsequent boosts of 12.5µg were delivered in alternating 2 and 3 week intervals in the same manner as boost one until a sufficient titre was achieved. In preparation for the final boost, the animals were rested for 4 weeks prior to administration and were sacrificed 7 days post IP injection. The spleens (SP) of several mice were harvested for hybridoma production.

2.3.3.2 *Anti-serum titre analysis of immune response to epitope-2 of cTnI*

cTnI (1µg/mL) and neutrAvidin (2.5µg/mL) were prepared in PBS and 100µL applied to a series of wells in duplicate and placed at 4°C overnight (O/N) or alternatively at 37°C for 1 hour. Coated plates were then blocked with 5% (w/v) PBSM for 1 hour at 37°C. After washing with PBS (x2), 1µM peptide-1-CT and peptide-2-CT in 1% (w/v) PBSTM were applied to separate series of neutrAvidin-coated wells. The plate was incubated at 37°C for 1 hour and washed with PBST (x3) and PBS (x3). Serial dilutions of serum (tail vein bleed) were prepared in 1% (w/v) PBSTM ranging from 1 in 1,000 to 1 in 1million. The prepared dilutions were applied in duplicate (100µL) across the cTnI, peptide-1 and peptide-2-coated wells. The plate was incubated and washed, as described in the previous step and 100µL of a 1 in 2,000 dilution of anti-mouse-Fc-specific HRP-labelled secondary antibody applied to all wells. The plate was washed as before and developed with 100µL TMB for 10 minutes followed by quenching with 50µL 10% (v/v) HCl. The plate was then read in the Tecan sunrise™ plate reader at 450nm.

2.3.3.3 *Fusion of splenocytes and myeloma*

Note: all work was carried out in laminar flow hood employing aseptic technique. Media was prepared as described in section 2.1.4.1 and sterile filtered through a 0.2µm filter unit.

Immediately after harvesting the spleen was perforated in several locations using two 2.5mL syringe and needles loaded with DMEM w/o FCS in a Petri dish containing 10mL of the same medium. The two syringes of media were used in tandem to 'flush' out the lymphocytes from the spleen. The media was removed and placed in a 50mL tube and the procedure repeated. The spleen was then crushed using a syringe plunger and washed a final time. The collected splenocytes were then centrifuged at 2,000rpm at 4°C for 10 minutes followed by resuspension in 10mL of DMEM w/o FCS. In addition, from four T175 (at approximately 75-80% confluence) SP2/0-Ag14 myeloma cells were harvested and placed in 40mL DMEM w/o FCS. Both the splenocytes and the myeloma cells were pelleted by centrifugation at 2,000rpm at 4°C for 10 minutes and washed twice as described. After the final wash the cells were counted and viability determined by trypan blue exclusion (**SP2/0-Ag 14:** 2.32×10^7 and **Splenocytes:** 1.56×10^8 cells/mL). The splenocytes were mixed in a 6.5:1 ratio with the myeloma cells. The mixed cell population was then collected by centrifugation at 1,250rpm at 4°C for 10 minutes and washed with (DMEM w/o FCS). This was repeated twice after which the supernatant was removed and the pellet disrupted by gentle agitation. The cell tube was placed in ice-cold water (ice cubes were glass vials containing frozen water). 1.5mL 50% (w/v) PEG was added drop-wise over 1 minute with constant vigorous swirling in the ice cold water and continued to mix vigorously for an additional 90 seconds. The fused cell mix was then clasped tightly in the palm of the hand during which 4mL/minute DMEM w/o FCS was added to a volume of 20mL with constant swirling. The cell solution was then heated to 37°C in a water bath for 20 minutes and centrifuged at 2,000rpm for 10 minutes at 37°C. The pelleted, fused cell mix was then resuspended at 1.0×10^6 cell/mL in selection media (HAT) (approximately 179.2mL). About 0.15mL/well of the inner 60-wells of 20x96-well plates was propagated and the cells grown at 37°C with 5% (v/v) CO₂ un-stacked for 7 days without being disturbed.

2.3.3.4 Analysis of fused hybridoma progeny

Initial analysis of 1170 individual wells post fusion was carried out by a direct binding ELISA. Wells were visually examined and scored for the presence of growing hybridoma/cell clusters. Wells were also scored for the number of distinct colonies formed to identify single cell-derived hybridomas where possible.

2.3.3.4.1 Direct Binding ELISA

Cardiac troponin I (1µg/mL) was coated onto Nunc™ ELISA plates (100µL/well) in PBS for 1 hour at 37°C (or alternatively overnight at 4°C). The solution was ejected from the plate and free sites blocked using 5% (w/v) PBSM as above and washed with PBST (x 1) and PBS (x 1). Crude supernatants were diluted 1 in 2 with 1% (w/v) PBSTM and 100µL applied to each well. After incubation the plates were washed with PBST (x3) and PBS (x3) using a plate washer. Bound secreted IgG was detected using an anti-mouse-Fc-specific-AP-labelled antibody (1 in 2,000 dilution in 1% (w/v) PBSTM). Secondary antibody was removed by washing (as described in the previous step) and colour development achieved using p-nitro phenyl phosphate (p-NPP) (12 minutes development time) as a substrate. Absorbance was then read using a Tecan Sapphire™ spectrometer at 405nm.

2.3.3.4.2 Epitope-specificity mapping on Biacore™ 4000

Subsequent to identification of positive clones by direct binding ELISA, epitope-specificity was confirmed on a Biacore™ 4000 (at the time called the A100). A chip surface was prepared by activation of the surface with 1:1 mix of 100mM *N*-hydroxysuccinimide (NHS) and 400mM *N*-ethyl-*N*-(dimethyl-aminopropyl) carbodiimide hydrochloride (EDC) for 10 minutes at a flow rate of 10µL/minute. NeutrAvidin in NaOAc pH4.2 (15µg/mL) was immobilised using amine-coupling chemistry with a flow rate 10µL/minute and a contact time of 10 minutes followed by capping with 1mM ethanolamine-HCl, pH 8.5 and cleaning

of the surface with desorb solution 1 and 2 (GE Healthcare). Individual spots within each of the four flow cells were addressed with an excess of biotinylated peptides (1, 2, 3 and 4) using the hydrodynamic addressing power of the instrument. Peptide concentrations were adjusted to 10 μ M in 10mM NaOAc, buffer line A placed in water, buffer line B was placed in 10mM NaOAc, pH 4.2 and buffer lines 1-4 in HBS-EP⁺ facilitating addressing of the spots. The hybridoma supernatants were diluted 1 in 5 with running buffer (HBS-EP⁺) and placed in 96-well plates. Analysis was carried out by injection of the diluted supernatants at 30 μ L/minute and monitoring the dissociation of the antibodies for 15 minutes post injection stop. Binding responses were evaluated using the dedicated BiaEvaluation software and antibody-secreting clones ranked by their binding levels and stability early versus stability late.

2.3.3.4.3 Competitive ELISA for hybridoma ranking

Two ELISA plates were coated with 0.5 μ g/mL cTnI in PBS at 4°C O/N. The plates were blocked with 5% (w/v) PBSM at 37°C for 1 hour. Supernatants for 24 clones were diluted 1 in 2 with 1% (w/v) PBSTM (1 in 2 A0) and also with 10 μ M peptide-2 in 1% (w/v) PBSTM (1 in 2 competition). The supernatants were also diluted 1 in 5 with 1% (w/v) PBSTM before dilution (1 in 2) with 1% (w/v) PBSTM (1 in 10 A0) and with 10 μ M peptide-2 in 1% (w/v) PBSTM (1 in 10 competition). The mixed dilutions were applied to the cTnI-coated wells and incubated for 1 hour at 37°C followed by washing with PBST (x3) and PBS (x3). A 1 in 2,000 dilution (1% (w/v) PBSTM) of anti-mouse-Fc HRP-labelled secondary antibody was then applied to the wells, incubated and washed as described in the previous step. The plate was developed with TMB and quenched with 10% (v/v) HCl before reading absorbance at 450nm on the Tecan SunriseTM.

2.3.3.4.4 Capture ranking of hybridoma supernatants on Biacore™ 3000

The surface was activated initially by mixing equal volumes of 400mM EDC and 100mM NHS and passing the mixture over the sensor surface for 10 minutes at a flow rate of 5µL/minute. A donkey anti-murine-IgG-Fc-specific antibody (Gallus Immunotech) was immobilised (50µg/mL in 10mM NaOAc, pH 4.2) onto the surface of a CM5 dextran chip (research grade) (FC: 4) at a flow rate of 5µL/minute for 20 minutes. The surface was then capped with 1M ethanolamine HCl, pH 8.5 for 10 minutes. The surface was further cleaned with two 30 second injections (30µL/minute flow rate) of 20mM NaOH removing any unbound or extraneous material. Conditioned media from the hybridomas was diluted 1 in 10 in running buffer (1X HBS-EP⁺) and a custom program written on Biacore™ 3000 was used to analyse the secreted antibodies. The IgG from the various supernatants was captured (flow rate: 10µL/min) and 30nM cTnI (flow rate: 30µL/min) passed over the captured monoclonal surface (FC: 4) and FC: 3 to act as a surface online reference. Reference subtracted sensorgrams were collected and the surface regenerated with a 30 second pulse of 10mM H₃PO₄ (optimised regeneration conditions).

2.3.3.4.5 Sandwich ELISA for cTnI

To perform the sandwich ELISA undiluted supernatant or purified mAb (typically 2-5g/mL) were coated onto the wells of an ELISA plate at 4°C O/N. The plate was blocked with 5% (w/v) PBSTM for 1 hour at 37°C and washed with PBST (x2). cTnI of various concentrations (a; for the analysis of crude supernatants; 1, 0.5, 0.25, 0.0025 and 0µ/mL and b; for purified mAb analysis; serial 1 in 3 dilution from 2000 to 0.3ng/mL) were applied to the wells, incubated at 37°C for 1 hour and washed with PBST (x3) and PBS (x3). MAb 16A11 (anti-peptide-3 HRP-labelled) was diluted 1 in 2,000 in 1% (w/v) PBTM and applied across the plate. After incubation and washing as above, the plate was developed with TMB and quenched with 10% (v/v) HCl. The absorbance was read at 450nm on the Tecan Sunrise™.

2.3.3.4.6 Isotyping of monoclonal antibody in crude supernatant

Isotype determination was carried out using the Pierce™ Rapid Isotyping kit (catalogue # 26179) on freshly diluted supernatant as directed by the manufacturer's guidelines. The presence of control and test lines indicated a valid test.

2.3.3.5 *Scale-up and cloning by limiting dilution of screened progeny*

Scale-up was carried out daily as required dependent on the specific growth rate of the individual clones. From a 96-well format at fusion, the cells were scaled up sequentially as illustrated in Figure 2.3-2 and cloned out by limiting dilution a total of three times to ensure monoclonality. Wells selected for continued expansion were identified by analysis and the cells resuspended in fresh hypoxanthine-aminopterin-thymidine (HAT) media (first scale-up procedure) or hypoxanthine-thymidine (HT) media (second and subsequent scale-up procedures). Cells were then transferred into the appropriate volume of medium for the scale (Figure 2.3-2) and placed at 37°C with 5% (v/v) CO₂ until nearing confluence. Once the cells were expanded to T75 scale, selected specific antibody-secreting hybrids were cloned by limiting dilution. Using the spent media, the cell monolayer was washed from the surface of the flask by pipetting and gentle tapping. The pooled cells were enumerated by Trypan blue dye exclusion (section 2.3.3.6.2). Individual clones were then seeded out at three cell densities (0.1, 1 and 10 cell/mL) in fresh 150µL HAT/HT media in a 96-well plate format and incubated for 7 days at 37°C with 5% (v/v) CO₂. Single hybridoma-containing wells were identified from the plates and expanded up to T75 flask scale with ongoing performance checking.

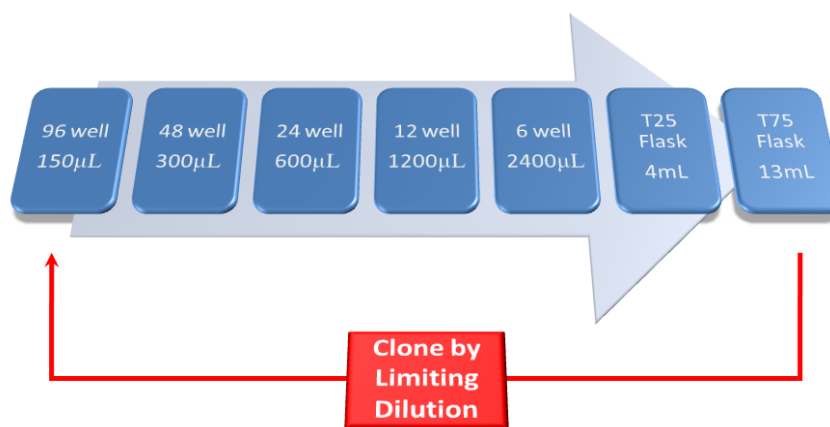


Figure 2.3-2: Flow diagram of scale-up and cloning by limiting dilution of generated hybridomas

Illustration of scale-up process indicating culture volumes used. Clones were serially expanded from 96-well master plates through to T75 flasks. At the flask-stage specific antibody-secreting hybrids were cloned by limiting dilution. Positives were re-confirmed and scaled up through the process again. This cloning by limiting dilution process was carried out three times to ensure monoclonality.

2.3.3.6 *General mammalian cell culture methods*

All methods involving the use of mammalian cells were carried out aseptically in a Laminar flow hood. Cells were grown at 37°C with 5% (v/v) CO₂ in a humidified atmosphere. Adequate precautions and sufficient care were taken to ensure prevention of contamination of the cultures and media. The media was prepared using the components listed in section 2.1.4.1, sterile filtered (0.2µm) and stored at 4°C for one month. Mycoplasma testing was carried out on all cell lines, purchased or acquired, not certified as ‘mycoplasma-free’ prior and, routinely, on all the cell lines held.

2.3.3.6.1 Recovery of frozen mammalian cells

Cells were recovered from LN₂ storage by rapid thawing at 37°C (clasped in the palm of the hand) and transferring to a flask (generally T75) containing 30mL of relevant media (dependent on cell line) and incubated at 37°C with 5% (v/v) CO₂.

2.3.3.6.2 Mammalian cell counting and viability determination by trypan blue exclusion

Cell counts were performed routinely to assess seeding densities and cell viability. The counts were carried out using an improved Neubauer counting chamber. An aliquot of resuspended cells (50 μ L) was diluted 1:5 with fresh media in an eppendorf tube. This 1 in 5 dilution was further diluted 1:1 with 0.25% (w/v) Trypan blue solution for no longer than 5-10 minutes. The cells were applied to the counter chamber beneath the cover-slip. Viable cells remained uncoloured due to their intact cell membranes. The dye is able to traverse the cell membrane in non-viable cells which are stained blue. The count was performed under phase contrast on an inverted microscope (Leica DMIL) at 40X magnification.

2.3.3.6.3 Storage of mammalian cell lines

Cells were harvested from 90% confluent flasks (T75/T175) by flushing from the surface with an aliquot (~5mL) of the conditioned culture media. The resuspended cells were counted (section 2.3.3.6.2) and recovered by centrifugation at 3000rpm at 4°C for 10 minutes. The cells were resuspended in fresh media (DMEM with 50% (v/v) FCS) to give a cell density of 2×10^6 cells/mL and this was mixed 1:1 with cryoperservative media (DMEM with 50% (v/v) FCS and 8% (v/v) DMSO) to give a final cell density of 1×10^6 cell/mL in DMEM supplemented with 50% (v/v) FCS and 4% (v/v) DMSO. The cells were distributed into 1mL aliquots in screw-threaded cryovials and placed in a Mr. Frosty freezing container (filled with pre-chilled isopropanol) at -80°C for 12 hours. The vials were then transferred to the liquid phase of LN₂.

2.3.3.7 Purification of anti-epitope-2 monoclonal antibody

2.3.3.7.1 Protein G purification of 20B3 monoclonal antibody

Protein G sepharose™ fast flow was resuspended in 1mL of 20% (v/v) EtOH in mol. G. H₂O and allowed to settle in a 10mL column. The buffers required were prepared as described in section 2.1.4.6.1. The resin was then washed with 25mL of equilibration buffer. Supernatant collected from T175 flasks over a number of days was concentrated from approximately 500mL to 5mL with an Amicon® stir cell system (GE Healthcare) with a molecular weight cut-off membrane (100kDa). The concentrated supernatant was diluted to 10mL with equilibration buffer before application to the column (a 150µL sample of the ‘flow-through’ was taken for analysis). The column was washed twice with 15CV wash buffer (wash 1 and 2). The retained protein was then eluted from the column with 10mL elution buffer collecting 850µL in 1.5mL tubes containing 150µL neutralisation buffer. The fractions containing significant amounts of protein were identified using the ND-1000™ and then desalted using a PD-10 column (GE Healthcare). The PD-10 was equilibrated with 25mL PBS and a maximum of 3mL of eluted protein applied to the column. The ‘flow-through’ was discarded and the retained protein eluted with 3.5mL PBS in 350µL fractions. The desalted protein fractions were quantified using the ND-1000™ and concentrated using a Vivaspinn 6 (10kDa cut-off). The final protein determination was carried out using the ND-1000™.

2.3.3.7.2 Size exclusion chromatography-HPLC analysis of monoclonal antibody, 20B3

Size exclusion chromatography was carried out on a Shimadzu HPLC at 20°C.

Column: Phenomenex BioSep-SEC-S200 (300 x 7.80mm)

System: LC20AB (pump), CT02AC (oven), CBM20A (control), SIL20A (auto sampler) and SPD20A (UV detector).

Three dilutions of mAb were prepared to generate a strong UV_{280nm} peak. Monoclonal antibody 20B3 was adjusted to 0.125, 5 and 495 μ g/mL in PBS corresponding to total protein quantities of 6.25ng, 0.5 and 24.75 μ g being applied to the column (50 μ L injection volume, 0.5mL/min flow rate). The resulting chromatograms were analysed using the LC solution software package.

2.3.3.8 *Kinetic analysis of monoclonal antibody on Biacore™ 3000*

20B3 (50 μ g/mL in 10mM NaOAc buffer) was pre-concentrated onto the dextran surface over a range of pH values to determine the optimal pH to promote efficient immobilisation. The pH of the buffer was adjusted with 10% (v/v) acetic acid to pH values 3.8, 4.0, 4.2, 4.4, 4.6 and 4.8. 10 μ L (50 μ g/mL) of the protein at the respective pH was passed over an unmodified carboxymethylated dextran chip at a flow rate of 10 μ L/minute. The pH demonstrating the highest response unit (RU) level, hence greatest pre-concentration, was employed as the carrier buffer for immobilisation. A surface of 20B3 mAb was then created using the immobilisation chemistry and parameters, outlined in section 2.3.3.4.4, resulting in a surface of approximately 5000RU. Kinetic analysis was carried out with serial cTnI concentrations prepared in HBS-EP⁺ at a flow rate of 30 μ L/minute to minimise mass transfer limitations.

2.3.4 Recombinant antibody generation

2.3.4.1 Immunisation of chickens

Chicken Designation: Y20.03.09

cTnI peptide-1-KLH immunisations were administered via 1mL subcutaneous injections. On day one, the chickens (adult Leghorn) were immunised with 100µg of the relevant peptide-conjugate in 550µL PBS emulsified in a 1:1 ratio with 550µL Freund's complete adjuvant (FCA). The first boost was delivered 3 weeks later by administration of 75µg of peptide-conjugate, emulsified 1:1 in Freund's incomplete adjuvant (FICA). Subsequent boosts of 50µg were delivered in alternating 2 and 3 week intervals in the same manner as boost one until a sufficient titre was achieved. In preparation for the final boost, the animal was rested for 4 weeks prior to administration and was sacrificed by lethal injection (*pentobarbital*) and cervical dislocation 7 days post subcutaneous injection. Both bone marrow (BM) and spleen (SP) were harvested for library building.

2.3.4.2 Extraction of RNA and cDNA synthesis from chicken

Total RNA was recovered from BM and SP of the immunised chicken (Y20.03.09) by chloroform-based extraction carried out immediately after sacrifice. All reagents used are molecular grade and all materials treated with RNaseTM Zap where possible.

All surfaces of the laminar flow unit were decontaminated with 70% (v/v) isopropyl alcohol (IPA) and RNaseTM ZAP. SP and BM (x 2 thigh/hip) were processed separately. The spleen was placed in 50mL RNase-free tube immediately containing 10mL ice-cold Trizol. The bone marrow was first extracted by cutting away the joint knuckles at either end of the bone and flushing out as much marrow as possible using a syringe and needle loaded with 10mL Trizol reagent. Both BM and SP were homogenised using a homogeniser probe (previously precepted, RNaseTM Zap washed, rinsed, autoclaved and dried) at 50% output for 1 minute followed by 100% output for 20 seconds. 20mL of Trizol was added to both tubes and allowed to stand at room temperature (RT) for 5 minutes followed by centrifugation at 3,530rpm at 4°C for 20 minutes. The supernatant was carefully transferred

to a 50mL polypropylene tube and 6mL chloroform was added. The tube was shaken vigorously for 15 seconds and left to rest for 15 minutes at RT. After centrifugation at 12,000rpm at 4°C for 25 minutes the upper aqueous layer was carefully pipetted away into a 50mL polycarbonate tube (note: a residual layer was left to ensure no protein contamination) to which 15mL isopropanol was added and mixed vigorously for 15 seconds. After standing at RT for 15 minutes the tube was centrifuged at 12,000rpm at 4°C for 25 minutes and the supernatant removed from the opaque pellet. The pellet was washed twice with 30mL ice-cold 70% (v/v) EtOH at 12,000rpm at 4°C for 20 minutes and air-dried for 2 minutes. Both the BM and SP pellets were resuspended in 500µL mol. G. H₂O and quantified on Nanodrop ND 1000™ using nucleic acid RNA-40 setting. A sufficient aliquot was retained for cDNA synthesis and the remainder was precipitated, as described in section 2.3.1.1 for storage at -80°C in several aliquots.

From the total RNA extracted, mRNA was oligo dT primed for cDNA synthesis which was carried using Superscript III® reverse transcriptase kit as per manufacturer's guidelines. The cDNA was stored in 10µL aliquots at -80°C post 1st strand synthesis.

2.3.4.3 *pComb3xSS vector preparation*

The pComb3 vector series was kindly provided by Carlos Barbas III (Scripps Institute, La Jolla, California) under an academic material transfer agreement (MTA). The pComb3xSS vector was transformed into competent dam⁻/dcm⁻ *E. coli* for initial propagation and maintenance. An overnight culture (10mL SB supplemented with 12µg/mL tetracycline) was prepared from a single transformed colony and incubated at 37°C shaking at 230rpm. This overnight culture was then used to inoculate 100mL SB (12µg/mL tetracycline) and grown O/N at 37°C shaking at 230rpm. Bacteria were collected by centrifugation at 4000rpm at 4°C for 30 minutes and the plasmid purified using NucleoBond® Xtra Midi as per the manufacturer's guidelines. Purified plasmid was resuspended in a final volume of 250µL mol. G. H₂O and quantified on Nanodrop ND™ 1000 nucleic acid DNA-50 setting.

Purified vector (section 2.3.4.3) was initially verified using the digestion setup outlined in Table 2.3-3 and the digested products visualised for verification on a 0.5% (w/v) agarose gel (section 2.3.1.1).

Table 2.3-3: pComb3xSS vector digestion components

Component	SacI Digest	SfiI Digest
Vector	1µg	1µg
Buffer 4 (10X)	1X	1X
BSA (100X)	1X	1X
Mol. G. H₂O	to 50µL	to 50µL
SacI [20U/µL]	2U/µg	-
SfiI [20U/µL]	-	2U/µg
Total Volume	50µL	50uL
Temperature	37°C	50°C
Time	3 hours	3 hours

2.3.4.4 *Antibody (scFv) library construction*

Antibody construction was carried out as described by Andris-Widhopf and co-workers [88, 89]. The initial steps involved in generating the library require the amplification of the antibody variable domains from the synthesised cDNA isolated from both the spleen (SP) and the bone marrow (BM) of the chicken (Y20.03.09). The primers used for library building are those published in Chapter 9 of Phage Display: a laboratory manual and host-specific sub chapters [89]. All primers used were those to clone antibody fragments into the pComb3x vector series. The list of primers used to construct avian scFv fragments from immune libraries introducing the long linker (GGSSRSSSSGGGGSGGGG) between the variable heavy and light chains is shown in Table 2.3-4 [88, 89]. All primers were commercially synthesised by Integrated DNA Technologies (Interleuvenlaan 12A B-3001 Leuven, Belgium). The only exceptions were the sequence primer pair that were synthesised on demand by Source BioScience DNA Sequencing (Translational Research Lab - Room 1.18, Central Pathology Laboratory, St James's Hospital, Dublin 8. Ireland).

Table 2.3-4: Avian scFv library PCR primer list

Primer Name	Sequence 5' - 3'
<u><i>Variable H</i></u>	
CSCVHo-FL	GGT CAG TCC TCT AGA TCT TCC GGC GGT GGT GGC AGC TCC GGT GGT GGC GGT TCC GCC GTG ACG TTG GAC GAG
CSCG-B	CTG GCC GGC CTG GCC ACT AGT GGA GGA GAC GAT GAC TTC GGT CC
<u><i>Variable λ</i></u>	
CSCVK	GTG GCC CAG GCG GCC CTG ACT CAG CCG TCC TCG GTG TC
CKJo-B	GGA AGA TCT AGA GGA CTG ACC TAG GAC GGT CAG G
<u><i>SOE Overlap</i></u>	
CSC-F	GAG GAG GAG GAG GAG GAG GTG GCC CAG GCG GCC CTG ACT CAG
CSC-B	GAG GAG GAG GAG GAG GAG GAG CTG GCC GGC CTG GCC ACT AGT GGA GG
<u><i>Sequence Primers</i></u>	
Ompseq	AAG ACA GCT ATC GCG ATT GCA G
gBack	GCC CCC TTA TTA GCG TTT GCC ATC

2.3.4.4.1 Variable domain amplification

The first round of PCR involved separate amplification of variable heavy and light chains. Initially, the MgCl_2 concentration for the reactions was optimised to ensure high-yield specific-bands by titration in the concentration range as indicated in Table 2.3-5 followed by large-scale synthesis (15X) at the optimised 2.0mM MgCl_2 for both V_L and V_H .

Table 2.3-5: Amplification of avian variable domains from cDNA

Component	Optimisation Reaction (1X)	Large-Scale Reaction (1X)
Go Taq Buffer (10X)	1X	1X
MgCl_2 [25mM]	1.5/2.0/3.4/4.0mM	2.0mM
Mol. Grade H_2O	to final volume of 50 μL	to final volume of 50 μL
dNTP [100mM]	0.1mM	0.1mM
Forward Primer [60nMol]	30pM	30pM
Reverse Primer [60nMol]	30pM	30pM
cDNA	1 μL	μL
Polymerase [5U/ μL]	1.25U	1.25U

The PCRs were carried out under the following cycling parameters in the G-Storm thermocycler.

Table 2.3-6: Variable domain amplification PCR cycle parameters

Stage	Step	Temperature (°C)	Times (s)	# Cycles
1	Initial Denature	94°C	120	1
2	Denaturation	94°C	15	30
	Annealing	56°C	30	
	Extension	72°C	60	
3	Final Extension	72°C	600	1

Large-scale variable PCR products were resolved on 1.5% agarose gel (section 2.3.1.3). Strong bands at 350bp (LC) and 450bp (HC) were excised and purified using NucleoTrap® gel extraction kit according to the manufacturer's guidelines. Purified products were quantified using Nanodrop ND 1000™ using DNA-50 setting. Note: All PCR products were eluted from the column in washes of 20µL then followed by an additional 10µL of preheated (~70°C) molecular grade water.

2.3.4.4.2 Splice-by-overlap extension (SOE) PCR

The second round of PCR 'stitched' together the variable domains into a single scFv construct in the V_L-V_H orientation. This stitching is possible due to the overlapping 'tails' in the light chain reverse (CKJo-B) and heavy chain forward primers (CSCVHo-FL). This was carried out using the overlap primer pair (CSC-F and CSC-B) to complete the construct and introduce upstream and downstream SfiI sites for easy transition into the vector. In addition 'clamp' sequences (GAG)₆ on these primers promote efficient digestion of the PCR products. Platinum® Taq DNA Polymerase High Fidelity (Invitrogen) was employed at this stage of library construction and initial optimisation of MgSO₄ was carried out prior to the large-scale reaction. Table 2.3-7 details the reaction conditions for SOE optimisation and the subsequent optimised large-scale reaction. The PCRs were carried out under the following cycling parameters in the G-storm thermocycler (Table 2.3-8).

Table 2.3-7: Splice-by-overlap extension PCR

Component	Optimisation Reaction Concentration (1X)	Large-Scale Reaction Concentration (1X)
High Fidelity PCR Buffer (10X)	1X	1X
MgSO ₄ [50mM]	1.5/2.0/3.4/4.0mM	1.5mM
Mol. Grade H ₂ O	to final volume of 50µL	to final volume of 50µL
dNTP [100mM]	0.1mM	0.1mM
CSC-F [60nMol]	30pM	30pM
CSC-B [60nMol]	30pM	30pM
V _L	100ng	100ng
V _H	100ng	100ng
Polymerase [5U/µL]	1U	1U

Table 2.3-8: SOE amplification PCR cycle parameters

Stage	Step	Temperature (°C)	Times (s)	# Cycles
1	Initial Denature	94°C	120	1
	Denaturation	94°C	15	
2	Annealing	56°C	30	30
	Extension	68°C	60	
3	Final Extension	68°C	600	1

Optimisation reactions for SOE-PCR were visualised on 1.5-2% (w/v) agarose gel (section 2.3.1.1) to allow determination of the optimal conditions for the large-scale reactions. Optimised large-scale reaction products were taken forward for purification. SOE-PCR products were purified by resolution on a 2% (w/v) agarose gel (section 2.3.1.1) and extracted using the NucleoTrap® gel extraction kit as per the manufacturer's instructions. The purified products were eluted in 50µL mol. G. H₂O per gel slice.

SOE Product	Concentration	Total DNA
BM	87.6ng/µL	21.9µg
SP	131.02ng/µL	32.8µg

2.3.4.4.3 Restriction digests of vector and inserts for scFv library construction

Both the purified pComb3xSS and SOE-PCR products from the BM and SP were digested in large-scale for ligation of the library (Table 2.3-9).

Table 2.3-9: Large-scale SfiI digestion of scFv library and insert

Component	BM	SP	pComb3xSS
DNA	10µg	10µg	20µg
Buffer 4 (10X)	1X	1X	1X
BSA (100X)	1X	1X	1X
Mol. G. H ₂ O	to 200µL	to 200µL	to 200µL
SfiI [20U/µL]	36U/µg	36U/µg	6U/µg

All the reactions were incubated at 50°C in a G-storm thermocycler for 5 hours. The BM and SP were then stored as an ethanol precipitation until required (section 2.3.1.1). Table 2.3-10 outlines the subsequent treatment of the vector.

Table 2.3-10: Triple digestion and Antarctic phosphatase treatment of vector

Component	pComb3xSS
XhoI [20U/µL]	3U/µg
XbaI [20U/µL]	3U/µg
Temperature and Time	37°C for 1 hour followed by 65°C for 30 minutes
Antarctic phosphatase buffer (10X)	1X
Antarctic phosphatase [5U/µL]	1U/µg
Temperature and Time	37°C for 30 minutes followed by 65°C for 15 minutes

Post triple digestion and Antarctic phosphatase treatment the vector was stored as an ethanol precipitation (section 2.3.1.1) until required. All the digested product precipitations were completed, as described in section 2.3.1.1. The products were purified by resolution on 0.5% (w/v) (pComb3x) or 2% (w/v) (BM and SP) agarose gels, the relevant bands

excised and extracted using NucleoTrap® gel extraction kit as per the manufacturer's instructions (eluted in 50µL mol. G. H₂O).

2.3.4.4.4 Library ligation and transformation

The purified *SfiI* digested scFv inserts were then ligated into the prepared pComb3x vector using T4 ligase (NEB) under the reaction conditions outlined in Table 2.3-11. The reaction was carried out overnight at room temperature. The ligations were then deactivated at 65°C for 20 minutes and ethanol precipitated overnight at -20°C as described in section 2.3.1.1.

Table 2.3-11: scFv library ligation reaction components

Component	BM	SP	Control
Vector DNA	1.4µg	1.4µg	1.4µg
Insert DNA	0.7µg	0.7µg	-
Ligase Buffer (10X)	1X	1X	1X
Mol. G. H ₂ O	to 100µL	to 100µL	to 100µL
T4 Ligase [400U/µL]	10U/µg	10U/µg	10U/µg

Once the precipitations were completed, the ligation reactions were resuspended in 15µL mol. G. H₂O for transformation. Transformations were carried out for BM and SP libraries separately. Each 15µL library ligation was split into 2 x 7.5µL transformation reactions (4 in total) to generate the avian anti-peptide-1 library.

300µL of electro-competent *E. coli* XL1-blue cells, prepared as per section 2.3.1.5.1, were placed into ice-cold 2.5mm electroporation cuvettes (Bio-Rad) and 7.5µL of the library ligation added to each 300µL cell aliquot. The cells and DNA were left to stand for 1 minute after gentle mixing. DNA was electroporated into the cells using the Gene Pulser xCell Electroporation system (Bio-Rad) with the following parameters; 2.5kV, 25µF and 200Ω ($\tau = 4.0\text{msec}$). Once electroporation was completed each cuvette was immediately

flushed with 1mL SOC media and transferred to a 50mL pre-warmed tube. This was followed by a further 1mL wash with SOC. All the electroporated samples (both BM and SP ~ 8mLs) were combined into the one 50mL tube and placed at 37°C shaking at 230rpm for 1 hour. The control ligation (2 x 7.5μL ligation) was also electroporated and treated in the same fashion. To both the library and the control 10mL of pre-warmed SB (with 3μL of 10mg/mL carbenicillin and 30μL of 5mg/mL tetracycline) was added. A 20μL sample of the library was removed into 180μL SB for titre determination by plating a 10-fold serial dilution range (plated 100μL of 10⁻³ to 10⁻⁶ inclusive on LB-Carbenicillin (50μg/mL) agar plates). A 2μL sample was removed from the control library and diluted into 200μL SB followed by plating 10μL and 100μL of this 1 in 100 dilution onto LB-Carbenicillin (50μg/mL) agar plates. The control was then discarded. The library was then placed at 37°C shaking at 230rpm for a further hour after which 4.5μL of Carbenicillin (100mg/mL) was added. After incubation for 1 hour at 37°C with shaking at 230rpm, 2mL of helper-phage (VCSM13: 1.0x10¹³cfu/mL) was added and the library transferred to a 500mL baffled flask containing 183mL SB with 92.5μL Carbenicillin (100mg/mL) and 370μL Tetracycline (5mg/mL). The culture was left static for 15 minutes followed by incubation for 2 hours as described in the previous incubation step. 280μL of Kanamycin (70mg/mL) was added and the cultures left to grow at 37°C with shaking at 230rpm overnight. At this stage the library is displayed on the phage particle and is ready for bio-panning.

2.3.4.5 *Bio-panning of phage displayed libraries*

2.3.4.5.1 Pre-optimisation of bio-panning conditions

Prior to carrying out any of the bio-panning strategies outlined in the subsequent sections the conditions were optimised with available control antibodies to maximise the success of the bio-panning stringencies.

2.3.4.5.1.1 *Wild-type antigen presentation*

The wild-type (WT) library was panned in a highly stringent antigen presentation manner using the mAb 20B3 to isolate compatible antibody-pairs for a diagnostic assay format. The strategy utilised 20B3 to capture cTnI to be subsequently interrogated by the library. Thus, isolating scFv fragments which could bind cTnI epitope-1 in the presence of the mAb bound in close proximity. The coating concentration of 20B3 and cTnI capture concentration were determined by preparation of a sandwich assay mimicking the presentation strategy. 20B3 mAb at 50, 10, 5 and 1µg/mL in PBS was coated in duplicate onto wells of an ELISA plate with 2µg/mL of the control mAb (Hytest 228) O/N at 4°C. The plate was blocked with 5% (w/v) PBSM for 1 hour at 37°C and concentrations of cTnI (15, 10, 5, 1, 0.5 and 0µg/mL) in 1% (w/v) PBSTM applied to the capture mAb wells. After incubation for 1 hour at 37°C and washing (PBST x3 and PBS x3) the captured cTnI was detected with a 1 in 2,000 dilution (1% (w/v) PBSTM) of anti-epitope-1 Hytest mAb 19C7 (HRP-labelled). The plate was incubated and washed as before followed by colour development with TMB and quenching with 10% (v/v) HCl after 10 minutes. The absorbance was read at 450nm in Tecan Sunrise™ plate reader.

2.3.4.5.1.2 *Mutant in-solution peptide concentration optimisation*

An ‘in-solution’ mode of bio-panning was selected to isolate improved mutants (MT) over the WT scFv. To optimise the bio-panning conditions 2µg/mL of purified WT scFv and

Hytest 19C7 HRP-labelled mAb were incubated with varying concentrations of biotinylated synthetic epitope-1 (10, 1, 0.5, 0.1 and 0nM) in 1% (w/v) PBSTM at 37°C shaking for 1 hour to assess the biotin-peptide-1 concentrations to optimally enrich and suitably challenge the library. The peptide-bound antibody was recovered by incubation with 10µL streptavidin-coated magnetic beads (NEB), application of a magnet and washing (PBST x3 and PBS x3). A 1 in 2,000 dilution in 1% (w/v) PBSTM of an anti-HA HRP-labelled secondary antibody was applied to the tubes containing scFv, incubated and washed as before. The resultant bead-peptide-antibody complexes were then resuspended in TMB and after 10 minutes, 100µL of the TMB was transferred to an ELISA plate containing 50µL 10% (v/v) HCl and the absorbance read at 450nm on the Tecan Sunrise™.

2.3.4.5.2 Phage rescue after each round of bio-panning

Phage rescue is the process carried out at each round of bio-panning to recover the selected antibody-displaying phage from culture supernatant. After incubation of the transformed library overnight (section 2.3.4.4.4) the phage were isolated by PEG₈₀₀₀ precipitation. This was carried out after each round of bio-panning e.g. R0 = transformed library recovery, R1 = recovered phage after 1st round of bio-panning and so on. The phage-scFv library culture was placed in 2 x 250mL or 2 x 85mL (depending on culture volume) centrifuge bottles. A 1mL sample was removed, centrifuged at 9,000rpm for 5 minutes at RT. The cells and supernatant were retained for DNA/soluble antibody analysis if required.

The centrifuge bottles were centrifuged at 9000rpm for 15 minutes at 4°C (Eppendorf 5810R) after which 4% (w/v) PEG₈₀₀₀ and 3% (w/v) NaCl was added to each supernatant after transfer to a set of clean centrifuge bottles. The phage rich supernatant was shaken at 230rpm for 5 minutes at 37°C. The precipitating phage was then put on ice for 30 minutes before centrifuging at 9000rpm for 15 minutes at 4°C. The supernatant was discarded and the tubes dried by inversion for 10 minutes. The phage pellet was then resuspended in 2 x 1mL of 1mg/mL KLH with 0.02% (w/v) NaN₃ in PBS. The phage preparation was then transferred to a 2mL micro-centrifuge tube and any residual cellular debris removed by centrifugation (full speed for 5 minutes at 4°C).

2.3.4.5.3 Wild-type scFv bio-panning

To a previously coated (100µL of 5mg/mL 20B3 mAb at 4°C O/N) and blocked (PBSM 5% (w/v) 1 hour at 37°C) immunotube, 850µL of the rescued phage was added and incubated with shaking for 1 hour at RT to deplete the library. Eight wells of a microtitre plate coated with 50µg/mL 20B3 mAb (4°C O/N) were blocked with 5% (w/v) PBSM (1 hour at 37°C) to capture 75µg/mL of cTnI (1 hour at 37°C) followed by washes of PBST (x3) and PBS (x3). 800µL of the depleted phage library was then applied to the captured protein wells (100µL/well) and allowed to interact while shaking for 1 hour at RT. Non-specific phage were removed with sequential PBST (200µL/well x 5) and PBS (200µL/well x 5) washes. Specific bound phage were eluted by incubation with 100µL/well of 10mg/mL trypsin in PBS at 37°C for 30 minutes. The eluted phage (~800µL) was then infected into 5mL of mid-exponential (O.D₆₀₀ ~0.4) *E. coli* XL-1 blue for 15 minutes, static at RT. Pre-warmed SB media (6mL) containing 1.6µL of Carbenicillin (100mg/mL) was added to the infected cells and a 2µL sample diluted in 200µL SB for output titre determination by plating 10µL and 100µL of this onto LB-Carbenicillin (50µg/mL) agar plates. The 8mL output library was placed at 37°C shaking at 230rpm for 1 hour followed by the addition of 2.4µL of Carbenicillin (100mg/mL) and incubation at 37°C shaking at 230rpm for 1 hour. Helper-phage (1mL of VCSM13: 1.0 x 10¹³ cfu/mL) was added and the culture transferred to a 250mL baffled flask containing 92mL SB with 46µL of Carbenicillin (100mg/mL) plus 184µL of Tetracycline (5mg/mL) and incubated at 37°C with shaking at 230rpm for 2 hours. In the final step 140µL of Kanamycin (70mg/mL) was added and the culture incubated as above overnight.

An input titre was performed during these incubation steps by addition of 10µL of the rescued phage in 90µL SB media and 10-fold serially diluting to 10⁻⁹. A 2µL sample of the 10⁻⁷, 10⁻⁸ and 10⁻⁹ dilutions were infected into mid-exponential phase *E. coli* XL-1 blue (100µL) and plated (50µL) onto LB-Carbenicillin plates (50µg/mL) after static incubation at RT for 15 minutes.

This bio-panning procedure was repeated on successive days (referred to as rounds), employing the stringency conditions delineated in Table 2.3-12, to exert selective pressure on the library to isolate high-affinity clones.

Table 2.3-12: Bio-panning conditions employed for isolating the wild-type anti-epitope-1 scFv

	O/N Culture Volume (mL)	[Capture mAb] ($\mu\text{g/mL}$)	[cTnI] x (wells) ($\mu\text{g/mL}$)	Washes PBST + PBS
R1	200	50	75 x 8	5 + 5
R2	100	50	75 x 4	5 + 5
R3	100	50	50 x 4	5 + 5
R4	100	50	25 x 4	5 + 5

2.3.4.5.4 Mutant scFv bio-panning

Solution-phase bio-panning was the mode of selection decided upon for the isolation of improved affinity clones from the LC-shuffled scFv library. The library was constructed in the same manner as for the WT with the V_H being amplified from the WT scFv plasmid by PCR as opposed to cDNA. The WT V_H was then recombined (by SOE-PCR) with the catalogue of light chains (SP and BM) from the original chicken cDNA. At this stage the mutant (MT) library construction process was carried out as for the WT where the SfiI digested BM and SP LC-shuffled libraries were ligated and transformed as previously described and displayed on phage (section 2.3.4.4.4). From the MT-rescued phage (section 2.3.4.5.2) 170 μL was incubated with 25 μL streptavidin-coated magnetic beads to deplete the library of non-specific-phage for 1 hour at 37°C. The beads were recovered by the application of a strong magnet for 2 minutes. The depleted library (150 μL) was then transferred to a 1.5mL tube previously blocked with 3% (w/v) PBS-BSA. To the tube 50 μL of 4X concentrated biotinylated peptide-1 (see Table 2.3-13) was added and incubated shaking at RT for 45 minutes. Streptavidin-coated magnetic beads (20 μL) blocked with 3% (w/v) PBS-BSA were added and the library-peptide-bead mix incubated for a further 15 minutes. Specific-phage were recovered by application of the magnet and the non-specific phage-containing supernatant discarded. The bead-peptide-scFv-phage complexes were washed by resuspension in 500 μL PBST and recovered using the magnet. This washing was repeated with PBST x5 and with PBS x5 with the beads being transferred to a clean blocked 1.5mL tube after the PBST washes. The phage were eluted with 500 μL of 10mg/mL trypsin in PBS for 30 minutes at RT and the beads recovered using the magnet.

The supernatant was then infected into 5mL of mid-exponential (O.D₆₀₀ ~0.4) *E. coli* XL-1 blue for 15 minutes, static at RT. At this stage, the bio-panning procedure for in-solution selection was carried out as described for the WT library bio-panning. The selection conditions exerting selective pressure on the mutant library are indicated in Table 2.3-13.

Table 2.3-13: Solution-phase bio-panning conditions for mutant anti-epitope-1 scFv selection

Round	4 x Peptide Concentration (nM)	Final Peptide Concentration (nM)	Washes PBS + PBST
1	40	10	5 + 5
2	4	1	5 + 5
3	2	0.5	5 + 5
4	0.4	0.1	5 + 5

2.3.4.6 Polyclonal-phage ELISA for specific antibody-displaying phage

After completion of the bio-panning experiments a polyclonal-phage ELISA was carried out to assess the success of the panning conditions and to identify the round in which enrichment of phage displaying antigen-specific antibodies had occurred. The ELISAs carried out for the WT and MT selection campaigns are described below.

2.3.4.6.1 Wild-type polyclonal-phage ELISA

cTnI (1µg/mL in PBS), neutrAvidin (2.5µg/mL), 20B3 mAb (10µg/mL) and KLH (1µg/mL) were coated over a series of wells on an ELISA plate at 4°C overnight. The plate was blocked with 5% (w/v) PBSM at 37°C for 1 hour. Biotinylated peptide-1 (10µM) was applied to the neutrAvidin-coated wells and cTnI (10µg/mL) to a series of the 20B3 mAb-coated wells (all other wells were placed in PBS). After incubation for 1 hour at 37°C the plate was washed with PBST (x3) and PBS (x3). Phage from each rescue (round: R0, R1, R2, R3 and R4) were diluted 1 in 5 with 1% (w/v) PBSTM and 100µL applied across the coated wells for each phage rescue. The plate was incubated and washed as described in the

above step and a 1 in 2,000 dilution (1% (w/v) PBSTM) of anti-M13 HRP-labelled secondary antibody applied to the wells. After incubation and washing as indicated above, the plate was developed with 100µL/well TMB and quenched after 10 minutes with 10% (v/v) HCl. The absorbance was read in the Tecan Sapphire™ at 450nm.

2.3.4.6.2 Mutant polyclonal-phage ELISA

A series of wells of an ELISA plate were coated with cTnI (1µg/mL) and KLH-peptide-1 (1µg/mL) in PBS overnight at 4°C to accommodate the four phage rescues and the WT scFv (pure) as a positive control. The entire plate was then blocked with 5% (w/v) PBSM for 1 hour at 37°C. The phage from each rescue (R0-R4) was diluted 1 in 5 with 1% (w/v) PBSTM and 100µL applied across the coated wells. After incubation for 1 hour at 37°C the plate was washed with PBST (x3) and PBS (x3). A 1 in 2,000 dilution (1% (w/v) PBSTM) of anti-M13 HRP-labelled secondary antibody was applied to the wells. After incubation and washing the plate was developed with 100µL/well TMB and quenched after 10 minutes with 10% (v/v) HCl. The absorbance was read in the Tecan Sapphire™ at 450nm.

2.3.4.7 Soluble scFv expression and lysis

Once the round corresponding to selective enrichment of the library was identified by the polyclonal-phage ELISA, the phage were infected into mid-exponential *E. coli* Top10F'.

A small amount of phage (1-20µL) was added to a growing culture of *E. coli* TOP10F' and incubated for 1 hour at 37°C, while shaking at 230rpm. The cells were then diluted serially from 10⁻¹ to 10⁻⁷ in SB media and plated onto LB-Carbenicillin (50mg/mL) agar plates to isolate single colonies. Single colonies were then transferred into the inner 60 wells of a 96-well plate containing 150µL SB (50µg/mL Carbenicillin and 1% (w/v) glucose). The plate was sealed and incubated at 37°C shaking at 230rpm overnight. The following day 25µL of the O/N cultures was subcultured into 875µL SB (50µg/mL Carbenicillin and 1X 505) in a 96-deep-well plate and grown for 3 hours at 37°C shaking at 230rpm. The individual

cultures were then induced with 100 μ L of 5mM IPTG (final of 0.5mM IPTG) overnight at 30°C shaking at 230rpm. The IPTG-induced single colonies were evaluated for specific-soluble antibodies by a number of analysis formats that were specific to the WT and MT screening campaigns. Prior to analysis the cells were recovered from the conditioned media by centrifugation at 4,000rpm for 30 minutes at 4°C. The cells were then lysed to release the soluble-expressed scFv. The cell pellets were then frozen at -80°C for a minimum of 1 hour. After thawing the cells were resuspended in 500 μ L PBS containing 1mg/mL lysozyme and incubated at RT for 30 minutes. The plate was freeze-thawed a minimum of 3 times with alternating cycles of -80°C and 37°C. The cellular debris was collected by centrifugation at 4,000rpm for 40 minutes at 4°C and the scFv-containing supernatant (clarified lysate) removed for analysis.

2.3.5 Screening for anti-epitope-1-specific scFv from bio-panned libraries

Both the WT and MT selected libraries from the bio-panning campaigns described above were screened in slightly differing fashions. The screening regimes undertaken for both are described separately in this section.

2.3.5.1 *Wild-type scFv screening approach*

A three pronged analysis was undertaken for the WT scFv screen. This consisted of bio-panning output-based genetic evaluation, plate-based ELISA and high-throughput (HT)-based screening which were all applied to exhaustively mine the selected WT library.

2.3.5.1.1 Fingerprint analysis of wild-type clones by restriction mapping

For fingerprint analysis single colonies were selected from the output titre plates from round four to allow PCR amplification of the scFv gene. Nineteen individual 1X reactions were prepared as outlined in Table 2.3-14. Eighteen colonies were randomly sampled and

added to 60µL of mol. G. H₂O, boiled and the debris collected by centrifugation (full speed at RT). This was then used as the water component specific to each clone for the PCR mix (the 19th tube served as a negative control). To all 19 tubes Go *Taq* polymerase (0.25µL) was added and the PCR carried out in a G-storm thermocycler as outlined in Table 2.3-8.

Table 2.3-14: Colony pick PCR master mix

Component	1X
Go Taq Buffer (5x)	1X
MgCl ₂ [25mM]	2.0mM
dNTPs [100mM]	0.1mM
Mol. G. H ₂ O	to 49.75µL
CSC-F [60nM]	30pM
CSC-B [60nM]	30pM

The amplified scFv genes were resolved on a 2% (w/v) agarose gel (section 2.3.1.3) to ascertain the percentage of colonies containing the gene fragment. This was followed by digestion with *AluI* and *BstNI* to generate a DNA fingerprint for each clone. The digestions were setup as delineated in Table 2.3-15 and were carried out for 2 hours at 37°C for *AluI* and 60°C for *BstNI*. They were then resolved on a 3% (w/v) agarose gel to visualise the patterns.

Table 2.3-15: *AluI* and *BstNI* digestion tube setup

Component	<i>AluI</i>	<i>BstNI</i>
SOE PCR Product	8µL	8µL
Buffer 2 (10X)	1X	1X
Mol. G. H ₂ O with 1X BSA	to 24µL	to 24µL
<i>BstNI</i> [10U/µL]	-	5U
<i>AluI</i> [10U/µL]	5U	-
Total	24µL	24µL

2.3.5.1.2 ELISA screening of wild-type clones

After bio-panning to screen for the most sensitive WT scFv, 300 individual colonies were selected from round 4 output plates and screened by steady-state and HT-analysis. The combined analysis regime provided classical ELISA-based ranking information and critically more defined binding analysis using SPR-based HT-instrumentation.

To initially determine the bio-panning success, the clarified lysates from plate # 1 only were assayed in a **direct binding ELISA** against the cTnI protein (1µg/mL), KLH-peptide-1 conjugate (1µg/mL) and KLH control (1µg/mL) in PBS coated onto separate plates at 4°C O/N. The plates were blocked with 5% (w/v) PBSM for 1 hour at 37°C. Lysates were freshly prepared, diluted 1 in 3 (1% (w/v) PBSTM) and applied to the cTnI, KLH-peptide-1 and KLH-coated ELISA plates. The plates were incubated at 37°C for 1 hour and washed with PBST (x3) and PBS (x3) followed by application of a 1 in 2,000 dilution of anti-HA HRP-labelled secondary antibody in 1% (w/v) PBSTM. The secondary antibody was incubated and washed as described in the previous step followed by development of colour with TMB. The substrate colour was quenched with 10% (v/v) HCl and absorbance read at 450nm on the Tecan Sunrise™.

A **sandwich assay format** was also employed to rank all 300 clones. The 20B3 mAb at 1µg/mL in PBS was applied to three ELISA plates (inner 60) per scFv plate to be screened at 4°C O/N. The plates were blocked for 1 hour at 37°C with 5% (w/v) PBSM and two plates were coated with 6-fold differing concentrations of cTnI (6nM and 36nM) for 1 hour at 37°C. This left the 3rd plate as a negative control. The plates were washed with PBST (x3) and PBS (x3) before adding 100µL/well of freshly prepared and diluted lysates (1 in 3 in 1% (w/v) PBSTM) over the three plates. The plates were incubated and washed as described in the previous step and a 1 in 2,000 dilution of anti-HA HRP-labelled secondary antibody in 1% (w/v) PBSTM was added. The secondary antibody was incubated and washed as described above followed by development of colour with TMB. The substrate colour was quenched with 10% (v/v) HCl and absorbance read at 450nm on the Tecan Sunrise™.

2.3.5.1.3 High-throughput ranking of wild-type clones

HT ranking of the lysates was carried out on the Biacore™ 4000 multiplexed surface plasmon resonance (SPR)-based instrument. A surface of 6000RU was prepared by amine-coupling of an anti-HA polyclonal antibody (contact time of 10 minutes) at 15µg/mL in 10mM NaOAc, pH 4.2, over spots 1, 2, 4 and 5 of the four flow cells on a research grade CM5 chip (Biacore, Sweden). The surface was then capped with 1M ethanolamine HCl, pH 8.5 and cleaned with desorb solution 1 and 2. This prepared surface could remain active for several weeks with continuous buffer flow (1X HBS-EP⁺).

All 300 clones were involved in the analysis which was divided over 4 plates. Clones were expressed and prepared, as described in section 2.3.4.7, and diluted 1 in 5 with 1X HBS-EP⁺. The diluted clones were applied to 96-well plates compatible with the system and racked in the dedicated temperature-controlled hotel (20°C) and the analysis carried out at 25°C. The diluted bacterial lysates were injected onto spots 1 (clone X) and 5 (clone Y) at a flow rate of 10µL/minute for 10 minutes. cTnI (25nM) in 1X HBS-EP⁺ was then passed over the whole surface at a flow rate of 30µL/minute and the active spots (1 and 5) online-reference subtracted using the reference spots (2 and 4). The surface was regenerated with a 30 second pulse of 20mM NaOH. Data was acquired at 1Hz/sec collection rate and evaluated using the dedicated BiaEvaluation software. The data based on stability (early and late) allowing percentage left ranking was prepared and exported, in addition to the subtracted sensorgrams.

2.3.5.2 *Mutant scFv screening approach*

In the case of the MT screening a much more HT-based approach was undertaken given the level and amount of quality data that could be acquired, yielding more information on kinetic parameters that allowed more efficient and knowledge-based selection of improved scFvs.

2.3.5.2.1 ELISA analysis of mutant scFv

The initial screening of the 192 clones (2 x 96-well plates) was undertaken in direct binding and sandwich ELISA formats. For the direct binding ELISA, a plate was coated with cTnI and blocked as described previously (section 2.3.5.1.2) and for the sandwich assay purified 20B3 mAb was coated and blocked on ELISA plates followed by capture of cTnI (1µg/mL). In both cases 192 clones were expressed and lysed as described in section 2.3.4.7. The lysates were diluted 1 in 3 with 1% (w/v) PBSTM and applied to the direct and sandwich assay plates. After incubation for 1 hour at 37°C the plates were washed (PBST x 3 and PBS x 3) and a 1 in 2,000 dilution of anti-HA HRP-labelled secondary antibody in 1% (w/v) PBSTM added to the plates. The plates were incubated and washed (PBST x 3 and PBS x 3) followed by colour development with TMB and quenching with 10% (v/v) HCl prior to reading absorbance at 450nm on the Tecan Sunrise™.

2.3.5.2.2 High-throughput ranking of mutant scFv

2.3.5.2.2.1 HT - 'off-rate' ranking

A surface of ~6000RU was prepared by amine-coupling of anti-HA antibody as described in 2.3.5.1.3. 192 clones were involved in the analysis and the clones were expressed and prepared as described in section 2.3.4.7 followed by dilution in 1X HBS-EP⁺ (1 in 5). The diluted clones were analysed as described in section 2.3.5.1.3 with the inclusion of a 0nM cTnI concentration into the analyses. Data was acquired at 1Hz/sec collection rate and was evaluated using the dedicated BiaEvaluation software. Data based on stability (early and late) allowing percentage left ranking was prepared and the curves acquired modelled for crude k_a and k_d values using the 1:1 Langmuir equation with the global fit parameter.

2.3.5.2.2.2 HT - '2 over 2' ranking of wild-type and mutant scFv

Two different scFv densities were captured for each clone in a cycle (two clones per cycle: spots 1 and 5 – high density and spots 2 and 4 – low density) in the capture approach at 25°C. Diluted lysates (1 in 3 and 1 in 30 in 1X HBS-EP⁺) for a selected group of 15 MT clones and the pure WT (1µg/mL and 0.1µg/mL in HBS-EP⁺) were passed across the chip surface at a flow rate of 10µL/minute for 10 minutes. Post scFv capture two concentrations of cTnI were passed across the two capture densities (75nM and 25nM) in 1X HBS-EP⁺. The data was collected at 1Hz/sec and the surface regenerated after 12 minutes dissociation for the next cycle. The data was evaluated using the dedicated BiaEvaluation software using the '2 over 2' template. Curves were fitted with 1:1 Langmuir binding equation with the global fit parameter allowing determination of more precise k_a and k_d values for the 15 mutant clones.

2.3.5.2.2.3 Full kinetic profiling of wild-type and mutant scFv

The anti-HA surface prepared on Biacore was readily employed to carry out full kinetic profiling of the clones. In this case a clone was captured repeatedly on spot 1 and a second clone on spot 5 over the four flow cells (a total of 8 clones). Seven MT clones and the WT scFv were taken forward for full kinetic analysis over a significant cTnI concentration range [12, 6, 3(x2), 1.5, 0.75, 0.375, 0.1875 and 0nM cTnI]. The run typically took in the order of 12-14 hours. The data was collected at 10Hz/sec and allowed acquisition of vast amounts of kinetic data to fit with 1:1 Langmuir binding model. Owing to issues with the commercial protein the data collected was fitted with a local R_{max} to improve the quality of the data fits.

2.3.6 Inhibition ELISA comparison of wild-type and mutant scFv

Inhibition analysis was carried out to evaluate the WT in comparison to the selected panel of MT clones, increasing the confidence in the demonstrated improved sensitivity of the clones.

2.3.6.1 *Titre*

Analysis was carried out with freshly prepared lysates. A plate was coated with 0.5µg/mL cTnI in PBS O/N at 4°C and blocked with 5% (w/v) PBSTM for 1 hour at 37°C. Doubling dilutions (1 in 100 to 1 in 204,800) of lysates in 1% (w/v) PBSTM were applied to the wells and incubated for 1 hour at 37°C. The plate was washed with PBST (x3) and PBS (x3) followed by application of a 1 in 2,000 dilution of anti-HA HRP-labelled secondary antibody in 1% (w/v) PBSTM. The plate was incubated and washed with PBST (x3) and PBS (x3) and colour developed with the addition of TMB followed by quenching with 10% (v/v) HCl. Absorbance was read at 405nm using a Tecan Sunrise™

2.3.6.2 *Inhibition*

The optimised scFv lysate dilutions (double strength) were diluted 1:1 with free a cTnI concentration range (200 to 0.39nM and including zero cTnI in 1% (w/v) PBSTM) and incubated at 37°C for 1 hour in 1.5mL tubes. The inhibition mix (100µL) was then applied to a plate coated with cTnI (0.5µg/mL in PBS) as described for the titre. After 1 hour incubation at 37°C the plate was washed, the secondary antibody applied and the plate absorbance read (as described for the titre determination). Each clone A0 (Absorbance at zero cTnI) was divided into the response at each free cTnI concentration resulting in an inhibition curve.

2.3.7 Full kinetic profiling using fatty acid binding protein fusion

The precise determination of the kinetic constants was important to critically evaluate the clones. Despite the issues encountered using the commercial cTnI protein the surrogate epitope fusion protein proved invaluable. To carry out the kinetic evaluation the exact determination of the FABP-P1&2 fusion concentration was required as for evaluation of kinetic interactions exact protein concentrations are necessary to accurately model the data. Absorbance measurements are inherently inconsistent and give the total protein concentration. In this assay any protein contaminants were not involved in calculation of the actual fusion protein concentration.

2.3.7.1 *Determination of fatty acid binding protein fusion concentration*

The exact concentration of the FABP fusion was determined by an inhibition assay format using an 'in-house' anti-FABP scFv [90] and commercial hFABP (c-hFABP) of known concentration. Initially, the optimal scFv concentration for the analysis was determined by titration against 0.5µg/mL hFABP in PBS coated onto the wells of an ELISA plate O/N at 4°C. The plate was blocked with 5% (w/v) PBSTM for 1 hour at 37°C. Serially diluted scFv was then applied to the coated well, incubated for 1 hour at 37°C and washed (PBST x 3 and PBS x3). The bound scFv was detected using a 1 in 2,000 dilution of anti-HA HRP-labelled secondary antibody in 1% (w/v) PBSTM. From this titre the optimal scFv dilution for the inhibition format was determined. In this assay a plate was coated with FABP and blocked as described for the titre. The scFv was diluted with a range of c-hFABP concentrations incubated in 1.5mL tubes for 1 hour at 37°C before transfer to the hFABP-coated wells. In parallel, the FABP-P1&2 fusion protein was diluted in the same manner with the scFv for accurate concentration determination. After incubation and washing the bound scFv fraction was detected with the anti-HA HRP-labelled secondary antibody as described for the titre above. Using the c-hFABP inhibition curve values a calibration plot was generated. This allowed for the unknown (FABP-P1&2) response to be back calculated resulting in precise determination of the concentration. The analyses described here were carried out in triplicate and on three individual occasions.

2.3.7.2 *Kinetic evaluation of wild-type and mutant scFv*

An anti-HA pAb surface was prepared as previously described (section 2.3.5.1.3) over the spots of two flow cells only. This allowed for kinetic characterisation of the WT (180) and MT (2B12) in duplicate (spot 1 and spot 5) per kinetic run. Purified WT and MT scFv dilutions in 1X HBS-EP⁺ were prepared to obtain a consistent $R_{\max} < 100\text{RU}$ required for reliable kinetics. Using these optimised scFv concentrations the FABP-P1&2 fusion was adjusted to a suitable concentration range for the kinetics to be carried out [25, 12.5, 6.25, 3.125(x2), 1.5625, 0.78125, 0.390625 and 0nM]. The kinetic data was collected at the higher (10Hz/second) rate and the dedicated BiaEvaluation software utilised to prepare the data and fit the kinetic parameters with 1:1 Langmuir binding global fit equation.

2.3.8 *Sequence analysis and protein modelling of scFv*

2.3.8.1 *Sequence analysis of two selected scFv clones*

Sequence analysis was carried out by Source-Bioscience Ireland using the sequence primers delineated in Table 2.3-4 from purified plasmids or cell stocks treated by the company. The DNA sequence was then translated using the Expasy online translate tool (<http://www.expasy.ch/tools/dna.html>). The amino acid sequence was then aligned using ClustalW (<http://www.ebi.ac.uk/Tools/msa/clustalw2/>) to compare sequences. Aligned sequences were exported to PowerPoint and the significant regions highlighted.

2.3.8.2 *Protein modelling of two scFv clones*

The amino acid sequences for WT and MT clones were submitted to the Web antibody modelling server (WAM) at <http://antibody.bath.ac.uk/> using the auto align program. As this system is for human antibodies the CDRL2 caused errors for the modelling program, for that reason the ‘N’ residue in the ‘SNIP’ sequence of complementarity determining region of the light chain (CDRL2) was removed from both the wild-type and mutant clones

to allow the program to apply its models. The models were returned as pdb files and viewed using the Swiss-PDB deep view program 4.0.1. The structures were energy minimised and corrected for side chain clashes using the in program functionality. Following colouring and augmentation of the view point the images were saved as high-quality POV Ray scenes or bmp files.

2.3.9 Thermal challenge assay for assessment of improved stability

The thermal challenge assay was modified from [91, 92] by incubation of 0.1µg/mL (130µL/tube) of the purified scFv in PBS over a range of temperatures. In the G-storm thermocycler a gradient was programmed from 47.9°C to 72.5°C in which the proteins were placed for 90 minutes. For both scFvs, an aliquot was retained at RT to act as an unheated control. After thermal challenge the 11 heat treated proteins and control were diluted 1 in 4 in 1% (w/v) PBSTM and applied in triplicate, to a plate previously coated with 0.5µg/mL cTnI and blocked with 5% (w/v) PBSTM. The plate was incubated at 37°C for 1 hour and washed with PBST (x3) and PBS (x3). The bound non-denatured scFv was detected with a 1 in 2,000 dilution of anti-HA HRP-labelled secondary antibody in 1% (w/v) PBSTM. The plate was incubated and washed with PBST (x3) and PBS (x3) and developed with TMB followed by quenching with 10% (v/v) HCl. The absorbance was then read on the Tecan Sunrise™ at 450nm. The individual responses for each temperature were expressed as a percentage retained binding activity and the clones compared at 50% loss of binding activity (T₅₀).

2.3.10 Determination of crystal structure

2.3.10.1 Gel filtration of purified scFv

A S75 (16/60) analytical gel filtration column (GE Healthcare) was equilibrated with 1X TBS prepared as described in section 2.3.1.9 (1CV = 50mL). A 0.5mL sample of scFv 180 (2.0mg/mL) previously purified by IMAC (section 5.2.2.5.3) was applied to the column at a

flow rate of 0.5mL/minute. Fractions were collected after 0.3CV until 1CV was reached. Protein was monitored online by $A_{280\text{nm}}$ using the dedicated Unicorn control and evaluation software (GE Healthcare). Protein peaks were evaluated and significant monomeric protein-containing fractions concentrated to approximately 150 μ L in 1X TBS.

2.3.10.2 Coarse screening for optimal crystal formation conditions

2.3.10.2.1 Manual tray setup

Coarse screening was carried out in 24-well plate format. The concentrated protein was centrifuged at 13,000rpm at 4°C to remove any formed precipitates or contaminating matter. 24-well plates were prepared by application of a ring of petroleum jelly to the circumference of each well. 500 μ L of mother liquor from the Sigma Basic Crystallisation Kit for Proteins (catalogue # 82009) conditions 1 to 48 were placed in the appropriate number of wells (2 x 24-well plates). A 0.6 μ L drop of mother liquor was placed in the centre of the siliconised glass slides (Hampton Research catalogue # HR3-277) and 0.6 μ L of scFv 180 (at 6mg/mL) was mixed into the mother liquor drop before inversion of the slide and sealing of the well using a 1mL pipette tip. All plates were then placed in a vibration excluded temperature controlled environment at 20°C and monitored daily for crystal formation.

2.3.10.2.2 Crystallisation tray setup

As the crystal suite was automated the protein was provided to the facility for robotic dispersion of 100nL drops. The concentrated protein was centrifuged at 13,000rpm at 4°C to remove any formed precipitates or contaminating matter which could block the nano-needle. 100nL drops of protein were mixed with 100nL drops of mother liquor in the 96 conditions for the Hampton Research PEG/ION and SaltRx screening kits (Table 8.1-2). Plates were housed in temperature controlled racks at 20°C and imaged daily. Plates could be viewed remotely using the CrystalTrack online software.

2.3.10.3 Fine screening to refine optimal crystal formation conditions

Fine screening conditions were prepared for the Sigma Basic Crystallisation Kit condition number 40 (0.1M Na-citrate pH 5.6, 20% (v/v) 2-propanol and 20% (w/v) PEG-4000). The fine screen was carried out as described in Table 2.3-16. Each Na-citrate at a pH was prepared as a 1.8M stock and 28µL added to the corresponding rows of the plate. Each mix of salt and organic solvent was prepared individually from stocks of 50% (v/v) 2-propanol and 50% (w/v) PEG-4000 in MilliQ water as described in Table 2.3-17. The prepared solutions was added to each corresponding column (472µL) and mixed on a plate shaker for 5 minutes to fully mix the mother liquor. Individual hanging drops were prepared by application of 0.6µL of the relevant mother liquor to the siliconised glass slide and mixing in 0.6µL of scFv 180 (6mg/mL). The wells were sealed using petroleum jelly and placed at 20°C to incubate.

Table 2.3-16: Layout of the fine screening conditions for scFv 180 crystal formation





















Conditions		1	2	3	4	5
% 2-propanol (v/v)		18	19	20	21	22
% PEG-4000 (w/v)		18	19	20	21	22
A	Na-Citrate pH 6.0					
B	Na-Citrate pH 5.8					
C	Na-Citrate pH 5.6					
D	Na-Citrate pH 5.4					

Table 2.3-17: Preparation of mother liquor for fine screening of crystal conditions

Final %	Final volume (mL)	50% (v/v) 2-propanol (µL)	50% (w/v) PEG-4000 (µL)	MilliQ Water (µL)
18:18	2.3	828	828	412
19:19	2.3	874	874	326
20:20	4.3	1720	1720	430
21:21	2.3	966	966	134
22:22	2.3	1012	1012	48

2.3.10.4 X-ray diffraction of scFv 180 crystals

Individual crystals from the coarse screens (both manual and automated) were collected in a goniometer loop of an appropriate size (decided visually under a microscope) and locked onto the goniometer. Using the adjustment screws the crystal was brought into the X-ray path. X-ray measurements were made using the Rikagu *RU-3HBR* rotating anode generator with helium purged *OSMIC* focusing mirrors as an X-ray source. The data was collected using an R-AXIS IV++ detector by rotation through 90°C. Collected images were data processed using a custom written program and displayed as jpeg files for the purposes of display in this thesis.

2.3.11 Evaluation of selected scFvs and the industry standard

In this inhibition analysis, the purified WT (180) and MT (2B12) and the Hytest 19C7 HRP-labelled antibody were titred as described in section 2.3.6.1. The optimal antibody dilution was determined and the inhibition carried out as described in section 2.3.6.2 with a cTnI concentration range of 5 to 0.0195µg/mL (serially doubling) in 1% (w/v) PBSTM. The analysis for each antibody was carried out in duplicate and on three individual occasions.

2.3.12 Conversion of scFv to scAb format

2.3.12.1 Genetic manipulation of scFv construct

pComb3x-based scFv were converted to scAb format by addition of a chicken constant domain (C_λ) to the end of the V_H chain. To achieve this, the C_λ amplified from chicken cDNA was cloned into pMopac16 (Figure 8.1-7) in place of the existing HuC κ designed by Dr. Stephen Hearty and carried out by Dr. B. Vijayalakshmi Ayyar. To subclone in the pComb3x-scFv into pMopac C_λ the *SfiI* sites needed to be modified to be compatible. This was carried out using the primers as outlined in Table 2.3-18.

Table 2.3-18: Primer sequence to transfer pComb3x-based scFv to pMopacC_λ

Primer Name	Primer Sequence
ChiVL-VHPac-F	GGA AAT CGC GGC GGC CCA GCC GGC CAT GGC GCT GAC TCA G
ChiVL-VHPac-R	TTA CTC GCG GCC CCC GAG GCC GCA CTA GTG GA

The pMopacC_λ and pComb3-based 2B12 and 4G5 vectors were purified as described in section 2.3.1.2. The scFvs were modified by PCR using the reaction mix outlined in Table 2.3-19 in the G-storm thermocycler with the cycle parameters delineated in Table 2.3-20.

Table 2.3-19: Amplification and modification of scFv from pComb3x vector

Component	Large-Scale Reaction Concentration (1X)
Go Taq Buffer (10X)	1X
MgCl ₂ [25mM]	2.0mM
Mol. Grade H ₂ O	to final volume of 50μL
dNTP [100mM]	0.1mM
Forward Primer [60nMol]	30pM
Reverse Primer [60nMol]	30pM
Plasmid DNA	1μL
Polymerase [5U/μL]	1.25U

Table 2.3-20: Modified scFv amplification PCR cycle parameters

Stage	Step	Temperature (°C)	Times (s)	# Cycles
1	Initial Denature	94°C	120	1
2	Denaturation	94°C	15	30
	Annealing	56°C	30	
	Extension	72°C	60	
3	Final Extension	72°C	600	1

Post large-scale amplification the scFv inserts were purified by resolution on a 2% (w/v) agarose and extraction using the NucleoTrap® gel extraction kit as per the manufacturer's

guidelines. The modified scFvs and pMopacC_λ vector were SfiI digested as described in Table 2.3-21.

Table 2.3-21: Large-scale SfiI digests of pMopacC_λ vector and modified scFv inserts

Component	2B12	4G5	pMopacC _λ
DNA	10μg	10μg	20μg
Buffer 4 (10X)	1X	1X	1X
BSA (100X)	1X	1X	1X
Mol. G. H ₂ O	to 200μL	to 200μL	to 200μL
SfiI [20U/μL]	36U/μg	36U/μg	6U/μg

All the reactions were incubated at 50°C in G-storm thermocycler for 5 hours. The scFv digests were then stored as an ethanol precipitation until required (section 2.3.1.1). The vector was further treated with Antarctic phosphatase (1X Buffer and 1U/μg enzyme) for 1 hour at 37°C followed by inactivation at 65°C for 20 minutes. Post digestion and Antarctic phosphatase treatment the vector was stored as an ethanol precipitation (section 2.3.1.1). All the digested product precipitations were completed, as described in section 2.3.1.1, and subsequently purified by resolution on 0.5% (w/v) (vector) or 2% (w/v) (insert) agarose gel, followed by excision of the relevant bands and extraction using NucleoTrap® gel extraction kit as per the manufacturer's instructions (eluted into 50μL mol. G. H₂O). The modified scFv inserts were ligated into the pMopacC_λ vector and transformed into *E. coli* TOP10F' as described in 2.3.1.4.

2.3.12.2 scAb expression analysis

Single colonies were selected and grown up for small-scale analysis as described in 2.3.1.7 and glycerol stocks prepared as described in 2.3.1.6. The presence of correctly expressed protein was identified by direct binding ELISA against KLH-peptide-2 at 1μg/mL (2B12_scAb) and neutrAvidin (2.5μg/mL) captured 1μM biotinylated peptide-3 (4G5_scAb). Both plates were blocked with 5% (w/v) PBSTM and diluted lysates applied

(1 in 5). Bound scAb was detected using anti-HIS HRP-labelled secondary antibody. The plates were developed using TMB followed by quenching with 10% (v/v) HCl and the absorbance read on a Tecan Sunrise™ at 450nm.

2.3.13 Purification of generated recombinant antibodies

Purification of the recombinant antibodies generated followed the generic recombinant protein purification protocol in section 2.3.1.9 using the buffer compositions outlined in section 2.3.1.9. The clones were grown overnight in 5mL starter cultures (SB with 50µg/mL Carbenicillin and 1% (w/v) glucose) from glycerol stocks. The 5mL starter culture was then used to inoculate 400mL SB (with 50µg/mL Carbenicillin) in a 2L baffled flask. The culture was grown at 37°C with shaking at 230rpm until an OD600 of ~0.6 was reached. At this stage the clones were induced with 0.5mM IPTG O/N at 30°C. The induced cultures were collected and lysed as described in 2.3.1.7. All proteins (scFv 180, scFv 2B12, 2B12_scAb, scFv 4G5 and 4G5_scAb) were purified on 1mL settled Ni²⁺ charged resin using the PBS-based buffers outlined in section 2.1.4.6.2.

Chapter 3: Cardiac Troponin I antigen

3.1 Introduction

Prior to any monoclonal antibody generation campaign careful consideration with respect to antigen source and quality is advised. The necessity for the epitope-specific strategy employed to successfully isolate diagnostically relevant antibodies became apparent and strategies to overcome some of the antigen quality-based limitations encountered in characterisation of the selected antibodies were required.

3.1.1 Cardiac Troponin I (cTnI)

Cardiac Troponin I is a critical component of calcium mediated muscle contraction in thin filament-based Tn-tropomyosin interaction, as described in section 1.3.3.4. Due to its ‘gold standard’ status for the diagnosis of AMI, the ability to detect ultra-low levels of cTnI is of paramount importance. Currently, the new generation of *sensitive* cTnI assays have overcome problems associated with non-specific issues found in first generation devices, pushing assay reliability and sensitivity much higher. The associated problems (illustrated diagrammatically in Figure 3.1-1) include patient heterophile antibodies, human anti-mouse antibodies (HAMA), cTnI auto-antibodies [93] and the varying forms of circulating TnI (Table 1.3-5). However, these have largely been overcome by targeting the stable N-terminal region of cTnI [66]. Major challenges exist for the generation of epitope-specific antibodies against cTnI. Directing the immune response to several specific and discrete epitopes was a significant challenge. This issue, coupled with the lack of standardised reagents for troponin-based diagnostics and suboptimal antigen quality, presented significant barriers for screening, characterisation and assay development [66].

3.1.2 Design of cTnI peptides

The initial approach to overcome the problems associated with antigen quality and directing the epitope-specificity was introduced early in the immunisation regime. In the primary screening of existing whole protein immunised libraries, the synthesis of specific epitope-associated peptides facilitated evaluation of the selected library for epitope-specific antibodies. *Figure 3.1-2 A* is an alignment of cardiac and skeletal TnI indicating the regions of similarity. To a large extent the two proteins are similar and this presents an obstacle for specific antibody generation. The N-terminal cardiovascular-specific region was identified and subsequently targeted as a key antigen in line with current trends to ensure cardiovascular-specificity. Two adjacent peptides, peptide-1 (epitope-1) and peptide-2 (epitope-2), were designed as outlined in Table 3.1-1, and are overlapping continuous regions within the cardio-specific N-terminus of cTnI. For antibody targeting, combined with discrimination between skeletal (s) and cTnI, these two epitopes were used in conjunction during selection and screening to identify optimal antibody pairs for diagnostic purposes. *Figure 3.1-2 B* illustrates a model of the cTnI molecule indicating the conformation of each peptide region in the context of the whole protein.

A	P48788	MGD-----EEKRNRAITARRQHLKSVMLQIAATE	29
	P19429	MADGSSDAAREPRPAPAPIRRRSSNYRAYATEPHAKKSKISASRKLQKTL LLQIAKQE	60
		. :*.: :*: :*: :*: :*	
	P48788	LEKEESRREAEEKONYLAEHCPPLHIPGS-MSEVQELCKQLHAKIDAAEEEEKYDMEVRVQK	88
	P19429	LEREAEERRGEKGRALSTRCPLELAGLGFAELQDL CRQLHARVDKVD EERYDIEAKVTK	120
		**:* ..*.* . *: :* **..* :*: :*: :*: :*: :* .: :*: :*: :* .*	
	P48788	TSKELEDMNQKLF DLRGKFKR PPLRRVRMSADAMLKALGSKHKVCMDLRANLKQVKKED	148
	P19429	NITEIADLTQKIF DLRGKFKR PTLRRVRISADAMQALLGARAKESLDI RAHLKQVKKED	180
		. .*: *: :*: :*: :*: :*: :*: :*: :* .: :*: :*: :*	
	P48788	TEKERDLRDVG DRKNIEE SGMEGRKKMFES	182
	P19429	TEKEN --REVGDWRKNIDALSGMEGRKKKFES--	210
		****. *: :*: :*: :* :* :*	

B

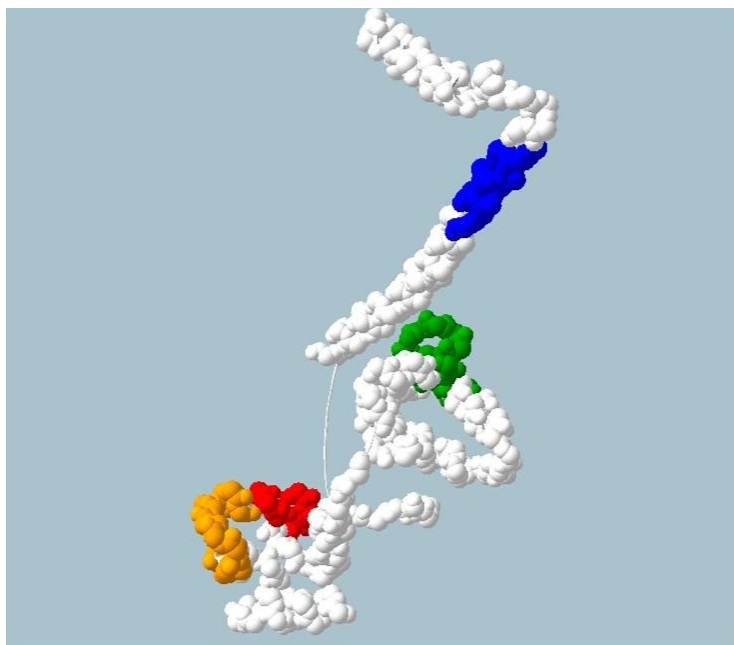


Figure 3.1-2: Cardiac Troponin I amino acid sequence and model

A) CLUSTAL 2.0.11 multiple sequence alignment of c- and s- TnI

Amino acid alignment of cTnI (P19429) and sTnI (P48788) using ClustalW at <http://www.uniprot.org/>. Amino acid identity is indicated by the symbols as follows; “*” identical, “:” conserved and “.” semi-conserved. Epitopes are highlighted on the P19429 sequence and in the cardiac troponin model as follows; 1: red, 2: gold, 3: green and 4: blue.

B) cTnI molecule model

A hypothetical 3D structure of TnI was constructed using SWISS-MODEL [95] and the PDB files 1J1D and 1J1E as a templates (release date 15-Jul-2003) [96]. PDB files were viewed using Swiss-PDB Viewer program 4.0.1.

The amino acid composition of each peptide and its associated properties are summarised in Table 3.1-1. These peptides were synthesised commercially by Anaspec with N-terminal conjugation to biotin. Due to the reasons outlined in section 3.2.2, peptides 1 and 2 were synthesised using C-terminal conjugation chemistry to include KLH (CT-peptide-1- or -2 - KLH) and biotin conjugation (CT-peptide-1- or -2-B).

Table 3.1-1: Cardiac Troponin I peptides

Peptide	Amino acid residue	MW (Da)	Theoretical pI	Amino Acid Sequence
1	39-50	1372	11.26	KISASRKLQLKT
2	24-40	2005	10.00	NYRAYATEPHAKKKSKI
3	79-93	1485	3.79	QPLELAGLGFAELQ
4	169-180	1452	9.70	RAHLKQVKKEDT

3.1.3 Recombinant antigen expression

The expression of recombinant proteins in *E. coli* is of considerable importance for a significant number of biological fields and applications including proteomics, structural genomics and vaccines. The widespread use of *E. coli* as a host for heterologous protein production has come about due to gargantuan improvements in our understanding of transcription, translation and protein folding in the organism. These leaps have been made possible by improved genetic tools at the disposal of scientists intermixed with much good fortune [97]. *E. coli* is advantageous in many respects including; its growth on inexpensive carbon sources, rapid biomass accumulation, suitability for high-density fermentations and relatively simple scale-up. *E. coli* is not without its disadvantages and is typically only suited to expression of soluble proteins that do not require complex post-translational modifications. In addition, incorrect conformation, degradation and aggregation may commonly occur, complicating expression [98].

The choice of expression vector and *E. coli* host is of considerable importance, impacting on the quality, quantity and purification potential of the recombinant protein. Many expression vectors exist and each has a wealth of experience and publications supporting

their use for numerous applications. These vector systems rely on the use of ‘good’ promoter systems. Typical characteristics of a good promoter include high potency and capability to reach expression levels in excess of the 10-30% of the total protein content [99]. Many of these promoters are based on or around the *lac* operon. Indeed, despite some of its disadvantages it is still widely and successfully adopted to drive heterologous protein expression. Both the *lac* and *lacUV5* are weak promoters and tend to be extremely useful to achieve graded expression of recombinant proteins in conjunction with the non-hydrolysable analogue, isopropyl- β -D-1-thiogalactopyranoside (IPTG). The *tac* and *trc* are synthetic promoters that comprise of the -35 region of the *trp* promoter and the -10 region of the *lac* promoter. The *tac* and *trc* promoters differ by a single base pair between the two regions and are relatively strong promoters, routinely achieving specific protein content of 15-30% of the total cell protein content [97]. To circumvent the leakiness of the *lac*-based promoters repression can be achieved by *lacI*^Q which is a single point mutation of the chromosomal *lacI* promoter in the host strain. This causes a 5-10 fold increase in the number of *lacI* repressor molecules available in the cell allowing efficient repression of protein expression until induced by IPTG.

The pET system of vectors were developed from the original vectors constructed by Studier and co-workers [100] and commercially developed by Novagen [101]. The system allows cloning of target genes downstream of the bacteriophage T7 late promoter. These medium copy number plasmids require T7 RNA polymerase that is engineered into *E. coli* by prophage (λ DE3), is controlled by the *lacUV5* promoter and is inducible by IPTG. In this powerful system, very high target protein concentrations can be achieved (up to 50%) due to the synthesis of large amounts of mRNA. This expression mechanism is not without disadvantages as such high levels of mRNA can cause ribosome destruction and cell death. In addition, leaky T7 polymerase expression may contribute to plasmid and/or expression instability [97]. In an already crowded environment, where a protein exits a ribosome every 35 seconds and macromolecule concentrations can elevate to 300-400mg/mL, this high-level of expression can contribute to protein misfolding and the formation of inclusion bodies [98]. To mitigate against these events strategies have evolved including co-expression of phage T7 lysozyme and insertion of *lac* operator sequence downstream of the plasmid-encoded T7 promoter. In the former strategy, T7 lysozyme is encoded on a plasmid (pLysS and pLysE) and inhibits T7 RNA polymerase, repressing expression of T7

RNA polymerase-dependent genes. In the latter strategy, the inclusion of a chromosomal copy of the *lac* repressor gene (*lacI*) allows repression of both the *lacUV5* and T7 promoters integrated with segments of the *lac* (*T7lac* - Figure 3.1-3) [102].

In combination with these numerous strategies to control induction, the vectors encode several other components such as leader sequences, fusions to promote expression or stability, purification and affinity tags. Leader/signal sequences (e.g. *ompA* and *pelB*) mark the protein for export to the periplasm *via* the *sec*-dependent transport pathway (vector: pET26b+). Numerous other signal sequences and mediators exist in the pET armamentarium and a full listing of the components of the pET vectors can be found in the pET system manual [102]. Three pET vectors were exploited in the course of heterologous expression of the various forms of recombinant TnI (rTnI), pET 26b+, 28b+ and 32b+.

The above mentioned technologies were exploited for the successful cloning, heterologous expression and purification of recombinant forms of the cTnI protein in conjunction with the methodologies outlined in section 2.3.2

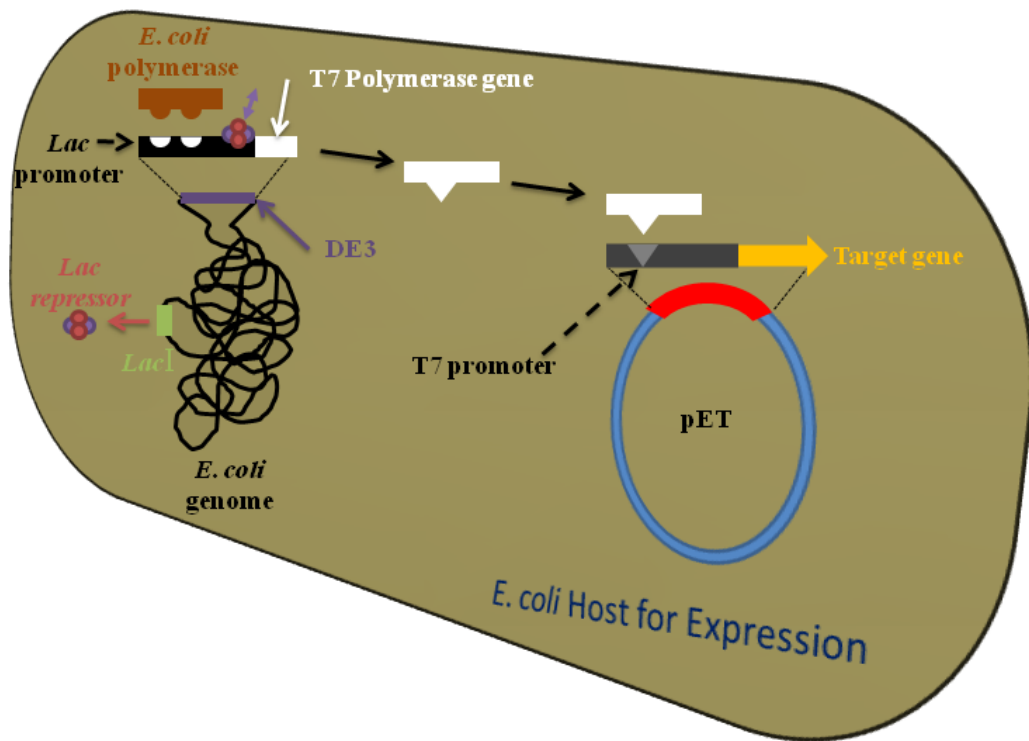


Figure 3.1-3: Control and production of recombinant protein expression by T7lac

The *E. coli* host strain are lysogens of bacteriophage DE3 and contain a chromosomal copy of the T7 RNA polymerase gene (white) in addition to fragments of DNA encoding the *lacI* gene (green) and the *lacUV5* promoter (black). The *lac* repressor (red and purple) acts on the *lacUV5* promoter on the host chromosome repressing T7 RNA polymerase transcription. Additionally, it acts on the T7lac promoter (grey) in the pET vector to block transcription of the target gene (yellow) by T7 RNA polymerase. Upon induction with IPTG translation of the T7 RNA polymerase gene by *E. coli* polymerase provides T7 RNA polymerase to interact with the T7lac promoter and express the target gene.

3.2 Results

3.2.1 cTnI antigen quality

SDS-PAGE and Western blot (WB) analysis of the cTnI commercially sourced from Life Diagnostics allowed for the antigen quality to be evaluated (section 2.3.2.1). As illustrated in Figure 3.2-1 on SDS-PAGE a single band was observed for cTnI. However, when probed with three industry gold standard antibodies by WB numerous bands were observed at higher and lower molecular weights, suggesting aggregation and degradation of the antigen was a factor. This was likely to be exasperated by the purification process where the buffer contains significant levels of urea and EDTA, which can lead to carbamylation, and thus is not representative of the naturally occurring circulating forms of cTnI [66].

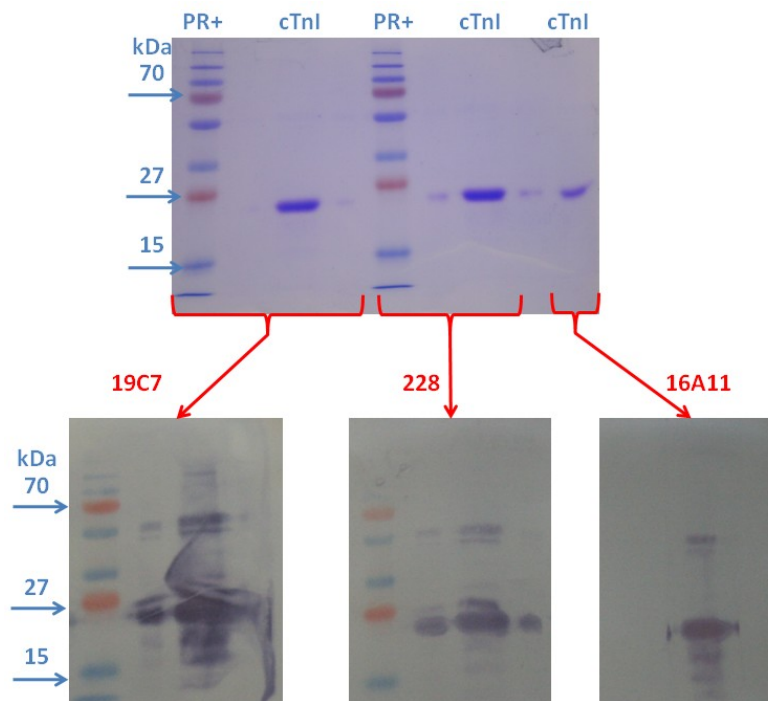


Figure 3.2-1: 12.5 (w/v) SDS-PAGE and Western blot of commercially available cTnI

Top: SDS-PAGE, bottom: WB. The commercially sourced cTnI was loaded onto lanes of the SDS-PAGE and WB probing was performed using three industry ‘gold’ standard monoclonal antibodies available from Hytest (19C7; peptide-1. 228; peptide-2 and 16A11; peptide-3. Monoclonal antibodies 19C7 and 228 were detected using an anti-mouse HRP-conjugated secondary antibody. 16A11 was directly HRP-conjugated facilitating direct detection. PR⁺: Prestained protein ladder.

3.2.2 Initial immunisations with whole cTnI

Immunisations of a chicken were previously performed with the whole cTnI protein. Subsequently, a library was constructed and bio-panned against the immobilised cTnI protein (Dr. Stephen Hearty and co-workers). This library showed a poor spread of epitope-specificity which was analysed for by solid-phase ELISA against the designed peptides and the library exclusively yielded anti-peptide-3 scFvs (4G5- see section 5.3).

Potential epitope-1 and -2-specificity was evaluated from the chickens serum taken at expiry (section 2.3.2.2). Figure 3.2-2 is the serum titration result for the synthetic peptides in various forms. Reactivity for epitopes-1 and -2 was analysed in C- and N-terminal conjugation strategies to biotin. Additionally, the peptides C-terminal conjugated to KLH and the cTnI protein were included in the analysis.

When comparing the C- and N-terminal conjugated peptide-2, Figure 3.2-2 shows the major difference in the animal's response to the conjugation terminus of the peptide. The antiserum to the C-terminally conjugated peptide-2 (both biotin and KLH) had a relatively high titre. However, the N-terminal conjugated peptide-2 (to biotin) did not show a titre. This suggests that the conjugation terminus impacted the display of the synthetic epitope to the antibodies available in the serum. Peptide-1 binding responses were not observed for either the N- and C-terminal conjugation chemistries.

Overcoming this demonstrated lack of epitope-specificity was the main goal of the work presented in this thesis. To overcome the limited epitope spread, synthetic epitope-based immunisations were employed throughout and this approach was successful for antibody generation.

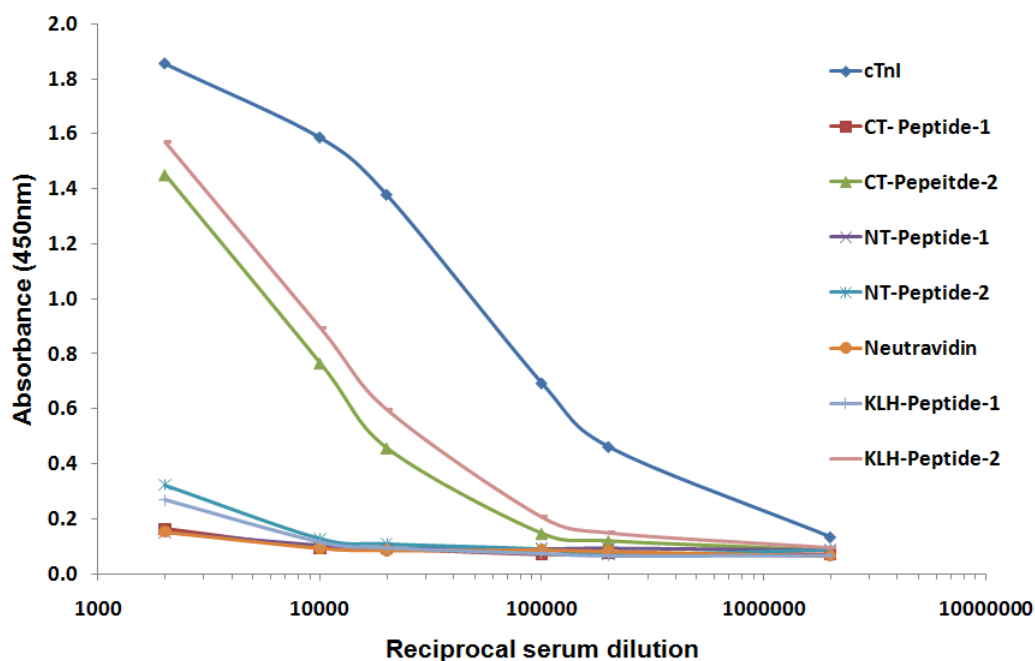


Figure 3.2-2: Evaluation of immune response to the synthesised peptides from a chicken immunised with cTnI

The serum from a chicken previously immunised with cTnI (commercial protein) and from which an anti-cTnI scFv library was constructed was tested for its antibody reactivity to the synthetic peptide epitopes. The serum was titrated in a typical serum ELISA format against the cTnI protein and various formulations of the synthetic epitopes and a control, neutrAvidin. Peptide-1 and -2 were assayed in N-terminal (NT) and C-terminal (CT) conjugations to biotin and also as CT-KLH conjugates. Specific IgY was detected using an anti-chicken IgY-Fc-specific antibody labelled with HRP.

3.2.3 Recombinant Troponin I

Due to the demonstrated antigen quality issues the availability of a recombinant form of the cTnI protein would be advantageous and was investigated to provide a stable and consistent antigen. Full length cTnI, minus the initial regulatory region, was expressed and purified in work carried out by others, independently [103], and more typically co-expressed with TnC and cTnT in *E. coli* [104-106]. Initial efforts sought to achieve soluble expression of the truncated Troponin I protein (rTnI) as an ideal antigen. This was the most logical and desired construct as it would have approximated the natural isoform well. To this end a gene construct was designed and synthesised.

3.2.3.1 Cloning strategy for recombinant Troponin I

A gene construct was synthesised commercially by Genscript (USA, Inc.), following optimisation for expression in *E. coli*. It contained the amino acid sequence shown in Figure 3.2-3. The construct was flanked by BamHI and HindIII sites for cloning into the pUC57 vector. Subsequently, the NcoI-HindIII sites were used to transfer the gene into a pET expression vector. The gene was designed without the 28 amino acid N-terminal regulatory sequence of cTnI which is known to hinder its expression in *E. coli* [104, 105]. The N-terminal methionine sets the frame for translation and results in cleavage of the signal sequence from the protein in vectors that transport the protein to the periplasm. The N-terminal alanine, exposed due to proteolytic cleavage of the leader sequence, was selected by accounting for the “N-terminal amino acid rule for *E. coli*” and both Met and Ala are known to be stabilising in terms of protein degradation [107].

GSHAMAN¹NYRAYATEPHAKKK²SKIS³ASRKLQ⁴LKTLLQIAKQELEREAEERRGEKGRALST
 RCQPLELAGL³GFAELQDLCRQLHARVDKVDEERYDIEAKVTKNITEIADLTQKIFDLRGKF
 KRPTLRRVRISADAMMQALLGARAKESLDLRAHLKQVKKEDTEKENREVGDW⁴RKNID
 ALSGMEGRKKKFESKL

Figure 3.2-3: Design and amino acid composition of the rTnI gene

This is the gene sequence that was synthesised with BamHI (blue shading) and HindIII (purple shading) restriction sites for insertion of the gene into pUC57. Sub-cloning *via* the NcoI (red shaded) and HindIII restriction sites was carried out into a number of pET vectors. Peptide 1-4 are coloured (1: Red, 2: Gold, 3: Green and 4: Blue).

3.2.3.2 Results

The rTnI gene (pUC57 - Figure 8.1-6) was transformed into *dcm⁻/dam⁻ E. coli*, propagated and plasmid purified, as described in section 2.3.1.2. Subsequently, the gene was prepared for transfer into the pET26b vector by restriction digest (section 2.3.2.3.1). Post digestion, the rTnI gene (~600bp) and pET26b vector (~5.4kb) were resolved (Figure 3.2-4), purified by gel extraction, ligated and transformed into BL21(DE3)pLysS cells. Additionally, the gene was ligated into pET32b(+) and pET28b(+) and transformed into the same cell type.

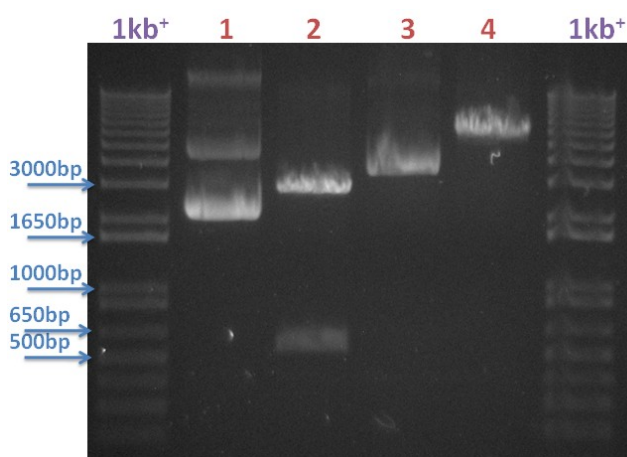


Figure 3.2-4: rTnI gene cloning from the maintenance vector into an expression vector

The restriction digestions were analysed by 0.5% (w/v) agarose gel electrophoresis. Lane 1: undigested pUC57 containing the rTnI gene. Lane 2: double NcoI and HindIII digested pUC57 with a drop out band at approximately 600bp (expected 582bp). Lane 3: pET26b(+) vector. Lane 4: double NcoI and HindIII digested pET26b(+). 1kb⁺: DNA ladder.

Expression of the protein from individual clones (section 2.3.2.3.2) was screened for by SDS-PAGE and WB using the Hytest 16A11 HRP-labelled mAb (anti-epitope-3) and the anti-HIS HRP-labelled antibody as probes. Figure 3.2-5 shows specific bands at a slightly higher molecular weight (~27kDa) than was expected (~24kDa). However, this apparent molecular weight increase is a known phenomenon in electrophoresis of TnI [103] due to the very high positive charge at neutral pH. In both Western blots specific bands were observed suggesting correct heterologous expression of the construct.

Purification of the expressed protein sought to exploit the hexa-HIS-tag by IMAC (section 2.3.2.3.3). Repeated attempts to purify the protein from *E. coli* lysate were unsuccessful despite extensive efforts at optimisation of the buffers, purification steps and lysis conditions (results not shown). Some success was experienced using cation exchange (section 2.3.2.3.3) due to the extremely high positive charge of cTnI at neutral pH. However, attempts to drive the expression levels higher, in larger scale protein production, did not result in increased levels of protein from the purification. The expression of rTnI also became variable, possibly due to the toxicity of the protein to the *E. coli* host leading to plasmid instability.

The relatively poor expression of rTnI as a soluble antigen was not overly surprising as the high pI of the protein was anticipated to be problematic to express in *E. coli*. Recombinant TnI was expressed readily as inclusion bodies from *E. coli* when cloned into the pET28b(+) vector. When cloned into this expression vector (removing the associated solubility enhancing fusions) large protein quantities could be expressed as insoluble protein as illustrated in Figure 3.2-6. The challenge outlined in this chapter was to develop an easily *solubilised* antigen free of modifications due to harsh denaturants (e.g. urea) that would be required to solubilise the protein for purification under denaturing conditions. Despite its successful expression as an inclusion body in its current form the antigen was not as what was required and the recombinant antigen strategy was further refined.

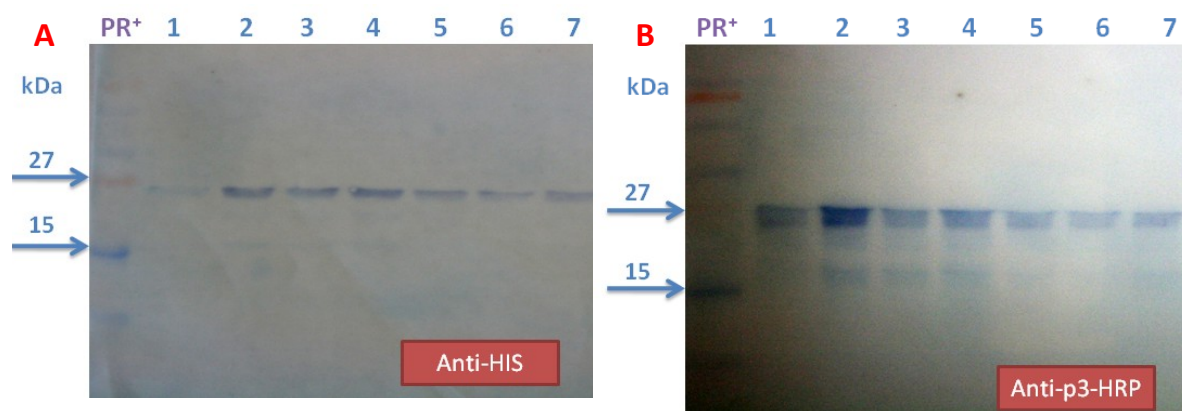


Figure 3.2-5: Western blot detection of rTnI secreting clones

Western blots were prepared from SDS-PAGE of *E. coli* lysates and probed with anti-HIS HRP-labelled (A) and anti-epitope3 HRP-labelled (B) antibodies. Specific bands were visualised at approximately 27kDa for the soluble protein. PR⁺: Prestained protein ladder. Lanes 1-7: individual clones expressing the protein.

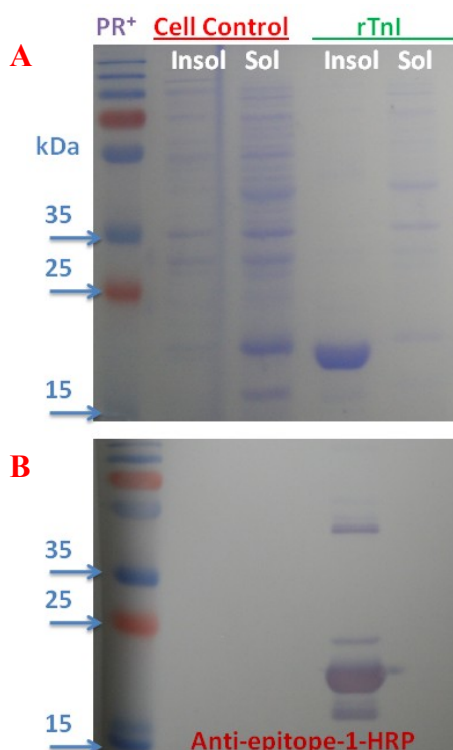


Figure 3.2-6: Expression of rTnI as an inclusion body in the pET28b vector

The expression of rTnI in the pET28b(+) vector in BL21pLysS cells. The cell control was the BL21pLysS cells without the vector. Both the test and control were induced and prepared in a similar fashion. 'Insol' and 'sol' labels are the insoluble and the soluble protein fractions, respectively. The soluble fraction was obtained by lysis of the cells and removal of the cellular debris by centrifugation. The insoluble fraction was prepared from the soluble fraction pellet. The SDS-PAGE (A) and transferred WB (B) show the presence of the protein (rTnI) in the insoluble fraction which is relatively pure, but is absent in the soluble fraction. PR⁺: Prestained protein ladder

3.2.3.3 *Conclusion and adaption of the cloning strategy*

rTnI was successfully cloned into and expressed in *E. coli*. However, its purification by IMAC was not feasible from the soluble expressed protein fraction. This suggested that the HIS-tag may have been associated with some region of the rTnI protein and was unavailable to interact with the nickel resin. Purification by cation exchange chromatography protocol could not be achieved with the soluble protein. Attempts to re-express these clones proved unsuccessful suggesting plasmid instability due to the toxicity of the protein. It must also be noted that the rTnI gene was also examined in pET32b+ vector as an alternative strategy (results were not shown). With marginally greater success in the IMAC purification, where the rTnI bound to the column, the eluted protein was truncated and highly contaminated. Polishing steps to isolate the rTnI by cation exchange were unsuccessful in this construct which may have been impacted by the presence of the S-tag and Trx-tag as fusions to the protein altering the overall charge. Soluble fusions and leader sequences in this case did not lend themselves to improving the quality or solubility of the recombinant protein. The cytoplasmic expression of rTnI in pET28b yielded inclusion bodies of relatively high-purity. This was not the ideal means of protein isolation, as the re-folding of proteins is not a trivial exercise. This methodology was further complicated by the use of harsh denaturants, such as urea. The use of urea can potentially cause disadvantageous modifications to the protein, for example, carbamylation resulting in a protein preparation that was not representative of native antigen. To simplify the issue, it was decided to heavily truncate the TnI gene to be expressed removing the highly-charged regions which are involved in interactions with cTnT and TnC.

3.2.4 Expression of epitope 1 and 2 regions as a fusion to the fatty acid binding protein (FABP)

It was discovered in our laboratory that a small cytoplasmic human protein, heart-type fatty acid binding protein (h-FABP), was notable for its high level of expression and ease of purification. Hence, it was proposed as an optimal fusion partner to assist the expression of the epitope-1 and -2 regions of TnI in a more efficient way than the multiple tags introduced by the pET vector systems.

3.2.4.1 Cloning strategy for the FABP fusion construct

Owing to the small size of the combined epitope region (27 amino acids), to effectively express it in *E. coli*, a strategy to fuse it to a ‘carrier’ protein was adopted using h-FABP. The small size (14.8kDa) and cytoplasmic nature of the protein was beneficial coupled with the availability of several high-affinity antibodies to the protein which could aid detection and if required purification [90]. A gene construct was designed ‘in-house’ (section 2.3.2.4.1) and synthesised commercially by Genscript (USA, Inc.) as illustrated diagrammatically in Figure 3.2-7. FABP was linked to the N-terminus of the epitope-1 and -2 regions via a flexible serine-glycine linker which is well tolerated in *E. coli*. Within the construct restriction enzyme sites provide directionality to the gene for cloning into the expression vector (*NcoI* and *NotI*) and modularity allowing insertion of different linker/non-linker variants (*BamHI*, *SacI* and *NotI*). With no requirements for the formation of disulphide bonds the gene was cloned into pET28b+ (Figure 8.1-4) removing the N-terminal His-Tag and T7-Tag by virtue of the *NcoI* restriction site. Transformation was carried out into *E. coli* Tuner™ (DE3) cells, which are *LacZY* BL21 mutants (Novagen) and uptake IPTG in a uniform fashion allowing homogenous expression of vectors under control of *T7lac* promoter. The biophysical properties of the expressed protein are summarised in Table 3.2-1.

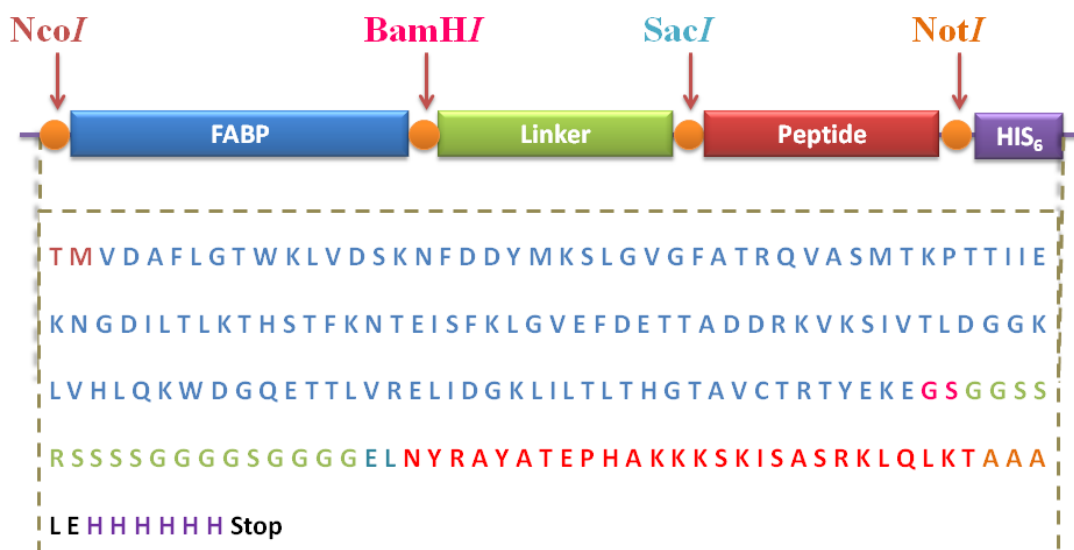


Figure 3.2-7: Schematic overview of FABP peptide 1 and 2 fusion construct

The epitope one and two region gene was synthesised as fusion protein to heart-type fatty acid binding protein (h-FABP) joined by a flexible linker (GGSSRSSSSGGGSGGGG) and cloned into the pET28b+ vector encoding a hexa-histidine tag *via* *NcoI* and *NotI* restriction sites. The *SacI* and *BamHI* restriction sites facilitate any further utility of this vector construct as an expression partner. The amino acid sequence for the gene in the pET28b vector is shown, as colour coded in the diagrammatic representation.

Table 3.2-1: Biochemical properties of FABP-P1&2 fusion protein

Molecular Weight (kDa)	20.89
Number of Amino Acids	192
Estimated pI	9.19
Charge at pH7.00	7.3
Extinction Coefficient at 280nm (M⁻¹ cm⁻¹)	16500

3.2.4.2 *Screening, expression and purification*

Initial selection of colonies post transformation was carried out by SDS-PAGE and WB (section 2.3.2.4.2). Three clones were taken forward to screening and compared in parallel to Tuner™ cells containing no plasmid. All the selected clones were tested with and without induction by IPTG on 12.5% (w/v) SDS-PAGE and WB (Figure 3.2-8). From the initial screening SDS-PAGE gel, over expression bands were observed in the induced clones at an apparent MW above 15kDa (suggested to be 20.8kDa expected band) with no bands in the un-induced cells combined with complete absence in un-transformed Tuner™ cells. The specificity of this band was confirmed by a WB transfer probed with an anti-HIS HRP-labelled antibody. To further evaluate the reactivity of the expressed fusion protein a series of SDS-PAGE and WB were performed in parallel on one selected clone (clone # 1), which was taken forward due to its marginally greater apparent expression in Figure 3.2-8. In these Western blots, six available antibodies were utilised to probe the protein. In Figure 3.2-9 broad bands were observed for virtually all the antibodies used, save the anti-HIS HRP-labelled probe. This suggested that there may have been some truncation of the protein possibly due to degradation in lysate (lysate was retained at 4°C O/N), but more likely due to premature termination of translation of the protein. However, the discrete anti-HIS band was encouraging as the C-terminal HIS-tag resides at the end of the full-length protein permitting purification on IMAC of only the correctly expressed full-length protein.

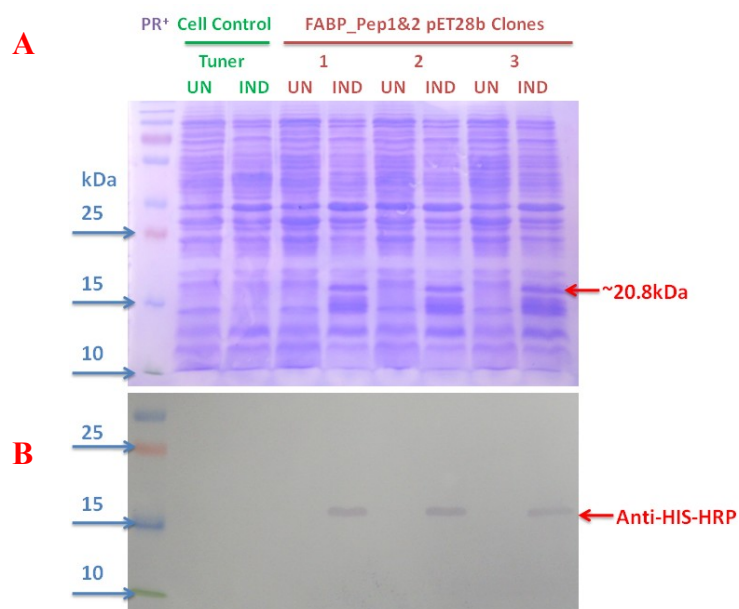


Figure 3.2-8: Initial screening of FABP-P1&2-expressing clones

The vector was transformed into Tuner™ cells and three clones were compared to an un-transformed Tuner™ cell control in a small-scale expression experiment (10mL SB, 0.2mM IPTG, 4 hours at 30°C) by SDS-PAGE (A). All clones were tested in un-induced (UN) and induced (IND) states. For all three selected clones over-expression bands (approx. 20kDa apparent molecular weight) were observed in the IND lanes only as verified in WB (B) using an anti-HIS HRP-labelled probe. In addition, the Tuner™ control shows no over-expression bands. The molecular weight was assigned by comparison to the prestained protein ladder (PR⁺).

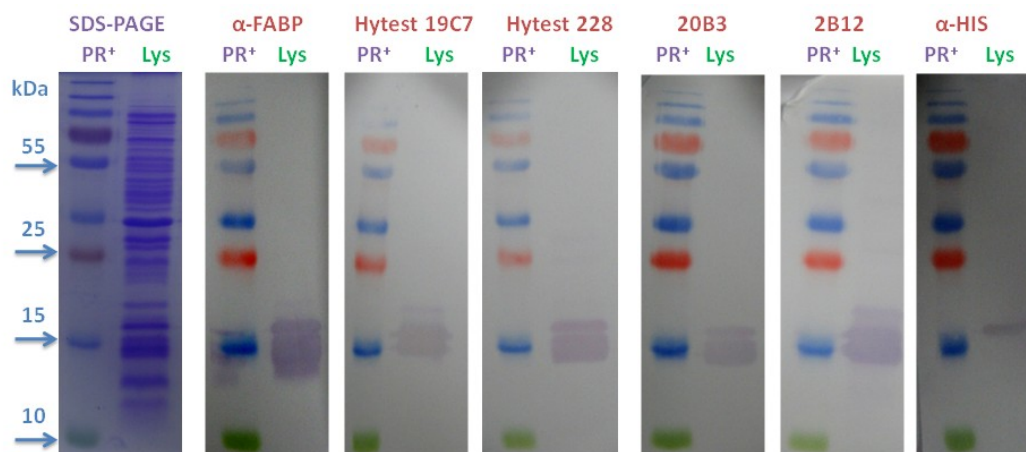


Figure 3.2-9: SDS and WB analysis of antibody reactivity with expressed FABP-P1&2 fusion

Analysis was carried out using a battery of anti-cTnI-epitope antibodies. SDS-PAGE (LHS) of clone # 1 induced and lysed. Multiple transfers of the resolved lysate were prepared in series and probed with various antibodies; anti-FABP ('in-house'), Hytest control antibodies 19C7 (epitope 1) and 228 (epitope 2), 'in-house' anti-epitope antibodies (20B3 – epitope-2 and 2B12 – epitope-1) and the anti-purification tag antibody (anti-HIS). 19C7 and anti-HIS were both HRP-labelled facilitating direct detection. MAbs 228 and 20B3 were detected using an anti-mouse HRP-labelled secondary antibody and the recombinant antibodies (anti-FABP and 2B12) were detected using anti-HA HRP-labelled secondary antibody. PR⁺: Prestained protein ladder.

To ensure maximal protein expression to support efficient purification yields a small-scale study of the effect of IPTG concentration and induction time was carried out at 30°C (section 2.3.2.4.3). From Figure 3.2-10 it was concluded that irrespective of IPTG concentration after 5 hours induction, the protein expressed well, but the appearance of a slightly increased MW band was observed. From the 2.5 hour induction profile, an IPTG concentration independent expression profile was observed, where even minimal IPTG concentration fully turned on protein expression. This was likely as a result of the uniform uptake of IPTG by the Tuner™ cells due to the *lacZY* mutation. Marginally more protein appeared to be expressed at 0.2mM IPTG and this was adopted as one of the optimal conditions for large-scale expression.

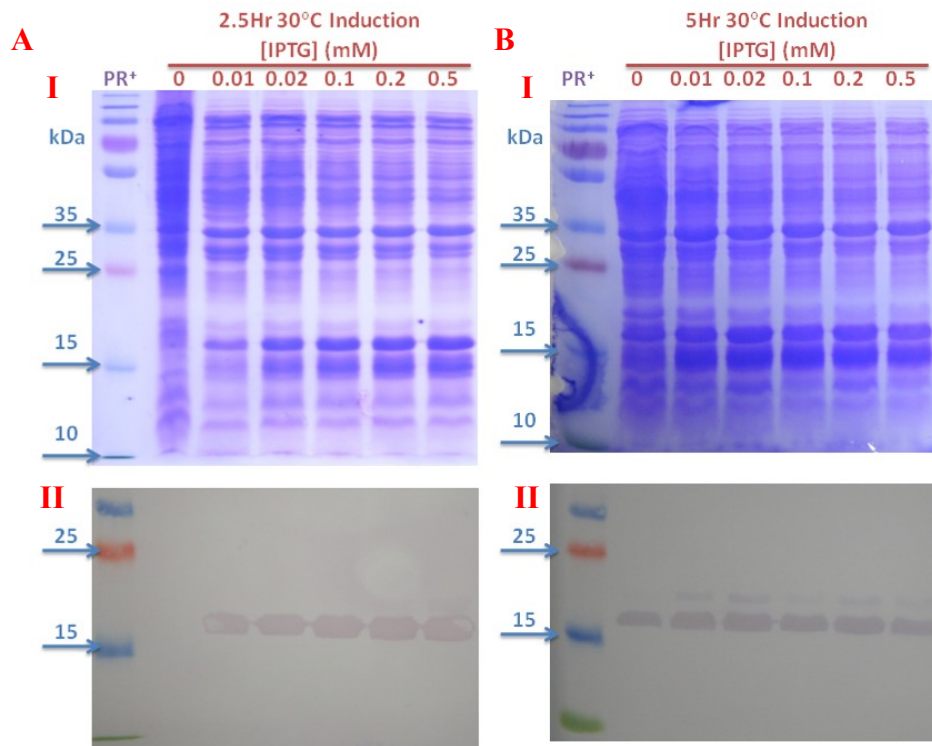


Figure 3.2-10: Optimisation of expression of the selected FABP-P1&2 clone

The IPTG concentration and length of induction time were examined by SDS-PAGE (I) and WB (II). Samples were taken at two time points; 2.5 hours (A) and 5.0 hours (B) over a range of IPTG concentrations (0-0.5mM) as indicated above the lanes. SDS-PAGE of the cytoplasmic cell extractions were subsequently WB transferred and probed with anti-HIS HRP-labelled detection antibody. PR⁺: Prestained protein ladder.

The protein was expressed in large-scale and then purified by IMAC as detailed in section 2.3.2.4.4. Initial purifications were hampered by removal of the protein from the column by simply washing in PBS-based wash buffers. Adoption of NaH_2PO_4 buffers for purification (with the removal of Tween®20) followed by optimisation of both salt and imidazole concentration proved more efficient than the PBS-based buffers (Figure 3.2-11). Subsequently, large-scale purification yielded 1.68mg/mL (3.3mg total from a 400mL culture) of fusion protein as determined by absorbance (280nm) measurement. The purified fusion protein was visualised on SDS-PAGE, transferred to nitrocellulose and probed with commercial and in-house antibodies for purity. The anti-epitope-1 (Hytest 19C7 and 2B12), anti-epitope-2 (Hytest 228 and 20B3) antibodies were used in a WB confirming specificity as illustrated in Figure 3.2-12. Some additional bands were visible, but a high proportion of the desired MW protein was purified. Polishing steps to improve the purity were undertaken at this stage to reduce the number of bands in combination with an alternative purification strategy, cation exchange chromatography. However, when carried out with crude lysate another similarly charged protein bound to and eluted from the exchange column. This strategy from crude lysate was inefficient, but could easily be combined with an initial IMAC purification to form a two step purification protocol. When combined with gel filtration chromatography, the protein preparation was found to be extremely pure and to exist predominantly as a monomeric fraction (even after prolonged storage at -20°C). Figure 3.2-13 is the gel filtration profile for the fusion protein, as described in section 2.3.2.4.5. In this case the purity was $\geq 98\%$ and suitable for kinetic studies. Prior to this, precise measurement of the concentration of protein was necessary. This was carried out using hFABP from a commercial source (c-hFABP) and the anti-hFABP clone (H2) in an inhibition assay (section 2.3.7.1). The inhibition assay was carried out at a pre-determined antibody dilution by titration and a standard curve constructed by inhibition of binding to the immobilised hFABP with free c-hFABP. Prepared dilutions of the purified FABP-P1&2 fusion were assayed in parallel allowing determination of the true protein concentration from the standard curve. An average of $56.86 \pm 3.56 \mu\text{M}$ ($n=3$) FABP-P1&2 fusion was calculated which equated to a true protein concentration of $1.19 \pm 0.07 \text{mg/mL}$. The correct determination of protein concentration was critical for its use in 1:1 interaction kinetics where the concentration of the analyte is crucial for accurate kinetic constant analysis.

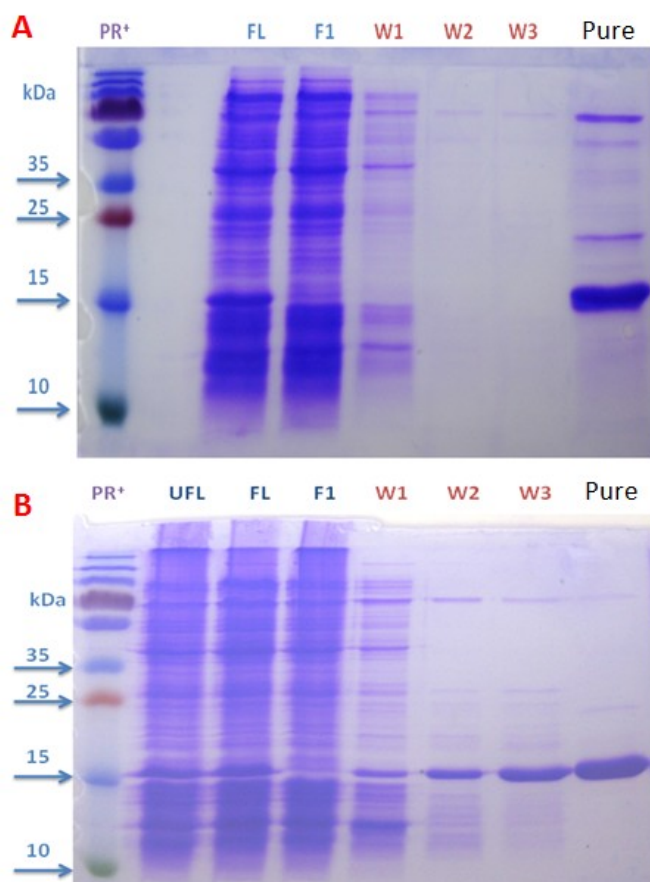


Figure 3.2-11: Optimisation of salt and imidazole concentration for purification of FABP-P1&2 fusion

SDS-PAGE analysis of the purification conditions was carried out. The lanes are labelled as follows; PR⁺: Prestained protein ladder, UFL: unfiltered lysate, FL: flow-through, F1: flow-through, W1-3: washes 1-3 and Pure: purified fraction

- A) Variation of the salt concentration with a fixed imidazole concentration (10mM). W1: 100mM, W2: 150mM, W3: 300mM NaCl. Little difference was observed greater than 100mM NaCl. However, some higher MW bands were present in the pure fraction. To overcome the presence of these bands imidazole concentration was optimised.
- B) Variation of the concentration imidazole in the wash buffers at 100mM NaCl. W1: 10mM, W2: 15mM and W3: 20mM imidazole. These modified buffers yielded pure protein without any contaminating bands. In this case the use of increasingly stringent washing caused some loss of the desired protein. However, this was countered by the relatively pure protein fraction collected.

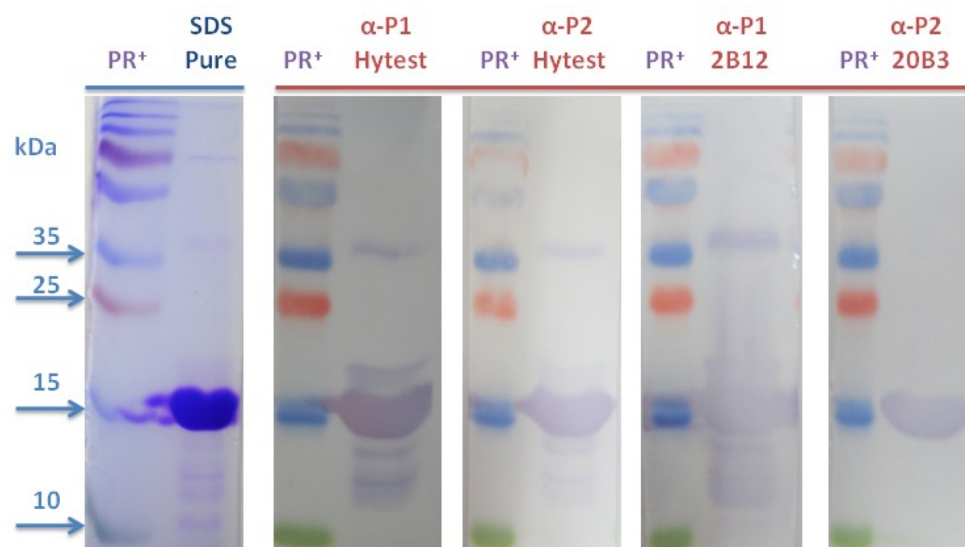


Figure 3.2-12: Large-scale, optimised purification of recombinant FABP-P1&2 protein by IMAC

The protein was purified by IMAC adopting the optimised NaH_2PO_4 -based buffers and yielded a pure fraction by SDS-PAGE analysis. Furthermore, the presence of FABP-P1&2 fusion protein was confirmed by WB using the epitope-specific antibodies available, as labelled on the image. PR⁺: Prestained protein ladder.

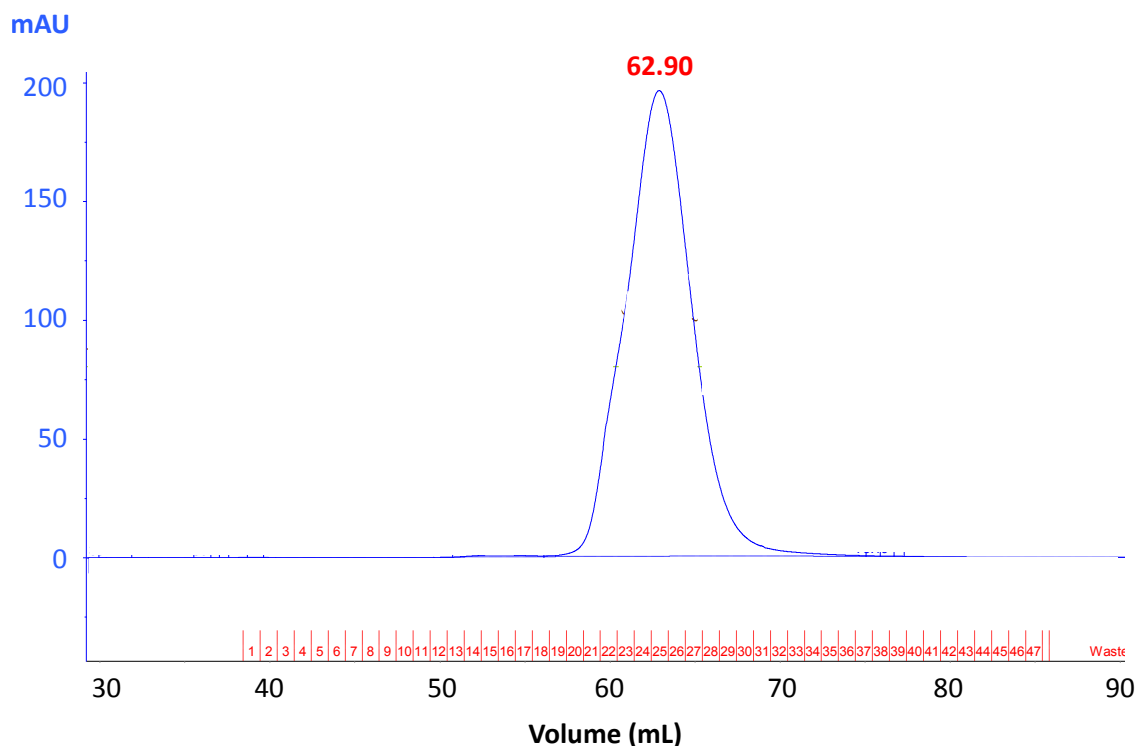


Figure 3.2-13: Gel filtration elution profile of recombinant FABP-P1&2 protein

The purified protein was applied to a HiLoad S75 16/60 gel filtration column at a flow rate of 1 mL/minute in 1X PBS buffer containing 0.02% (w/v) NaN_3 . The image is cropped to show only the volumes where the fractions were collected and the peaks observed. At 62.90mL the peak maximum was reached and demonstrated the FABP-P1&2 fusion protein to be highly soluble and stable.

3.3 Chapter conclusions

At the onset of the project a previously existing, whole protein immunised, avian library was available and screened using the custom designed cTnI peptides to evaluate the spread of epitope-specificity. This library exclusively yielded anti-epitope-3 or undefined epitope anti-cTnI antibodies (section 5.3). To assess the coverage of other non-immuno-dominant epitopes in this library the serum was titred against the C- and N-terminally conjugated peptides. This comprehensively demonstrated that there was no specificity for epitope one, but potentially specific-antibodies for epitope two (only in the C-terminal conjugated peptide form). The terminus of conjugation is typically arbitrarily assigned, but sequences from N-terminal regions of a protein are recommended to be conjugated *via* their C-terminus and *vice versa*. It cannot be definitively concluded that the whole protein-based immunisation approach did not contain antibodies specific to the epitope-1 region, rather that the strategy did not elicit antibodies capable of recognising both the native and synthetic variants of the epitope. The likelihood of extracting conformationally-sensitive epitope-specific antibodies from this library for epitope-2 was severely diminished, as the bio-panning experiments would have to be carried out using the synthetic peptide. Indeed, numerous blocking bio-panning experiments (using anti-epitope-3 antibodies bound to cTnI) were undertaken to increase the likelihood of extracting anti-epitope-2 scFv which failed to isolate the required antibodies. Immunising with a protein and screening against a peptide epitope potentially fails to enrich for conformation-specific recombinant antibodies, as was seen in this case. The library described here was bio-panned against the cTnI protein and the unpanned library was only available as a cell stock not a cDNA stock. With differing levels of representation for each clone (i.e. each cell) in the transformed library, amplification from cell-stocks can often introduce a bias due to differences in the specific-growth rate of the cells. The best bio-panning experiments are carefully built upon efficient amplification of the genes into the vector, transformation and immediate display on the phage for bio-panning. While numerous factors affect various stages of that process (e.g. mRNA quality, PCR and transformation efficiency) moving immediately into the bio-panning experiments ensures that the representation of each of the antibodies displayed is not affected by cell-storage.

Immunisation strategies based on the use of the synthetic epitopes conjugated to a carrier protein (e.g. KLH) improve the chances of accessing those conformation-specific antibodies by bio-panning with the native protein and numerous examples of successful peptide immunisation strategies are available [108, 109] particularly in the area of vaccine development [110-112]. This strategy of synthetic epitope immunisation was adopted successfully and led to the development of both hybridoma (anti-epitope 2 – section 4.2) and recombinant antibodies (anti-epitope 1 – section 5.2) with potential applications in cTnI diagnostic platforms.

Overcoming the issues linked to the quality of the available antigen (section 3.2.1) was a significant challenge and the use of recombinant antigen expression proved to be a successful strategy that led to the efficient characterisation of the selected antibodies (section 5.2). The use of recombinant protein expression technologies is wide-spread with many examples of successes and at least as many, if not more, failures. The strategy proved multifaceted due to a number of intrinsic factors primarily surrounding the expression and purification of a difficult-to-express, highly charged, human protein in *E. coli*. Despite overcoming some of these barriers with truncated cTnI expression, downstream purification was a significant issue. This resulted in strategies that sequentially reduced the length of the protein to be expressed, culminating in successful expression and, crucially, purification of the epitope 1 and 2 regions as a fusion to FABP. The fusion protein proved to be a readily expressed and purified protein which was highly stable even after prolonged storage. The successful isolation of the FABP-P1&2 fusion protein permitted accurate characterisation of the developed antibodies with a soluble, stable and consistent representative antigen.

Broadly speaking, the availability of vast amounts of bioinformatic, structural and genetic information surrounding many human and animal proteins is unprecedented. A knowledge-driven and rational approach to epitope targeting is not only a possibility, but is strongly advised in light of such quality information being readily accessible. The source and availability of quality antigen prior to attempting to generate any antibody is paramount and is a widely accepted key factor. To rationally target specific epitopes multiple versions of an antigen are hugely beneficial and a prerequisite to highly-specific antibody generation: i) for immunisation, ii) to perform selections or screening campaigns with a different form of the antigen than was immunised and iii) to rigorously characterise the generated antibodies in multiple approaches. While not all antibody generation campaigns require such absolute

and dedicated epitope-specificity, it is of particular importance in the development of sensitive assays using novel antibodies in a clinical-diagnostic setting.

The approach to antigen development undertaken was dictated by the specific assay requirements; compatible sandwich assay pairs that were specific to absolutely defined epitopes on a human structural protein. The process was initially instigated due to the poor epitope spread found with cTnI protein-based immunisations and led to substantial optimisation of the procedures followed, including synthetic-peptide chemistry for antigen generation and recombinant methodologies for protein expression. The experience gives one an appreciation for the complexity of the process, but the successful application of the approach to antibody generation validates the feasibility of the strategy and the thought processes and stratagems needed for difficult to work with or scarcely available antigen.

Chapter 4: Monoclonal Antibodies

4.1 Introduction

4.1.1 Hybridoma technology

Nobel laureates (1984) Kolher and Milstein invented what has become the most freely available and hence, widely used method to generate monoclonal antibodies [113]. Hybridoma technology was exploited to generate anti-epitope-2-specific antibodies from a murine repertoire.

Hybridoma generation involves the immortalisation of B-lymphocytes, harvested from mice immunised with a specific antigen, by fusion with a myeloma cell to generate a stable hybrid cell line with characteristics of both parental cells. This hybridoma gains immortality from the myeloma parent and specific antibody production capacity from the lymphocyte parent (Figure 4.1-1). The most widely used fusion partners are Sp2/0-Ag14 [114] and P3X63Ag8.653 [115] and both were selected from a mouse lineage deficient in hypoxanthine-guanine phosphoribosyltransferase (HGPRT⁻). Fusion is most commonly mediated by the addition of polyethylene glycol (PEG) [116] and the fusion itself is a multifaceted process that includes cell agglutination, membrane fusion and cell swelling [117]. Often the optimal environmental conditions are variant leading to degrees of fusion efficiency that is largely thought to be affected by efficient cell-pairing [118]. More efficient strategies to fuse cells have developed, for example, bringing single lymphocytes in close contact with myeloma (cell pairing) and microfluidic control of this process [119].

Chromosome exchange occurs between the parent cells and following fusion, a heterogeneous mixture of myeloma cells, lymphocytes and many fusions of myeloma-myeloma, lymphocyte-lymphocyte and myeloma-lymphocyte are generated. To isolate hybridomas resulting from lymphocyte-myeloma fusions the following approach, involving a selective propagation regime based on the Hypoxanthine-Aminopterin and Thymidine (HAT) system, is adopted (Figure 4.1-2). This ensures that only correctly fused, potentially antibody-secreting clones are selected for. In addition, selecting for correctly fused myeloma-lymphocytes must also take into account the degree of genetic instability in the newly formed hybrid. Segregation of the chromosomes occurs at distinct periods, one occurring rapidly during the initial propagation of the fusions and another after prolonged culture [120]. With respect to mouse monoclonal hybrids this equates to large-scale loss of

hybrids in the initial scale-up followed by gradual decline in antibody-producing hybrids with increasing expansion. To counter the initial rapid segregation of chromosomes large numbers of positive clones are carried through the screening process. One of the main challenges in the procedure is the screening and characterisation of multiple potential antibody-producing clones in a rapid and judicious manner (Figure 4.1-1).

Figure 4.1-3 illustrates the concept of ‘cloning by limiting dilution’ which is vital for the isolation of clones derived from a single parental hybridoma. The methodology involves seeding the cells at such a range of densities as to maximise the probability of a single cell being distributed in a single well. This approach assumes that the majority of wells seeded (at ≤ 1 cell/well) do not demonstrate cell growth and Poisson-distribution dictates that the wells demonstrating growth contain single cells. The nature of cells disrupts this mathematical approach (due to clumping for example) and so cloning by limiting dilution must be carried out repeatedly to ensure monoclonality [99].

In parallel, the screening process must be designed to closely mimic the eventual analytical format that will be used to ensure the antibodies effectiveness in that format. The process of scale-up, specificity analysis and stability of the newly formed hybrids requires serious consideration. High-throughput interaction analysis systems offer an attractive means to assess the binding characteristics of secreted hybridoma-derived antibodies and provides valuable information to support the selection process e.g. on SPR-based instruments [121] or microarrays [122-124].

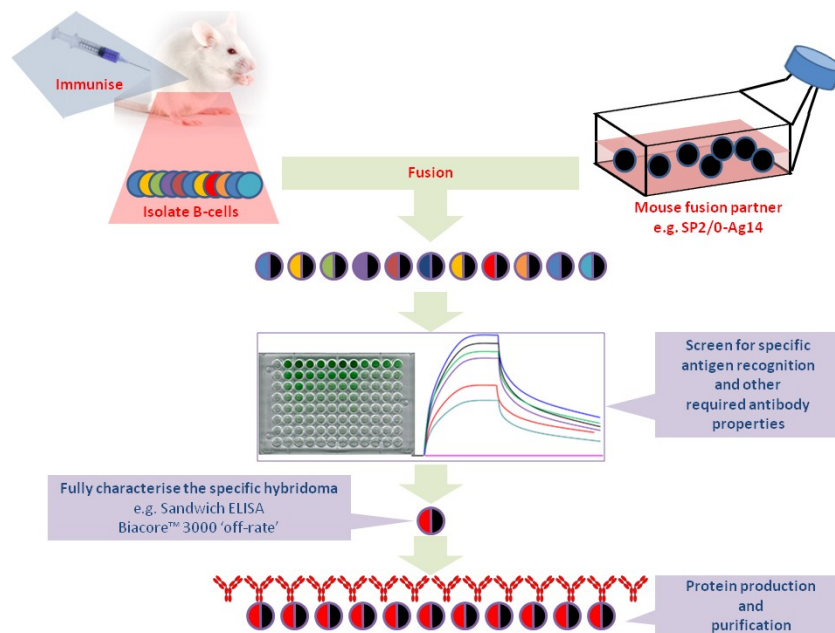


Figure 4.1-1: Schematic overview of mouse monoclonal antibody production

From an immunised mouse, B-lymphocytes are isolated and fused with a mouse myeloma cell line (Sp2/0-Ag14) creating a series of hybrid cells. Screening of the hybridoma pool is carried out to ensure only specific functional hybridomas are taken to the next stage of scale-up. Subsequently, specific clones are further characterised before expansion to purify the selected antibody.

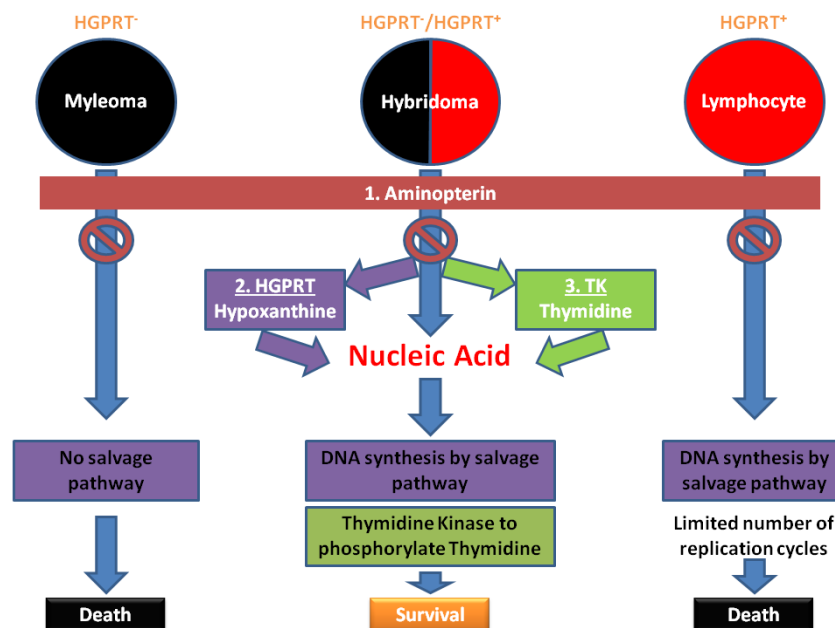


Figure 4.1-2: HAT selection for B-cell-myeloma fusions

Aminopterin blocks the *de novo* synthesis of purines (1). The enzyme HGPRT can incorporate Hypoxanthine, a source of purine precursors, into mature purines (2). Additionally, thymidine synthesis is blocked so an exogenous source of thymidine is provided which is absorbed by the cell and phosphorylated for inclusion into DNA synthesis (3). Therefore, only clones which are HGPRT⁺ can propagate in this system and only immortalised hybridomas can survive prolonged culture.

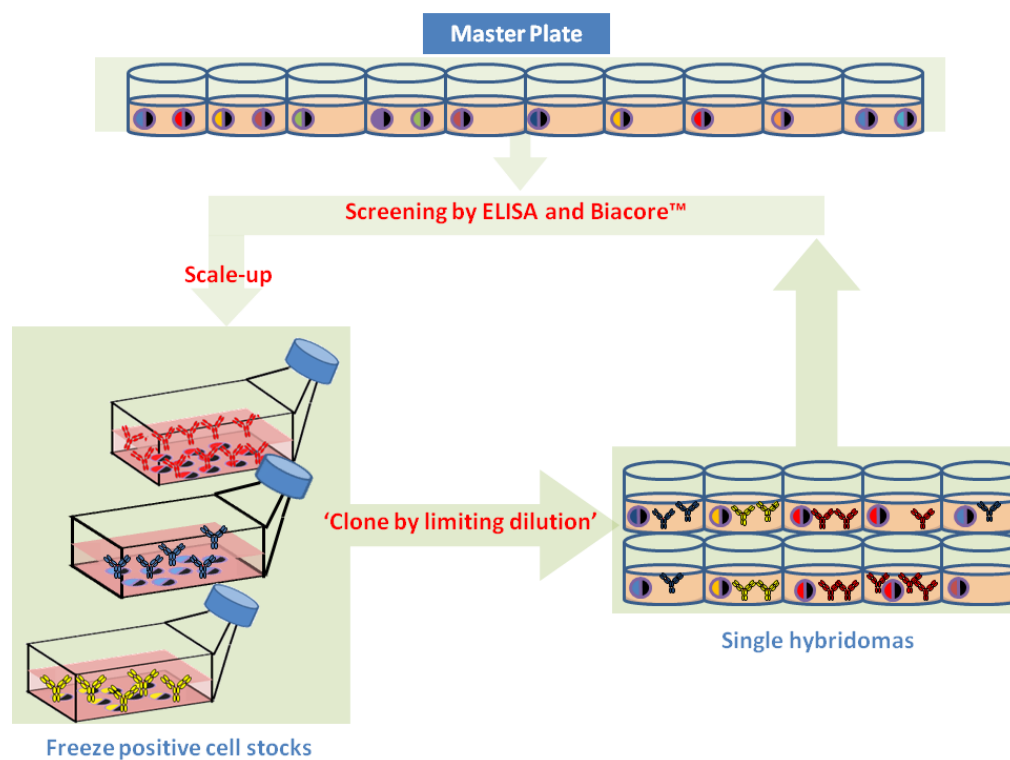


Figure 4.1-3: Schematic overview of identification and isolation of stable hybridomas

From the fusion master plate, positive wells are identified by a functional assay for the antigen of interest. Those clones secreting antibody of the required specificity, combined with other additional properties, are expanded from a 96-well format through to flasks of increasing size. Cells are harvested and plated at low concentrations to achieve one cell per well. This process must be carried out several times to ensure monoclonality. Preservation of positive hybridoma populations at numerous stages in the expansion process is necessary. The need to screen regularly to ensure continuous secretion of specific antibodies is of crucial importance.

4.1.2 Surface plasmon resonance (SPR)

The use of surface plasmon resonance (SPR)-based optical biosensors has seen tremendous growth over the last two decades, and this trend is predicted to continue as the technology becomes more accessible and its applications more diverse. SPR has emerged as the foremost and favoured technology for monitoring molecular interactions, due ostensibly to the fact that binding events can be monitored in ‘real-time’ and without the requirement for ancillary labels (Figure 4.1-4). These key attributes facilitate accurate kinetic measurements, rapid analysis times, reduced additional costs and possible heterogeneities or other complications associated with labelling of interactants.

SPR is a quantum electromagnetic phenomenon as a result of the interaction of light with free electrons at a metal-dielectric interface (surface plasmons) [125]. Most SPR-based instruments are designed in the Kretschmann configuration using a prism coupled to a dielectric metal e.g. gold (Figure 4.1-4) [126]. In this common and efficient arrangement, a metal film is deposited directly on top of a prism. P-polarised light from a light source (LED at 760nm in Biacore™ instruments) is incident on the surface (red wedge) after passing through the prism at an angle of incidence greater than the critical angle (θ_c) causing total internal reflection (TIR) to occur [125]. When the light vector matches the surface plasmon wave propagation vector, energy from the incident light couples into the surface plasmon wave leading to an enhancement of the evanescent field and a corresponding reduction in the reflected light (black line which is referred to as a minimum observed or θ_{SPR}). The minimum angle change ($\Delta\theta_{\text{SPR}}$) is a function of mass changes at the surface caused by molecular binding events. $\Delta\theta_{\text{SPR}}$ is the baseline minimum angle (θ_{SPR1} – solid black line) change after interaction between a ligand and analyte (θ_{SPR2} – dashed black line) and is reported as a change in response units (RU) in real-time [99].

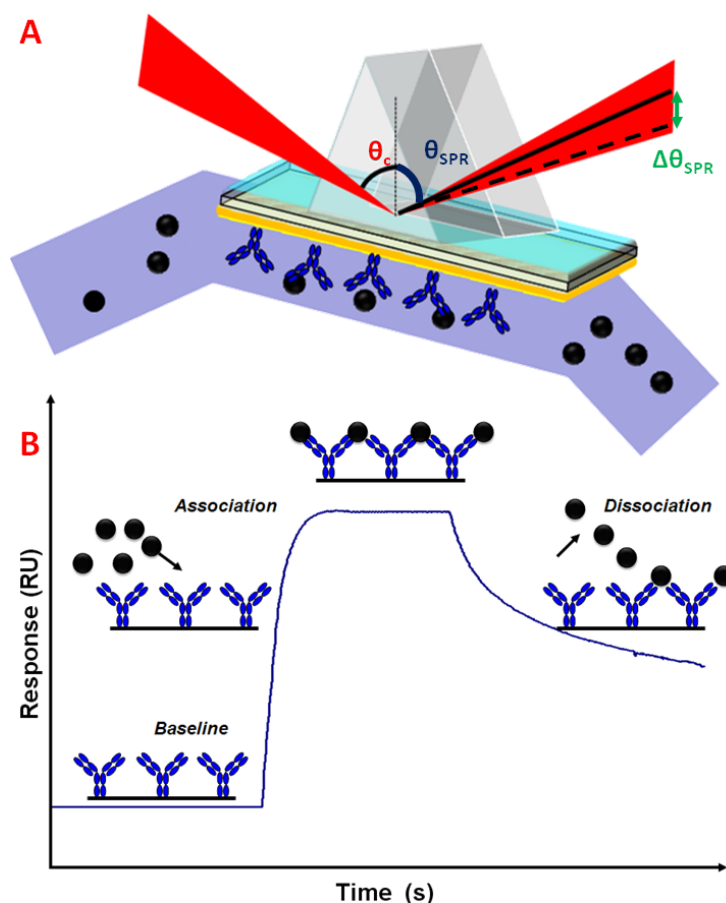


Figure 4.1-4: Overview of the surface plasmon resonance biosensor configuration

(A) Binding of analyte to ligand immobilised on the sensor chip surface is monitored in ‘real-time’ and the binding profile is reported as a ‘sensorgram’ as shown in (B). In the sensorgram buffer flow over the antibody-coupled surface establishes a baseline response. The continuous injection of analyte allows for association (binding) to occur. After the sample injection is finished, buffer flow is restored and dissociation (unbinding) is monitored. Regeneration restores the surface to baseline level (not shown). Interaction kinetics and binding affinities can be extrapolated readily from the resultant sensorgram data. RU: Response unit.

The simplest interaction is the 1:1 binding event, which can be described for immobilised ligand (A) binding to cognate analyte (B) forming a complex (AB) as illustrated by Equation 4.1-1. k_a is the association rate and k_d is the dissociation rate (see Table 4.1-1 for detailed explanation) [127].

Equation 4.1-1: 1:1 binding interaction for analytes A and B forming the complex AB

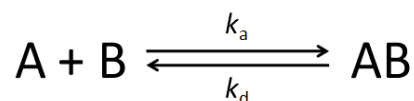


Table 4.1-1: Definitions of biophysical determinants for bio-molecular interactions

	Definition	Description	Proportionality	Units
k_a	Association rate constant (also referred to as ‘on-rate’)	No. of AB complexes formed per unit time at unit concentration of A and B.	Affinity $\propto k_a$	$M^{-1}s^{-1}$
k_d	Dissociation rate constant (also referred to as ‘off-rate’)	No. of AB complexes dissociating per unit time.	Affinity $\propto 1/k_d$	s^{-1}
K_A	Equilibrium association constant	Affinity propensity to association of A + B	$K_A = k_a/k_d = [AB]/[A][B]$	M^{-1}
K_D	Equilibrium dissociation constant	Affinity contribution to stability of AB complex	$K_D = k_d/k_a = ([A][B])/[AB]$	M

The value of truly high-throughput (HT) systems for studying bio-molecular interactions is discussed in section 5.1.10 with respect to recombinant libraries. HT-screening using SPR is also invaluable for the screening of hybridomas. The first use of such parallel screening on Biacore™ 4000 (known as the A100 at the time) was in the characterisation of hybridoma supernatants [121]. Biacore™ (GE Healthcare) is the predominant manufacturer of the SPR systems found in many research laboratories, due to its substantial market penetration, and the range of instruments that have developed since the first system in 1990. For these reasons, our lab has three Biacore™ instruments: 1000, 3000 and 4000. The 1000 and 3000 systems are low volume analysis systems and were typically used to evaluate a maximum of 20 clones in the process of this work. The HT and diverse nature of the 4000 made it the predominant workhorse for screening for specific antibodies from both hybridoma progenies and recombinant antibody libraries.

The strategies and technologies outlined above were combined with the methodologies delineated in section 2.3.3, to isolate epitope-specific antibody-secreting hybridoma clones. The synthetic-epitope immunisation regime was favoured for, with functional screening of the hybridomas using the cTnI protein. This permitted screening and isolation of hybridomas producing anti-cTnI-specific antibodies by a ‘data-rich’ selection approach.

4.2 Results of the generation and isolation of a monoclonal antibody against epitope-2 of cTnI

Hybridoma technology was employed and evaluated as an approach to isolate anti-cTnI-epitope-specific antibodies from murine repertoires. A strategy to isolate a stable, antibody-producing, specific hybridoma was developed based upon a successful immunisation strategy using the synthetic peptide-2 as antigen. To enhance the probability of isolating an antibody that was capable of binding the native protein, the initial screening of the hybridomas was carried out by solid-phase ELISA against intact native cTnI. In conjunction with this, epitope-specificity studies were carried out using the Biacore™ 4000 and ‘off-rate’ kinetics determined using the Biacore™ 3000. In combination, this approach provided accurate, high-quality, ‘data-rich’ information to rank the individual antibody-secreting hybridomas and judiciously aid in the selection process for the best candidate antibodies.

4.2.1 Immunisation of Balb/c mice with synthetic-epitope-2 conjugate

Balb/c mice were immunised with peptide-2 conjugated to KLH (section 2.3.3.1) and the antiserum produced was found to react specifically with the native epitope presented in the context of the cTnI protein (Figure 4.2-1), as confirmed by ELISA (section 2.3.3.2). To ensure that the response was specific for the synthetic epitope and not the linker, a negative control peptide was included. The ELISA showed a very high serum titre (cTnI: 1 in 1 million and peptide 2: >1 in 1 million) and the extracted spleen cells from the associated animal were used for hybridoma generation, as described in section 2.3.3.3.

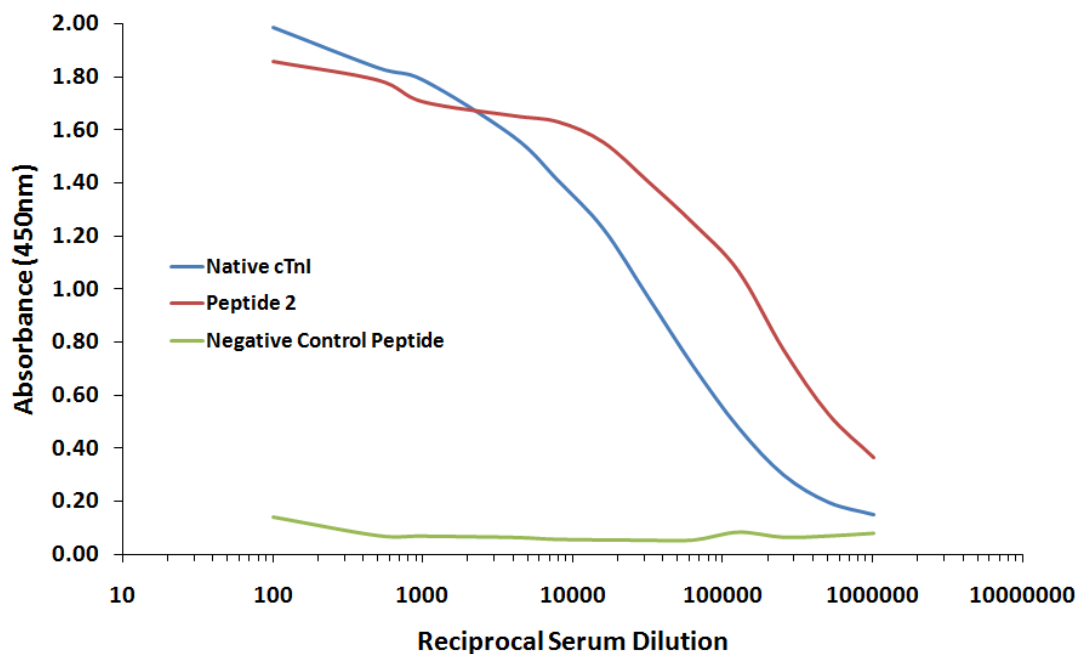


Figure 4.2-1: Anti-serum response in KLH-peptide-2-sensitised mouse

The commercial cTnI protein and neutrAvidin were coated onto the wells of a microtitre plate and blocked with 5% (w/v) PBSM. Subsequently, biotinylated peptide 1 and 2 were applied to a separate series of the neutrAvidin-coated wells. Antiserum was titrated from 1 in 100 to 1 in 1,000,000 in 1% (w/v) PBSTM and mouse IgG detected using a commercial anti-mouse-Fc-specific HRP-labelled secondary antibody. The response profile generated showed antibodies-specific for the required epitope in both its synthetic (peptide 2) and native (cTnI) forms.

4.2.2 Clone selection by data-rich screening

To strategically evaluate each clone in a judicious manner, a multi-platform analysis regime was employed with the initial focus on epitope- (on Biacore™ 4000) and protein-specificity (by ELISA and Biacore™ 3000). These core requirements were supplemented by further analysis based on functional assay screening (sandwich ELISA) and evaluation of antibody expression levels (section 2.3.3.4).

4.2.2.1 *Epitope and protein-specificity screening*

Post fusion 19.5 plates were prepared and analysed by direct binding ELISA (section 2.3.3.4.1) to identify specific antibody-secreting hybrids. The time between test and decision was typically in the order of 24 hours for ELISA-based analysis. In a steady-state analysis such as this, the signals obtained are due to unknown combinations of intrinsic affinity and the relative abundance of the secreted antibody in the supernatant [128]. However, as a starting point in the analysis it was a suitable method to identify potential positive antibody-secreting clones in the wells. To reduce the number of wells to a manageable level an absorbance level of 0.4A.U was applied as a cut-off limit. This yielded 112 clones to be carried forward for further analysis as illustrated in Figure 4.2-2.

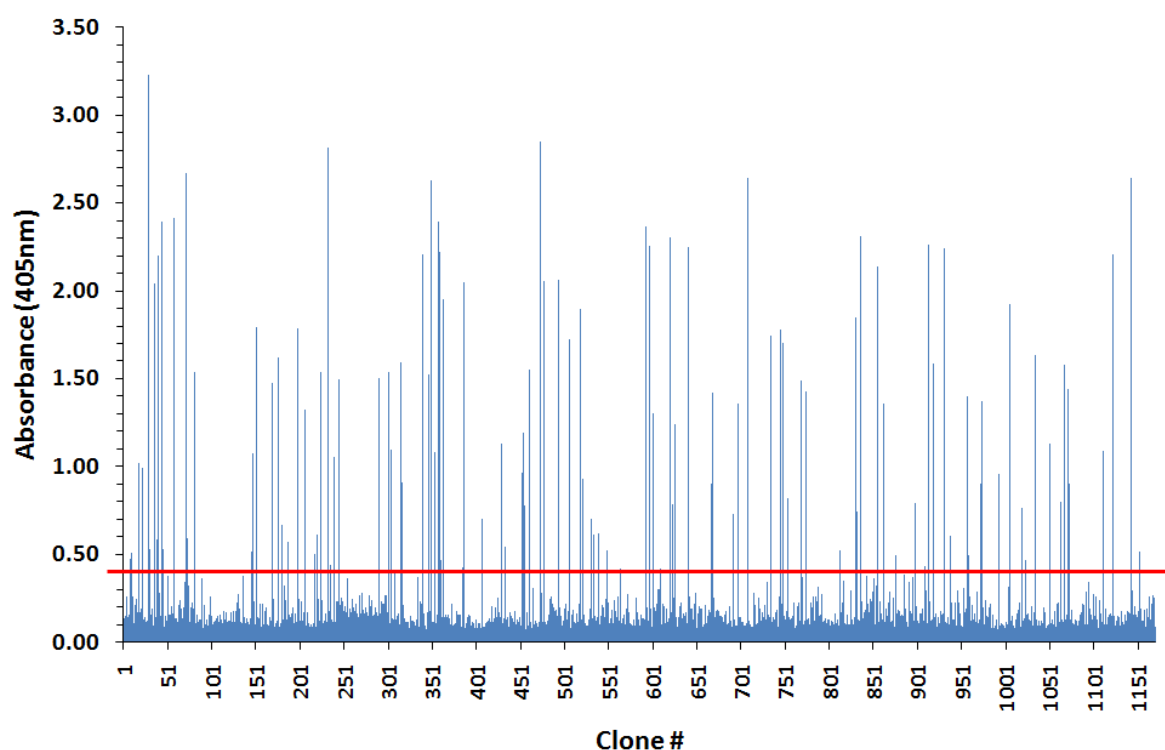


Figure 4.2-2: First screen of antibody-secreting hybridomas by a direct binding ELISA

Analysis of crude supernatants was carried out against the cTnI protein to assess for conformation-specific anti-epitope-2 antibodies. cTnI was coated onto wells of an ELISA plate at 1µg/mL followed by blocking. Diluted supernatants were applied to individual wells and specific murine IgG detected with an anti-mouse-alkaline phosphatase (AP)-labelled secondary antibody. The red line indicates the 0.4A.U. cut-off limit that was applied.

Peptide-specificity analysis was then carried out using the Biacore™ 4000 (then known as the A100) as described in section 2.3.3.4.2. This analysis confirmed epitope-specificity and eliminated issues with reactivity against the other cTnI synthetic peptides and linker chemistries. Figure 4.2-3 is an illustration of the screening experiment setup where four hybridoma supernatants per cycle were interrogated against the 4 peptides and a surface control. For each antibody, 5 independent sensorgrams were collected per cycle.

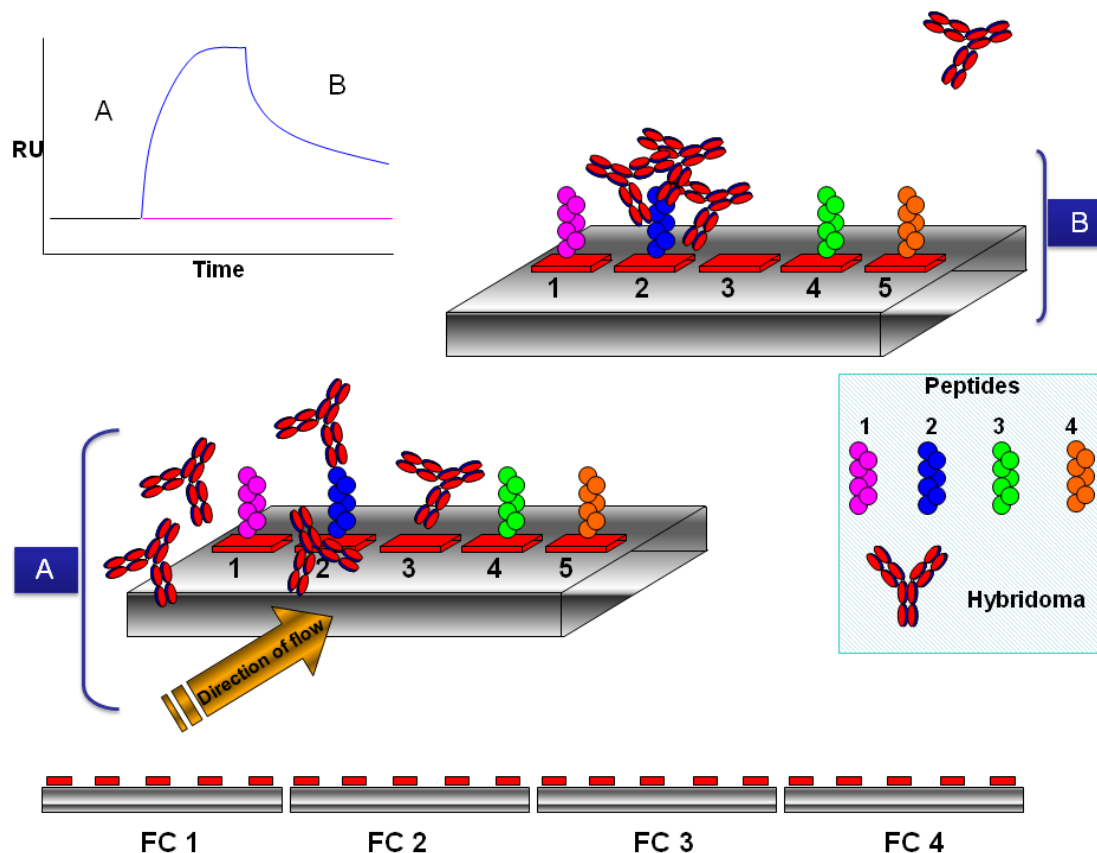


Figure 4.2-3: Biacore™ 4000 flow cell setup for epitope-specificity mapping of generated hybrids

Peptides 1, 2, 3 and 4 were immobilised on the outer spots of the flow cell with spot 3 retained as a surface control.

- Crude supernatants diluted in running buffer are applied across the flow cell, where association occurs (insert sensorgram).
- Hybridomas binding to immobilised peptide-2 and their subsequent dissociation were monitored for 12 minutes post injection.

This diagram illustrates binding of one hybridoma. In reality four hybridomas per cycle were interrogated generating curves for each spot (five per hybridoma) resulting in substantial data to rank the hybridomas.

The peptide-specificity maps collected at each stage of expansion were paired with direct binding ELISA data to ensure the isolation of specific antibody-secreting clones. Figure 4.2-4 shows the binding response levels for the 112 selected clones from the initial whole protein screen. A significant number of clones can be seen to bind exclusively to the spot where peptide-2 was immobilised.

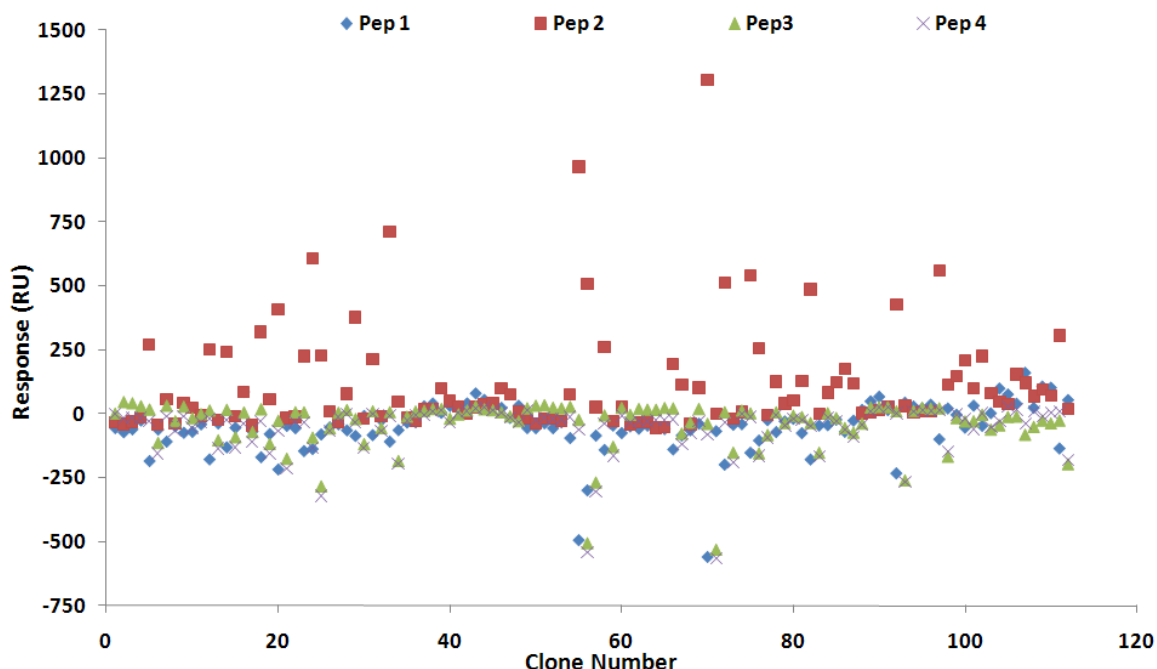


Figure 4.2-4: Epitope-specificity screening for anti-cTnI epitope-specific antibodies on Biacore™ 4000

Crude antibody-containing supernatants were diluted in buffer and each passed over the four peptides and a surface reference. The binding responses for each antibody for the peptides were plotted for the 112 hybridomas selected previously by the cTnI protein binding ELISA. A significant number of the antibodies reacted with the peptide-2 and crucially showed no cross reactivity with the other peptides.

Following scale-up to 48-well plate scale, the clones were retested by a direct binding ELISA (Figure 4.2-5) and the positives were reanalysed for peptide-specificity (Figure 4.2-6). Figure 4.2-5 demonstrates a dramatic loss of binding for several clones possibly due to chromosome loss or growth competition from other non-secreting cells present in the wells. This highlights the importance of examining each clone at each stage of scale-up. The epitope-specificity was also re-analysed to ensure no shift in the binding profile. Figure 4.2-6 shows retention of specificity for the majority of the clones. From this paired analysis data 24 clones were taken forward and expanded up to 24-well plate scale.

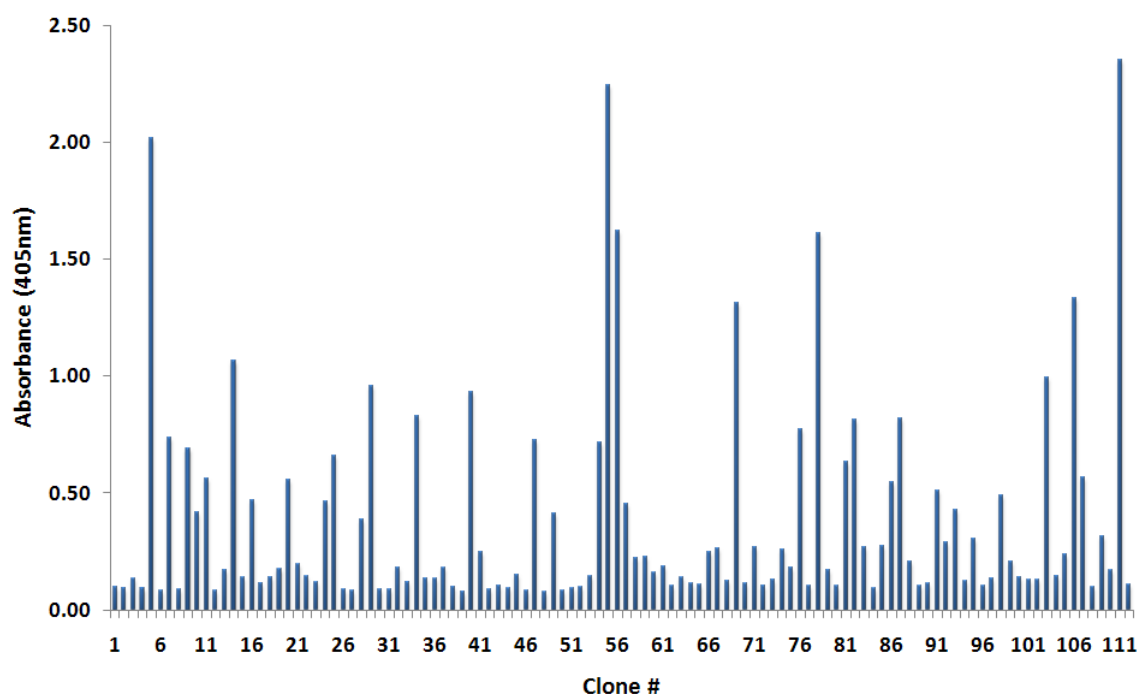


Figure 4.2-5: Direct binding ELISA to confirm retention of positivity at 48-well plate scale of hybridoma expansion

Direct binding to cTnI was carried out to assess retention of positivity post scale-up from 96- to 48-well plate format. A number of positive clones showed loss of binding either due to instability of the chromosomes or due to competition from other non-secreting clones in the wells.

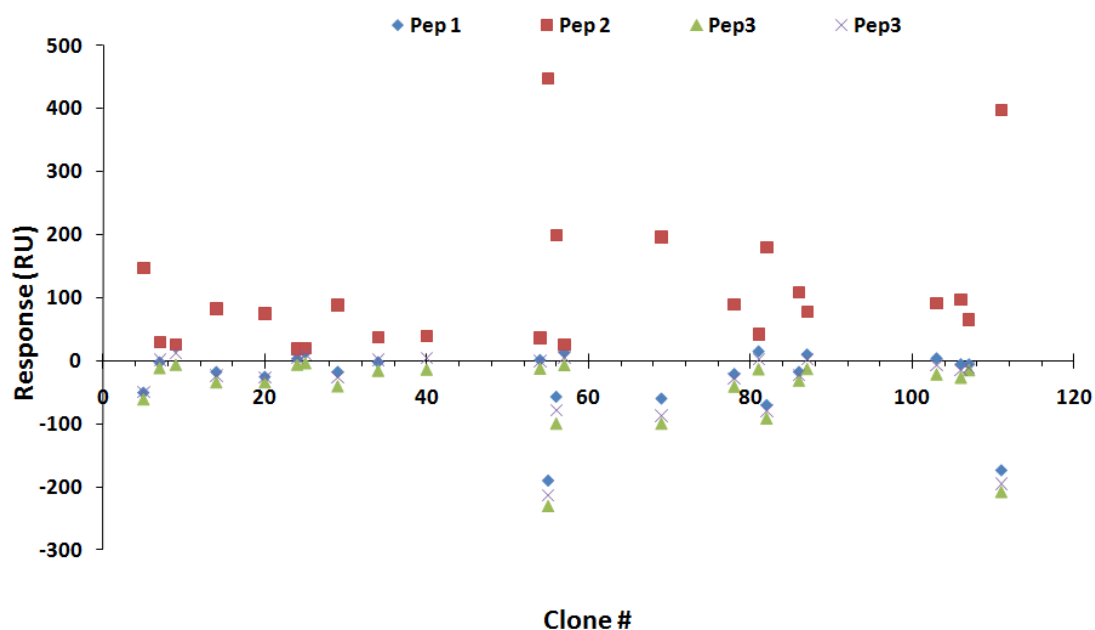


Figure 4.2-6: Epitope-specificity of expanded clones at the 48-well plate stage of hybridoma scale-up

Positive clones from the direct binding ELISA analysis were re-assessed for peptide-specificity on the Biacore™ 4000. Many of the strong binding clones retained their epitope-specificity. Crude supernatants were again diluted in running buffer (HBS-EP⁺) and binding responses assessed as described previously.

The format of analysis was then expanded, after scale-up from 48-well to 24-well plates, to include competitive ELISA (section 2.3.3.4.3). Figure 4.2-7 shows that binding to cTnI could be almost completely abolished by an excess of free peptide-2. The crude supernatants (two dilutions) were incubated with and without free peptide and assayed against the cTnI protein. The absorbances at zero free peptide concentration (A0) were compared to a 'one-shot' excess of free peptide aimed to completely reduce binding. This approach was employed as there was no reliable way to quantify the amount of secreted IgG in the supernatants without titration. Titration was possible, but for large numbers of clones it is inherently cumbersome. This 'one-shot' competition assay allowed for evaluation of 24 clones in one analysis at two supernatant dilutions. The collected data indicated that all clones were sensitive to free peptide thus indicating competition for binding and hence, cTnI specificity.

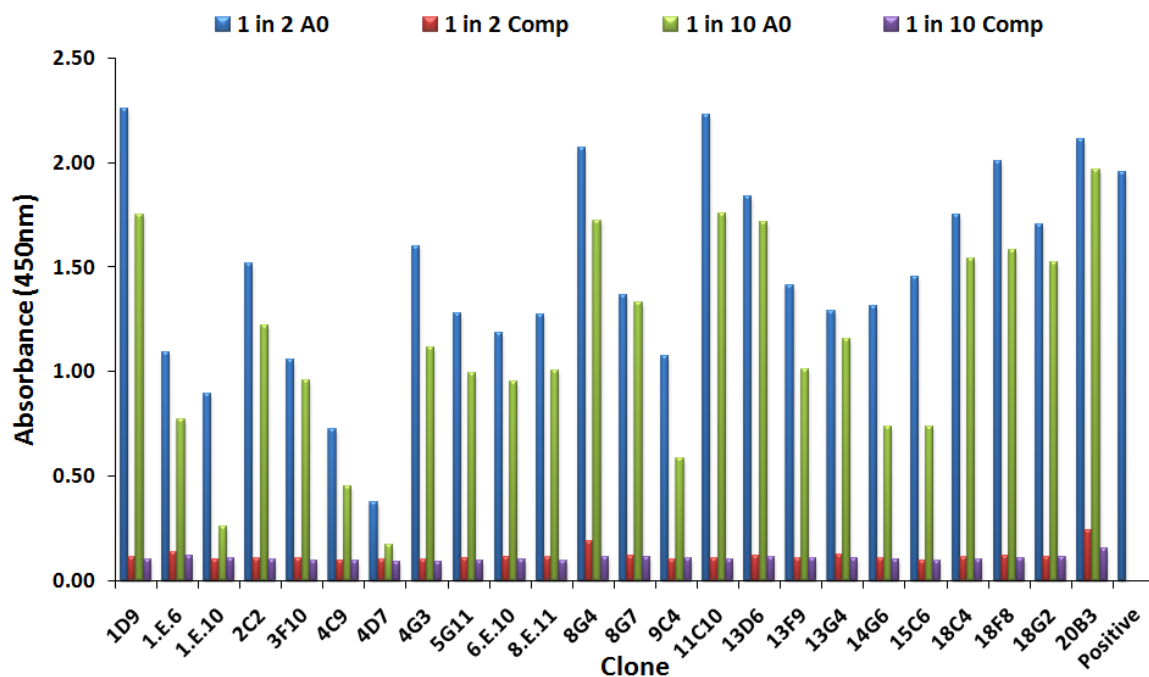


Figure 4.2-7: Competitive ELISA comparison of twenty-four selected hybridomas

Twenty four positive clones were evaluated for their sensitivity to the free peptide at the 24-well plate scale. cTnI was coated onto wells of an ELISA plate. Crude supernatants were diluted 1 in 2 and 1 in 10 with 1% (w/v) PBSTM (A0) and 10 μ M free peptide-2 (Comp) before being applied to the cTnI-coated wells. Absorbance without competitive antigen and signal reduction due to free antigen were plotted side by side for both dilutions of supernatant. It can be seen that all the clones were sensitive to the presence of free peptide antigen which competed for binding at both supernatant dilutions. cTnI bound mAb was detected using an anti-mouse HRP-labelled secondary antibody.

Until this stage of expansion all assumptions made were based on direct binding formats. Since affinity is a ratio of the thermodynamic constants k_a and k_d (Table 4.1-1) a method to examine at least one of these constants for ranking was required. The k_a constant is concentration dependent and therefore ranking guided by this parameter in crude samples was not feasible. k_d is independent of concentration and was examined in a stability study by monitoring the formation of an antibody-peptide binding event and its subsequent dissociation over a relatively long time period. Examination of the percentage left (% left, see Equation 4.2-1) for each of the selected hybridomas permitted ranking by evaluation of a parameter related to their affinity rather than basic binding assay. Table 4.2-1 outlines the stability early response (immediately after association) and stability late response (after 12 minutes dissociation) with the calculated percentage left values for each of the hybridomas in comparison to a commercial monoclonal antibody (Hytest 228).

Table 4.2-1: Ranking of hybridomas by percentage left

Clone	Clone #	Stability Early (RU)	Stability Late (RU)	% Left
1D9	5	180.13	154.90	86.00
1.E.6	7	75.30	57.33	76.13
1.E.10	9	87.85	63.38	72.14
2C2	14	127.45	103.70	81.37
3F10	20	127.10	107.78	84.80
4C9	24	71.25	52.55	73.75
4D7	25	83.18	55.65	66.91
4G3	29	123.60	101.50	82.12
5G11	34	119.98	96.75	80.64
6.E.10	40	160.35	136.85	85.34
8.E.11	54	96.70	72.95	75.44
8G4	55	386.13	361.80	93.70
8G7	56	234.83	212.15	90.34
9C4	57	90.85	66.33	73.00
11C10	69	253.25	228.45	90.21
13D6	78	168.20	141.70	84.24
13F9	81	97.73	72.45	74.14
13G4	82	238.68	214.40	89.83
14G6	86	158.55	130.28	82.17
15C6	87	108.68	81.73	75.20
18C4	103	130.60	105.98	81.14
18F8	106	142.88	112.75	78.92
18G2	107	123.23	95.65	77.62
20B3	111	453.28	426.43	94.08
Hytest 228	-	250.73	250.63	99.96

Figure 4.2-8 graphically maps the relationship between binding early and late, as described in Table 4.2-1. The clones can be observed to lie quite close to the ideal (100% left) with four clones showing percentage left values >90%. These clones (highlighted in red) were prioritised for continued expansion and cloning by limiting dilution.

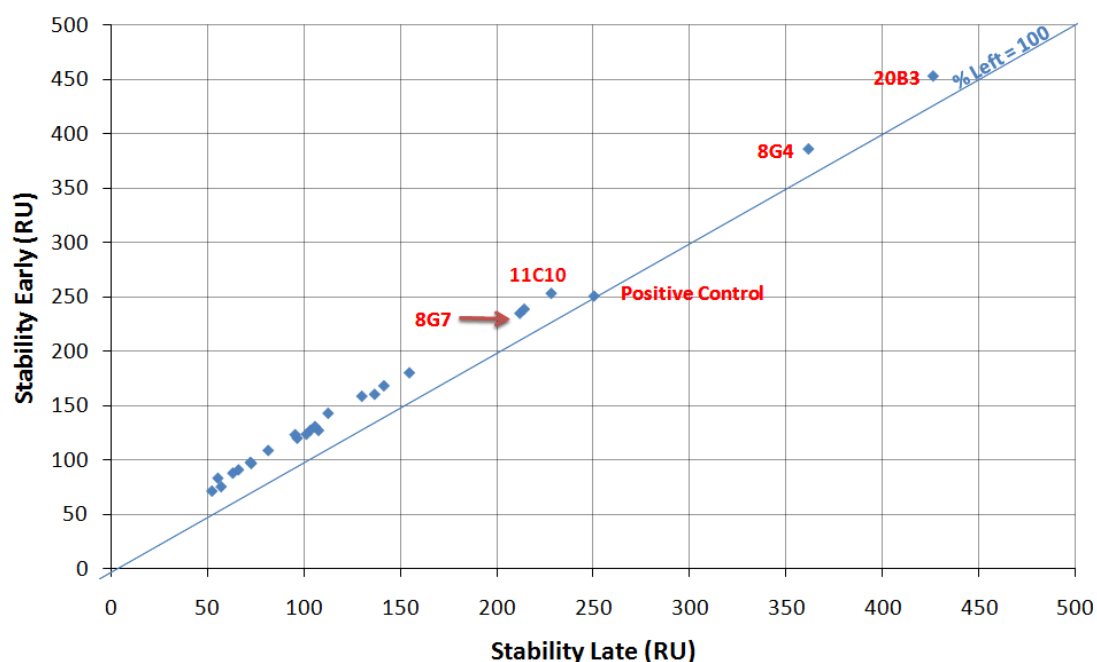


Figure 4.2-8: Biacore™ 4000 high-throughput percentage left ranking of anti-peptide-2 hybridomas

Plot of stability early versus stability late. Binding levels at a time-point early in the dissociation phase were collected and compared to a later time-point, after 12 minutes dissociation. The diagonal blue line represents 100% left, which is indicative of no dissociation of the antibody-antigen interaction.

4.2.2.2 *Capture ranking of Hybridoma clones on Biacore™ 3000*

With the number of clones reduced to a manageable number the format of the analysis was refined further to acquire more ‘assay relevant data’. As the final assay format is intended to be a sandwich assay, the selected mAb must function as an efficient capture antibody. The antibody selected must therefore recognise the antigen in a solution-dictated conformation which can often differ from the conformation adopted when the protein is absorbed onto polystyrene plates. To achieve this, four clones were evaluated on the Biacore™ 3000 in a low volume analysis. Figure 4.2-9 outlines the two flow cell experimental setup. In both flow cells, a surface was prepared using an anti-mouse Fc-specific antibody as described in section 2.3.3.4.4. The active surface captured mAbs from crude supernatants after which a fixed cTnI concentration (30nM) was passed over both flow cells. In this setup the reference cell allows for any contributions of non-specific cTnI binding to be subtracted. This analysis was limited somewhat as the dissociation for each mAb off of the capture antibody was not subtracted. However, this dissociation was constant for each of the hybrids and permitted ranking based on percentage left analysis.

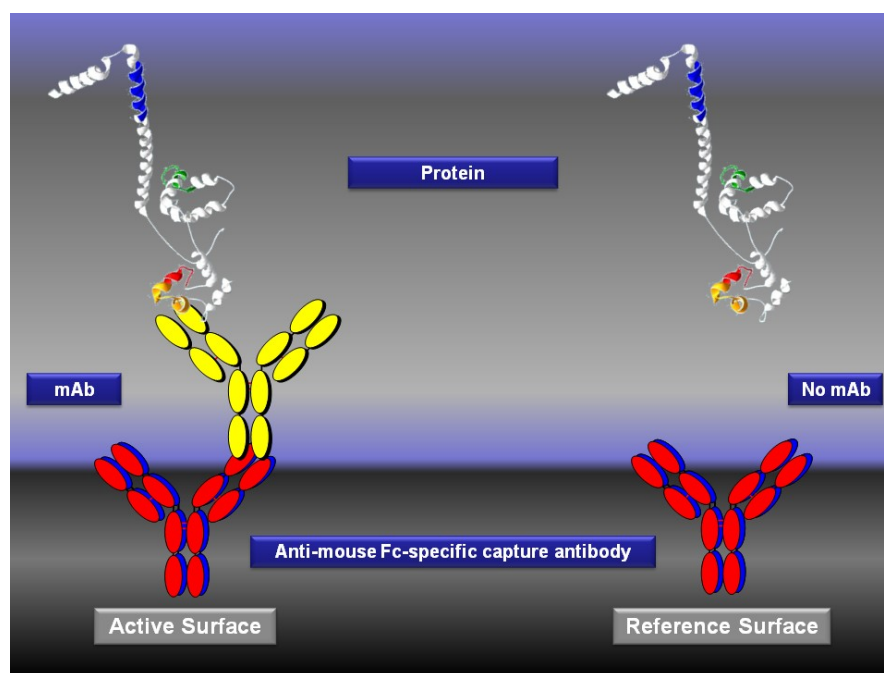


Figure 4.2-9: Biacore™ 3000 'off-rate' ranking flow cell setup

A commercial mouse-specific monoclonal antibody (red) was utilised to capture the Fc portion of the anti-peptide 2 monoclonal antibodies from crude supernatants (yellow). cTnI was then passed over the captured monoclonal antibodies and the Fc-specific capture antibody which was used as an online surface control.

This methodology was applied to the four prioritised clones at 6-well plate scale (section 2.3.3.4.4). Figure 4.2-10 illustrates the cTnI binding profile for the four clones. Indicated on the graph are the time points R_{Early} and R_{Late} which were used to derive the percentage left values for the four clones using Equation 4.2-1 (8G4: 59.4%, 20B3: 54.2%, 8G7: 52.6%, 11C10: 51.9% and Hytest 228: 53.1%). Of crucial importance from this analysis was the binding of the mAbs to the native protein in-solution. This orientation was more representative of the scenario in which the selected mAb would be deployed. The mAbs were also observed to perform comparably to the commercial standard mAb (Hytest 228).

Equation 4.2-1: Calculation of percentage (%) left values in Biacore™ 'off-rate' experiments

$$\% \text{ Left} = \frac{R_{\text{Late}}}{R_{\text{Early}}} \times \frac{100}{1}$$

Where R is the response units (RU). 'Early' was defined as 10 seconds after the end of the cTnI injection (end of the association phase) and 'late' as the response after several minutes dissociation in relation to the early time point. See Figure 4.2-10 for graphical representation of R_{Early} and R_{Late} .

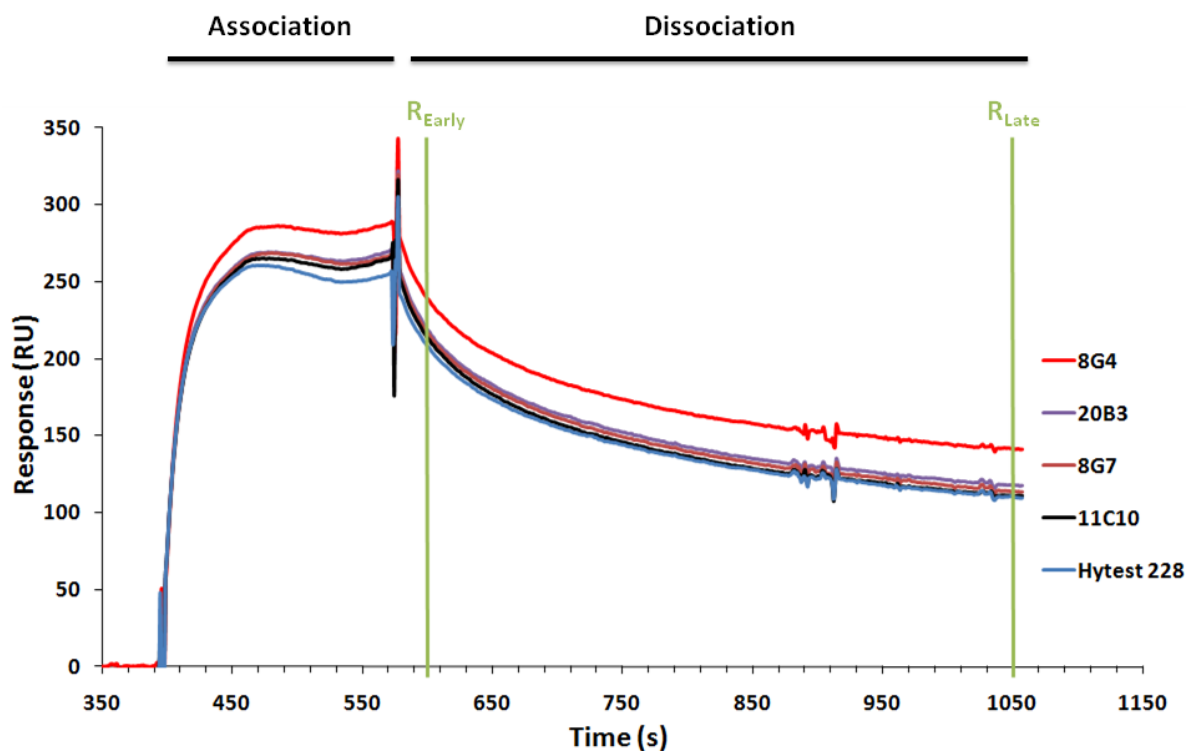


Figure 4.2-10: Biacore™ 3000 'off-rate' analysis of four selected hybridomas for the cTnI protein

This normalised graph (minus mAb capture level and non-specific interactions) indicates the association and dissociation of cTnI. Fixed time intervals R_{early} and R_{late} (7.5 minutes dissociation) are indicated on the graph. The response values (RU) at these time points were used in Equation 4.2-1 to calculate % left values.

The four clones were scaled-up to T75 flasks and subsequently cloned by limiting dilution as described in section 2.3.3.5. The other non-prioritised clones were banked, as described in section 2.3.3.6.3. Once cloned by limiting dilution, five clones from each parent were selected from direct binding ELISA data (not shown). Nineteen of the twenty selected hybridomas continued to secrete antibody through expansion (11C10#5 became non-viable) and were tested predominantly by ELISA as described for the primary expansion (data not shown). The 19 clones were analysed side-by-side with the Hytest equivalent antibody (mAb 228) on Biacore™ 3000 in the capture approach. Figure 4.2-11 shows the subtracted sensorgrams for all the clones and the commercial antibody. The response at the early time point (~600 seconds) and the late time point (~1020 seconds) was then expressed as % left values as calculated from Equation 4.2-1 and contained in Table 4.2-2. The analysis showed that all the 20B3 sub-clones performed best, with values from 61.50 to 63.26%, and compared well with the Hytest mAb (66.66%). To further differentiate between the 20B3 sub-clones (#1-5) a dilution series of supernatants was prepared to assess the

antibody expression levels between the daughter clones (section 2.3.3.4.1). Figure 4.2-12 shows no appreciable difference in expression levels and so 20B3#5, with a marginally greater percentage left value, was selected and expanded for further cloning by limiting dilution (section 2.3.3.5).

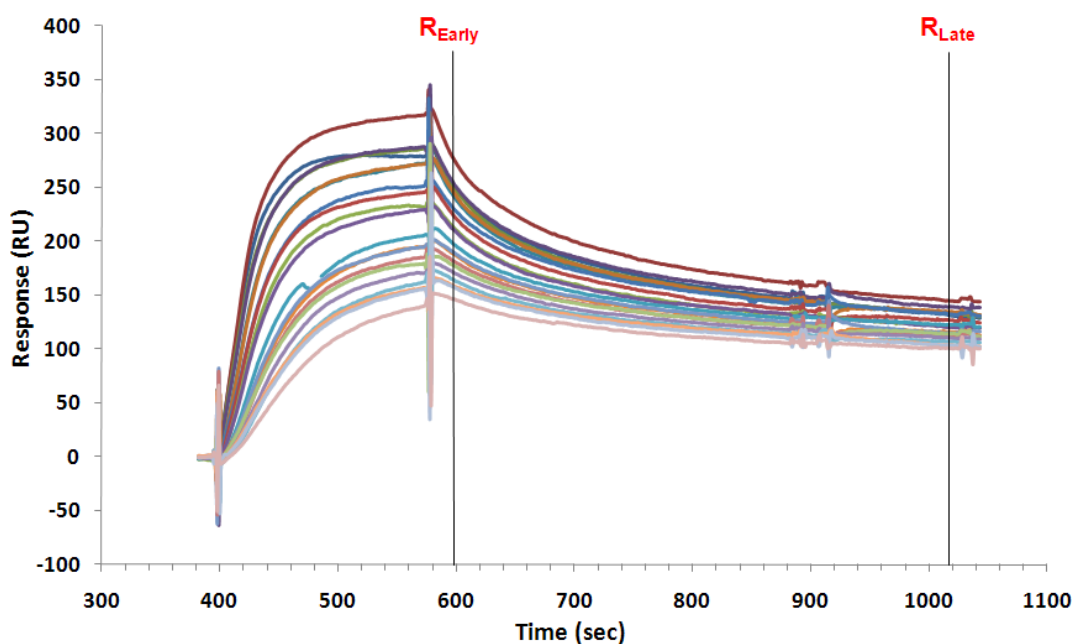


Figure 4.2-11: Biacore™ 3000 percentage left ranking of twenty clones for cTnI protein binding

This normalised (minus mAb capture level) reference subtracted graph indicates the association and dissociation of cTnI at fixed time intervals. R_{early} was defined as 10 seconds after the end of the cTnI injection and R_{late} as the dissociation after 7 minutes in relation to R_{early} .

Table 4.2-2: Percentage left values for nineteen hybridomas from Biacore™ 3000-based experiment

Clone #	Percentage (%) Left				Control
	8G4	8G7	11C10	20B3	
1	47.13	50.18	58.39	61.50	66.66
2	47.14	53.10	58.28	61.58	
3	47.90	51.82	57.98	62.00	
4	49.99	52.80	58.44	62.68	
5	49.96	52.86	-	63.26	

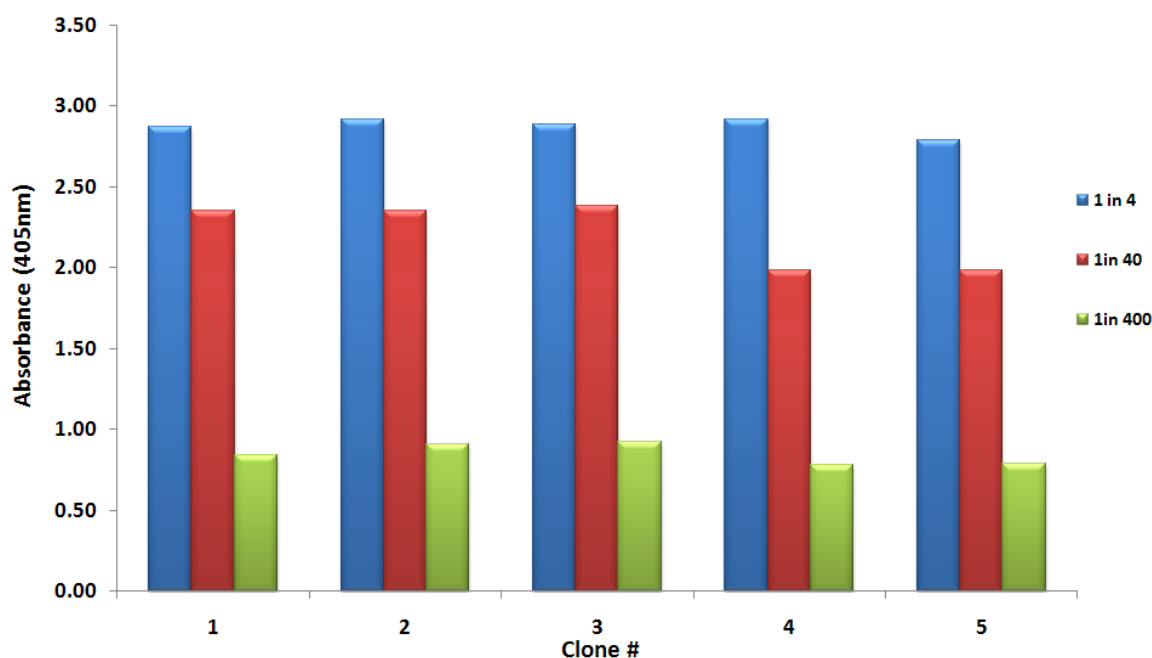


Figure 4.2-12: Direct binding ELISA-based analysis of hybridoma antibody expression levels

In a direct binding ELISA format three dilutions of supernatant (1 in 4, 1 in 40 and 1 in 400) were prepared in 1% (w/v) PBSTM and applied to a cTnI-coated (1µg/mL), blocked (5% (w/v) PBSM) plate. The bound mAb levels were detected using an anti-mouse-Fc-specific HRP-labelled secondary antibody. This allowed comparison of the antibody production levels between the five 20B3 daughter clones. The graph illustrates no major differences in expression levels between these closely related progenies. Clone #5 was selected for expansion and cloning by limiting.

4.2.2.3 Additional screening of the hybridoma progeny

After the second cloning by limiting dilution carried out on 20B3, the hybrids were then evaluated in a sandwich ELISA capturing various concentrations of cTnI and bound protein was detected using an anti-epitope-3 HRP-labelled antibody (Hyttest 16A11) as described in section 2.3.3.4.5. Figure 4.2-13 shows the cTnI concentration dependant signal obtained for all the captured mAbs over a significant cTnI concentration range with no non-specific interaction between the mAbs and reporter antibody. This demonstrated the ability of the antibodies to recognise the antigen in a number of formats and, in particular, one mimicking its envisaged endpoint assay application. Clone E (20B3.5.E) was isotyped using Pierce™ Rapid Isotyping kit and the selected monoclonal was found to be IgG₁κ as shown in Figure 4.2-14 (section 2.3.3.4.6).

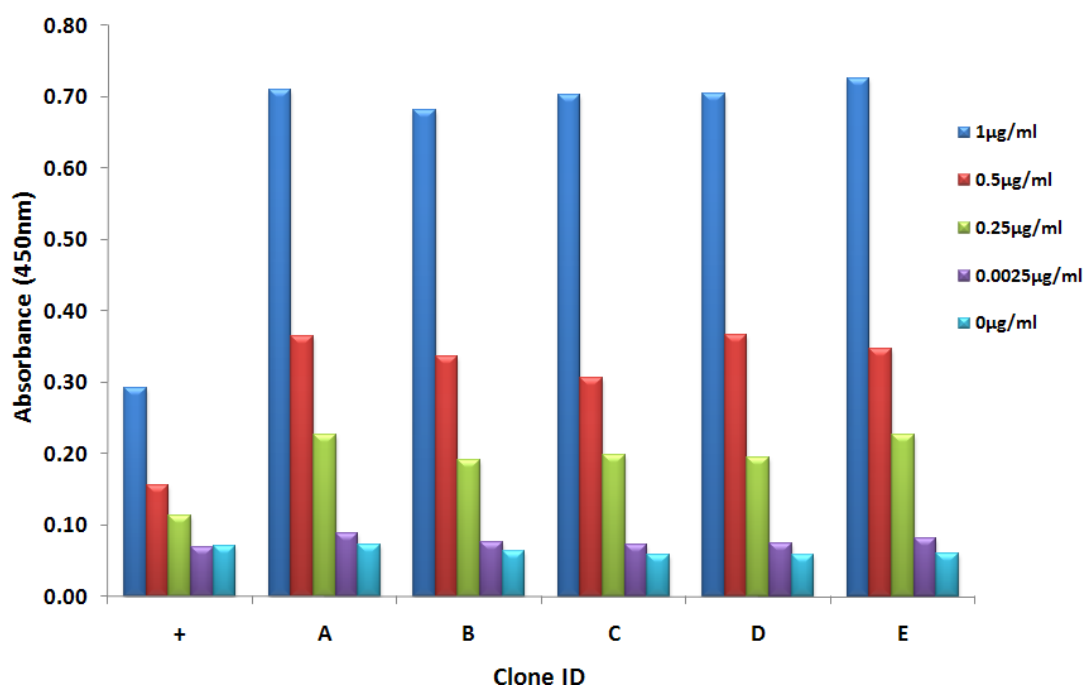


Figure 4.2-13: Sandwich ELISA for cTnI using hybridoma supernatant

Supernatants directly from hybridoma wells were applied to an ELISA plate to form the antibody capture surface. Hytest 228 (2 µg/mL) was also immobilised to serve as a positive control. Various cTnI concentrations were applied to the immobilised monoclonal antibodies. A buffer only control (0 µg/mL cTnI) was also applied to ensure there was no non-specific interactions with the monoclonal antibodies. Captured cTnI was probed using an anti-eptiope-3 HRP-labelled secondary antibody which completed the sandwich format. A cTnI dependent profile for each antibody surface was obtained.



Figure 4.2-14: Isotype determination of monoclonal antibody 20B3

This rapid kit allowed isotype determination for both the heavy and light chains directly from crude supernatant. The supernatants were diluted in sample diluent and applied to the bottom of the lateral flow cassette. There were three cassettes (2 heavy and one light) which contain control lines and areas corresponding to a specific isotype. The presence of the control and test lines indicates a valid positive result. The mAb was determined to be an IgG₁κ.

To ensure clonality, 20B3.5.E was cloned out by limiting dilution for a third and final time. The resulting hybridomas were considered to be truly monoclonal at this stage. To examine differences in expression levels all the output clones were diluted in a comprehensive 10-fold dilution series (1 in 3 \rightarrow 1 in 300,000) and assayed by direct binding ELISA against cTnI (section 2.3.3.4.1). Figure 4.2-15 illustrated relatively uniform expression levels for all twenty sub-clones of 20B3.

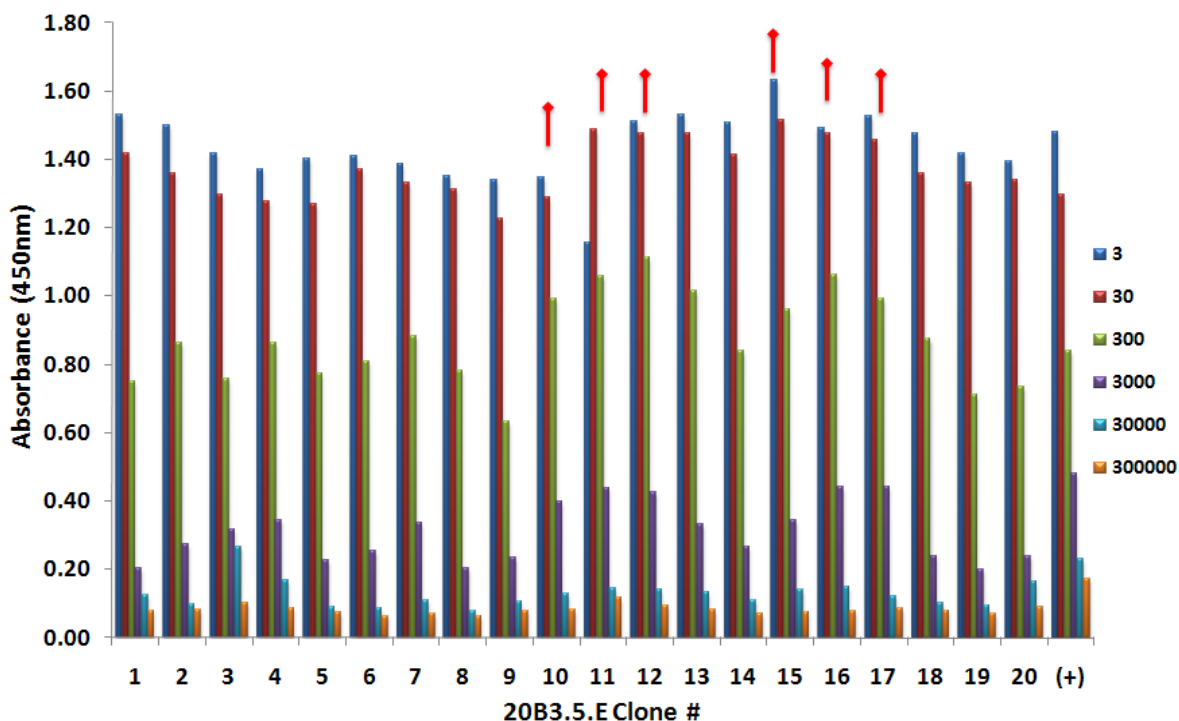


Figure 4.2-15: Analysis of the expression levels of individual hybridomas by direct binding ELISA

All the clones had comparable absorbance and were considered to be similar due to their common origin. cTnI was coated across an ELISA plate to which diluted supernatants were applied. Bound mAb was detected with anti-mouse-Fc-specific HRP-labelled secondary antibody.

As a final analysis six of the clones were evaluated in a competitive analysis format (as indicated in Figure 4.2-15). Competitive analysis was carried out during the initial scale-up and screening using free peptide and cTnI (cTnI data not shown). Six clones were selected from the expression analysis of the 20 clones above and were initially titred to obtain the optimal supernatant dilution to carry out the competitive analysis (Figure 4.2-16-A). Two of the clones were diluted accordingly and mixed 1:1 with a range of free peptide (Figure 4.2-16-B) and free cTnI (Figure 4.2-16-C) concentrations. Figure 4.2-16-B shows the competition profile with free peptide-2 for the selected hybrids and the control antibody Hytest 228. The two clones perform well, but the relatively low AU for the Hytest 228mAb results in a poorer competitive profile potentially indicating its limited usefulness. Figure 4.2-16-C shows the competition profile with free cTnI where there is no competition of the two selected clones or the 228 mAb. This mirrors the behaviour of all the clones and the control when tested early in the first scale-up and screening campaign.

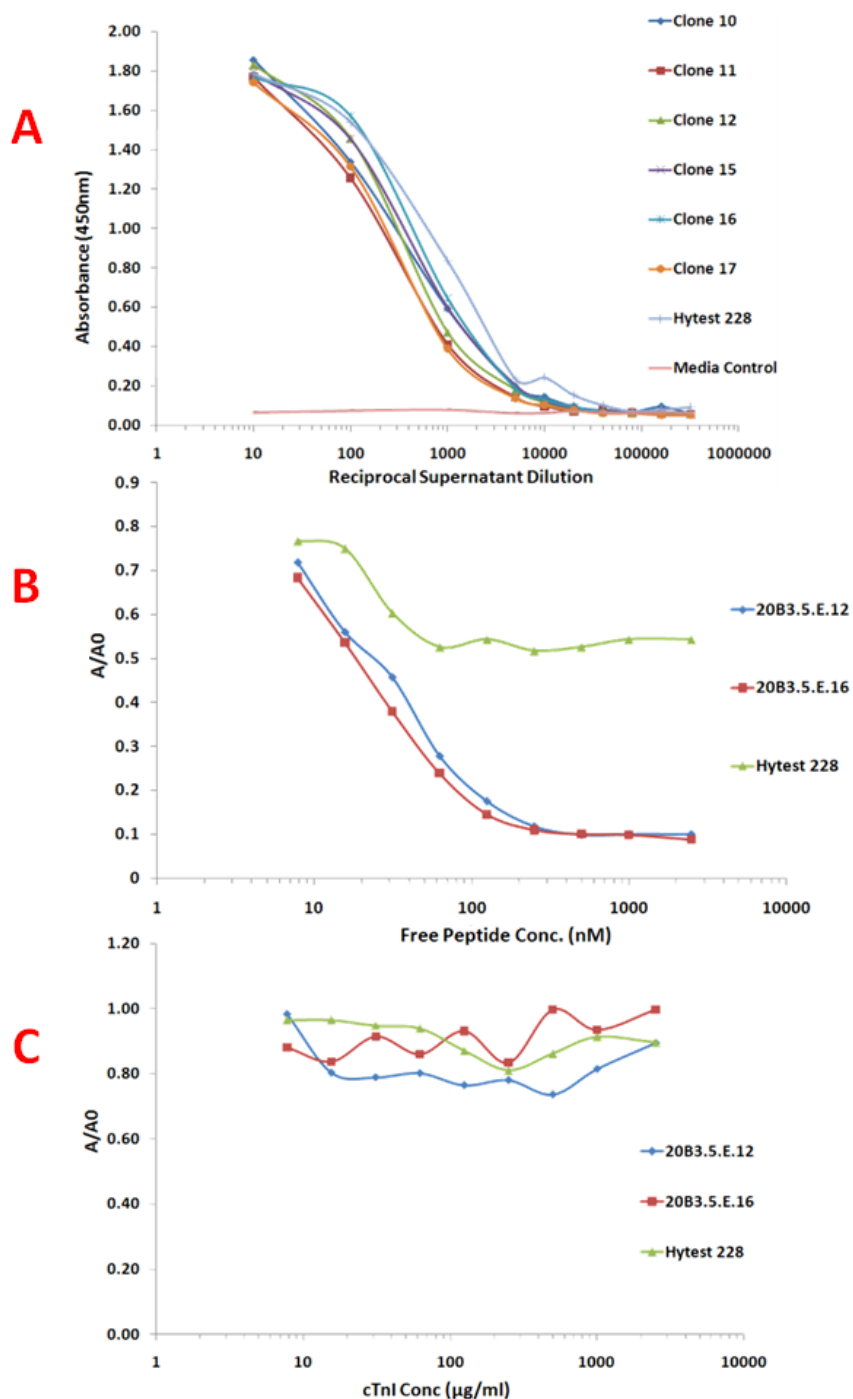


Figure 4.2-16: Titre and competitive analysis of selected monoclonal antibody 20B3

- A) Titre of all six clones plus Hytest 228 mAb to assess optimal supernatant dilution to use in subsequent competitive assay.
- B) Competitive analysis of selected two clones in direct comparison to Hytest 228 mAb for free peptide. The mAbs demonstrate sensitivity for the peptide.
- C) Competitive analysis of the two selected clones in direct comparison to Hytest 228 mAb for cTnI protein.

The control mAb and the selected mAbs behave equally in this assay. As shown previously, the selected clones can recognise cTnI directly bound, in sandwich ELISA and in a capture format on Biacore™ 3000. This suggests that for binding either the antibody/antigen must be immobilised in some way and may involve charge-determined properties that have a significant effect on binding. Accordingly, clone #12 was carried forward for large-scale antibody production and purification. The route to selection of the various sub-clones of 20B3 is outlined in Figure 4.2-17.

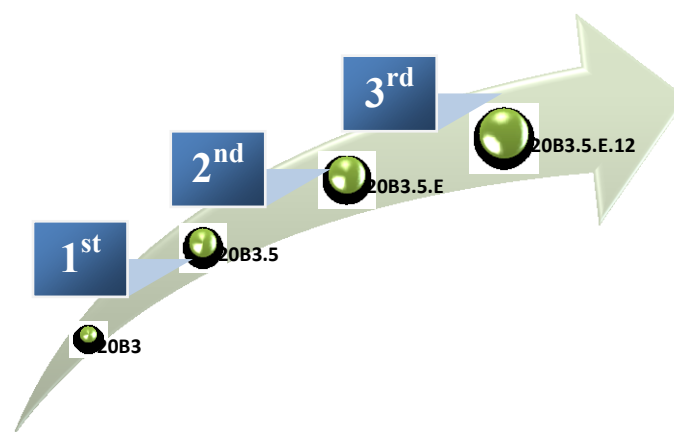


Figure 4.2-17: Route to the selection of lead monoclonal antibodies from the analysis strategy employed
From the initial master plate position (plate: 20 position: B3) three sequential limiting dilution steps through continuous culture resulted in the isolation of various daughter clones.

4.2.3 Purification of the monoclonal antibody 20B3

Large-scale expression of mAb 20B3 was carried out over a number of weeks in T175 flasks permitting the collection of approximately 30mL conditioned media per flask twice a week. This conditioned media was retained at 4°C until 500mL media was collected (with the addition of 0.02% (w/v) NaN₃). The ‘antibody-rich’ media was concentrated using an Amicon® stir cell system (GE Healthcare) with a molecular weight cut-off membrane (100kDa). This facilitated reduction of the supernatant volume to a manageable level for purification (10mL). Purification was carried out using protein G (reviewed by Darcy and co-workers [129]) (recombinant: sepharose™ fast flow – Sigma®) which was selected for its medium antibody-binding protein interaction for this isotype (see appendix, Figure 8.1-8), as outlined in section 2.3.3.7.1. The entire concentrated supernatant was applied to the settled resin, followed by washing and elution by acidic pH. Post elution the protein-containing fractions were collected (Figure 4.2-18), combined (~2.5mL) and desalted on a PD-10 (GE Healthcare) column. Significant protein-containing fractions (Figure 4.2-18) were pooled and concentrated using a Vivaspin™ column (30kDa MW cut-off).

To assess the success of the purification, samples from the column ‘flow-through’, washes and desalted protein were analysed by 12.5 % (w/v) SDS-PAGE and WB. Figure 4.2-19 shows the success of the purification protocol and the purified sample was compared to goat IgG. Bands corresponding to intact IgG, the heavy and light chains were observed in the purified fraction. To examine the purity of the final preparation, samples of the purified mAb were analysed by size exclusion chromatography (SEC) (section 2.3.3.7.2). SEC allowed separation of molecules as consequence of their size not molecular weight and was carried out in aqueous buffers that allowed retention of biological activity. To establish the ideal concentrations for use, three different concentrations of mAb (high, low and medium) were applied to the column and compared to a set of protein standards. Figure 4.2-20 shows the elution profile of the purified mAb and was overlaid with a second chromatogram of protein standards. From the figure, the purified mAb overlaps well with the IgG protein standard and no other significant peaks were observed. This simple one step purification successfully yielded a very pure monoclonal antibody preparation. Typically, this type of purification from 500mL conditioned media gave 6-8mg of protein (12-16µg/mL of culture media).

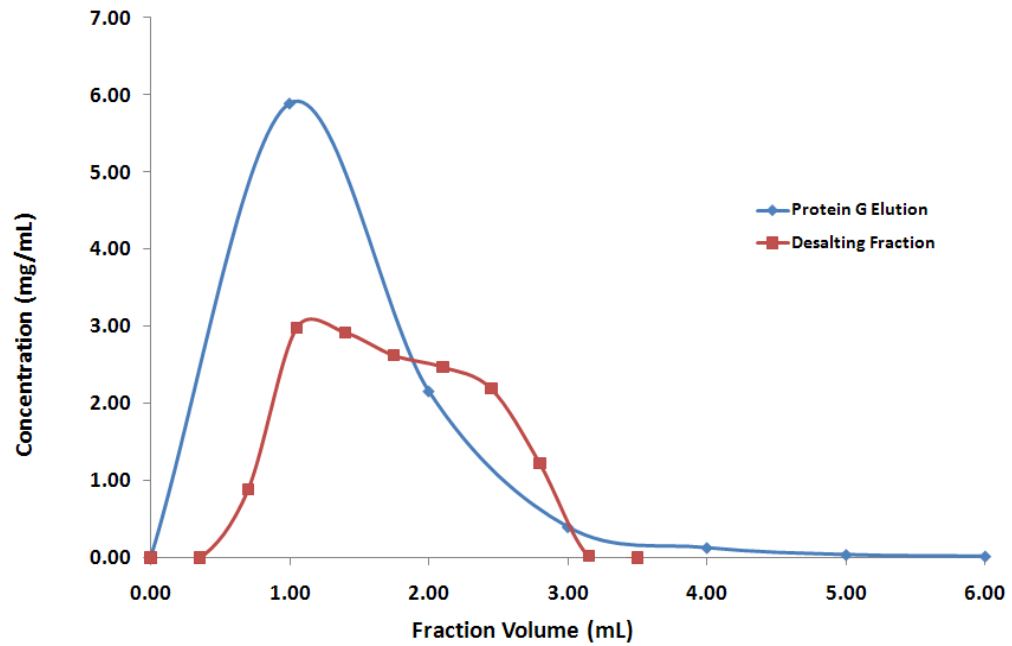


Figure 4.2-18: Elution profiles for protein G and PD10 columns used in the purification of 20B3

Absorbance (280nm) measurement of the eluted fractions collected from protein G and PD-10 desalt columns. Significant protein-containing fractions as visualised here were combined and carried forward to next stage of purification.

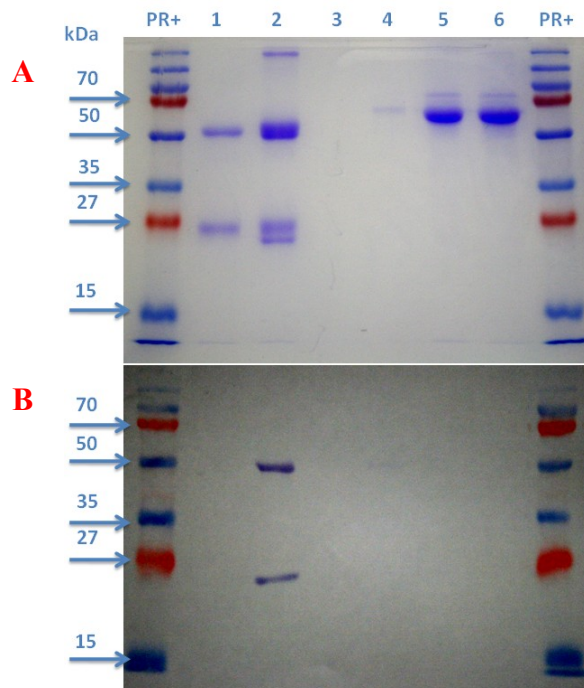


Figure 4.2-19: SDS-PAGE and WB analysis of the purification steps for monoclonal antibody, 20B3

The figure shows the SDS-PAGE (A) and WB (B) probed with anti-mouse-Fc-specific HRP-labelled antibody. The lanes were labelled as follows; PR⁺: Prestained protein ladder, lane 1: goat IgG control, lane 2: purified mAb 20B3, lane 3: column wash 2, lane 4: column wash 1, lane 5: flow-through 2 and lane 6: flow-through 1. From the results 20B3 was demonstrated to have purified successfully using protein G.

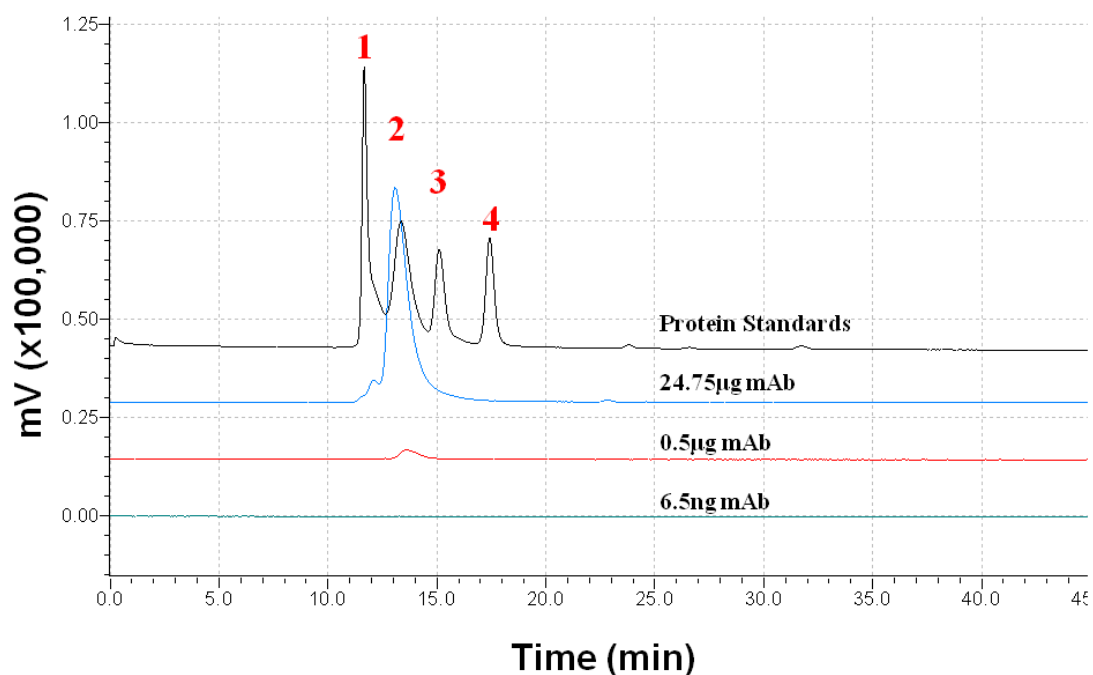


Figure 4.2-20: SEC-HPLC analysis of the 20B3 monoclonal antibody following purification

Protein standard peaks; 1: bovine thyroglobulin, 2: immunoglobulin, 3: myoglobin, 4: uridine. Analysis was carried out on SHIMADZU Prominence HPLC using a Phenomenex BioSep-SEC-S2000 column (dimensions 300 x 7.8mm 5micron) at 20°C. The buffer was 1X PBS and the analysis was carried out at 0.5µL/minute.

To ensure that the purification conditions did not compromise the activity of the purified mAb, a series of ELISAs were carried out. Initially, the mAb was titrated against cTnI in a direct binding ELISA (section 2.3.3.4.1) in parallel to the Hytest mAb228 (Figure 4.2-21). The mAb (8.76mg/mL) titred out at approximately 1 in 30,000 compared to the commercial mAb228 (9.3mg/mL) titring at approximately 1 in 70,000. Figure 4.2-22, a sandwich assay (section 2.3.3.4.5), illustrates mAb 20B3 and mAb 228 as capture reagents for various concentrations of cTnI. Bound cTnI was detected using an anti-epitope-3 HRP-labelled secondary antibody (16A11) and mAb20B3 again compares well with the equivalent commercial antibody. In this non-optimised assay format both antibodies can detect cTnI concentrations between 70-100ng/mL.

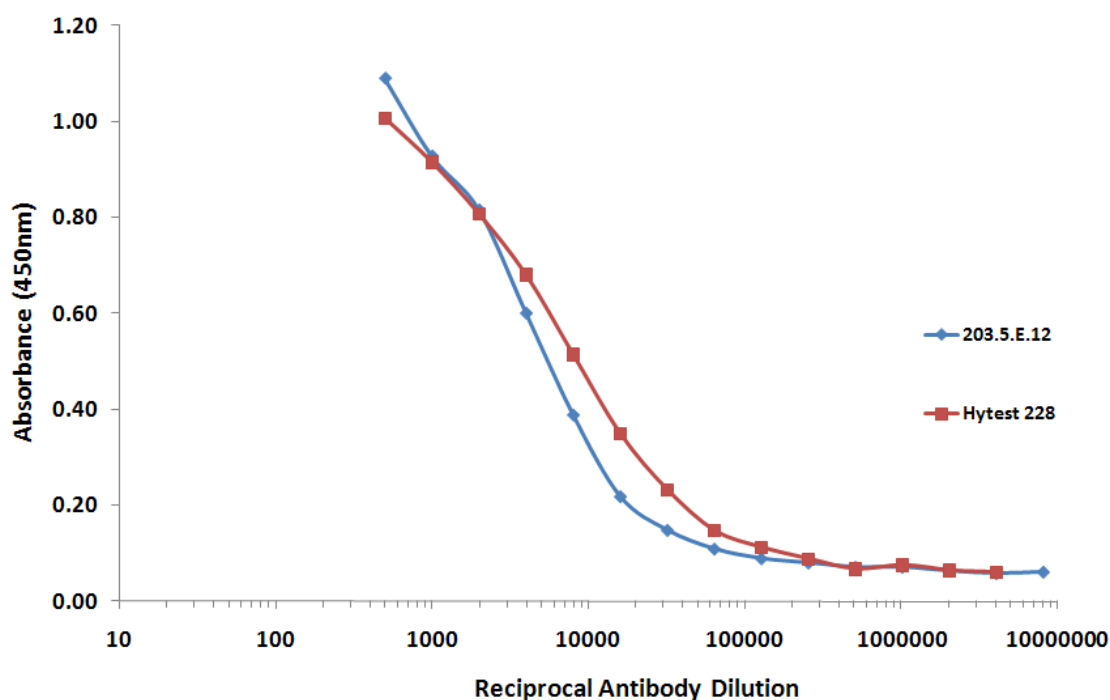


Figure 4.2-21: Titrations of purified the 20B3 and Hytest 228 antibodies

Reciprocal antibody dilutions in 1 % (w/v) PBSTM titrated against cTnI-coated onto the surface of a microtitre plate. The purified mAb titred in a similar fashion to the commercial standard and indicated no adverse loss of activity due to the purification strategy.

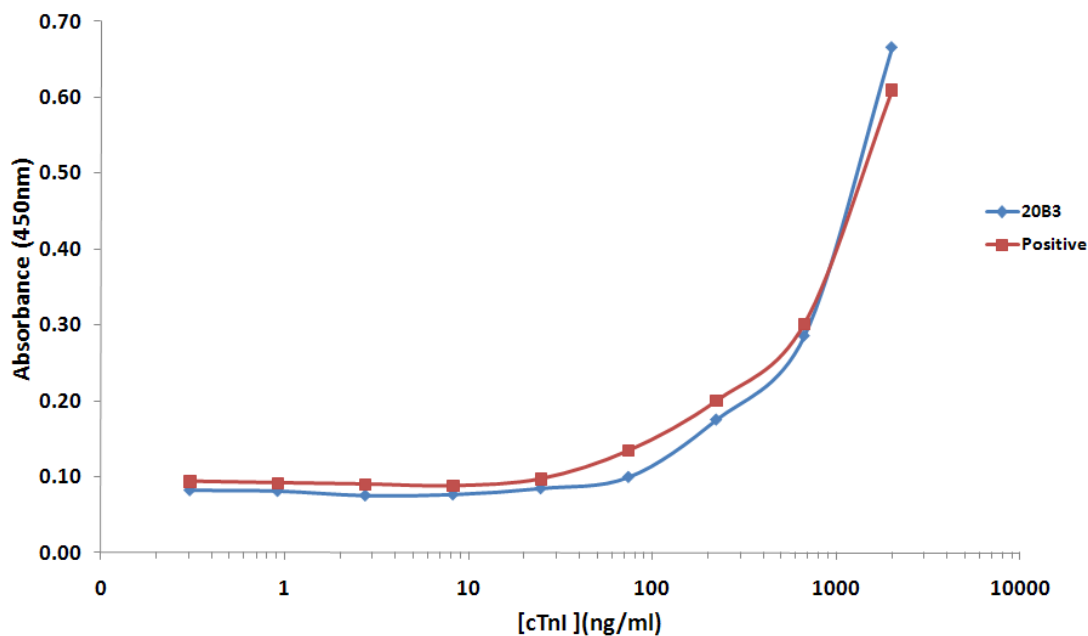


Figure 4.2-22: Sandwich ELISA using the 20B3 antibody and equivalent control antibody for cTnI

MAb 20B3 and Hytest 228 were coated onto the surface of an ELISA plate capturing cTnI over a relatively wide concentration range (0.2 to 2000ng/mL). Captured cTnI was detected using the Hytest anti-epitope-3 HRP-labelled mAb (Hytest 16A11). Both the Hytest and ‘in-house’ monoclonal antibody (20B3) behave similarly.

4.2.4 Determination of antibody affinity on Biacore™ 3000

The determination of affinity, by a capture approach, was hampered by non-specific interaction between the cTnI antigen and the antibody used to capture 20B3. This was a typical event when batches of cTnI (commercial) were changed and was a result of the inconsistencies between purification batches and highlights the significance of the antigen quality issues. This did not manifest as a problem in ranking experiments, but in true 1:1 binding any additional interactions represent a significant barrier to efficient modelling of affinity.

To overcome this, the 20B3 mAb was directly immobilised to a Biacore™ 3000 chip (see section 2.3.3.8). Due to the stabilisers and preservatives (e.g. BSA) present in the commercial antibody it could not be immobilised and compared in this format. However, determination of the kinetic constants for the mAb was of interest. Figure 4.2-23 is a sensorgram of the immobilisation of mAb 20B3 to the chip surface. The dextran was activated using EDC-NHS and the mAb (20µg/mL) injected across the flow cell linking the antibody to the surface. The surface was capped to block any un-reacted sites and regenerated twice. This resulted in a 20B3 mAb surface of approximately 5000RUs. In this fashion the kinetics were examined in the simplistic 1:1 Langmuir binding interaction (Figure 4.2-24).

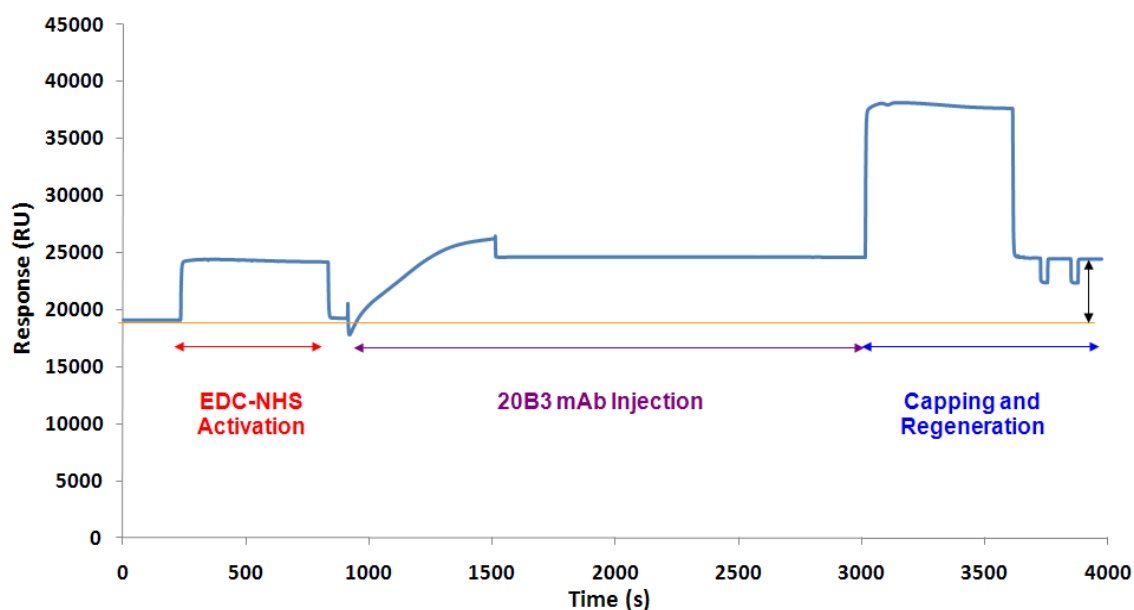


Figure 4.2-23: Immobilisation of monoclonal antibody 20B3 onto the surface of a Biacore™ 3000 chip
Flow cell (FC) 2 of a CM5 dextran (research grade) chip was activated by EDC-NHS for 10 minutes and the antibody linked *via* primary amine groups to the surface. Un-reacted sites were capped using ethanolamine-HCl, pH 8.5 and regenerated with two 30 second pulses of 10mM NaOH. A total of 5027.1 RU of mAb was covalently linked to the surface, as indicated by the multi-directional arrow compared to the flow cell baseline (gold line).

Kinetic constants were modelled on the curves with 1:1 Langmuir binding with drifting baseline model and local R_{\max} parameter. This was carried out using the dedicated BiaEvaluation software. The simplest model (and therefore the most reliable) did not fit the data well and the drifting baseline degree of freedom was required to accurately model the data (Figure 4.2-24). From the χ^2 (χ^2) value (0.137) the fits were found to be good and even residual distribution reinforces the ‘goodness’ of the fit. From the kinetic evaluation the derived constants are outlined in Table 4.2-3.

Table 4.2-3: Kinetic constants derived for monoclonal antibody 20B3

	20B3
k_a ($M^{-1}s^{-1}$)	1.27×10^6
k_d (s^{-1})	2.33×10^{-4}
K_D (M)	1.84×10^{-9}

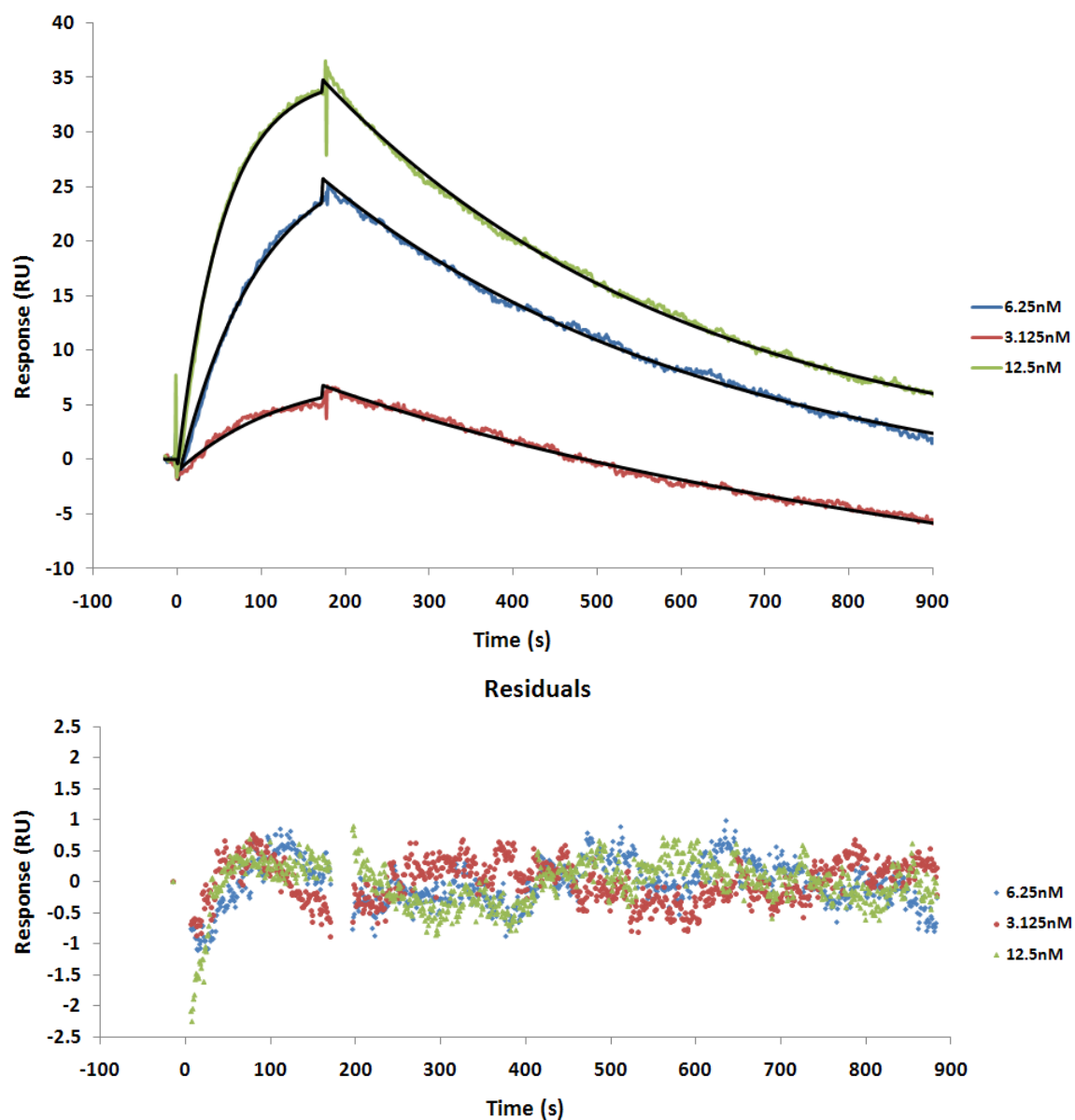


Figure 4.2-24: Kinetic analysis of the 20B3 antibody-immobilised surface

Kinetic analysis of interaction between cTnI and the mAb 20B3. Four cTnI concentrations were used in the analysis (12.5, 6.25, 3.125 and 0nM) to fit the kinetics using 1:1 Langmuir binding model with drifting baseline (black line). The residuals (below) show the ‘goodness’ of the fits with even distribution of the data points. The following kinetic parameters were derived; k_a : $1.266 \times 10^6 \text{ Ms}^{-1}$, k_d : $2.325 \times 10^{-3} \text{ s}^{-1}$ and K_D : $1.836 \times 10^{-9} \text{ M}$ with χ^2 value of 0.137.

4.3 Chapter conclusions

The 20B3 antibody was developed by fusion of a SP2/0-Ag14 myeloma fusion partner with splenocytes from a mouse showing a significant titre to cTnI in a synthetic epitope-based immunisation regime. Screening the resultant progeny was undertaken combining direct, sandwich and competitive ELISA formats, HT-epitope mapping and ‘off-rate’ ranking. The ability to acquire rapid information in a timely manner dramatically increased the chances of success, minimising sources of error not related to chromosome loss or competition by non-secreting cells. Adopting an ‘information-rich’ approach allowed the successful isolation of a panel of antibodies specific for the N-terminal epitope-2 region of cTnI. From 112 positive clones identified, a single progeny of 20B3 was isolated as the optimal anti-cTnI mAb generated in this campaign. The antibody was successfully purified in large quantity, tested in direct binding and sandwich assay formats before evaluation of its affinity on Biacore™ 3000. The mAb20B3 was found to have an affinity of 1.84nM demonstrating the isolation of a high-affinity reagent ideal for use for cardiovascular risk assessment.

The development of an antibody by the traditional hybridoma approach demonstrated was primarily dictated by the differential response of the host animal during the immunisation regime. Interestingly, but inexplicably the synthetic peptide-2 conjugate only raised cTnI-specific responses in mouse. This was in direct contrast to the synthetic peptide-1 conjugate which raised a cTnI-specific response exclusively in chicken. Owing to the extremely high titre obtained the chances of developing a hybridoma were favourable and mitigated against the ‘sampling problem’ encountered when amplifying variable domains from mouse repertoires. The sampling problem referred to is the use of complex, degenerate primer mixes to amplify variable domains which can introduce a sampling bias preferentially selecting dominant variable domains. This sampling issue is greatly reduced in avian hosts due to the simplistic nature of the genes encoding for avian antibodies. Also, the patent-free status of hybridoma technology surpasses patent issues that surround the use of recombinant antibodies in downstream POC-device development. However, by adopting the hybridoma approach to antibody generation a finite pool of candidate clones were developed which require continuous attention, analysis and culture without the ability to ‘shelve’ the clones at any stage prior to achieving monoclonality.

The continuous nature of hybridoma generation requires significant support in terms of analysis and the utility of HT-screening tools for hybridoma characterisation is abundantly clear. The HT-SPR-based analysis took in the order of 6 hours to analyse hundreds of hybridoma supernatants with minimal manipulation and reagent consumption. However, the epitope-mapping strategy adopted was a relatively suboptimal approach to harness the parallel processing power of the instrument. The instrument and screening technology was recently acquired and exploiting its power was balanced with ensuring maximal value in terms of prepared surfaces and reagents. At the time of screening the hybridoma supernatants, the instrument was also in use mining a recombinant anti-cTnI protein library for epitope-specificity. The ease at which the instrument could be switched between bacterial lysate and crude supernatant analysis, using only one prepared surface, facilitated analysis of hundreds of individual monoclonal and recombinant antibodies. In fact, in many analyses the hybridomas and recombinant lysates were analysed in the same run. A more generic approach to hybridoma screening using a capture surface would have facilitated acquisition of a greater wealth of information. However, the transition to recombinant library screening with the same surface would not have been possible. In laboratories where many hybridoma screening campaigns are routinely undertaken, a single surface created on a multiplex instrument like the Biacore™ 4000 would aid selection by providing real-time interaction analysis in a time-scale to promote efficient scale-up, typically analysing 386 clones in 12 hours [121].

The 20B3 hybridoma also represents a potential source of genetic material for isolation and formation of a recombinant library. Using recombinant technologies it is possible to significantly modify the properties of the antibody in ways not possible with monoclonal antibodies. This would be advantageous as it would allow the evolution of affinity by *in vitro* mutagenesis, to drive down the possible assay limit of detection using *ultra-sensitive* antibodies. Additionally, the ability to tailor the biophysical properties of the antibody, in a retrospective fashion from the hybridoma, would greatly enhance the plasticity of the molecule for differing assay formats and applications [6].

Chapter 5: Recombinant Antibodies

5.1 Introduction to recombinant antibodies for diagnostic-based applications

5.1.1 Applications and potential

Although numerous useful diagnostic kits exist for a multitude of disease states, such as cardiac disease [130] and biological threat detection [54, 131, 132], few biosensor devices employing recombinant antibody technology are commercially available. Biosensors have huge potential in the areas of clinical diagnosis/monitoring, environmental and food safety, biothreat analysis on the battlefield and counter-terrorism [133]. In addition, POC testing can obviate long delays by providing relatively short testing times. However, for POC and other biosensor-based detection devices to become mainstream, current biological formats require reductions in size, sample and reagent volume requirements coupled with significant advances in reliability, ease-of use for multi-analyte determinations and high-throughput capabilities [134]. Table 5.1-1 outlines some examples of recombinant antibody-based biosensors incorporated on various transduction platforms.

Table 5.1-1: Examples of recombinant antibody-based biosensors for important applications

Analyte	Antibody Format	Transducer	Ref.
Disease			
HIV-1 virion infectivity factor	scFv	Piezoelectric	[135]
<i>Listeria monocytogenes</i>	scFv	SPR	[136]
	scFv (phage bound)	Amperometric	[137]
Severe acute respiratory syndrome virus	scFv	Imaging Ellipsometry	[138]
Bio-warfare			
Venezuelan equine encephalitis virus	scFv	Potentiometric	[139]
<i>Bacillus anthracis</i> S-layer protein	scFv	Resonant Mirror	[140]
Haptens			
Morphine-3-glucuronide	scFv	SPR	[141]
Contaminants			
Aflatoxin B1	scFv	SPR	[142]
Parathion (insecticide)	scFv	Piezoelectric	[143]
Atrazine	scAb	Amperometric	[144]

5.1.2 Emergence of recombinant antibody technology

In the late 1980s, the use of vectors in bacterial expression systems demonstrated that correctly folded antibody fragments could be produced [145, 146]. Since then, recombinant antibody fragments have been produced in mammalian [147, 148], insect [149, 150], yeast [151], plant [152] and ‘cell-free’ systems [153]. A factor limiting several of these expression systems is the inability to express large amounts of active protein. The relative advantages and disadvantages of each expression system is reviewed by Verma and co-workers [154]. There are two main sources of antibody genes; V-gene repertoires rearranged from animal or human donors and synthetic antibody V-gene repertoires constructed *de novo, in vitro* [58]. Cloning of antibody fragments into such systems begins with the isolation of mRNA coding for the V-genes from donor cells [155, 156]. Such sources of mRNA include hybridomas, peripheral blood lymphocytes, spleen and bone marrow cells [157]. The mRNA is in turn reverse transcribed into cDNA [156] and the subsequent amplification of the antibody genes is then carried out by PCR-based methods. This strategy for recombinant antibody generation clones all the mRNA molecules encoding for the antibody genes present in the mRNA pool. For the antibodies to be useful it is imperative that the antibody genes be cloned reliably [157]. Hoogenboom and co-workers [58] and Azzazy and co-workers [156] have provided comprehensive reviews of recombinant antibody libraries and their screening.

5.1.3 Antibody fragments and formats

Prior to the development of recombinant antibody technologies, antibody fragments were generated by proteolytic cleavage yielding $F(ab')_2$ and Fab. The ability to generate fragments of antibodies that retain their stability and specificity is essential. Recombinant technologies have facilitated the generation of a number of distinct antibody fragments (Figure 5.1-1) with desirable attributes and specificities for use in diagnostic applications. The smallest fragment of the whole antibody practically used is the Fv which consists of the V_H and V_L domains associated *via* a disulphide bond. Stability problems at lower concentrations were overcome by incorporating a flexible peptide linker into the Fv

fragment generating the single chain Fv (scFv) [158, 159]. Typically, a flexible (Gly₄Ser)₃ linker is used due to its tendency not to form secondary structures and the fact that it is found naturally in the M13 pIII protein and, is well tolerated in phage display. However, it was demonstrated that selection based on linker mutations can influence production, stability and recognition properties of the scFv [160]. Diabody production by incorporating a shorter polypeptide linker (5–12 amino acids) forces the association of two scFv molecules [161]. Genetically encoding alkaline phosphatase (AP) as a fusion to the scFv facilitates direct detection of bound antibody fragments [162, 163]. Dimeric scFv consists of two scFv fragments brought together *via* a naturally dimeric protein [157, 164]. An interesting variation on the dimeric scFv is a bifunctional scFv comprised of AP-labelled scFv [156, 157, 165]. Once these antibody fragments are generated, an appropriate or tailored selection method is used to isolate high-affinity antibodies from a vast library.

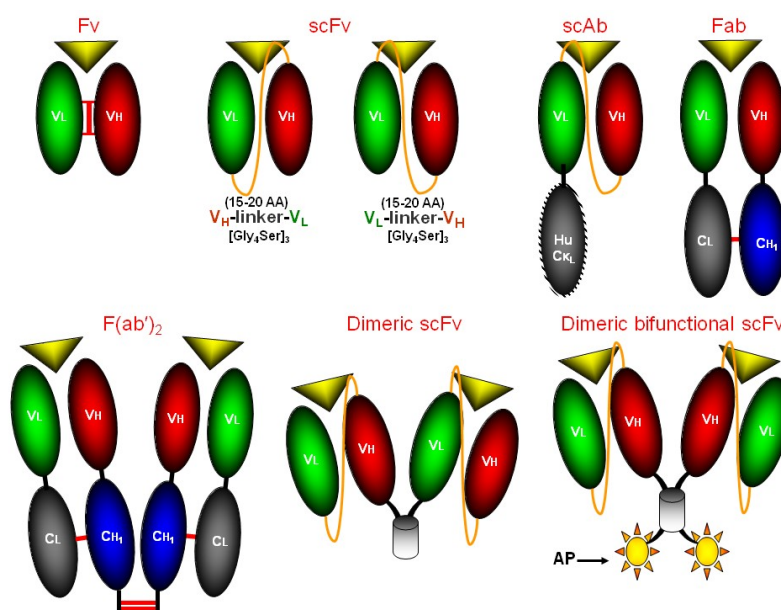


Figure 5.1-1: Recombinant antibody formats

The Fv consists of the V_H (red) and V_L (green) chains. The scFv consists of the Fv with a flexible linker joining the terminal ends of the V_H to V_L (or V_L to V_H). A scAb incorporates a human constant κ light chain or similar species-specific constant domain to the terminal of the V_L or V_H chains. The Fab consists of the Fv with both constant heavy and light chains. F(ab')₂ involves linking two Fab fragments by disulphide bonds (it can also be achieved by proteolytic cleavage of an IgG molecule). A dimeric scFv is generated by fusion of two scFv molecules *via* a naturally dimeric protein. A dimeric bifunctional scFv incorporates an alkaline phosphatase (AP) label to facilitate direct detection. The locations of the antigen binding sites are indicated by the yellow triangles.

5.1.4 Antibody libraries

Antibody libraries mirror what would naturally be present in individuals allowing them to generate antibodies against antigens that might be encountered during normal everyday life. This is the basis of our immune response and permits our survival despite the prevalence of many pathogens, toxins and life-threatening infections. The availability of combinatorial libraries is of major importance in antibody engineering. These libraries may be generated from immunised hosts (animal or human) or are available from academic or industrial sources (naïve or non-immunised libraries). The isolation of antibodies from such libraries is achieved by non-covalent interaction between the library member and its cognate antigen. Efficient high-throughput screening has enabled scientists to screen large libraries thus enhancing the probability of enriching for highly-specific antibodies [166, 167]. This capability has also allowed engineering of antibodies with improved affinity, stability and facilitated the possibility of ‘tailor-made’ antibodies for a wide range of applications.

5.1.5 Advantages of display technology

The advent of display techniques has enabled the generation of very large antibody libraries, thus increasing the probability of selecting antibodies with high-affinity and specificity [168]. In phage display, the antibody fragment is fused to a phage coat protein which provides a link to the encapsulated genetic information [169]. This physical link between the phenotype and genotype simplifies the selection of binders in the antibody library [12]. In contrast, in ribosome display the mRNA, ribosome and nascent antibody form a stable, stalled antibody–ribosome–mRNA (ARM) complex allowing for RT-PCR-mediated recovery of specific fragments [153, 170]. Table 5.1-2 outlines the attributes of phage (plasmid library) and ribosome display (mRNA/PCR fragment) [171].

Table 5.1-2: Phage and ribosome display compared

	Phage Display	Ribosome Display
Largest Library Size	10^{10} [172]	10^{13} [58] potentially 10^{14} [173]
Recovery of selected binders	Various (Figure 5.1-3)	RT-PCR (Figure 5.1-4)
Diversification	Mutagenesis	Mutagenesis (<i>in situ</i>)
Transformation and cloning	Required	Not required
Highest affinity mAb reported	Picomolar [174]	Picomolar [175]

Table adapted from [171].

Other display technologies include yeast [176, 177], bacterial [178] and mRNA display [179, 180]. A major advantage of the use of combinatorial display libraries is the generation of an immunised repertoire of antibodies from practically any species [181]. However, hybridoma technology applied to rabbit [182], cow [183], chicken [184] and human [185] lymphocytes has shown some success. The ability to generate antibodies recognising human epitopes, e.g. in biomarkers of diseases, is essential for many diagnostic tests and for therapy. Generally this can be achieved in a range of species, but the antigenicity is often dependent on how phylogenetically distant the species are from humans [88]. To date antibody libraries have been generated from a number of species including human [186], mouse [187], chicken [88, 188], rabbit [189, 190], camelids [191], shark [192], cattle [193] and sheep [194]. The availability of naïve and synthetic repertoires facilitates the generation of antibodies without the need for immunisation of animals, since such libraries can recognise a wide range of antigens [195]. The ability to generate recombinant antibodies to target-specific antigens, for example those demonstrated in Table 5.1-3, is crucial for the efficient development of the biorecognition elements for biosensor- and POC-based devices.

Table 5.1-3: Examples of recombinant antibodies generated to specific targets

Target	Analyte	Ref.
Human Disease		
<i>Cardiac disease</i>	Cardiac troponin (cTn)	[196]
	C-reactive protein (CRP)	[167]
	Heart-type fatty acid binding protein (h-FABP)	[90]
	Myeloperoxidase	[197]
<i>Hormones</i>	Thyroid stimulating hormone (TSH)	[198]
Haptens		
<i>Environmental</i>	Atrazine	[199]
<i>Illicit drugs</i>	Morphine-3-glucuronide	[200, 201]
Animal Disease		
<i>Foot and mouth</i>	Non-structural protein 3ABC	[202, 203]
<i>Mastitis</i>	<i>N</i> -acetyl-beta-D-glucosaminidase	[204]
<i>Bovine immunodeficiency virus</i>	Capsid protein	[205]
Security		
<i>Biological warfare pathogen</i>	<i>Brucella melitensis</i>	[206]
Contaminants		
<i>Food stuffs</i>	Aflatoxin B1	[59, 207]
	Halofuginone	[208]
	<i>Salmonella Typhimurium</i> (OmpD)	[209]

5.1.6 Phage display

5.1.6.1 Introduction

Phage display has become a widely exploited selection platform for antibodies since it was first described in 1985 by Smith and co-workers [210]. Use of the novel bacteriophage lambda expression system facilitated rapid identification of antibodies, and was suggested as a method to supersede hybridoma technology [211]. McCafferty and co-workers initially isolated an antibody from a large combinatorial library [212], and due to its robust nature phage display has become the ‘work-horse’ of antibody isolation [213]. Library diversities of up to 10^{10} have since been achieved [58]. Antibody selections performed on immobilised antigen [214, 215], antigen-coated magnetic beads in-solution [216-218], Biacore™ [219, 220], surface-displayed targets [221, 222], mammalian tissue culture [223] and *in vivo* approaches [223, 224] have all been successfully used in phage display.

5.1.6.2 The principle of phage display

Filamentous phage particles encapsulate single stranded DNA (ssDNA) and are capable of infecting *Escherichia coli* cells. Filamentous phage (Figure 5.1-2) infect and replicate without killing the host cell, unlike lytic phage (e.g. T4) [225]. The phage coat is composed of 5 different proteins (pIII, pVI, pVII, pVIII and pIX) [89, 213]. The pVIII (~50 amino acids) is the major coat protein and covers the surface of the phage cylinder. The hydrophobic 33 amino acid pVII (5 particles) and the 32 amino acid pIX proteins are located at one proximal end of the phage particle. The other end contains the pVI (112 amino acids) and pIII (406 amino acids) [89]. The pIII consists of the N1, N2 and CT domains. The interaction of the phage with the cell is mediated by the pIII protein (specifically N1 and N2 domains) and phage biology is well understood and documented [213, 226, 227]. The N1 domain is required during infection of the cell facilitating translocation of DNA into the cytoplasm and the N2 region is responsible for binding to F pilus, while the CT domain is essential for the formation of a stable phage particle [89, 213]. Antibodies consist of heterodimeric heavy and light chain variable domains that

combine to form the antigen-binding site and phage display of such a scFv is depicted in Figure 5.1-2. The two variable domains are linked by a polypeptide linker and integrated into the phage genome as a fusion to the gene of the pIII protein.

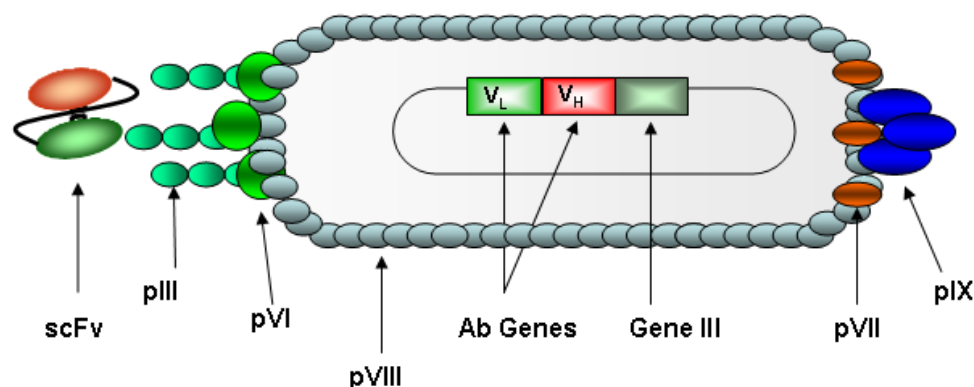


Figure 5.1-2: Phage display of a single chain fragment variable antibody

ScFv is displayed as a fusion to the pIII phage coat protein retaining a link between the antibody phenotype and the encapsulated genetic information. The phage remains infective to *E. coli* via pIII-mediated attachment to F pili. pIII proteins consist of N1 and N2 domains responsible for interaction with the F pilus of the cell and insertion of the phagemid DNA into the cytoplasm.

The development of phagemid vectors [214] has taken over from the initial use of phage vectors [211] due in part to the simplified transition to soluble expression of the antibody fragment, using an amber stop codon mutation between the geneIII (or pIII) and the antibody chain [156, 228]. This facilitates antibody fragment expression without continued fusion to the phage pIII by use of non-suppressor strains of *E. coli* [156, 228, 229]. Phage systems are also limited as fusions of large polypeptides to the amino acid terminus of the coat protein, lead to compromised protein function [230]. Phagemid systems permit the display of polypeptides that could not be displayed in simple phage systems by fusion to alternative coat protein genes encoded on the phagemid vector. This attenuates the effects of the fusion protein as the wild-type coat proteins are available from the helper-phage [230]. Table 5.1-4 outlines considerations to be taken into account when choosing phage or phagemid methods of recombinant antibody production.

Phagemid vectors contain *E. coli* and phage origins of replication. The phagemid DNA is packaged in the phage coat and propagated by super-infection with helper-phage [213].

This infection step allows the phagemid vector in the cell to be packaged into the phage particle in an identical way to phage DNA. The helper-phage serves to provide the proteins and enzymes necessary for phage replication and also the structural proteins required for encapsulation. To prevent over expression of the helper-phage genome, commercially available helper-phage contain a defective origin of replication (M13KO7 or VCSM13) and/or packaging signal [89, 213, 225].

Selection of such displayed antibodies is achieved by multiple rounds of binding to a target which selectively enriches phage with the relevant cognate antibody fragment expressed on their surface (Figure 5.1-3) [229]. Specific phage are eluted and re-infected into *E. coli* for sequential rounds of bio-panning [213] or soluble expression of antibody in non-suppressor strains which facilitates downstream purification and characterisation of the selected antibody fragments [156, 227].

Table 5.1-4: Phage and phagemid systems compared for antibody production

Phage	Phagemid
Better suited to peptide display	Suited to antibody display
Large proteins effect pIII production and assembly	Carries the fusion-coat protein to be displayed (e.g. pIII)
Large proteins present on pIII can affect infectivity	Large inserts are better maintained
Lower transformation efficiency	Higher transformation efficiency
Misfolding of large proteins more likely	Multiple copies of gene inserts per phage particle (valency)
No requirement for helper phage	Requires helper-phage to select
Avidity effects – lower affinity antibodies	Monovalent display – higher affinity antibodies
Sub-cloning required for soluble expression	Direct expression of soluble antibody
Not suited for affinity maturation	Suited for affinity maturation

This table was adapted from [89, 227, 231].

5.1.6.3 *Selection considerations for successful phage display*

Despite phage display of antibodies being widely practiced and mainstream in many molecular laboratories [58], the successful selection of specific antibodies remains a challenge [176]. The selection conditions exploited (Figure 5.1-3) can dramatically influence the quality of the selected antibody fragment and not all standard conditions lead to the selection of phage-displaying antibodies-specific to the target antigen. Selection aims to isolate high-affinity antibodies. However, the level of display may preferentially recover the antibody with the highest display level (avidity) on an individual phage particle. Monovalent display has been utilised to combat this phenomenon [58, 225, 231].

After transformation, the phage selection cycle illustrated in Figure 5.1-3 (steps 2–6) is sequentially repeated in order to isolate specific phage-displayed antibodies. In theory, only one round of selection from a phage library should be necessary. However, in practice non-specific binding of ‘sticky’ phage limits the enrichment that can be achieved. Typically between two and five rounds of bio-panning are required to isolate specific antibody-displaying phage as the ratio of binders to non-binders before and after each round of selection varies from 5- to 1000-fold [231]. Selection conditions such as elution strategy, stringency of washing, use of solid- or solution-phase methodologies, antigen form and the number of cycles (increasing cycles leading to decreased diversity) impact on the quality of the isolated antibody and require significant consideration [232, 233].

Antigen presentation is of particular importance and several presentation strategies are outlined in Figure 5.1-3. Conformational changes as a consequence of direct immobilisation on solid supports [156] or the use of peptide antigens, may result in the selection of antibodies that fail to recognise native epitopes in the context of the whole target molecule. Schier and co-workers have shown that affinity-driven selections of mutated scFv on immobilised antigen preferentially selected spontaneously dimerising scFv, with higher apparent K_D values, due to avidity effects compared to selection on biotinylated antigen with streptavidin-coated magnetic beads [215]. This demonstrated the dramatic influence of solid and solution-phase modes of selection, impacting upon the type and binding characteristics of the isolated antibodies. Lowering the antigen concentration in successive rounds of selection enriches for higher-affinity antibodies in a similar fashion to

B-cell selection *in vivo* [58, 231]. Low-concentration selections are employed to select antibodies with the highest affinity avoiding multimer formation [231]. Selection can also be tailored to favour affinity or ‘off-rate’ kinetics by gradual limitation of available antigen [229], limiting interaction time of the phage with the antigen, performing solution phase selection or competitive interaction with free antigen. To isolate specific, high-affinity antibodies the first round of selection should be regarded as an enrichment step, as excessive stringency leads to a decrease in the library diversity [227]. The multiplicity of infection of the helper-phage is also of considerable importance ensuring that each antibody is represented within the library. It is imperative to add sufficient phage (10–20:1) to infect the whole library and failure to do so in the initial amplification of the library leads to a reduction in diversity [234].

Suitable blocking agents to reduce non-specific binding are required and typical agents are semi-skimmed milk powder, bovine serum albumin (BSA) and keyhole limpet haemocyanin (KLH). Inclusion of detergents such as TweenTM-20 in washing steps and in the phage preparation contributes to reducing non-specific interactions [231]. Initially, each phage is represented in low numbers and washing should be less stringent to allow recovery of all antigen-bound phage. After the initial cycle, the stringency can be increased as the phage particles populate the library in higher numbers and it is necessary to exert selective pressure to isolate strong binders [231]. When bio-panning with immobilised antigen washing is performed by rinsing the wells or the immunotube with an increasing number of washes per round with a wash solution, e.g. PBS containing 0.05-0.1% (v/v) Tween®-20 [233]. Bio-panning in-solution typically involves using magnetic beads coated with the biotinylated antigen to capture phage-displaying antibodies [231]. Subsequently, the beads are washed and then recovered using a magnet. Bio-panning by cell surface display (e.g. surface/membrane proteins) requires centrifugation and re-suspension in wash solution [231].

Elution of specific-phage can be achieved in a number of ways (Figure 5.1-3). Elution by altering pH uses acidic (e.g. glycine-HCl, pH 2.2 [235, 236]) or basic (e.g. triethylamine [232, 237]) solutions followed by immediate neutralisation with a suitable reagent. Neutralisation is critical to prevent protein denaturation. It is also necessary to optimise elution as increasingly stringent elution may be required as antibody affinity increases [220]. Elution, without breaking the antigen-antibody interaction, can be facilitated by

trypsin [238], cleavage of a protease-sensitive site [239], NHS-SS-biotin cleavage by DTT [240] or use of commercially available paramagnetic beads containing a nuclease-cleavable DNA linker between the bead and streptavidin [241]. These methods for site-specific cleavage provide a means of decreasing background phage elution. Interaction between the phage and the *E. coli* cell can also be evoked to elute phage through the natural affinity for F pili [237].

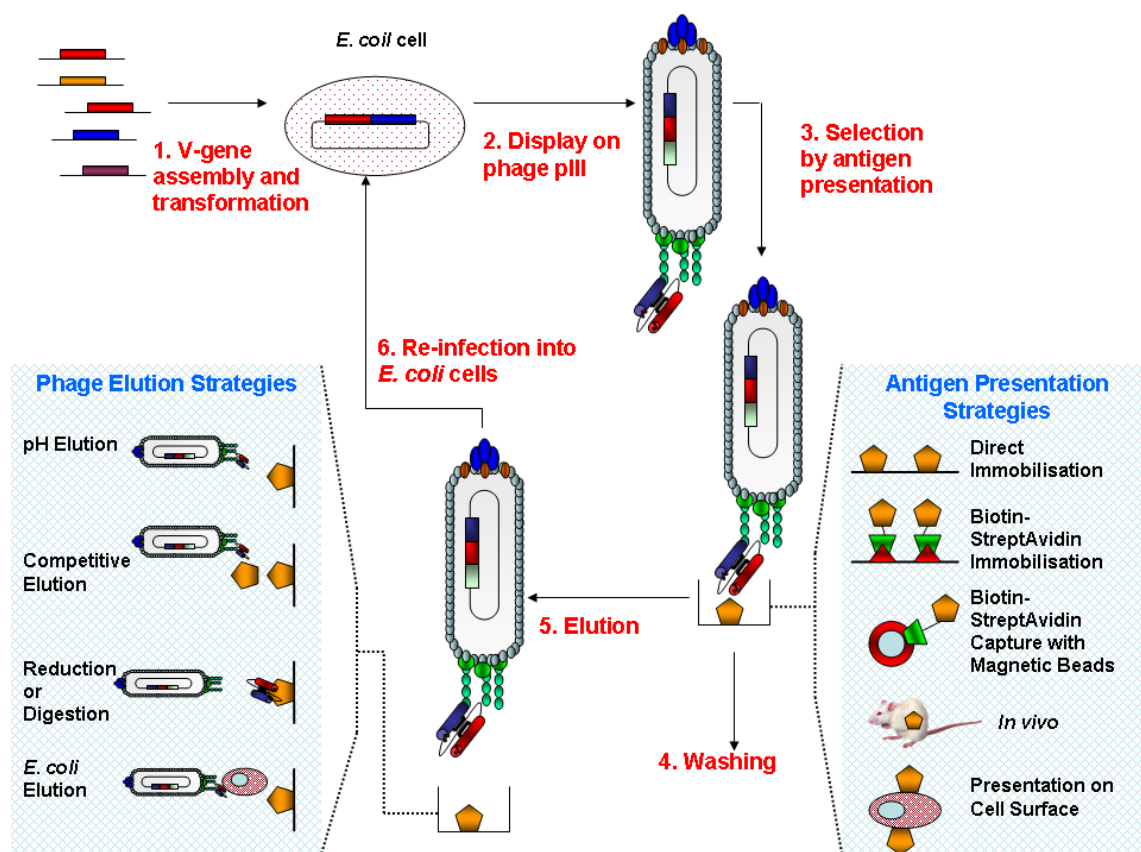


Figure 5.1-3: Overview of phage selection strategies

The iterative selection strategy shown is a multistep process. V-gene assembly by PCR allows cloning of the recombinant antibody library into *E. coli*. Subsequent rescue by helper-phage permits the propagation of the phage antibody library (scFv is shown). Antigen presentation is a key consideration and there are many modes of antigen-phage-antibody interaction. Serially increasing the stringency of washing after antigen presentation selects those phage displaying antibodies with highly-specific binding properties. Elution strategies are also illustrated. This figure was adapted from [176].

5.1.7 Ribosome display

5.1.7.1 Introduction

Ribosome display is a totally ‘cell-free’ method of selection and evolution of proteins that is not limited by any cell-based transformation steps [242-245]. It is an *in vitro* selection method for the isolation of proteins and peptides from large libraries that was successfully applied to the affinity maturation of antibodies using eukaryotic and prokaryotic systems [246]. The use of ribosome display overcomes current limitations for protein selection technologies as diversity is not limited by transformation efficiency, but by the physical number of ribosome molecules present and differing mRNA molecules available *in vitro*. Ribosome display couples the individual emerging protein (phenotype) with its corresponding mRNA (genotype) by the formation of stable protein–ribosome–mRNA (PRM) complexes, and after selection, PCR amplification of corresponding DNA for concurrent selection or diversification [247].

5.1.7.2 The principle of ribosome display

The generation of antibody–ribosome–mRNA (ARM) complexes [170] was developed from two experimental achievements: i) the production of single chain antibodies *in vitro* using rabbit reticulocyte lysate [248] and ii) the experimental demonstration that nascent proteins can remain stably associated with their mRNA as a polypeptide–ribosome–mRNA (PRM) complex in the absence of a stop codon or with the inclusion of antibiotics [249, 250]. The generation of the ARM complex, illustrated in Figure 5.1-4, allows the stalled complex to be selected for by interaction of the nascent protein with its cognate antigen. This captured complex permits the recovery of the genetic information directly from the ribosome-bound mRNA [170]. Ribosome display has two important functions: i) it allows selection, using proofreading polymerases and antigen-coated beads or plates [251] and ii) evolution of antibody affinity. The combination of both of these functions facilitates the selection of specific antibodies from a combinatorial library with simultaneous evolution of the protein by successive diversification of the pool with each round [153, 179, 252, 253].

The ribosome display construct is generally composed of the T7 promoter, a ribosome-binding site, a translational enhancer (such as the β -globin gene of *Xenopus laevis*), a translational initiation signal (such as Shine-Dalgarno for prokaryotic systems or Kozak sequence for eukaryotic systems) and an open reading frame (ORF) in which the library is fused to a C-terminal polypeptide spacer without a stop codon [244, 250, 253, 254]. The absence of a stop codon is crucial as it facilitates recovery of the intact, stalled ARM complex. Spacer length is of importance as it facilitates folding of the nascent protein by ensuring exit from the ribosomal tunnel. Typically, at least 20–30 amino acids are required and a spacer of 116 amino acids was shown to be more efficient in displaying proteins [255]. The spacer also provides a known sequence for designing primers for the RT-PCR recovery of the selected library [247]. Commonly used spacer sequences include human antibody light chain (C κ) and filamentous phage geneIII [244, 255]. The inclusion of 5' and 3' stem loop structures serve to improve mRNA stability by protecting it against degradation by RNases [253, 256].

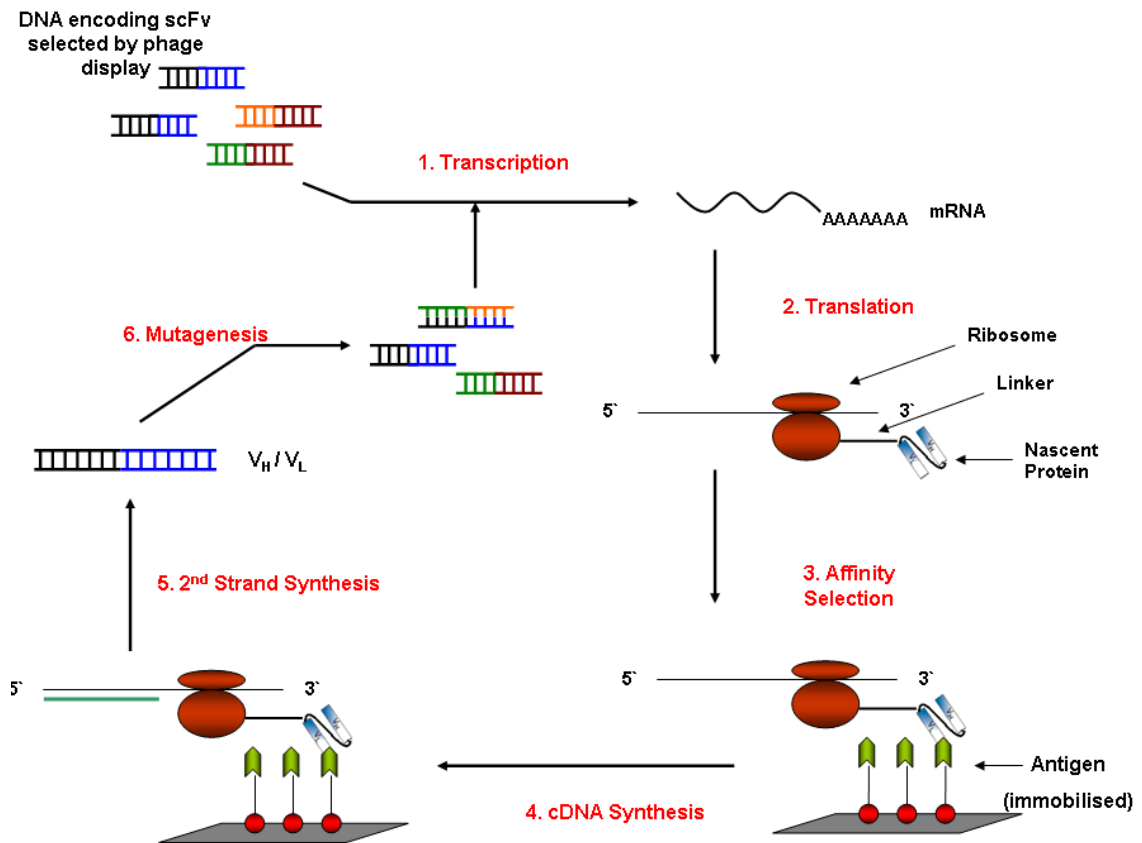


Figure 5.1-4: Overview of the principle of ribosome display

Overview of eukaryotic ribosome display, selection and evolution of antibody affinity. Selection is based on the formation of the antibody-ribosome-mRNA (ARM) complex by stalling the ribosome. The complex can then be isolated by affinity interaction with biotinylated antigen. RT-PCR then allows for the *in situ* recovery of the mRNA encoding for specific ARM complexes. Affinity evolution can be facilitated by the use of error prone PCR (random), chain shuffling (random) or site directed mutagenesis. This figure was adapted from [170, 247, 256].

5.1.7.3 *Considerations for successful ribosome display*

For antibody generation using ribosome display the folding efficiency is affected by inclusion of transcription stabilisers, as transcription requires reducing conditions whereas translation requires oxidising conditions. Hence, the enzymatic activity of transcription (T7 RNA polymerase) requires monitoring in the absence of reducing reagents and, where reducing agents are used for transcription, oxidising conditions are required for the subsequent translational step [256, 257]. Time, temperature and the inclusion of various additives for *in vitro* translation impact upon the yield and efficiency of ribosomal display. These effects are summarised briefly in Table 5.1-5.

Table 5.1-5: Factors affecting translational efficiency in ribosome display

Translational Factor	Effect
<i>Temperature</i>	Enzymatic activity of polymerase.
	Degradation of mRNA by RNases.
	Folding efficiency of synthesised protein.
<i>Time</i>	Longer translational times required in eukaryotic versus prokaryotic systems.
	Critical in uncoupled systems as mRNA is continually produced.
	Accumulation of small MW molecules from hydrolysis of triphosphates with longer translation times.
	Time-dependent inactivation of α -subunit of initiation factor 2 (eIF-2) by Ca^{2+} .
<i>Additives</i>	Protein disulphide isomerase (PDI) catalysing the formation of disulphide bonds.
	16S rRNA inhibition by anti-sense DNA-oligonucleotides.

Adapted from [153, 242, 253, 256, 257].

5.1.8 Mutagenesis strategies for evolution of antibody affinity

Mutagenesis introduces errors or changes in the genetic blueprint which gives rise to modified proteins, products or functions. Mutagenesis is an efficient method applied to directed molecular evolution. Evolution *in vitro* is a powerful tool for protein generation and refinement with improvements in binding affinity, folding efficiency and enhanced thermodynamic stability demonstrated [258]. Mutagenesis of genes is generally carried out using two broad strategies. Site-directed mutagenesis introduces errors focused in a particular region (e.g. CDR or antibody conserved regions). Alternatively, random mutagenesis causes mutations scattered across the gene in a stochastic manner by use of error prone PCR and/or DNA shuffling. Figure 5.1-5 outlines mutagenesis strategies for affinity improvement of selected antibodies by manipulation of the V-genes [6, 242].

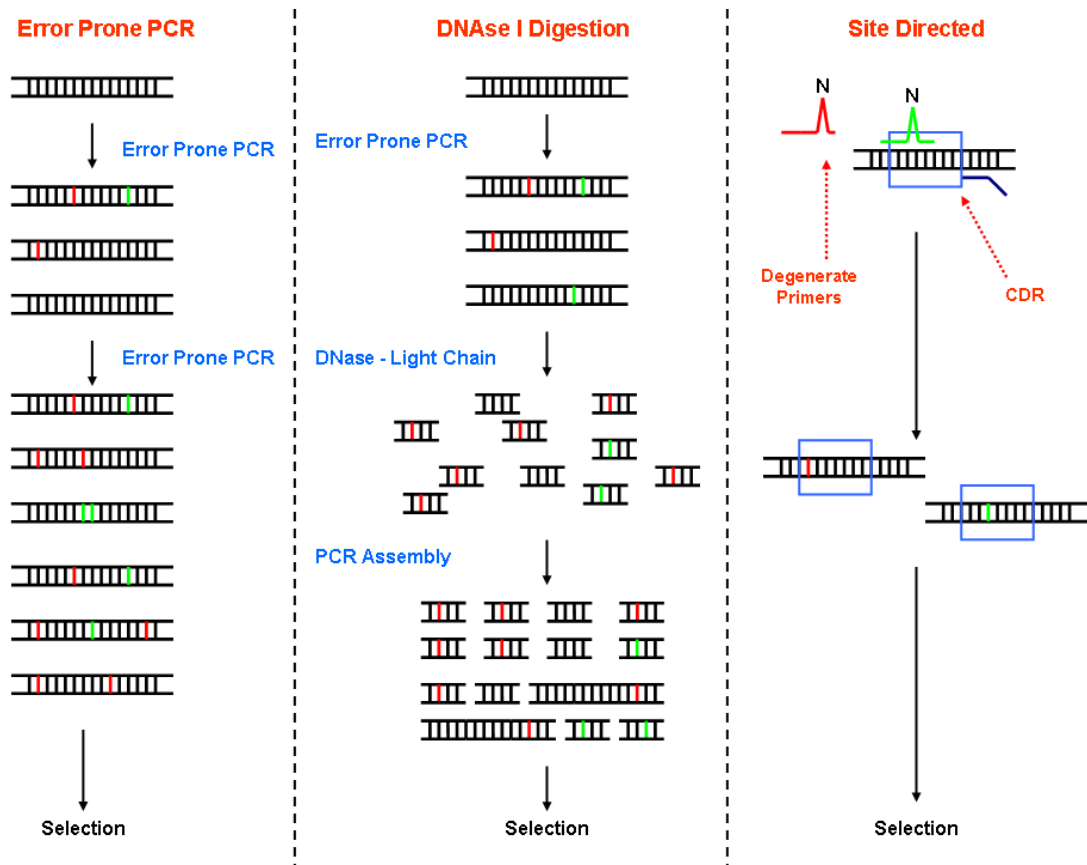


Figure 5.1-5: Overview of mutagenesis strategies for the evolution of antibody affinity

Strategies for the introduction of mutations for altering/improving the affinity of recombinant antibodies. Advantageous (red) and deleterious (green) mutations are shown. Error prone strategies introduce mutations randomly across the gene. With increasing number of PCR cycles more mutations are introduced. The useful mutations can be masked by deleterious ones and DNA shuffling of the light (and/or heavy) chains offers a solution by cleaving the gene with *DNase I* and allowing the gene to randomly reassemble (shotgun approach). Site directed mutagenesis of the CDR incorporates degenerate primers to introduce mutations in the antigen recognition sites. This figure was adapted from [258].

5.1.9 Genetically coded-tags for biosensor development

The inclusion of certain known peptide tags in recombinant antibody expression vectors offers a rapid and reliable method of purification and characterisation [259]. These tags may also prove useful as capture sites in biosensor development.

Oligohistidine tagging of antibody fragments has long been hugely beneficial for enhancing the purification process [260], but may also be useful in non-covalent coupling of the antibody to sensor surfaces using anti-histidine monoclonal antibodies [261], or potentially direct coupling to sensor surfaces, as demonstrated by Lori and co-workers [262]. The anti-HA (YPYDVPDYA) tag derived from influenza virus is extensively used in recombinant protein technology as a useful tag for capture methodologies [167]. FLAG (DYKDDDDK) residues incorporated into antibody fragments have utility as a useful ‘capture’ methods for recombinant protein characterisation. Mersich and co-workers demonstrated the detection of FLAG-tag fusion proteins facilitated by the use of anti-FLAG monoclonal antibodies in a SPR-based system [263]. The AviD tag is a neutrAvidin- (or avidin)-specific moiety that has useful applications in the immobilisation and purification of recombinant proteins [264]. Despite the absence of examples of biosensors utilising this specific AviD tag, there are many reports of the use of avidin, streptavidin and neutrAvidin surfaces or beads immobilising biotinylated antibodies for use in biosensors [265-267]. Purification using streptavidin-binding peptide (SBP tag) has also been demonstrated as a useful approach [268]. The SBP tag interacts specifically with streptavidin, but is a weaker interaction than between biotin and avidin. Hence, dissociation can be controlled and this SBP tag was utilised in surface preparation as demonstrated in both SPR- [269] and TIRF-based [270] systems.

Additionally, site-specific modification made possible by recombinant antibody techniques permits the incorporation of unnatural amino acids (e.g. selenocysteine [271]) or reactive amino acids (e.g. cysteine) into the antibody construct. This is of considerable value for specific ordered immobilisation or labelling of diagnostically-relevant antibodies for efficient incorporation into POC or biosensor devices.

5.1.10 High-throughput screening of antibody libraries

The real value of large and highly diverse recombinant libraries can only be efficiently exploited if the most judicious and discriminatory selection and enrichment regimes are employed [272]. This is particularly true in the case of extremely large ribosome displayed libraries and especially following focused *in vitro* directed evolution campaigns that can generate large pools of closely related yet heterogeneous clones. In order to exhaustively ‘mine’ such libraries it is important to ensure that a suitably comprehensive number of individual clones, rather than a small representative subset, are analysed. Interestingly, some of the most useful means of accomplishing such high-throughput data-rich ranking of binding interactions is provided by the newest generation of multiplexed SPR-based biosensors. Currently, the GE Healthcare Biacore™ 4000 instrument offers extremely high-sensitivity kinetic ranking of ligand interactions [121, 167]. It can accommodate multiple 96- or 384-well plates in temperature-controlled integrated rack housing. Four flow cells, each containing five interaction spots, employ hydrodynamic addressing to control interaction flow paths. Dedicated LIMS integration software facilitates compatibility with existing LIMS systems that are now increasingly established in high-throughput screening labs. The ProteOn XPR36 system from Bio-Rad is a unique 6×6 multichannel SPR platform that enables automated multiplex analysis of up to 36 biomolecular interactions in one experiment [273-275]. The powerful parallel processing abilities of the ProteOn XPR36 and 4000 are apparent, but the cost associated with running and the acquisition of such instruments is substantial [127]. An alternative system from ICx Nomadics (www.discoverensiq.com), the SensiQ Pioneer, is an SPR-based three flow cell and fully automated system that maintains affordability [276]. Interestingly, the system removes the need for manual preparation of individual concentrations in an experiment, but rather employs a continuous concentration gradient allowing the kinetic evaluation of 192 clones over a concentration range of 2-3 orders of magnitude [277]. The availability of such truly high-throughput instruments represents a powerful capacity for candidate screening. In addition, the capability to assess key binding events with many interaction partners in real-time and in parallel is of considerable value.

It is worth also mentioning that numerous emerging parallel instruments/technologies which are versatile alternatives to more refined HT-SPR systems are available [127]. Planar

protein arrays bring existing methods, for example ELISA, into the forum of HT and parallel. Several commercial systems exist and the development of SPR imaging brings together the advantages of traditional SPR with HT capabilities [278]. The Octet from ForteBio is another such system in which biolayer interferometry monitors biomolecular interactions. The system does not have the same sensitivity as the Biacore or ProteOn XPR36 instruments, however, its disposable tips obviate the requirement to regenerate and additionally the system operates without micro-fluidics making it an interesting complementary technology [274].

Several experiments carried out by Abdiche and co-workers compare a number of SPR platforms, namely Biacore™ 3000 (GE healthcare), Octet (ForteBio) and ProteOn XPR36 (Bio-Rad) in several blocking assay configurations [279]. Such epitope-based analysis allows binning of antibodies with similar epitopes. These assays are amenable to high-throughput analysis where often the affinity of the interaction is not the primary concern, as affinity can be engineered, but rather antibodies targeting specific-epitopes are of paramount interest. Blocking assays can also answer the question “does the binding of one molecule to a second prevent a third binding event?” The study demonstrates three interaction configurations (tandem, premix and classical sandwich) and the epitope bins correlated well when tested in each interaction configuration and on each analytical system [279]. Finally, the 20 country-wide benchmark study of affinity-based biosensors conducted to determine the variability in biosensor studies, by Rich and 150-colleagues, demonstrates the worldwide usage of SPR [280]. This publication employed a wide-breath of instruments from the Biacore™ range (A100, T100, S51, 3000, 2000, 1000, X100, flexichip and X), ProteOn XPR36, Octet and SensiQ to name a few. The data presented highlights the reliability of the systems in kinetic determination with individual user-designed experiments using a common interaction partner set (Fab fragment and GST-tagged antigen) on a range of surfaces [280].

5.1.11 Avian and mammalian repertoires as sources of antibody libraries

IgY is the typical low molecular weight antibody of several species (Table 5.1-6) and an evolutionary ancestor of IgG and IgE which are found only in mammals [281-283]. The chicken IgY, like IgG, consists of four polypeptide chains, but it differs by the presence of an additional constant heavy domain ($Cv_1 - Cv_4$) with an additional carbohydrate moiety, as illustrated in Figure 5.1-6. IgY by virtue of its lack of a hinge region, has significantly reduced flexibility in comparison to IgG. Its limited flexibility is derived from proline-glycine rich regions around the Cv_1 - Cv_2 and Cv_2 - Cv_3 domains [281].

Table 5.1-6: Properties of IgG and IgY

	IgG	IgY
Species	Mammals	Birds, reptiles, amphibians and lungfish
Molecular weight (kDa)	150	180
Isoelectric point (pI)	6.4-9.0	5.7-7.6
Concentration (mg/mL)	10-12 (serum)	15-25 (Egg Yolk)
Number of constant domains	4 (3 H and 1 L)	5 (4 H and 1 L)
Hinge	Yes	No
Complement binding	Yes	No
Rheumatoid factor binding	Yes	No
Fc receptor binding	Yes	No
Mediates anaphylaxis	No	Yes
Binding to protein A	Yes	No
Binding to protein G	Yes	No

This table was adapted from [283, 284].

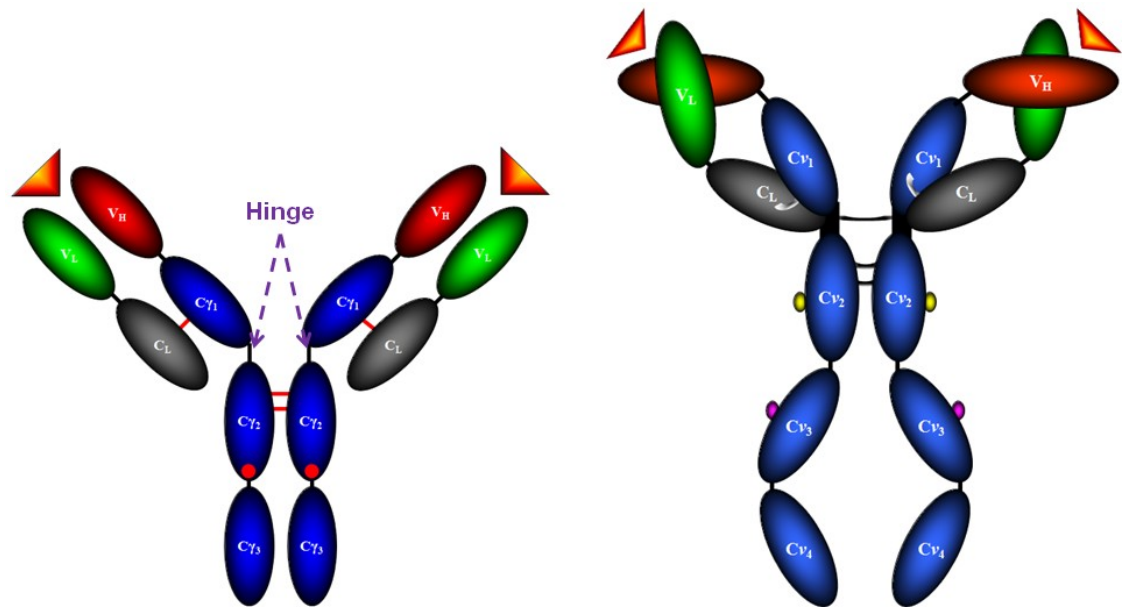


Figure 5.1-6: Illustration of the structural differences between IgG and IgY

IgG (left) is composed of four constant heavy domains with a single carbohydrate site (red dot) on each heavy chain. In contrast, the additional constant domain introduces a second carbohydrate site (yellow and purple dots). The flexible hinge region in the evolutionary ancestor (IgY) is absent and thus restricts flexibility in comparison to IgG.

Of considerable advantage is the simplicity of the germline genes in the avian immune system (single V_H and V_L germlines) in comparison to the primary antibody repertoire diversity mechanism in most vertebrates. In the chicken system, diversity is not achieved by a diverse set of Ig variable (V), diversity (D) and joining (J) gene segments as is the case in the mammalian system. Diversity is achieved rather by gene conversion (7-10 random conversions or transplantation of upstream pseudogene blocks) of single functional Ig V and J segments of both the heavy and light chains causing rearrangement of genes during the developmental stage of B-cells in the *Bursa of Fabricius* (Figure 5.1-7) [281, 283, 285]. In the IgH loci, 80-100 pseudo- V_H genes and in the IgL loci, 26 pseudo- V_L genes exist upstream of the functional V gene segment which are unable to undergo recombination with the (D)J gene segment due to lack of a 5' promoter and a functional recombination signal sequence (RSS) [282]. Although a limited number of genes are involved, gene rearrangement of heavy V_H - D_H - J_H and light V_L - J_L followed by subsequent gene conversion results in a large combinatorial diversity ($\sim 3 \times 10^9$) for chicken [282]. This limited Ig V functional gene pool is advantageous for recombinant antibody generation as it affords ready sampling of the entire antibody repertoire with a small primer set. This saves on time

and resources, in addition to ensuring that rare transcripts are not lost due to primer inefficiencies that are associated with complex primer mixes used to clone the mammalian antibody repertoire [286]. Many targets, especially those with therapeutic potential, are highly conserved in the evolution of mammals. This renders the immune response limited at best in both mice and rabbits as a result of immunological tolerance conferred during foetal development [88]. The use of chickens is advantageous in this respect as human proteins may be significantly different from those in the avian system giving rise to greater immunogenicity. Furthermore, several other advantages exist in terms of diagnostic applications and those are summarised in Table 5.1-7.

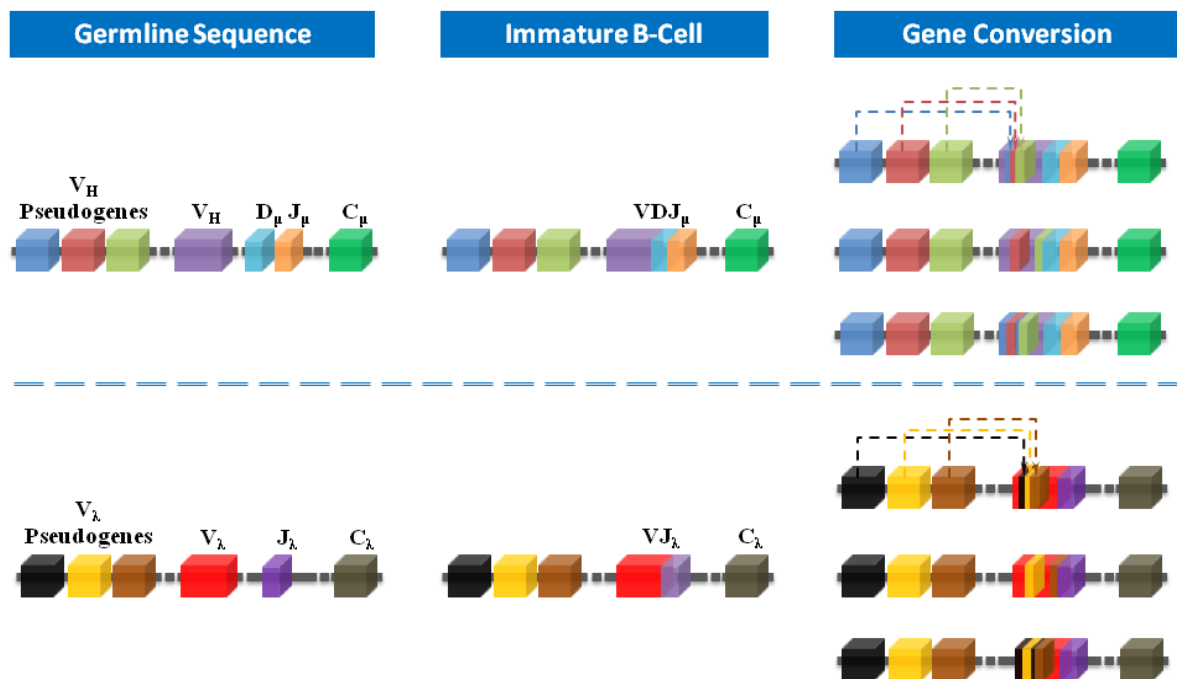


Figure 5.1-7: Overview of the process of gene conversion in chicken Ig genes

Both the V_H and V_L germline sequences undergo a process known as gene rearrangement as an initial stage of antibody generation. In the H germline, a functional V_H domain is comprised of unique V_H and J_H gene segments with one of a family of D_H elements (~ 15). In the L germline, only one light chain exists (λ) and every light chain is composed of the same V_L - J_L arrangement which in itself generates minimal diversity. Inter-chromosomal gene conversion in immature B-cells gives rise to massive diversity by translocation of pseudogene sequences into the V-genes. Typically the closest pseudogene is used more frequently in gene conversion, but in the light chain the pseudogenes are distributed across a 20kb region preceding the V_L gene [282].

Table 5.1-7: Advantages of exploiting the avian immune system for diagnostic antibody generation

Avian Antibodies	Benefit	Reference
Simplistic genes	Single primer sets. Efficient sampling of immune repertoire.	[88, 282, 285-288]
Phylogenetically distant	Respond strongly to mammalian protein antigens.	[285, 286, 289]
Stable at higher core temperature (41°C)	Stable antibodies (half-life in order of months).	[281]
Increased CDRH3 Length	Potential for greater diversity.	Personal observations, [290]
Lacking Fc effector function	Advantageous in diagnostic tests – reducing interference and false positives.	[281, 291, 292]
Multiple antigen immunisations tolerated	Multiple V-gene specificities available from a single animal and reducing costs.	[289]
High antibody yield in egg	Non-invasive, plentiful source of polyclonal Ab.	[281, 282]
High ratio of B-cells (100x compared with mouse)	Rich source of V-gene mRNA, facilitates efficient sampling of V-gene repertoire.	[285]
Not yet used in therapeutics	No HAMA responses – reduction in instances of false positives.	[281]
Increased levels of antibody produced	Reduction in number of laboratory animals required leading to reduced costs.	[281]

5.2 Results of the generation and isolation of recombinant antibodies against epitope-1 of cTnI

Recombinant antibody-based techniques for the development of highly tailored specific antibodies for cTnI epitopes one and three were evaluated. The epitope recalcitrance found with whole protein-based immunisation strategy was overcome with a focused, synthetic peptide immunisation regime for epitope one in common with the generation of the 20B3 monoclonal antibody. In contrast, epitope three-specific scFvs were readily isolated from an immunisation campaign using the commercial cTnI protein. The more established and routine methodology of phage display was opted for over ribosome display due to nature of the panning experiments undertaken where complex antigen presentation methodologies required a robust selection methodology.

The main rationale behind the use of chickens in the course of this project was the phylogenetic distance from man leading to greater cTnI protein heterogeneity (Figure 5.2-1). In the epitope one and two region human and mouse have identical amino acid compositions. In chicken, the amino acid sequence differs by four residues in this region and that was postulated to lead to increased immunogenicity. Epitope-specificity has proven recalcitrant in a whole protein-based immunisation regime for epitope one which could possibly be explained by the identical amino acid sequence in chicken and man. Again in the approach taken, native epitope recognition was paramount in the synthetic peptide-based immunisation strategy.

```

P19429 MADGSSDAAREPRPAPAPIRRSS--NYRAYATEPHAKKSKISASRKLQLKTLILLQIAKQ 59
P48787 MADESSDAAGEPQPAPAPVRRSSANYRAYATEPHAKKSKISASRKLQLKTLMLQIAKQ 60
Q6S7R6 MAE-----EEEPKPPPLRRKSSANYRGYAVEPHAKRQSKISASRKLQLKTLILLQRAKR 53
      **:          * . * *:*** ***.***.*****:*****:*** **:

P19429 ELERAEAEERRGEKGRALSTRCQPLELAGLGFAELQDLRCQLHARVDKVDEERYDIEAKVT 119
P48787 EMERAEAEERRGEKGRVLRTRCQPLELDGLGFEELQDLRCQLHARVDKVDEERYDVEAKVT 120
Q6S7R6 ELEREEQERAGEKQRHLGELCPPELEGLGVAQLQELCRELHARIGRVDEERYDMGTRVS 113
      *:*** :** *** * * * * * ** ***. :***:***:***:..:*****: :*:

P19429 KNITEIADLTQKIFDLRGKFKRPTLRRVRISADAMMQALLGARAKESLDLRAHLKQVKKE 179
P48787 KNITEIADLTQKIYDLRGKFKRPTLRRVRISADAMMQALLGTRAKESLDLRAHLKQVKKE 180
Q6S7R6 KNMAEMEELRRRVAG--GRFVRPALRRVRISADAMMAALLGSKHRVGTDLRAGLRQVRKD 171
      **:***: :* :*: . *:* **:*****:***** *****: : . **** *:***:

P19429 DTEKENREVGDWKKNIDALSGMEGRKKKFES----- 210
P48787 DIEKENREVGDWKKNIDALSGMEGRKKKFEG----- 211
Q6S7R6 DAEKESREVGDWKKNVDALSGMEGRKKKFEAPGGGQG 208
      * ***.*****:*****.

```

Figure 5.2-1: Alignment of human, mouse and chicken cardiac Troponin I

Chicken shows an increased level of heterogeneity compared to human cTnI in contrast to the murine protein. The alignment was generated with the clustalW program using the sequences from the universal protein resource knowledge base (UniProtKB - <http://www.uniprot.org/uniprot/>) with the sequences TNNI3_Human (P19429), TNNI3_Mouse (P48787) and cTnI_Chick (Q6S7R6). Amino acid identity is indicated by the symbols as follows; “*” identical, “.” conserved and “.” semi-conserved. Significant regions of the protein are conserved across the species. However, chicken shows amino acid variance in the regions of interest for development of cTnI epitope-specific antibodies.

5.2.1 Anti-epitope-1 wild-type scFv development

5.2.1.1 Immunisation

Throughout immunisation (section 2.3.4.1) the development of the antibody response to the antigen was evaluated using the biotinylated peptide and cTnI using a direct binding ELISA (section 2.3.4.1). Prior to the final boost and sacrifice the antiserum titre was determined. Serum was diluted (1 in 150 to 1 in 2,952,450) in 1% (w/v) PBSTM and the response against cTnI determined to be in excess of 1 in 20,000 with the titre against the biotin-peptide approaching 1 in 100,000. The difference in titre was attributed to several factors;

- i) a high proportion of the antibody response to the synthetic epitope does not recognise the epitope in the context of the cTnI protein,

- ii) there was no accurate way to normalise for coating of neutrAvidin and subsequent capture of the peptide-biotin conjugate. With 4 binding sites per neutrAvidin there could be an excess of peptides compared to a single epitope per cTnI molecule.

In spite of this, the response to cTnI was encouraging and owing to the simplicity of the avian immune system efficient sampling of the entire repertoire was ensured by the relatively small number of PCRs required to build the library.

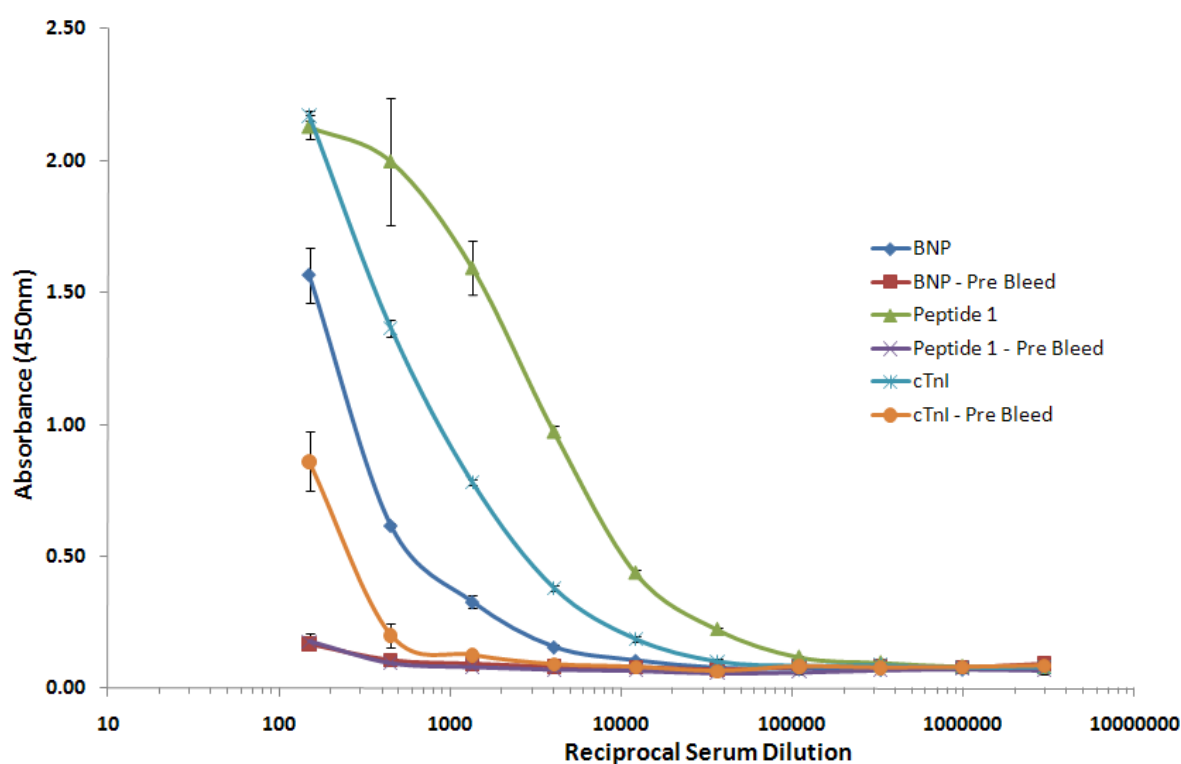


Figure 5.2-2: Avian antiserum titration for a chicken sensitised with the peptide-1-KLH conjugate

Avian host (designation Y.22.03.09) sensitised against peptide-1 of cTnI and N-terminal pro-brain natriuretic peptide (NT-proBNP). Serum was collected from an adult Leghorn chicken (male) 10 days after boosting, diluted in 1% (w/v) PBSTM and bound IgY (chicken antibody) detected using anti-chicken-Fc-specific HRP-labelled antibody. The graph indicates a significant antibody response for the synthetic peptide and crucially for the peptide in the context of the cTnI epitope. NT-proBNP, another cardiac marker, was also immunised taking advantage of the chickens tolerance of multiple immunogens. A notable NT-proBNP response was observed.

5.2.1.2 *Library construction by PCR*

5.2.1.2.1 Amplification of variable heavy and light chains

Post sacrifice, RNA extraction and cDNA synthesis (section 2.3.4.2), the variable domains from the avian bone marrow (BM) and spleen (SP) were amplified (section 2.3.4.4). Initially, the MgCl₂ concentration for the PCR was optimised for the V_L and V_H of both the BM and SP. MgCl₂ optimisation allows for optimal yield with greatest specificity. The yield is influenced by activity of the *Taq* polymerase and the magnesium ion-dependent incorporation of dNTPs, which also affects the specificity of primer for the template. The PCR products for each variable domain at each MgCl₂ concentration for both the BM and SP were resolved on 2% (w/v) agarose gels. These indicated similar yield, shown by discrete-specific band formation at approximately 450bp for V_H and 350bp for V_L (Figure 5.2-3). With the apparent null effect on yield, the lowest MgCl₂ concentration was used in the subsequent large-scale reactions (Figure 5.2-4). Post large-scale amplification the correct size amplicons were isolated by gel extraction and clean up (as per the manufacture's guidelines). Both the V_L and V_H were brought together by the inclusion of a flexible serine glycine linker [(G₄S)₄] in a splice-by-overlap extension (SOE) PCR (section 2.3.4.4.2).

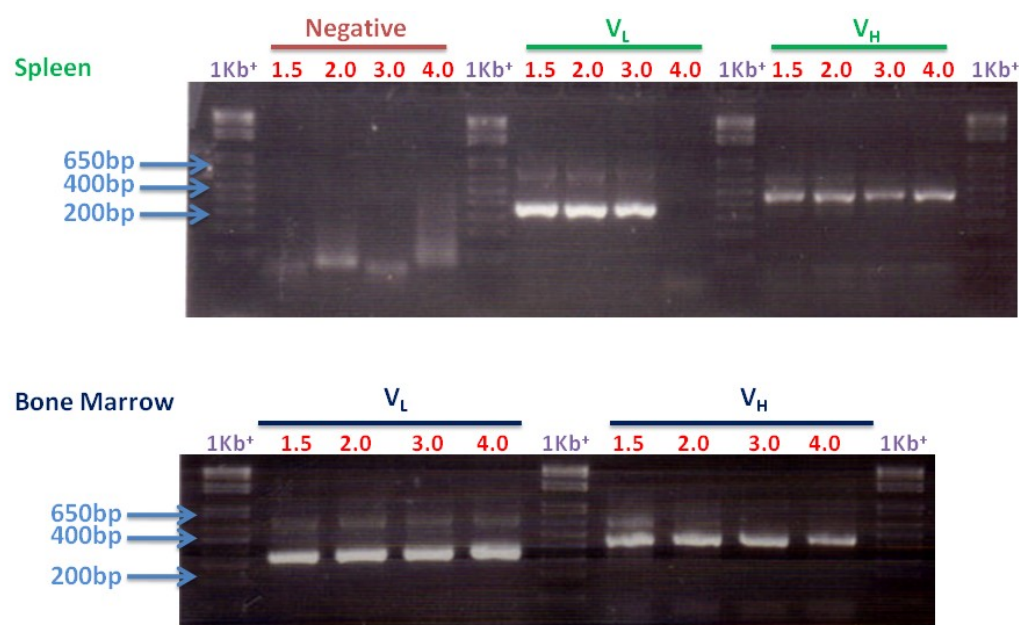


Figure 5.2-3: Optimisation of spleen and bone marrow V_L and V_H amplification from cDNA

Visualisation of the effect of MgCl₂ concentration on 2% (w/v) agarose gels. The amplification of BM and SP variable domains from chicken was initially optimised by magnesium chloride titration (MgCl₂). 1Kb⁺; DNA ladder, 1.5-4.0mM MgCl₂ concentration gradient. Negative reactions for each MgCl₂ concentration in the absence of cDNA showed no non-specific bands. Successful variable domain amplification was achieved with 1.5mM MgCl₂ for both the SP and BM.

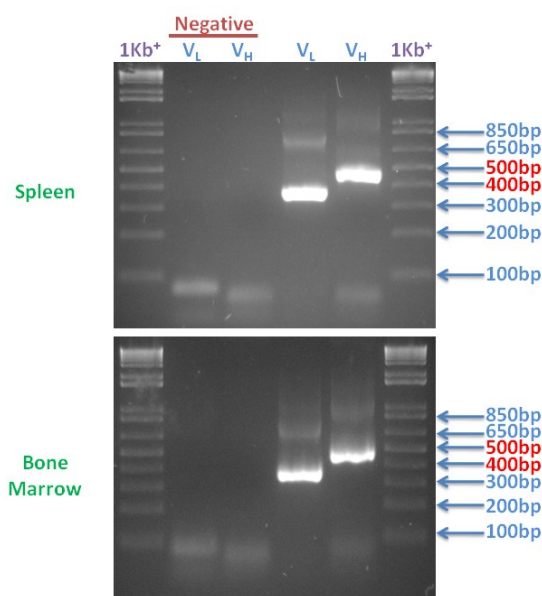


Figure 5.2-4: Large-scale V_H and V_L amplification from cDNA

MgCl₂-optimised large-scale amplification of V_L and V_H from SP (top) and BM (bottom) of Y20.03.09 chicken. In both cases V_L amplicons were observed at ~350bp and V_H amplicons at ~450bp. A negative control PCR showed no contaminating bands. The 1Kb⁺ ladder allowed approximation of DNA fragment size following resolution on a 2% (w/v) agarose gel.

5.2.1.2.2 SOE-PCR of variable heavy and light chains

The purified variable domains were incorporated in equimolar ratios into the SOE product corresponding to the scFv fragment (approximately 750-800bp) using the CSC-F and CSC-B primers (section 2.3.4.4.2). At this stage of the library construction process a high fidelity enzyme, Hi-Fi *Taq*, was used to ensure correct formation of the scFv fragment. Hi-Fi *Taq* requires inclusion of MgSO₄ in the PCR. The concentration was initially optimised and found to yield sufficient specific product at 1.5mM. The large-scale reactions were visualised on 2% (w/v) agarose gel and showed a diffuse band (Figure 5.2-5-A) that was discrete enough to be isolated and purified (Figure 5.2-5-B).

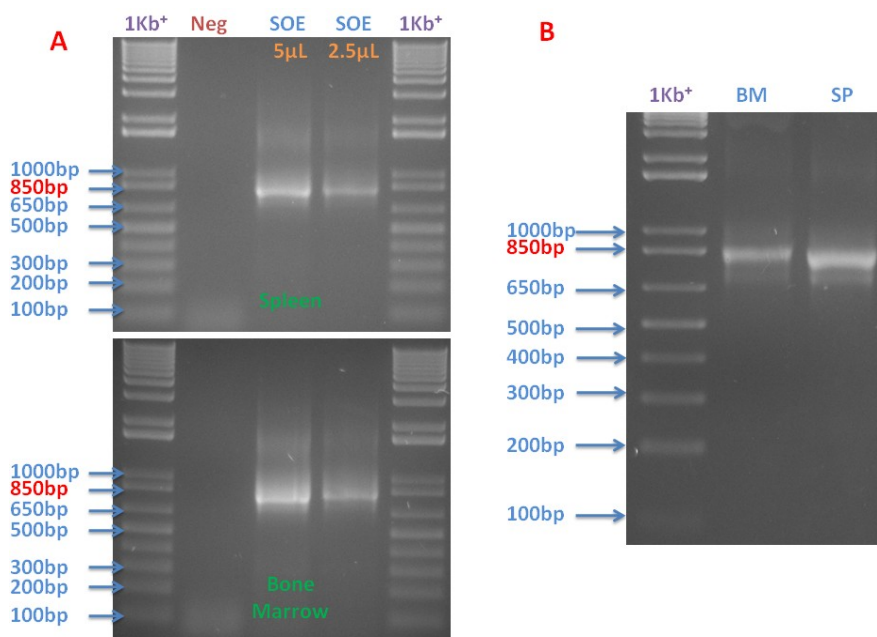


Figure 5.2-5: Splice-by-overlap extension (SOE) PCR of avian bone marrow and spleen V_H and V_L

Resolution of the PCR products was carried out on 2% (w/v) agarose gels.

A) Optimised large-scale SOE-PCR for SP (top) and BM (bottom)

An equimolar mix of V_L and V_H was overlapped by virtue of the overlap extension tails on the V_L reverse and V_H forward primers. Both the SP and BM show the formation of a specific band at ~800bp corresponding to the scFv SOE product. Negative control reactions show no non-specific products were amplified.

B) Purified SOE-PCR products:

SOE-PCR products after gel extraction and purification were visualised to ensure that a clean band was isolated from the large-scale SOE-PCR.

5.2.1.2.3 Construction of scFv library in the pComb3xSS vector

The pComb3xSS vector was made available by Professor Carlos Barbas III of the Scripps Institute, La Jolla, California, USA. The vector is a variant of pComb3x (accession number AF268281) containing a stuffer fragment (Figure 5.2-6). The vector contains both *E. coli* and phage origins of replication and can act as a shuttle vector for DNA encoding scFv (or Fab) fragments between *E. coli* cells and expression of the scFv on the surface of phage as a fusion to the geneIII protein. The vector was initially transformed into *dcm*⁻/*dam*⁻ *E. coli* for vector purification (section 2.3.4.3). To ensure the vector was intact and functional, small-scale restriction digestions were carried out and the vector was visualised on a 0.5% (w/v) agarose gel (Figure 5.2-7). *SfiI* digestion confirmed the presence of a ~1672bp stuffer fragment and concurrent *SacI* digest generated linear vector.

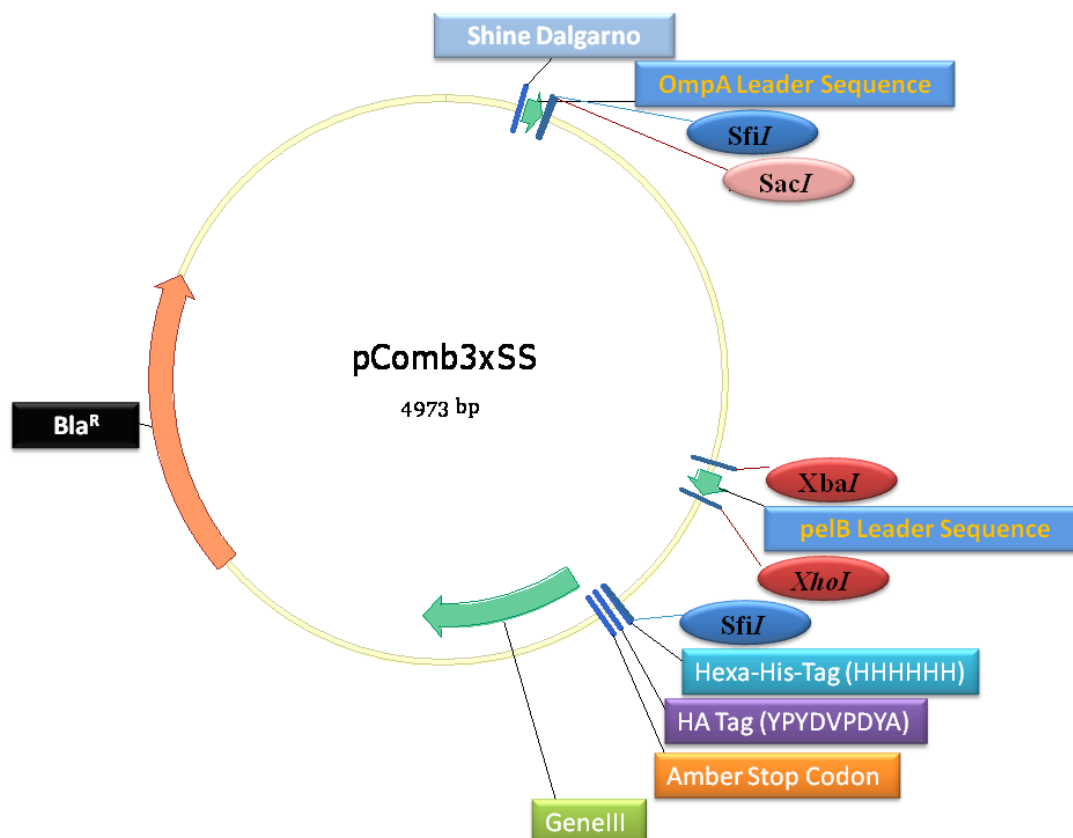


Figure 5.2-6: pComb3xSS vector map

The pComb3xSS vector is approximately 4973bp with both *E. coli* and phage origins of replication. Significant elements of the vector are highlighted. The stuffer fragment is located between the two *SfiI* sites.

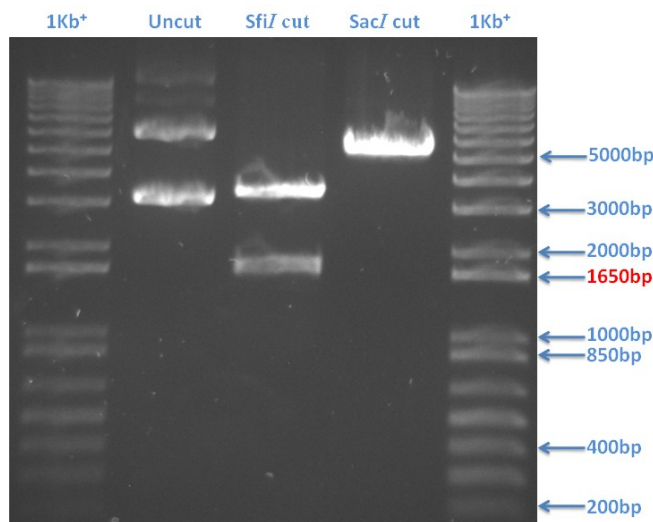


Figure 5.2-7: Test digestion of pComb3xSS vector

Examination of the vector prior to any library building, on a 0.5% (w/v) agarose gel. The undigested vector was resolved to ensure vector integrity. *SfiI* digestion results in drop out of the stuffer fragment at approximately 1650bp with *SacI* linearising the ~4973bp vector. Test digestions were compared to a 1Kb⁺ DNA ladder.

Large-scale digestion of the vector to incorporate the anti-epitope-1 scFv library (section 2.3.4.4.3) was carried out in a stepwise, triple digestion protocol (Figure 5.2-8). Digestion of the vector with *SfiI* may result in a significant amount of intact stuffer fragment or undigested vector, leading to library contamination, as observed in previous experiments despite de-phosphorylation of the cut vector (personal communication: Dr. Stephen Hearty and Dr. Barry McDonnell). To overcome this, subsequent digestion of the vector with *XhoI* and *XbaI* further degraded the stuffer fragment into three products (*SfiI* – *XbaI*, *XbaI* – *XhoI* and *XhoI* – *SfiI* see Figure 5.2-6) where only two were large enough (underlined) to be observed on a 0.5% (w/v) agarose gel (Figure 5.2-8). In addition, Antarctic phosphatase treatment of the entire vector digestion results in a de-phosphorylated vector, thus further preventing re-ligation. The fully digested, treated and purified pComb3xSS vector was visualised on 0.5% (w/v) gel showing a single band at approximately 3300bp (Figure 5.2-9).

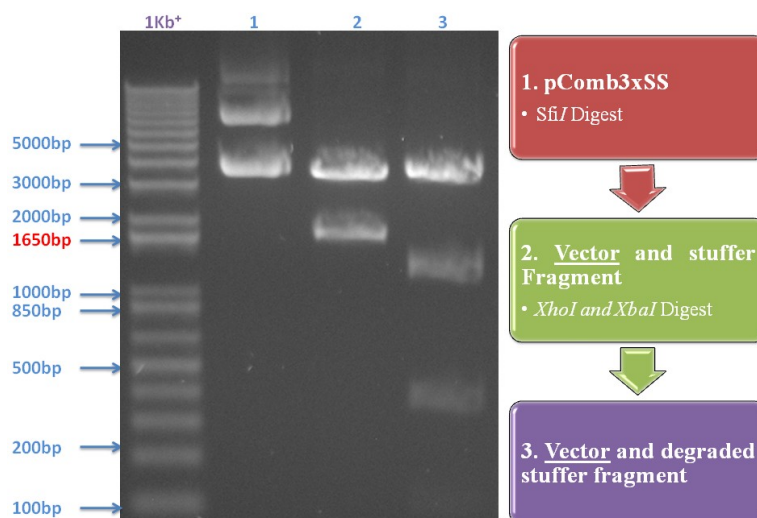


Figure 5.2-8: Large-scale triple digestion of pComb3xSS vector

Undigested pComb3xSS (lane 1), *SfiI* digested (lane 2) and triple digested (lane 3) reactions are shown. Triple digestion involved further degradation of the stuffer fragment (already *SfiI* digested) with *XhoI* and *XbaI* (flow diagram). The triple digestion (lane 3) reduces the potential for contamination of the downstream library building process. The digestions were resolved on a 0.5% (w/v) agarose gel and were compared to a 1Kb⁺ DNA ladder.

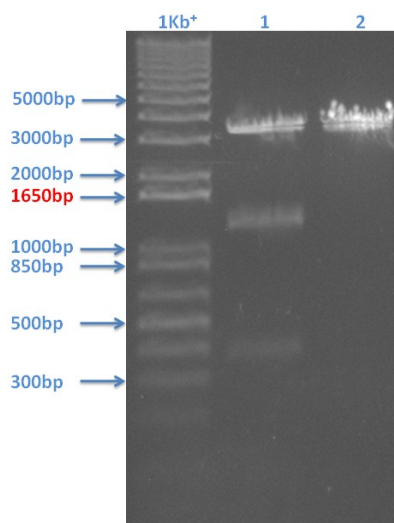


Figure 5.2-9: Purified triple digested pComb3xSS vector

Unpurified triple digestion (lane 1) and purified vector (lane 2) were resolved on a 0.5% (w/v) agarose gel. Post triple digestion, the vector backbone was purified by gel excision and clean-up resulting in a pure preparation of *SfiI* ready vector. The digestions were compared to a 1Kb⁺ DNA ladder.

Successful *SfiI* digestion of the SOE products was confirmed on a 2% (w/v) agarose gel (Figure 5.2-10) with cleavage of the restriction site plus the (GAG)₆ sequence readying the insert for ligation into the triple digested pComb3x vector (section 2.3.4.4.4). Post ligation

the antibody libraries (BM and SP) were transformed into electrocompetent *E. coli* generating a combined library size of 9.0×10^8 members which was subsequently rescued with helper-phage for bio-panning. The background re-ligation/contamination of this library was found to be zero, or at least less than 1000, as confirmed by control titring of vector religation reaction without insert. This highlights the success of the triple digestion methodology in combination with de-phosphorylation of the pComb3xSS vector during the library building process, generating a specific and uncompromised antibody library.

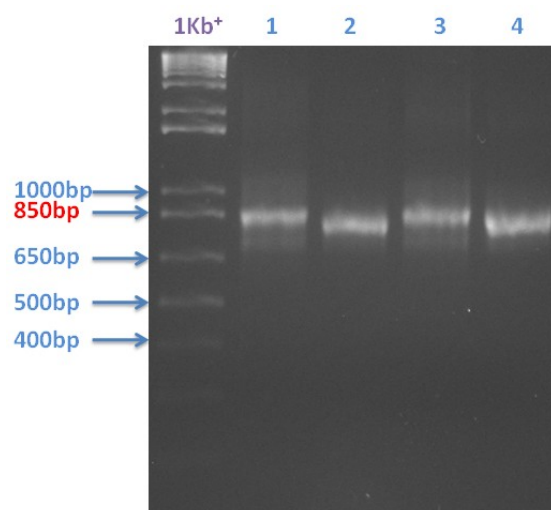


Figure 5.2-10: SfiI digestion of avian anti-peptide-1 scFv SOE-PCR inserts

Unpurified SP (lane 1) and BP (lane 3) and purified SfiI digested SP (lane 2) and BM (lane 4) SOE-inserts are shown. Examination of the SOE-PCR products post digestion on a 2% (w/v) agarose gel allowed visualisation of the digestion success due to the slight shift in the position of the product, compared to the undigested insert. 1Kb⁺: DNA ladder.

5.2.1.3 Phage display of the anti-epitope-1 scFv library

The library was evaluated in a highly stringent antigen presentation manner to maximise the probability of selecting scFvs for compatible assay pairing with the 20B3 mAb, in addition to ensuring high-affinity and specificity. The phage library was interrogated by capture of cTnI using the previously established anti-epitope-2 monoclonal antibody 20B3

(Figure 5.2-11-A). Integrating this ‘pairs-by-selection’ approach mitigates the requirement to mine for antibody pairings post bio-panning (section 5.1.10). This has advantages in terms of time-saving, ensuring compatible pair isolation and removing the need to re-select or screen should an antibody to only one dominant epitope be selected (i.e. no second pair available). Prior to carrying out this bio-panning approach, the concentration of the 20B3 mAb to use as a capture for cTnI was determined in a sandwich-type ELISA with comparison to the commercial antibody, Hytest mAb228 (section 2.3.4.5.1.1). This confirmed adequate capture density to efficiently evaluate the library and enrich for epitope-1-specific binders in very close proximity to the anti-epitope-2 mAb (Figure 5.2-11-B).

Notably, from the results obtained for the antibodies 20B3 (50µg/mL) and Hytest 228 (2µg/mL) capturing equal cTnI concentrations, with a fixed dilution of 19C7 (Hytest anti-epitope-1 HRP-labelled antibody), there was substantial a difference in absorbance values. This may be attributed to inaccuracies in the ‘in-house’ protein determination compared to the commercially sourced protein. Overlapping of the ‘in-house’ mAb epitope compared to the epitopes defined in Hytest catalogue also may have contributed to the result (Figure 5.2-11-C). Where the Hytest antibody pair (anti-epitope-2 capture and anti-epitope-1 reporter) were used there was a 5 amino acid spacer between the defined epitopes for both these antibodies. In contrast, where 20B3 was used as a capture reagent the epitope designed overlaps with the defined epitope for Hytest anti-epitope-1 mAb.

A high density (50µg/mL) of 20B3 capturing an excess of TnI (75µg/mL) for the first two rounds of bio-panning was adopted (section 2.3.4.5.3) to ensure enrichment of the library. To complement the stringency element introduced by this presentation strategy, a further level of selective pressure was introduced by gradual limitation of the concentration of antigen available for binding, but fixing the number of washes throughout (Table 2.3-12). Analysis of the input and output titres provides some information in relation to the successful shuttling of phage from input to output, as indicated in Table 5.2-1. Inbuilt into the selection campaign, was consideration for assay parameters such as temperature (room temperature) and blood collection regimes (presence of EDTA).

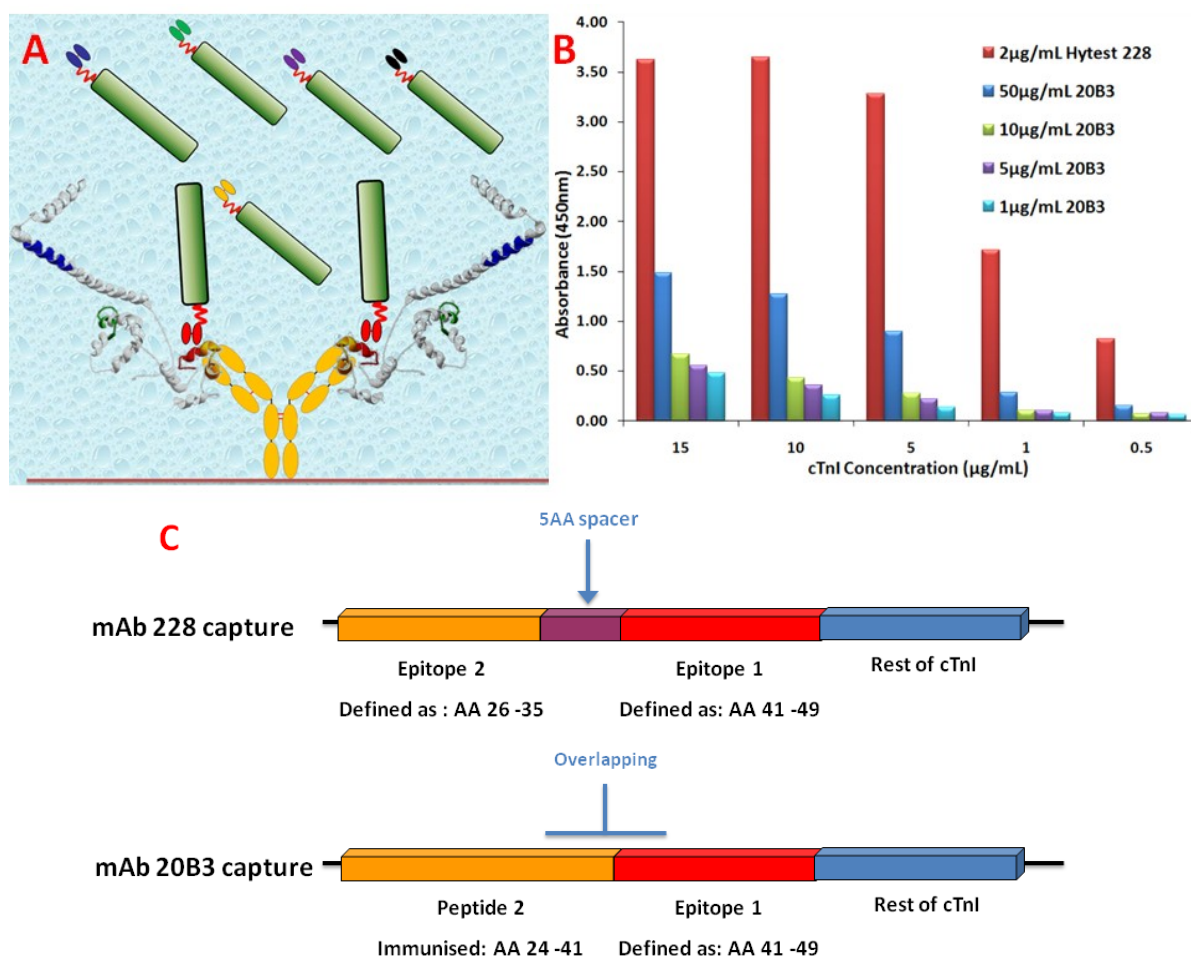


Figure 5.2-11: Antigen presentation strategy and optimisation for bio-panning of the anti-epitope-1 library

- A) Bio-panning presentation: Stringent conditions for anti-epitope-1 library members to bind to cTnI were created by this antigen capture approach. MAb 20B3 (yellow) was coated onto the ELISA plate surface capturing cTnI and presenting the protein to the scFv library (multiple colours) displayed on phage particles (green). This rigorous format ensured the isolation of compatible assay pairings.
- B) Optimisation of bio-panning conditions: Varying concentrations of monoclonal 20B3 were coated on to an ELISA plate to capture cTnI. Bound cTnI was detected using anti-epitope-1 HRP-labelled mAb (Hytest 19C7). For comparison purposes the commercial antibody Hytest 228 was also used as a capture reagent.
- C) Graphical explanation of the difference in signal obtained for the two captures mAbs: Capture with Hytest 228 and probe with Hytest 19C7 contains a 5AA spacer between the defined epitopes. The ‘in-house’ monoclonal epitope (which was used as the immunogen) overlaps with the 19C7 mAb-defined epitope and may cause an element of steric hindrance.

Table 5.2-1: Bio-panning input and output titres for anti-epitope-1 scFv

	Input Titre (cfu)	Output Titre (cfu)	% Recovery
R1	1.1×10^{12}	2.9×10^6	2.6×10^{-4}
R2	9.6×10^{11}	2.6×10^6	2.7×10^{-4}
R3	8.2×10^{11}	4.2×10^5	5.1×10^{-5}
R4	5.6×10^{11}	1.3×10^6	2.4×10^{-4}

Post-panning, the selected antibody-displaying phage from each round of selection were evaluated in a polyclonal-phage ELISA for enrichment against cTnI in its presented, immobilised and synthetic forms (section 2.3.4.6.1). To increase confidence in the result, negatives such as the capture monoclonal, blocking solution and KLH (carrier) were included. The presence of specific-antibody-displaying phage was detected by an anti-M13 HRP-labelled secondary antibody. Figure 5.2-12 illustrates the dramatic increase in specific-antibody-displaying phage at round four, suggesting enrichment of scFv-harbouring phage within the panned library. This specific signal was directed to no less than three different formats of the epitope: cTnI (native), KLH-peptide-1 (synthetic epitope) and mAb presented cTnI. There was minimal or no background binding to any of the included controls. Round four phage were subsequently infected into mid-exponential *E. coli* Top 10F' for expression of soluble scFv fragments (section 2.3.4.7) and taken forward into the screening campaign (section 2.3.5.1).

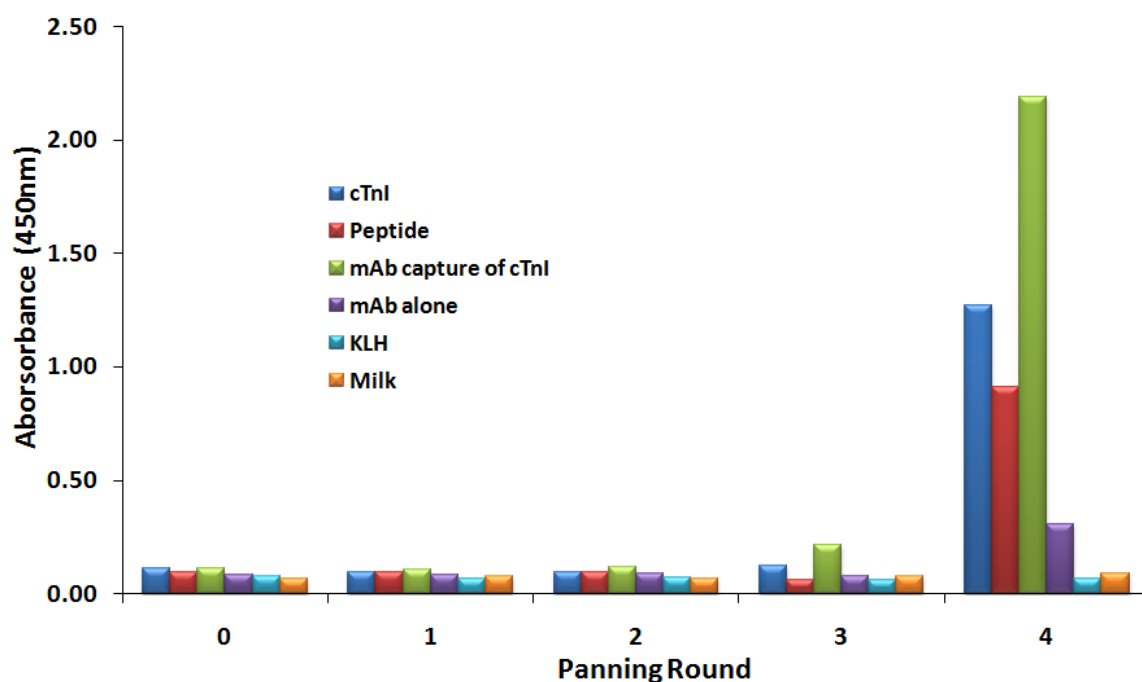


Figure 5.2-12: Polyclonal-phage ELISA after four rounds of stringent bio-panning

The phage preparations were assayed for specific binding against a number of positive and negative elements. Phage from each round was diluted 1 in 5 in 1% (w/v) PBSTM and 100µl applied to each well. Bound phage were detected using anti-M13 HRP-labelled secondary antibody. The ELISA plate was developed using TMB and the absorbance read after quenching with 10% (v/v) HCl at 450nm. The graph shows the dramatic increase in phage-displaying specific scFvs for the various formats of the epitope.

5.2.1.4 *Screening of anti-peptide-1 scFv library post selection*

Three hundred single colonies were isolated and grown up for screening (section 2.3.5.1). The screening approach was carried out at two levels. At the genetic level to assess the diversity of the rigorously panned library and at the protein level to assess binding in two ways: i) capture ELISA and ii) Biacore™ 4000 HT-ranking by ‘off-rate’ analysis. The acquired data, most notably on the refined HT-system, offered a wealth of information to judiciously aid the screening process.

5.2.1.4.1 Genetic fingerprint analysis of a subset of scFvs

The initial DNA-based analysis employed the restriction enzymes *BstNI* and *AluI* (below) to randomly cut the scFv gene generating a genetic fingerprint (section 2.3.5.1.1). Variations in the recognition site patterns as a result of DNA sequence diversity provided a rapid and cost effective method to examine a relatively good number of clones.



A colony pick PCR of the scFv insert showed 100% presence of DNA of the correct size (Figure 5.2-13 - 18/18). Subsequent digestion with the two enzymes and resolution on a 2% (w/v) agarose gel resulted in a fingerprint-specific for each clone analysed (Figure 5.2-13). Of those clones, 12 unique clone types were identified based on the size and number of the resulting bands. Type 'Di' (Alphabetic = group from *BstNI* digestion and roman numerals = group from *AluI* digestion) was found to be the dominant clone (Table 5.2-2).

Table 5.2-2: Genetic fingerprint identification of eighteen selected clones

Clone #	Clone Type	Occurrence	% of Population
1,6	Ai	2	11.1
2	Bii	1	5.6
3	Ciii	1	5.6
4,9,11,14,18	Di	5	27.8
5,12	Ci	2	11.1
7	Eiv	1	5.6
8	Cv	1	5.6
10	Dvi	1	5.6
13	Fvii	1	5.6
15	Cviii	1	5.6
16	Dix	1	5.6
17	Gx	1	5.6
Total		18	100.0

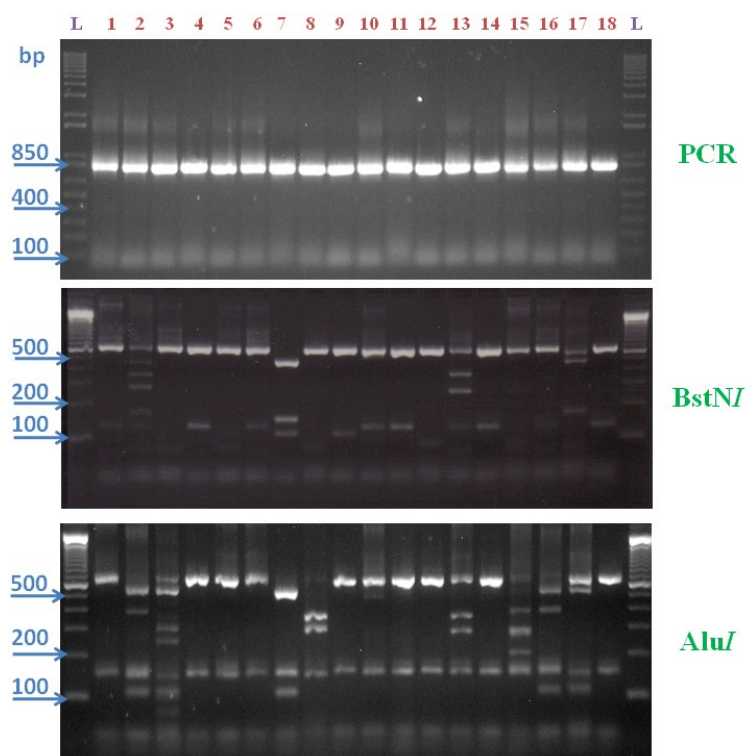


Figure 5.2-13: Genetic fingerprint analysis of eighteen clones after four rounds of bio-panning

L = 1Kb⁺ DNA ladder. Lanes 1-18 = selected single colony picks from which the scFv insert was amplified using CSC-F and CSC-B primers (top). Subsequently, the purified inserts were restriction fingerprinted with BstNI (middle) and AluI (bottom) to investigate the diversity in the DNA sequence of the clones isolated after stringent bio-panning.

5.2.1.4.2 Screening of anti-peptide-1 scFv in a functional assay format

Initial protein-specificity screening was performed as a preliminary evaluation of the success of the bio-panning procedures undertaken. Analysis by direct binding ELISA for cTnI, the peptide conjugate and KLH as a control was carried out as described in section 2.3.5.1.2. The subsequent functional screening was designed to consist of a sandwich assay format using mAb 20B3 as a capture reagent and kinetic evaluation using HT-Biacore™ 4000 system. The direct binding screen showed 98% binding-specificity for cTnI and KLH-peptide-1 with no background binding to KLH (Figure 5.2-14). A positive clone was defined as having a peptide and protein response greater than an absorbance of 0.2A.U. The screen highlighted the success of the bio-panning strategy, but was merely a pre-screen for the more rigorous analysis.

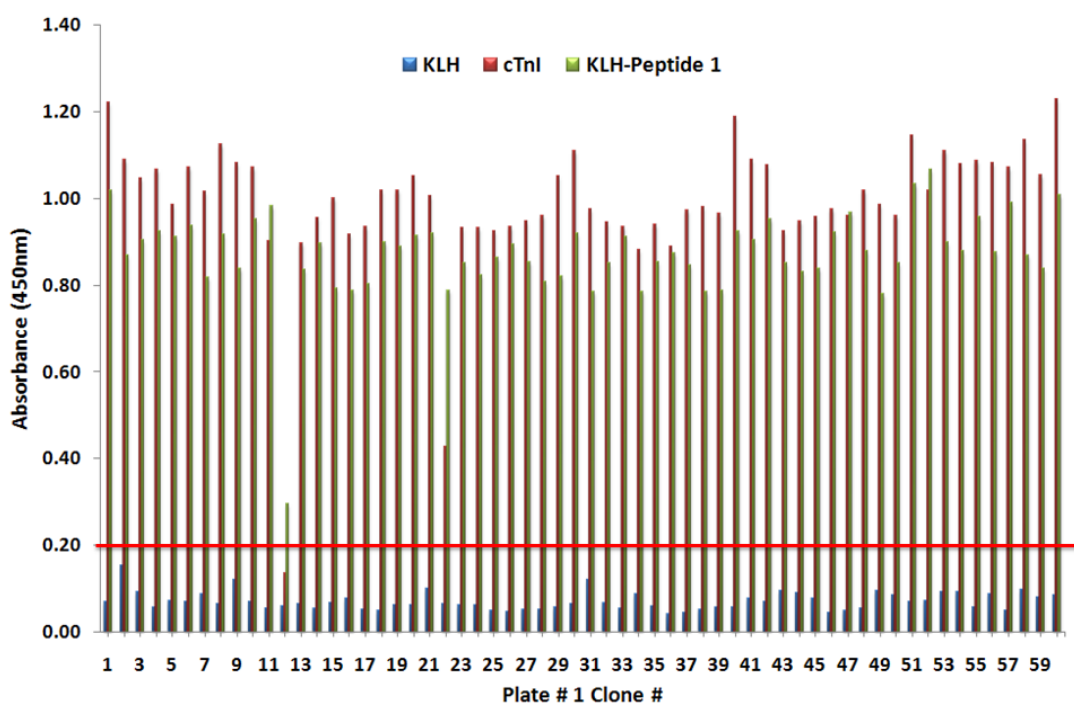


Figure 5.2-14: Initial screening of one anti-epitope-1 scFv bio-panned library output plate

This direct binding ELISA permitted approximate determination of the percentage of positive binders for cTnI, the peptide-1 conjugate and control KLH. Virtually all the clones bound to both cTnI and the peptide. cTnI, KLH-P1 and KLH were coated on three ELISA plates, blocked with 5% (w/v) PBSTM, to which diluted crude supernatants from overnight expressed single colonies were applied. Specific scFv were detected using an anti-HA HRP-labelled secondary antibody.

The second screen was instigated to challenge the scFvs in a sandwich format with the mAb 20B3. In this analysis the lysates were applied to plates on which the mAb 20B3 was coated to capture two concentrations of cTnI. This allowed comparison of the scFvs sensitivity for differential antigen concentrations. Figure 5.2-15 shows the response to both cTnI concentrations and to the negative control (0nM cTnI) for 4 out of 5 plates. From the graphs, varying degrees of response to the high and low cTnI concentrations was observed. With the exception of 3 clones (Plate #1 – 51, #5 – 29, #5 – 58 and #5 – 59) non-specific interaction with the 20B3 mAb was not observed.

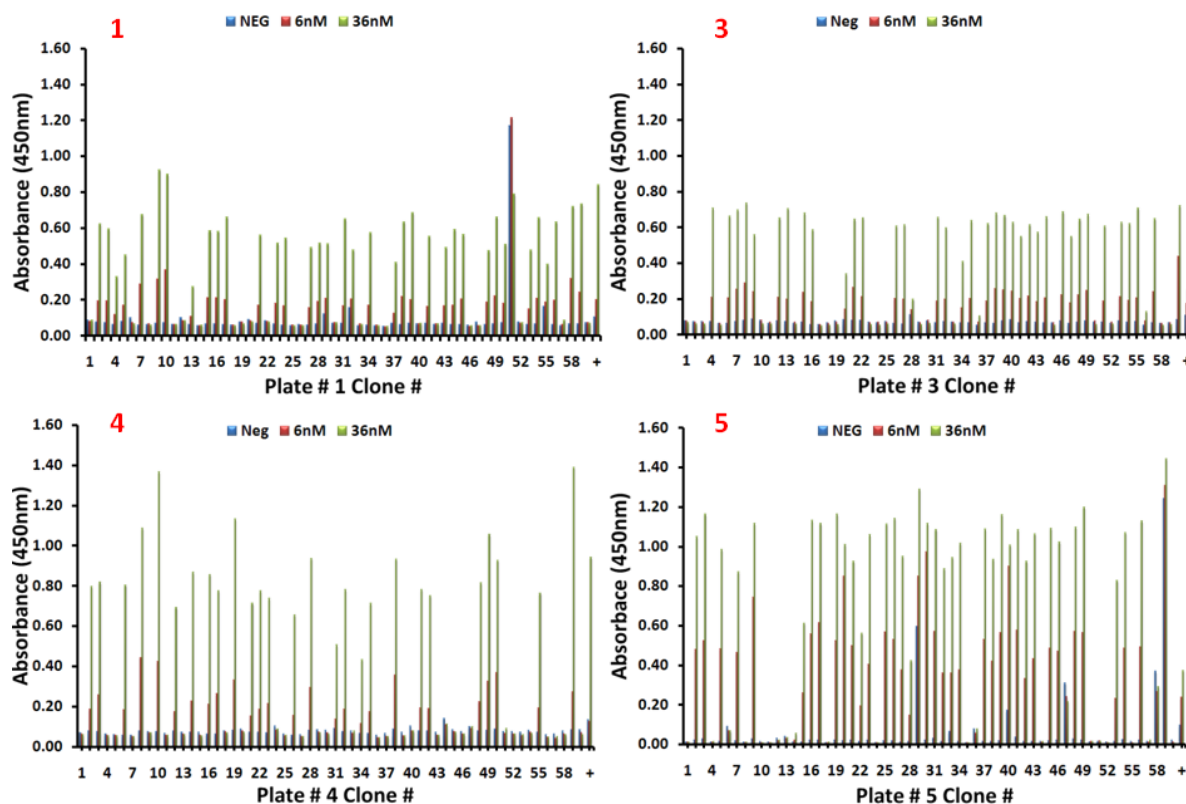


Figure 5.2-15: Sandwich ELISA screening for positive clones selected during anti-epitope-1 scFv bio-panning

Using the ‘in-house’ monoclonal 20B3 to create a capture surface, two concentrations of cTnI were applied to the immobilised mAb. In addition, a non-specific binding control plate (mAb coated only) was prepared. The crude lysates for four plates were diluted in 1% (w/v) PBSTM and applied over the three plates. Bound scFv were detected using an anti-HA HRP-labelled secondary antibody. The graphs above are a plot of clone number versus absorbance at 450nm for each cTnI concentration and for the mAb only control.

This response was then evaluated as a ratio which was developed based on experiments which ranked hybridomas in a time-resolved fluorescence assay carried out by Diago and co-workers [293]. The signal from the 6nM cTnI concentration was divided by the response for the 36nM concentration. This was plotted on a graph by clone number (Figure 5.2-16). Not all the clones had binding responses and resulted in very low ratio values. Clones with high 36nM binding signals and low 6nM signals resulted in a lower ratio value, for example highlighted clone #201 (purple): 6nM = 0.15AU and 36nM = 0.71AU gave a ratio of 0.215. In contrast, clone #270 (blue): 6nM = 0.97AU and 36nM = 1.180AU resulted in a higher ratio value of 0.871. Several other high performing clones were highlighted (green) in addition to the commercial control mAb 19C7 (red). This was a useful analysis to assist

in ranking a significant number of clones. However, some variability between plates (e.g. clones 1-60 on plate #1 compared to clones 241-300 on plate #5) was apparent with the control mAbs giving different ratio values between the plates (see “1+” = 19C7 ratio on plate #1 compared to the other highlighted controls in Figure 5.2-16). This was likely to be an artefact of variance in the washing steps as the plates were washed manually, and the analyses was performed over several days (1 set of plates per day). Use of a plate washer may assist in normalising such variability in addition to the assay being carried out within a day. To assist the ranking of these clones in a functional assay rather than a single cTnI concentration, a combination of 6-fold differing concentrations allowed the data to be presented in a useful way to aid the selection process by way of comparing scFv sensitivities to lower cTnI concentrations.

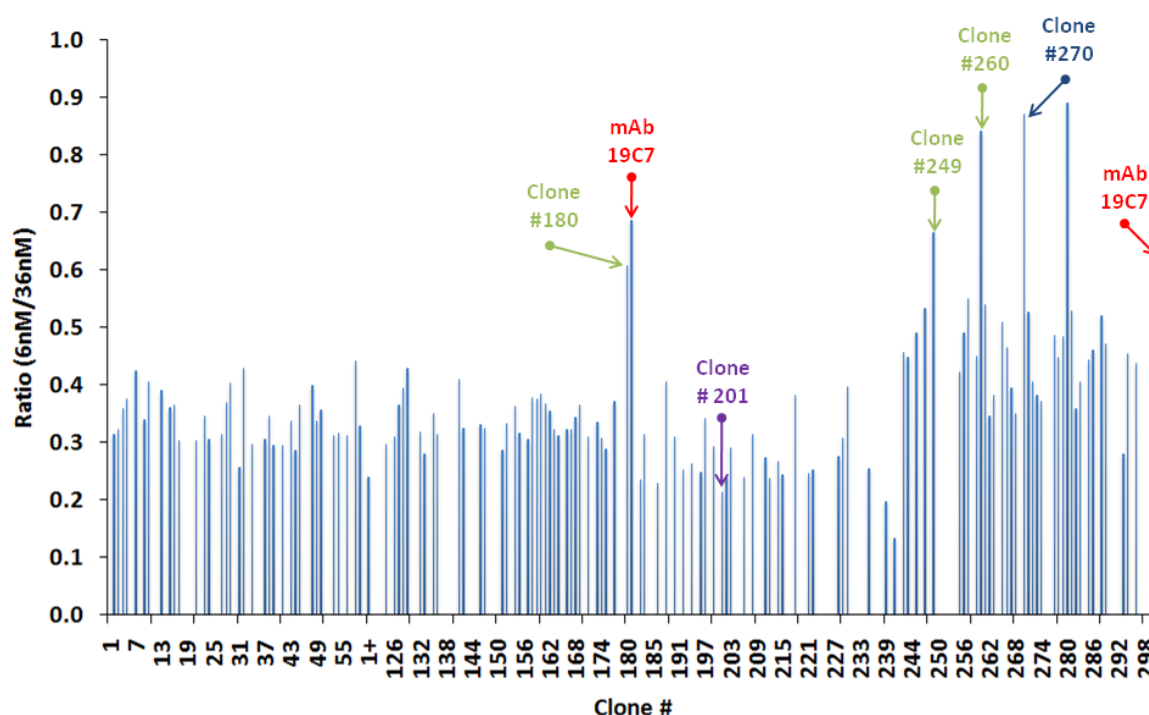


Figure 5.2-16: Ranking of anti-epitope-1 scFv based upon their binding ratio in a sandwich assay

Plot of 6nM signal divided by 36nM signal in 20B3-cTnI capture sandwich assay format for four out of the five plates of single colonies. This ratio permits ranking based on the ability of the scFv-clone to detect lower cTnI levels. Higher performing clones (#180, 249, 260 and 270) are indicated with a lower performing clone (#201) alongside the commercial equivalent mAb 19C7. Higher ratios are attributed to clones with greater sensitivity to lower cTnI concentrations.

5.2.1.4.3 High-throughput ranking of anti-peptide-1 scFv

In the selection campaign for the mAb 20B3 the ability to rank by a capture approach on the HT-Biacore™ was not feasible. In the screening campaign described for the scFv, the full parallel processing power of the instrument was harnessed and brought to bear on the panel of 300 anti-epitope-1 scFvs.

The scFvs were ranked by percentage left analysis in a capture format (section 2.3.5.1.3). Figure 5.2-17-A diagrammatically illustrates the flow cell setup. There are four flow cells each with five independently addressable and monitored spots within the system. An anti-HA pAb surface was created by immobilisation of approximately 6000RUs of the antibody onto spots 1, 2, 4 and 5. Crude lysates from overnight expressed clones were diluted in running buffer (HBS-EP⁺) and scFv captured on the outside spots (one scFv on spot one and another on spot five). cTnI (50nM in HBS-EP⁺) was passed over the entire surface with spots two and four acting as online references. The clones were ranked by the RU level at two time points (stability early and stability late). Stability late was set 12 minutes after stability early to allow for dissociation to occur. Figure 5.2-17-B is the raw sensorgram data acquired from a single run of 300 scFv clones. ScFv capture on spots one and five of each flow cell can be seen with a stabilisation step prior to zeroing the baseline. The binding of cTnI was then acquired before regeneration of the surface with 20mM NaOH.

Figure 5.2-18 is a plot of stability early versus stability late for the 300 clone screen and 100% left (or no dissociation) is signified by the diagonal blue line. The majority of clones resided within three sub-populations. Those with percentage left values $\geq 60\%$: high (1) and low (2) expressers and the remainder of the clones with percentage left values $< 60\%$ (3). High and low expressing clones were differentiated by the stability early values where greater levels of scFv capture gave higher cTnI binding responses. This was verified by the scFv capture level plot (Figure 5.2-19). In this case the high-level captured scFv # 23 and lower level captured scFv #17 are highlighted. In the stability early versus late plot (Figure 5.2-18) both clones were also highlighted and were both in the percentage left $\geq 60\%$ category. However, they exist in the high and low expresser groups, respectively. This extra information was useful for aiding the decision making process allowing for the identification of higher expressing clones. The data was also presented in a percentage left

plot versus clone number in Figure 5.2-20. This plot has value in identifying more stable binding events amongst a large panel of clones.

This screening approach demonstrates the wealth of information was be garnered from the HT-based methodology in a single analysis run. Using the cTnI antigen at all times ensured confidence in the antibody-antigen interaction in a conformation not compromised by direct immobilisation effects.

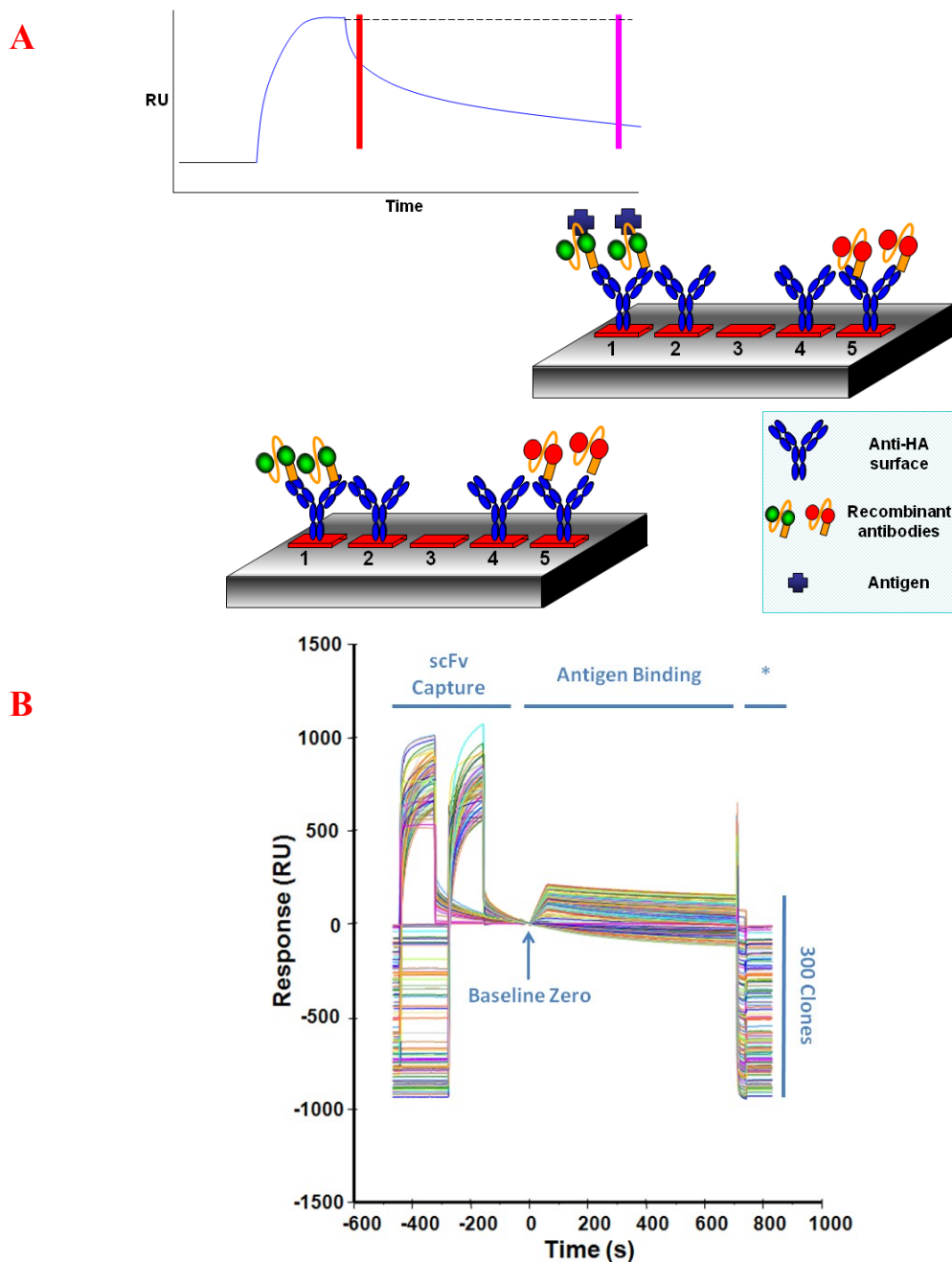


Figure 5.2-17: High-throughput screening by capture format on Biacore™ 4000 used for scFv analysis

- A) Overview of the experimental flow cell setup: The surface was composed of polyclonal anti-HA antibody on spots 1, 2, 4 and 5 of each flow cell (FC). The outer spots (1 and 5) were the active spots where recombinant antibodies were captured from crude lysate (two per FC by four FCs = 8/cycle). A fixed antigen concentration was then passed over the captured scFv with the inner spots (2 and 4) acting as online reference spots.
- B) Raw sensorgram data: Initially, the scFv were captured on spot 1 (1st peak on curve) and spot 5 (2nd peak) of each flow cell. This was followed by a stabilisation step before zeroing the baseline and injection of cTnI (antigen binding). After 12 minutes dissociation the flow cells were regenerated for the next cycle (*) with 20mM NaOH.

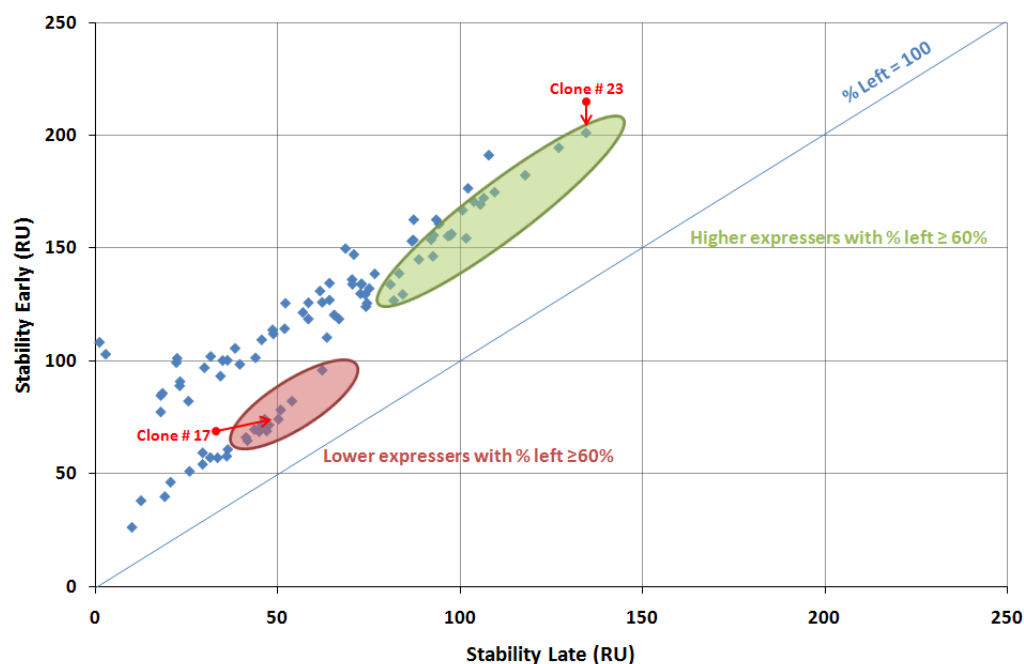


Figure 5.2-18: High-throughput stability early versus stability late ranking of anti-epitope-1 scFv

A plot of stability early versus stability late values for each of the 300 clones illustrated the overall stability of the binding events. From the graph, three distinct populations were identified - red circle: lower expressing clones with % left values ≥ 60 , green circle: higher expressing clones with % left values ≥ 60 and those clones with % left values < 60 . The blue diagonal line signifies a percentage left value of 100% where no dissociation has occurred.

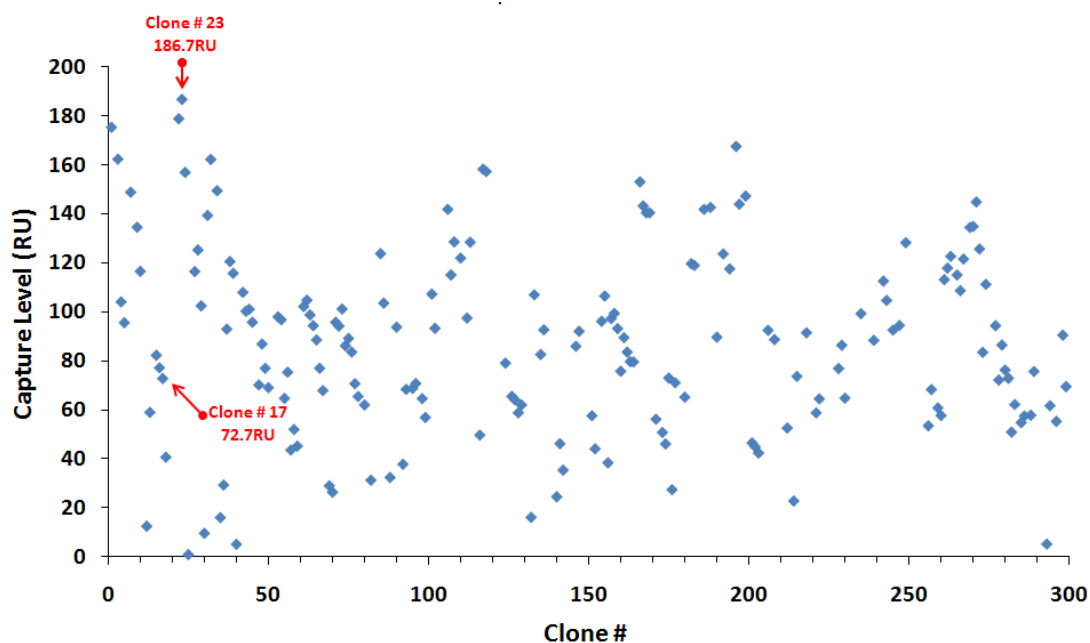


Figure 5.2-19: High-throughput scFv capture level plot for anti-epitope-1 scFv

Plot of the scFv capture level by clone number shown for 300 clones in the analysis. High capture level clone #23 and lower capture level clone #17 were highlighted. The capture level can be related to expression as all clones were cultured in equal volumes and diluted in the same fashion.

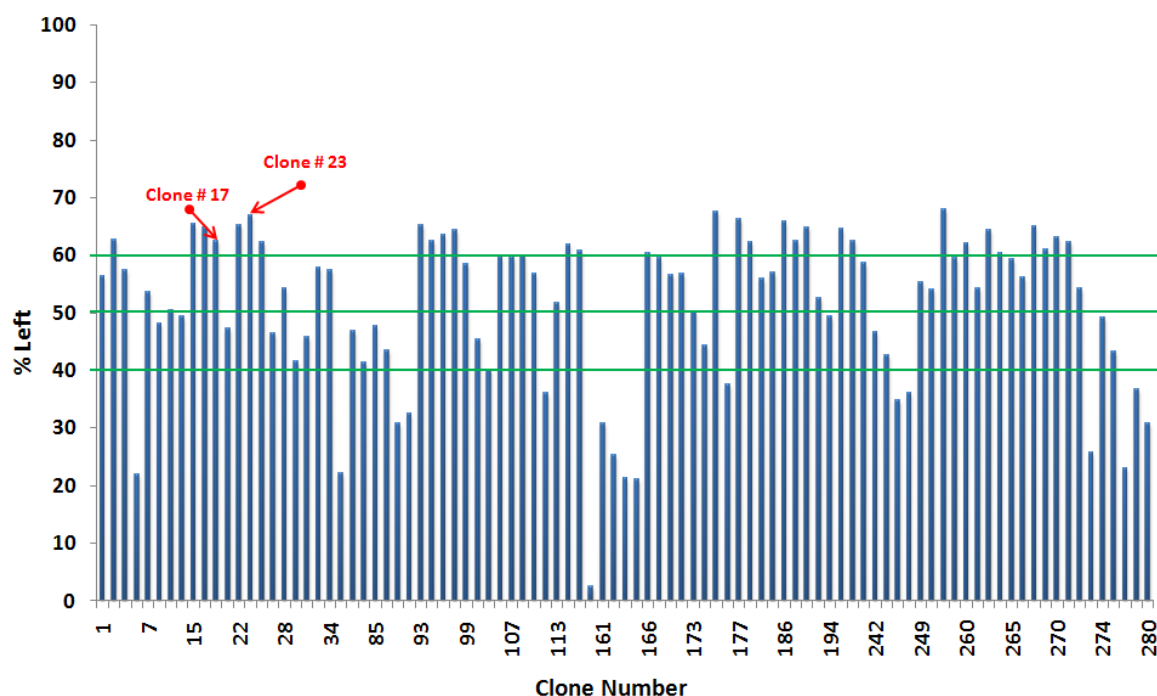


Figure 5.2-20: High-throughput percentage left plot for anti-epitope-1 scFv

Percentage left values were calculated using Equation 4.2-1. Percentage left values were plotted versus clone number and broken into three groupings ≥ 40 , 50 and 60% (green horizontal lines)

Vast amounts of data were acquired in a relatively short timeframe where the analysis of 300 clones took <12 hours. Combined with the functional sandwich assay screening substantial information was available to rationally select a panel of clones to carry forward. Table 5.2-3 is the correlated data for the top 58 performing clones from the HT-screening. This was then related to functional sandwich assay screen and a decision made on the top three clones (bold and red) to send for sequencing. As the plate position for the Biacore™ 4000 (where all 96-wells were used) was different from the original single colony plate (inner 60-wells only) the relevant plate positions are also tabulated for clarity. An additional clone that did not appear in the HT-screen (as it captured well, but had a fast cTnI dissociation rate), but did perform well in the functional assay screen was also selected for sequencing (clone_218). This trend occurred frequently on clones captured on spot five of the flow cells (FC) and suggested a bias in the instrument as all the clones that had performed superiorly were those captured on spot one (spot one FC:1 = plate position A, FC:2 = B, FC:3 = C and FC:4 = D compared to spots five of the four FC coming from plate positions E, F, G and H. Note: HT plate positions in Table 5.2-3).

Table 5.2-3: Rationalised selection of anti-epitope-1 scFvs

Clone #	% left	Positive by Sandwich ELISA	HT Plate Position	Original Plate Position
1	56.38	YES	1A2	1B3
3	62.59	YES	1A3	P1B4
4	57.43	YES	1A4	P1B5
7	53.63	YES	1A7	P1B8
10	50.47	YES	1A10	P1B11
15	65.45	YES	1B5	P1C6
16	64.75	YES	1C6	P1C7
17	62.40	YES	1B7	P1C8
22	65.30	YES	1C1	P1D2
23	66.88	YES	1C3	P1D4
24	62.32	YES	1C4	P1D5
28	54.32	YES	1C8	P1D9
32	57.85	YES	1D1	P1E2
34	57.44	YES	1D4	P1E5
93	65.21	-	2B3	P2E4
95	62.50	-	2B5	P2E6
96	63.64	-	2B6	P2E7
98	64.30	-	2B8	P2E9
99	58.49	-	2B9	P2E10
106	59.82	-	2C6	P2F7
107	59.71	-	2C7	P2F8
108	59.94	-	2C8	P2F9
110	56.78	-	2C10	P2F11
113	51.65	-	2D3	P2G4
117	61.79	-	2D7	P2G8
118	60.79	-	2D8	P2G9
166	60.31	YES	3A6	P3F7
167	59.54	YES	3A7	P3F8
168	56.63	YES	3A8	P3F9
169	56.71	YES	3A9	P3F10
173	50.29	YES	3B3	P3G4
175	67.52	YES	3B5	P3G6
177	66.34	YES	3B7	P3G8
180	62.33	YES +++	3B10	P3G11
182	55.93	YES	3C2	P4B3
183	57.07	YES	3C3	P4B4
186	65.80	YES	3C6	P4B7
188	62.47	YES	3C8	P4B9
190	64.75	YES ++	3C10	P4B11
192	52.54	YES	3D2	P4C3
196	64.62	YES	3D6	P4C7
197	62.40	YES	3D7	P4C8
199	58.62	YES	3D9	P4C10
249	55.19	YES	4A9	P5B10
256	54.06	YES	4B6	P5C7
257	67.97	YES	4B7	P5C8
259	59.54	YES	4B9	P5C10
260	62.11	YES ++	4B10	P5C11
261	54.32	YES	4C1	P5D2
262	64.43	YES	4C2	P5D3
263	60.34	YES	4C3	P5D4
265	59.24	YES	4C5	P5D6
266	56.24	YES	4C6	P5D7
267	65.02	YES	4C7	P5D8
269	61.10	Non-Specific	4C9	P5D10
270	63.18	YES ++	4C10	P5D11
271	62.16	YES	4D1	P5E2
272	54.33	YES	2D2	P5E3

5.2.1.5 *Sequence analysis of four selected scFvs*

Examination of the four sequences (section 2.3.8.1) indicated a ‘jackpot library’ with 100% sequence similarity (Figure 5.2-21). This ‘jackpot’ is a desirable outcome, because in a library of 9×10^8 members the probability of the same sequence appearing at random is low [12]. This was a relatively small cohort of clones to sequence. However, after four stringent rounds of selection and rigorous, specific screening it was anticipated that the diversity would be narrow given the focussed immunisation and stringent bio-panning regimes. This ‘jackpot’ result further validates the procedures followed.

It is widely accepted that the CDRH3 has by far the greatest sequence diversity compared to the remaining five CDRs and makes a significant contribution to antigen contact [6]. The CDRH3 in this case was 15 amino acids in length and dominated by serine (3/15), glycine (4/15), aspartic acid (4/15) and single tyrosine/isoleucine residues. Interestingly, the CDRL1 (14 amino acids) contains many tyrosine (5/14) and glycine (5/14) residues. The tyrosine residue content of the CDRs is attributed to specific antibodies in synthetic libraries with glycine, serine and tyrosine being dominant in naïve loops. Tyrosine, tryptophan and arginine residues are capable of mediating a wide-array of intermolecular interactions which are desirable in the composition of the CDRs. The frequency of tryptophan and arginine residues increases in antibodies having undergone affinity maturation, but it is tyrosine side-chains that mediate ~25% of antigen contacts. Furthermore, small residue prevalence in the CDR loops confers conformational flexibility which is crucial for effective antigen recognition [294]. With this in mind, almost all the CDRs are dominated by the small amino acids serine, glycine and aspartic acid. Four of the six CDRs contain tyrosine residues with the CDRL1 and CDRH2 showing higher frequencies. Interestingly, only two arginine residues occur in the CDRs (L1 and L2). In CDRL2, at this position the arginine residue was observed in many chicken-derived antibodies irrespective of the antigen (personal observation). The CDRL1 appears to be quite long i.e. longer than observed for other protein antigen binding clones developed in DCU including other avian and rabbit anti-cTnI antibodies. Of the 14 amino acids making up that CDR, tyrosine and the smaller amino acids (glycine, serine and aspartic acid) are abundant with only a single arginine residue. Based upon what is known about flexibility and tyrosine/arginine content this would suggest that CDRL1 may be important for avian

anti-cTnI peptide one binding. In the absence of any structural data this observation remains a supposition.

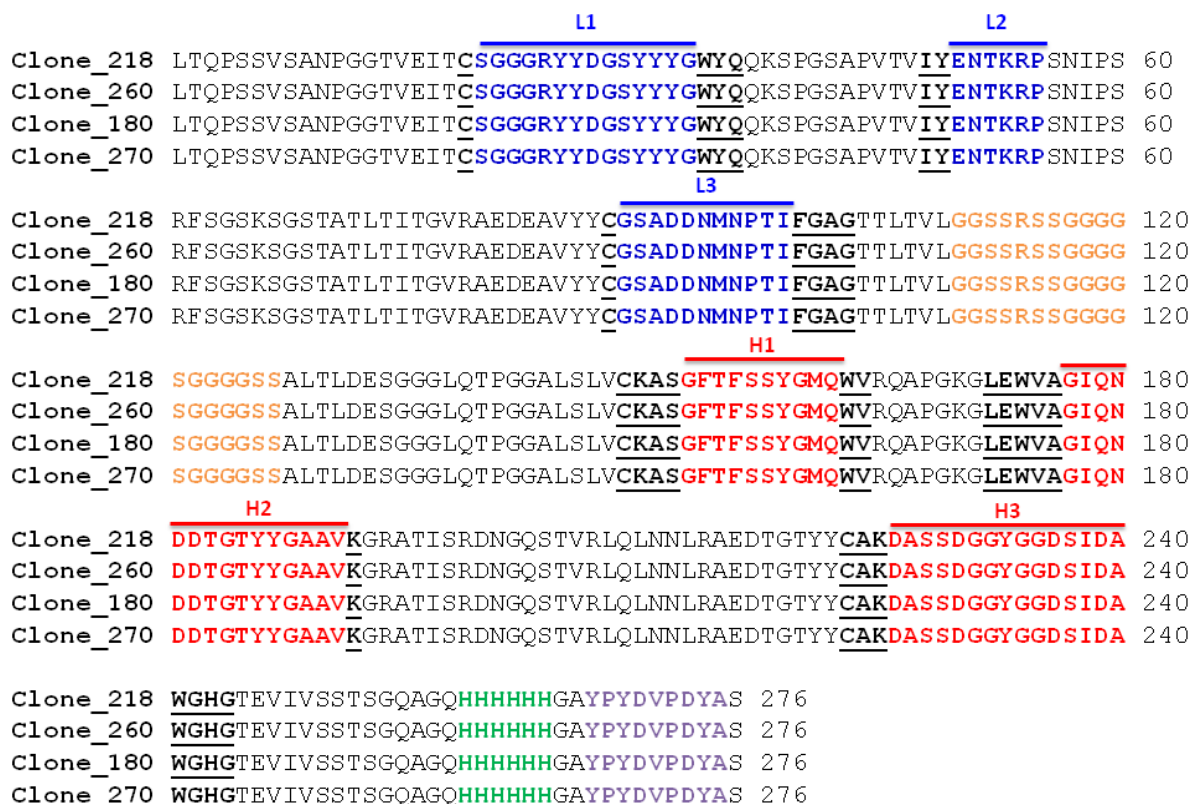


Figure 5.2-21: Alignment of four selected wild-type scFv for sequence comparison

The CDRs are highlighted using the Kabat numbering system. Conserved CDR flanking regions are highlighted (bold and underlined). Light chain CDRs 1-3 are indicated in blue with the heavy chain CDRs in red. Other highlighted regions: linker; gold, hexahistidine tag; green and HA-tag; purple. Sequences aligned using ClustalW at <http://www.uniprot.org/>.

It must be noted that scFv 218 which did not perform well in the HT-screening was identical in sequence as the other clones. It did perform well in the functional sandwich assay, but the rapid dissociation of cTnI in HT-analysis resulted in omission of the clone from selection. While no instrument issues/failures were found at the time (as the A100) when the machine was upgraded to Biacore™ 4000 a flow valve issue was found. In my opinion this introduced the selective bias noted in the screening of these clones (as one clone compared directly on spot one and five of the same flow cell also gave different dissociation rates). Post upgrade to Biacore™ 4000 positive hits came from all spots as demonstrated in the numerous plate positions in Figure 5.2-31.

5.2.2 Mutagenesis of anti-epitope-1 scFv

The primary decider of assay specificity and sensitivity is the antibody. The issue of specificity was well defined early in the antibody generation process by way of the epitope-focused immunisation and selection strategies. To ensure optimal sensitivity, the affinity of the antibody was of crucial importance. *In vitro* mutagenesis offers a rapid methodology to increase the diversity of the selected libraries and mine for improved clones by phage display.

5.2.2.1 Overview of the mutagenesis strategy

The mode of mutagenesis selected for this library was a conservative chain shuffle, considered an optimal approach for immune repertoires, as the chances of recapitulating the immune B-cell V_L - V_H pairing is statistically low [295]. Chain shuffling involves randomisation of the V_L - V_H pairing by re-combination of the one V chain with either the original or an alternative source of the other V gene. In the case of the anti-epitope 1 scFv 180, it was light-chained-shuffled against the catalogue of light chains from the original library, thus generating a second library (Figure 5.2-22-A) as described in section 2.3.4.5.4. This secondary library (3.1×10^8 members) based around the wild-type (WT) V_H contained many combinations of light chains from the immune catalogue with further diversity potentially introduced by errors during PCR amplifications. It is known from crystal structure determination and for genetic reasons that the V_H dominates antibody binding interactions and thus a light chain shuffle was an optimal method to improve the antibody binding energies [12]. The secondary library contains many combinations both specific and non-specific for cTnI in common with the primary library, in essence the libraries overlap greatly (Figure 5.2-22-B) and the selection strategy required significant modification to increase the statistical chances of finding new, higher-affinity V_H - V_L combinations.

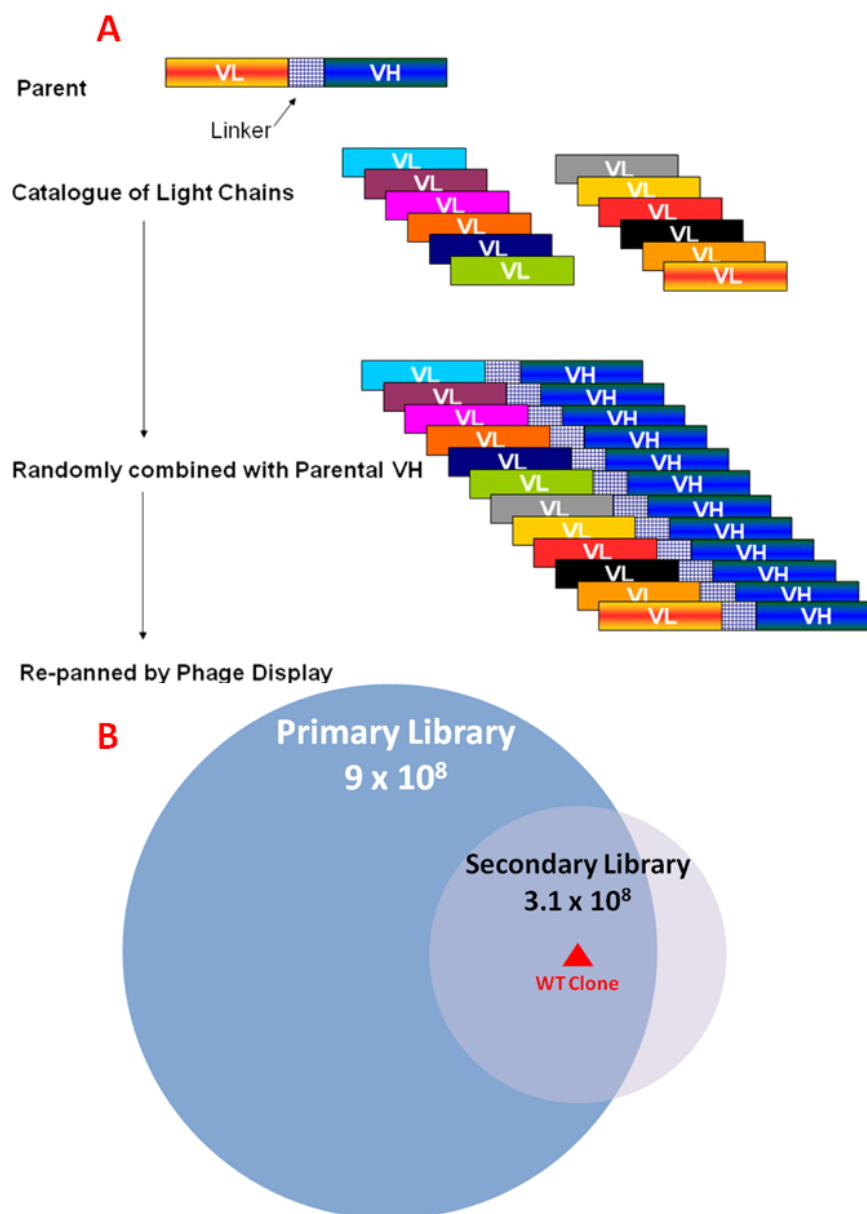


Figure 5.2-22: Overview of light chain shuffling mutagenesis strategy for the wild-type scFv library

- A. The parental scFv (180) heavy chain was isolated by PCR and recombined with a catalogue of light chains from the original library variable domain amplification, generating a secondary library. The recombined library was then subjected to bio-panning by phage display.
- B. This secondary library, biased by the V_H of the WT, contained many combinations of the light chains previously found in the primary library, but may also contain new light chain combinations not selected for in the WT campaign. Additional diversity could be introduced by the error rate of the polymerase potentially leading to new clones. This is diagrammatically represented by the bubble plot and highlights the significant overlap of the two libraries demonstrating the requirement for a new selection strategy to favour the isolation of improved affinity clones.

To favour an increased statistical probability of finding advantageous V_L - V_H combinations, solution-phase bio-panning was chosen as the optimal approach to select for specific mutants (section 2.3.4.5.4). With solid-phase selection, it is problematic to accurately control the concentration of the available antigen during selection experiments [89]. This is primarily due to the uncontrollable mechanism of absorption of proteins onto the surface of microtitre plates. Solution-phase bio-panning was a superior methodology in terms of selection of affinity improved mutants. In this case the concentration was precisely controlled during the phage-displayed antibody and free antigen interaction. Biotinylated peptide one was employed in the selection experiments. This was carried out by incubating the library with sequentially reduced concentrations of antigen. The specific phage displayed scFvs were subsequently recovered from the mixed population using streptavidin-coated paramagnetic beads followed by washing and infection into *E. coli* for the next round of bio-panning (Figure 5.2-23).

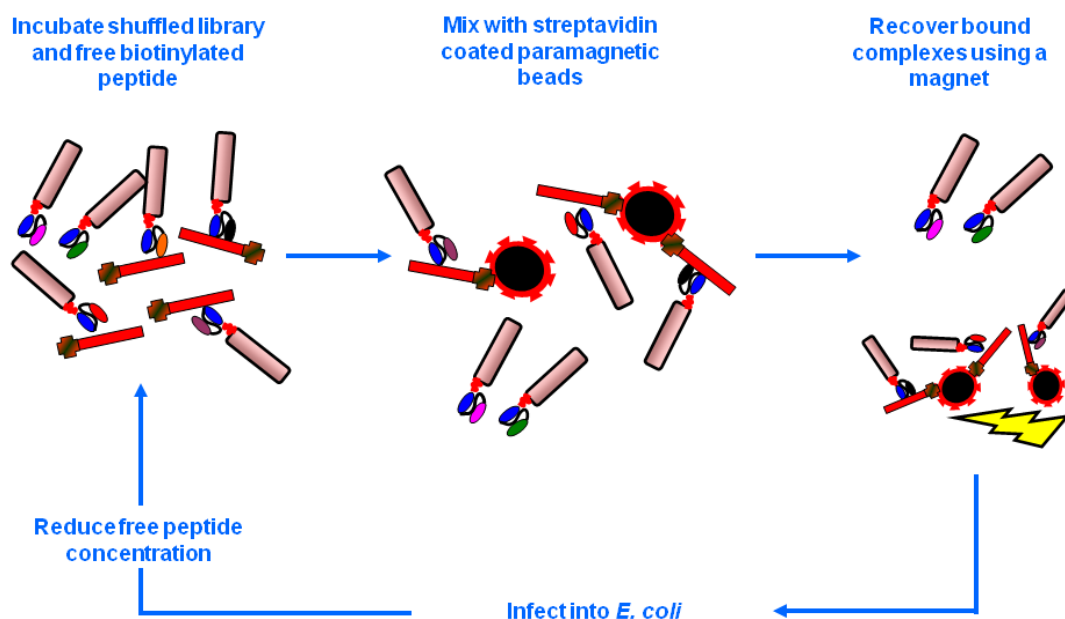


Figure 5.2-23: Solution-phase bio-panning for anti-epitope-1 mutant scFv

The chain shuffled library was displayed on phage and incubated with biotin conjugated peptide-1 in-solution. Bound peptide-phage antibody complexes were recovered using streptavidin-coated paramagnetic beads and a magnet followed by washing away of non-specific phage. The specific-phage were eluted by trypsin treatment and infected into *E. coli* for repeated rounds of bio-panning with decreasing free peptide concentrations.

Prior to bio-panning the capture of the WT clone and mAb 19C7 (HRP-labelled) by the biotinylated peptide-1 was evaluated (section 2.3.4.5.1.2). A dilution series of free-peptide was incubated with a fixed scFv (pure) or 19C7 concentration and recovered using streptavidin-coated paramagnetic beads. Post washing the bound scFv was detected using an anti-HA HRP-labelled secondary antibody and the signal developed using TMB. The signals were quantified by transferring the TMB to a microtitre plate (Figure 5.2-24) facilitating absorbance determination at 450nm. From the graph the lowest concentration of peptide (0.1nM) showed loss of signal for the WT scFv, with the Hytest 19C7 signal virtually abolished at 1nM. Owing to the relative low instance of each clone in the mutant (MT) library, the selection strategy that was employed mimicked the methodology demonstrated in these optimisation experiments (Table 2.3-13). This ensured that all peptide-binding antibodies were captured and enriched prior to significant challenge with low peptide concentration (0.1nM).

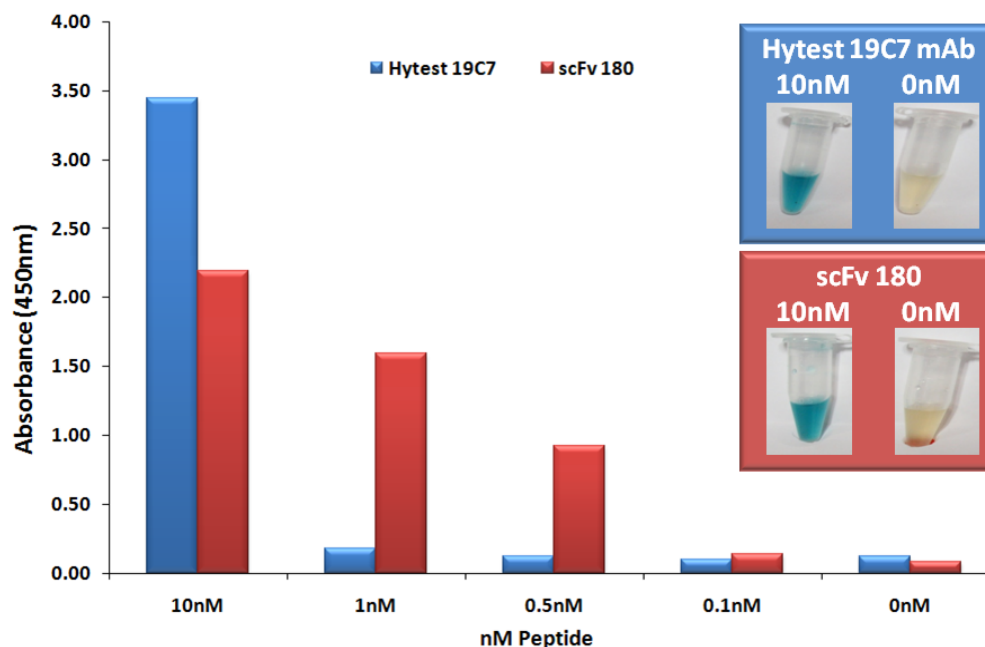


Figure 5.2-24: Pre-panning optimisation of peptide concentrations for in-solution bio-panning

The WT scFv and control mAb (19C7) were incubated with free peptide-1 and recovered using paramagnetic beads. The recovered bead-peptide-antibody complexes were incubated with TMB. The inset pictures show the 10nM and 0nM peptide concentrations for both Hytest (blue) and scFv 180 (red) after incubation with TMB. Visually the zero peptide concentration gave little or no colour change while the 10nM peptide showed strong colour development. The developed TMB for each concentration was then transferred to an ELISA plate for quantitation. This permitted optimisation of the bio-panning conditions prior to selection.

5.2.2.2 Library construction by PCR

The light chain shuffled library was constructed in the same manner as the WT library. The catalogue of V_L chains was prepared in large-scale, as previously optimised and described in section 2.3.4.4. In this instance the V_H was amplified from the scFv 180 plasmid directly using the V_H primer set (Table 2.3-4). The $MgCl_2$ concentration was optimised for this process prior to large-scale amplification. Figure 5.2-25 illustrates the specific bands amplified with 1.5mM $MgCl_2$ and this was used for the large-scale amplification. Finally, the V_H and catalogue of V_L were overlapped by SOE-PCR, as previously described using the optimised conditions (section 2.3.4.4.2) keeping the BM and SP V_L separate (Figure 5.2-26). The SOE-PCR was then ligated into pCom3xSS vector, as described for the WT library, and transformed into *E. coli* XL1 blue in preparation for bio-panning (section 2.3.4.4.4).

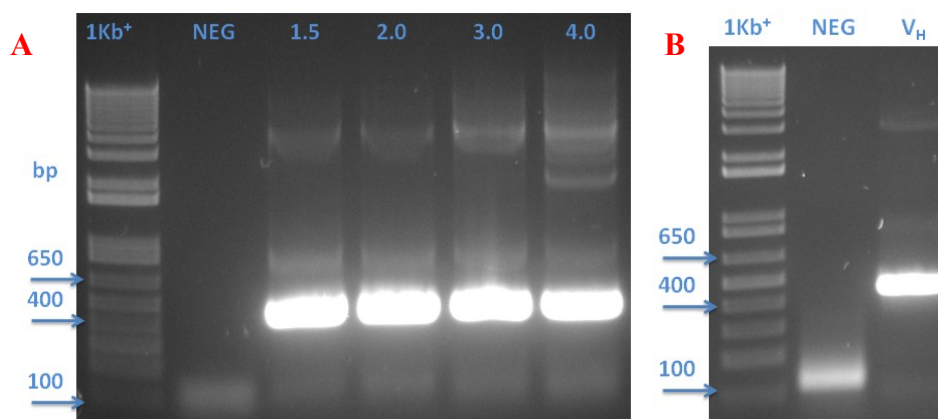


Figure 5.2-25: V_H amplification from wild-type gene

- A) Optimisation of the V_H amplification from the selected scFv 180 plasmid. $MgCl_2$ was titrated from 1.5mM to 4.0mM and demonstrated no significant increase in yield of the amplified product at ~450bp.
- B) The large scale amplification of the V_H was carried out at 1.5mM $MgCl_2$ as the optimised concentration.

The amplified products were resolved on 2% (w/v) agarose gels and in both cases negative reactions (no template DNA) were included. The size of the amplified products was estimated by comparison to the 1kb⁺ ladder.

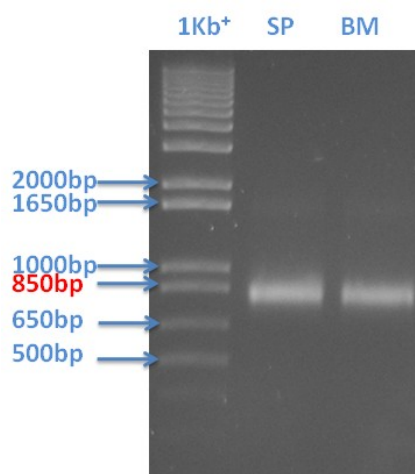


Figure 5.2-26: Mutant library SOE-PCR

The SP and BM catalogue of V_L chains were ‘stitched’ together with the V_H chain from the WT scFv by SOE-PCR. This resulted in the formation of a band at approximately 800bp corresponding scFv gene segment (V_L -linker- V_H). This product was subsequently digested with *SfiI* and ligated into the pComb3xSS vector for transformation. The SOE-PCR products were resolved on a 2% (w/v) agarose gel. 1Kb⁺: DNA ladder.

5.2.2.3 *Bio-panning of the anti-epitope-1 mutant library*

The transformed MT library was composed of both the SP and BM V_L catalogues which were pooled post transformation, yielding a library of 3.1×10^8 members. The scFv fragments were rescued by helper-phage and displayed on filamentous phage surface. The solution-phase bio-panning strategy outlined in section 2.3.4.5.4 was exploited incorporating the optimised bio-panning conditions and stringencies that are delineated in Table 2.3-13. After four rounds of bio-panning the phage preparations for each round were analysed by polyclonal-phage ELISA (section 2.3.4.6.2). Figure 5.2-27 demonstrates the immediate enrichment for both cTnI and KLH-P1 after one round of bio-panning and reinforces the need to perform at least one selection to enrich even a heavily-biased library. Despite gradual limitation of free antigen the enrichment sequentially increases for cTnI. Based on this strong positive polyclonal-phage ELISA, the round four phage population was infected into mid-exponential *E. coli*. Top 10F' for expression of soluble scFv and brought forward to screening (section 2.3.4.7).

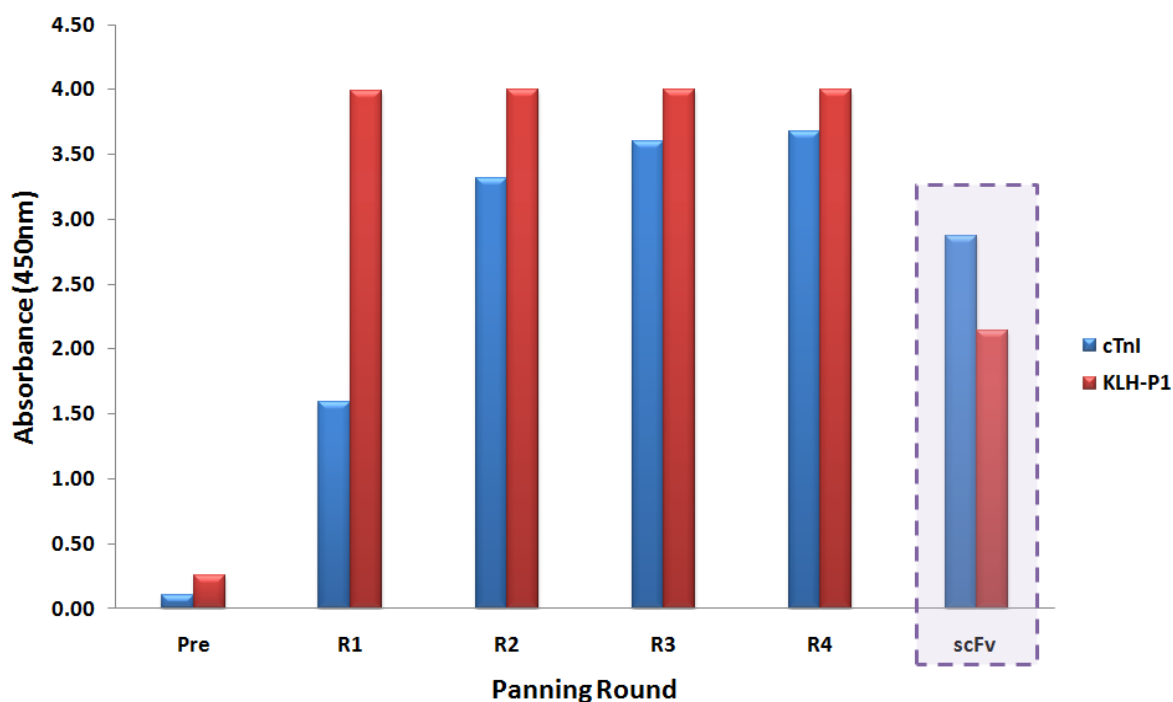


Figure 5.2-27: Polyclonal-phage ELISA for the light chain shuffled library

The phage preparations were assayed for specific binding against cTnI and the KLH-peptide-1 conjugate to demonstrate anti-epitope-1 scFv enrichment. Phage from each round was diluted 1 in 5 with 1% (w/v) PBSTM and the WT scFv (boxed) was also included as a positive control. Bound phage were detected using anti-M13 HRP-labelled secondary antibody and bound scFv with anti-HA HRP-labelled secondary antibody. Specific phage-displayed antibodies for cTnI (epitope one) were enriched after a single round of bio-panning. Even in such a biased library the transformed unpanned library signal was low due to the low representative numbers of each clone present.

5.2.2.4 *Mutant screening for improved affinity clones*

The mutant library generated contained a large pool of closely related yet heterogeneous clones that required differentiation from the WT in an efficient way. The primary screening regime (section 2.3.5.2) again utilised direct binding and sandwich ELISAs and the HT power of the Biacore™ 4000, but in this case applying some of the lessons learned and ‘tricks of the trade’ to garner more information per run. For example, zero antigen concentrations for each clone on Biacore™ 4000 allowed estimation of very crude k_a/k_d and the newly described ‘2 over 2’ kinetic evaluation permitted further refinement of the kinetics of the interactions in a HT-fashion. Use of the purified scFv 180 as a benchmark throughout the analysis allowed clear differentiations to be drawn in ‘side-by-side’ comparison to the MT lead candidates.

Initially, the 192 clones were evaluated in direct binding and sandwich assays (section 2.3.5.2.1). Figure 5.2-28 shows a significant population of positive clones in both sandwich (77.6%) and cTnI direct binding ELISA (81.3%). In general, most of the scFv that bound to cTnI directly also recognised the antigen presented by the 20B3 mAb. However, approximately 3.7% failed to bind the presented antigen (~7 clones) and thus represented sub-optimal V_L - V_H combinations for efficient pairing with the 20B3 mAb. The analysis was valuable as it demonstrates the success of the ‘in-solution’ selection campaign. The information acquired in this experiment does not provide a means to separate the clones in terms of improvement in affinity. However, this positive result allowed confident progression into HT-ranking of the clones on Biacore™ 4000.

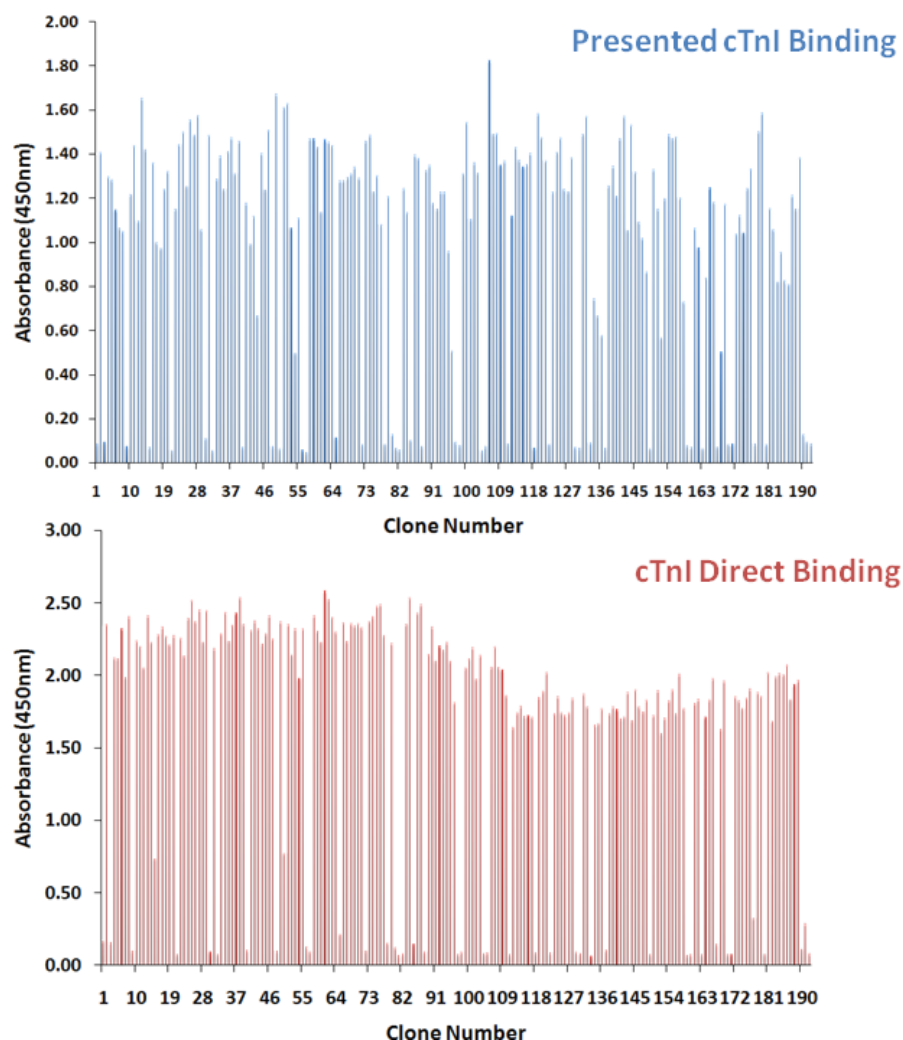


Figure 5.2-28: Functional assay screening of mutant scFv for immobilised and captured cTnI protein

cTnI was presented using the 20B3 mAb. ScFvs from crude lysates were applied to the captured antigen and bound scFv detected using an anti-HA HRP-labelled secondary antibody. A significant proportion of the population recognised cTnI in this presented form. In parallel, the same scFv supernatants were applied directly to wells coated with cTnI antigen and detected with the same secondary antibody. Again the majority of clones bound to the antigen specifically. This analysis alone gives a positive result to the bio-panning experiment, but lends no information to rank the clones in terms of improved affinity mutants.

The second more ‘information-rich’ screening method relied on the parallel processing power of the Biacore™ 4000. Figure 5.2-29 is the sensorgram data for the 192 mutant scFvs, analysed with a fixed concentration of cTnI in a capture approach (as described in Figure 5.2-17-A). The inclusion of a zero antigen concentration corrected for the dissociation of each captured scFv from the anti-HA surface and allowed the MT screen to evaluate each scFv by basic binding kinetics in a very HT-fashion (section 2.3.5.2.2.1).

Figure 5.2-30 is an ‘on/off-rate’ map of the 192 MT clones and the WT clone. A plot of this type allows affinity isotherms to be graphically represented giving an insight to the effective k_d/k_a . With little variance in the k_a a dramatic ‘slowing’ of the k_d was apparent. Given that K_D (affinity) = k_d/k_a , this dramatic improvement in k_d was advantageous, giving rise to a sharp improvement in the affinity values, as approximated from the position relative to affinity isotherms. The clones were also compared by % left analysis in the same experiment. By inclusion of the WT clone a threshold % left value of ~63.6% was applied. Figure 5.2-31 illustrates the dramatic improvement in percentage left value, indicating improved stability of the binding events. Only 15 clones (7.8%) showed reduced percentage left values in comparison to the WT. For the vast majority of clones the percentage left values increased above 70% up to a maximum of 94.8%.

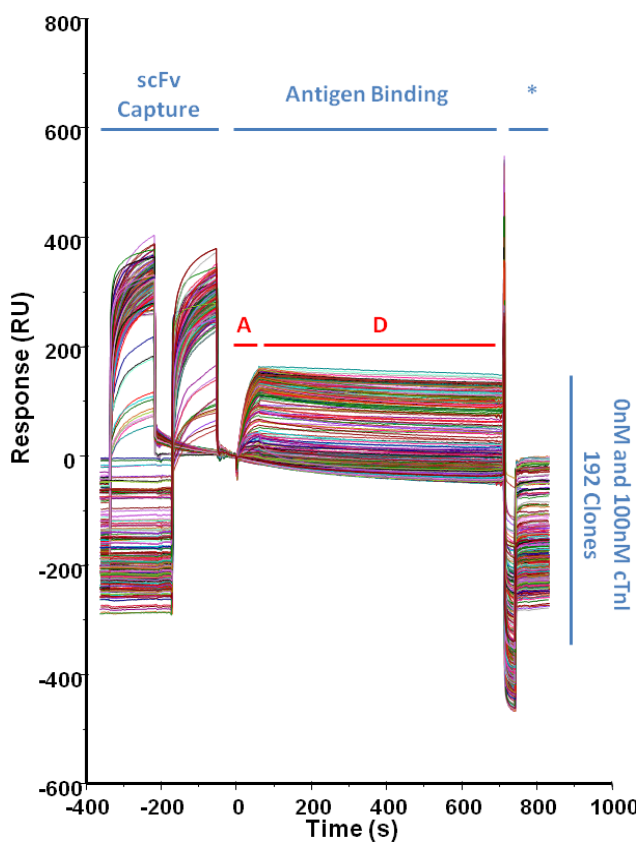


Figure 5.2-29: High-throughput (HT) screening of the mutant scFv on the Biacore™ 4000

Reference subtracted sensorgram data of the screening process. In each cycle individual scFvs were captured on spot 1 (1st peak) and 5 (2nd peak) followed by injection of both 0nM and 100nM cTnI. Inclusion of a zero for each scFv clone allows evaluation of the binding kinetics in a preliminary way by assigning association (A) and dissociation (D) curves. Regeneration of the surface (*) was achieved using 20mM NaOH.

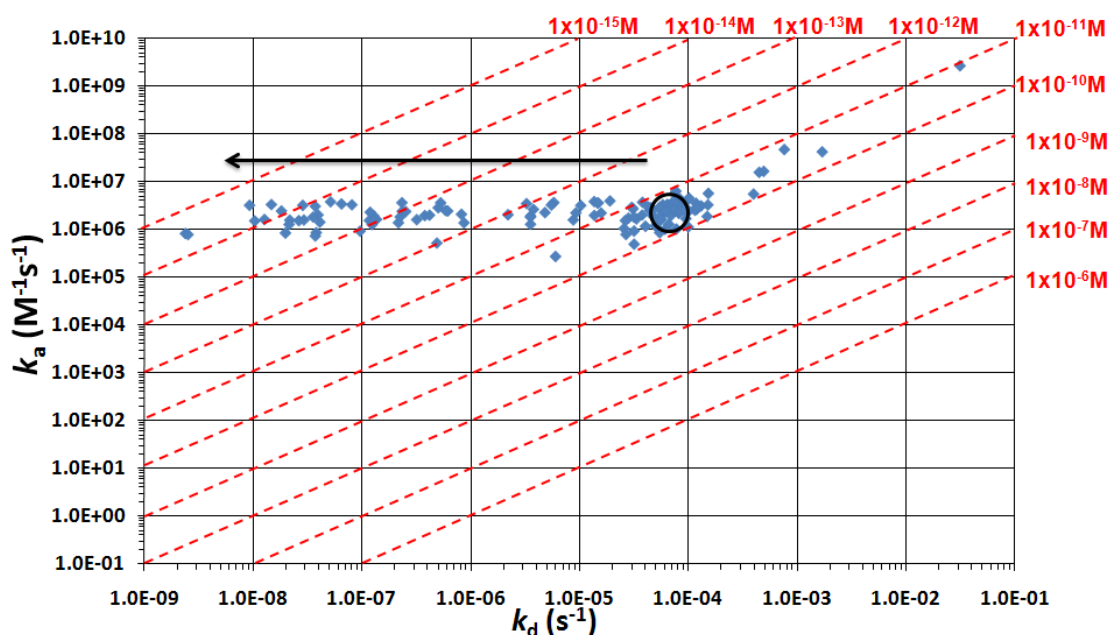


Figure 5.2-30: 'On/off-rate' map of phage selected scFv mutants for anti-epitope-1

From the Biacore™ 4000 experiments crude association (k_a) and dissociation (k_d) constants were modelled. The plot of k_a and k_d gives rise to the affinity isotherm map shown above. The affinity isotherms are indicated by diagonal red lines and allow visualisation of approximate affinity (M). The circle indicates the area where the WT lies on the plot. Visually there appears to be very little variance in k_a introduced by the light chain shuffle. However, a spread in the k_d was noticeable where the mutant clones predominantly move to significantly slower k_d values (directional arrow).

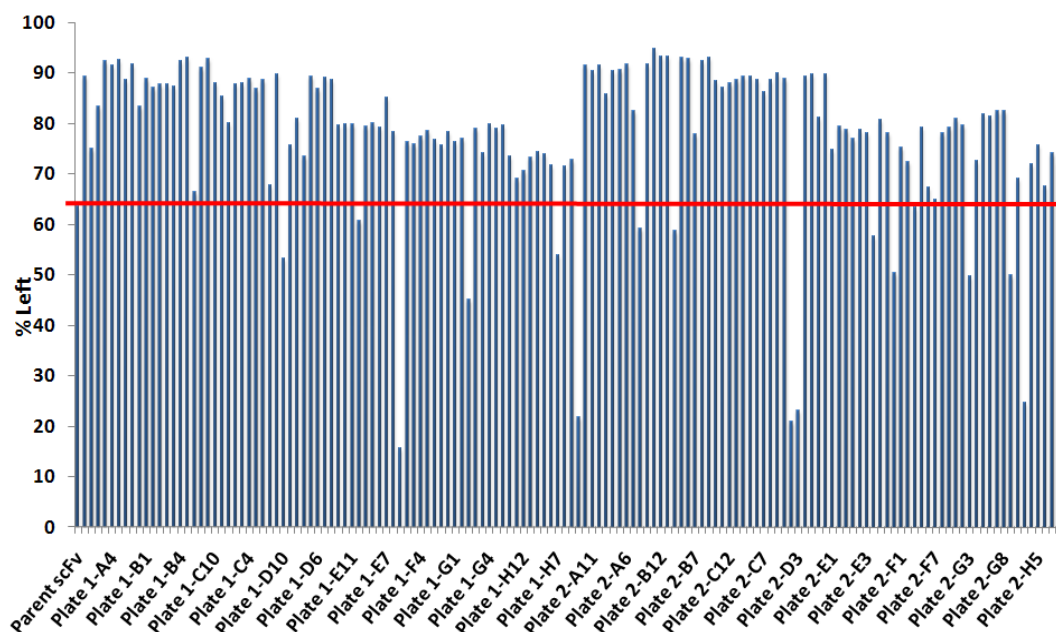


Figure 5.2-31: HT 'percentage-left' ranking of scFv mutants in comparison to the wild-type clone

In the same HT-experiment as the 'on/off-rate' map, the binding level early versus binding level late data was plotted as percentage left graph. This shows the stability of the binding event with a notable increase to a higher binding stability for the mutants compared to the WT (red line).

To delve further into this affinity improvement a relatively small subset of clones at the highest affinity range (14 clones) and one not so high (1 clone) plus the WT were taken into a ‘2 over 2’ kinetic experiment (section 2.3.5.2.2.2). This involved the capture of two different densities of the scFvs from the crude lysates, as illustrated in Figure 5.2-32. Data was then acquired for three antigen concentrations (0, 25 and 75nM cTnI) and provided a greater number of curves per clone for the software to fit kinetic constants. This resulted in improved reliability of the calculated values while retaining HT nature of the analysis. An example of the reference subtracted, fitted curves for two scFvs is illustrated in Figure 5.2-33. The curves were fitted with the 1:1 Langmuir binding model and a sharp ‘flattening’ of the dissociation phase observed for the mutant example. Figure 5.2-34 plots the extrapolated k_a and k_d values highlighting the dramatic shift in affinity towards 10^{-15} M. Although this was an exciting result the extremely high-affinity for the clones here was somewhat suspicious in magnitude and raised concerns about underlying antigen quality issues contributing to the derived k_d .

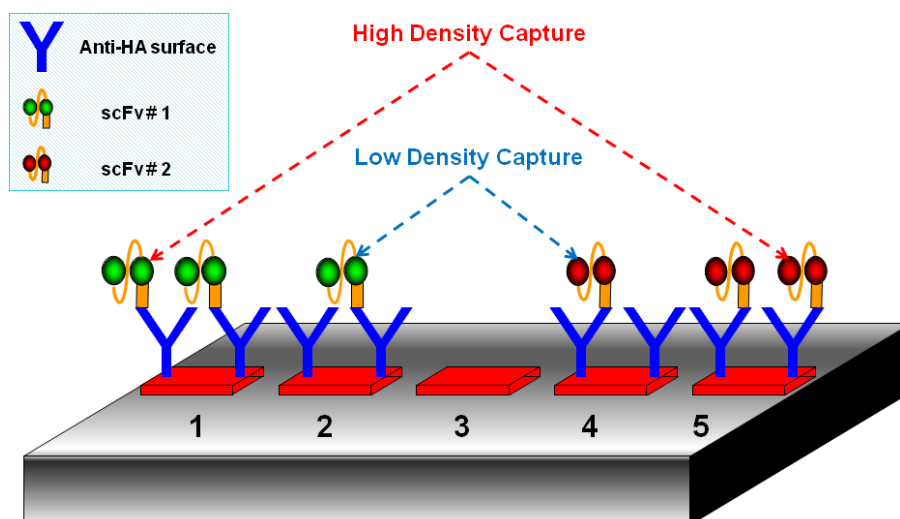


Figure 5.2-32: Flow cell setup for ‘2 over 2’ kinetic experiment

A polyclonal anti-HA surface was created within the flow cell. In this setup two scFvs are captured from diluted lysates; one scFv on spots 1 and 2 and a second scFv on spots 4 and 5. The lysates were diluted such that two different densities of scFv were captured; high density on spots 1 and 5 and low density on spots 2 and 4. Three cTnI concentrations (0nM, 25nM and 75nM in 1XHBS-EP⁺) were passed over the two capture densities and were referenced against the unmodified surface on spot 3. Two densities of each clone interacting with three cTnI concentrations formed the basis of kinetic constant determination with the 1:1 Langmuir binding model. In the four flow cell system eight clones were evaluated per cycle.

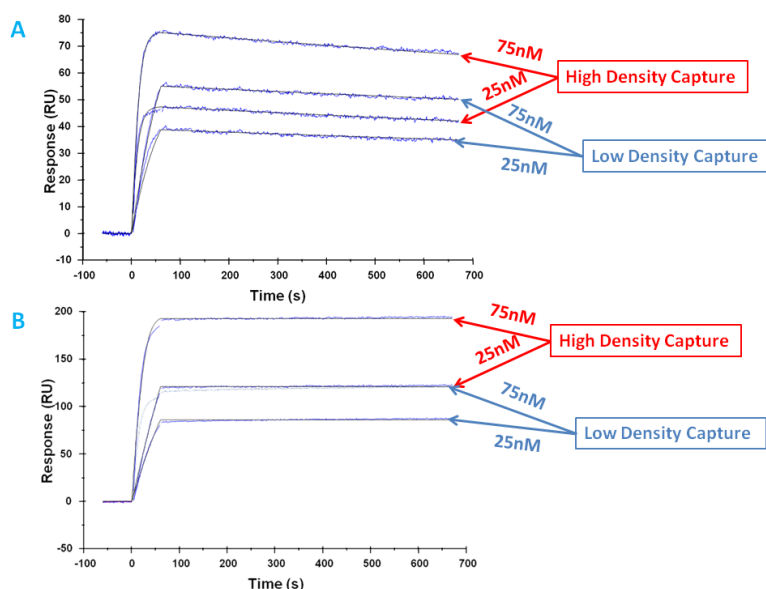


Figure 5.2-33: '2 over 2' kinetic curves for wild-type and one selected mutant

Representative reference subtracted curves from the '2 over 2' experiment. A: scFv 180 and B: scFv 2B12 with the high (red) and low (blue) density scFv capture levels for two cTnI concentrations (the 0nM cTnI curve was subtracted automatically by the software). The association and dissociation curves (blue lines) for each scFv were fitted with kinetic curves (black lines, a 1:1 Langmuir binding model) using a local fit. The fits were found to be good with χ^2 values of 0.56 for the WT and 1.0 for the MT. The corresponding affinities for all 15 selected clones and the WT were then plotted in Figure 5.2-34.

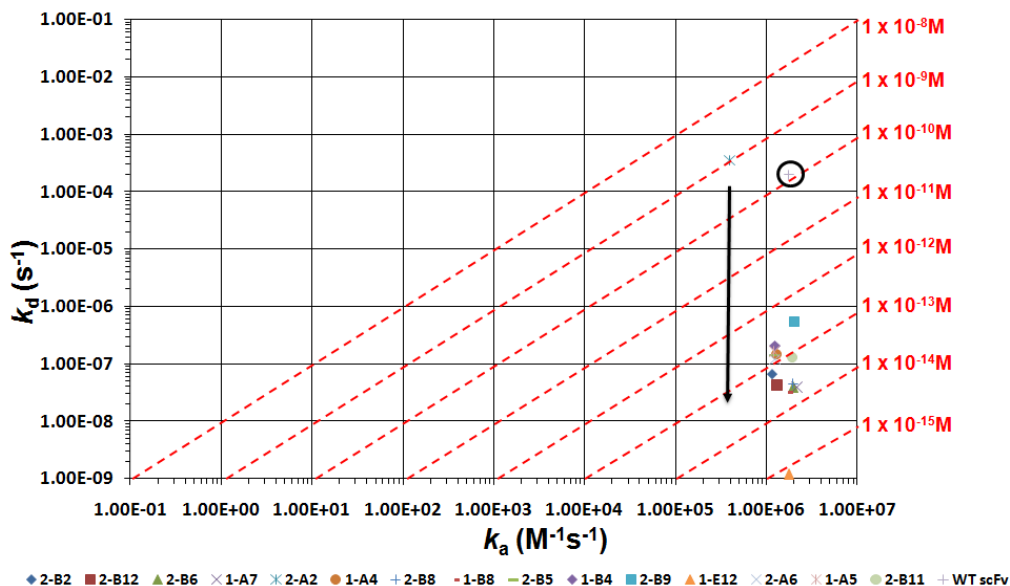


Figure 5.2-34: Plot of k_a and k_d from the '2 over 2' experiment for anti-epitope-1 mutant selection

The accuracy of the k_a and k_d values was improved by the '2 over 2' screening format while continuing to evaluate a significant number of scFvs. The k_a and k_d values were determined by fitting of the kinetic curves (as illustrated in Figure 5.2-33) and plotted on the graph. The affinity isotherms are indicated by diagonal broken red lines and again demonstrate little variance in k_a , but significant k_d improvement. The WT scFv is highlighted by the black circle.

5.2.2.5 Comparison of wild-type and mutant clones

From the ‘2 over 2’ kinetic evaluation, six clones were selected for full kinetic characterisation alongside the WT clone. The next section describes the challenges that presented themselves in acquiring accurate kinetic information and the approach taken to improve the quality of the interaction using the FABP-P1&2 fusion protein. Subsequent sections outline the route to selection of the ‘best’ clone largely based on the kinetic evaluations and inhibition analyses.

5.2.2.5.1 Full kinetic evaluation of the scFvs

Table 5.2-4 lists the clones selected for further kinetic analysis on Biacore™ 4000.

Table 5.2-4: Mutant clones selected for further characterisation

Clone	Percentage left (%)	Crude Analysis of K_D (M)	‘2 over 2’ K_D (M)
2B11	94.8	1.21×10^{-13}	6.80×10^{-14}
1E12	60.8	2.83×10^{-11}	6.60×10^{-16}
2B12	93.1	1.84×10^{-14}	3.20×10^{-14}
2B9	93.1	2.50×10^{-13}	2.65×10^{-13}
2B6	92.9	2.85×10^{-13}	1.98×10^{-14}
2B2	93.4	1.07×10^{-12}	5.77×10^{-14}
WT	63.6	-	1.12×10^{-10}

Full kinetic analyses were carried out for the six MT clones and the WT (section 2.3.5.2.2.3) with optimised dilutions for capture and cTnI concentrations to ensure that the R_{\max} was < 100RU. The cTnI concentration range used was: 12.0, 6.0, 3.0(x2), 1.5 0.75, 0.38, 0.19 and 0nM. Figure 5.2-35 shows the reference (buffer only) subtracted curves fitted locally by the Biacore™ software. A clear flat line for dissociation (k_d) was observed for each of the six MT clones which was indicative of high-affinity. Figure 5.2-36 shows the scFv 2B12 and the WT side-by-side illustrating the visual improvement in the ‘off-rate’

and thus suggests that the MT was a higher-affinity clone than the WT. Fitting kinetic constants on the dissociation phase proved extremely difficult owing to the apparent high-affinity of the clones. Significant and wildly varied k_d were obtained in inter- and intra-day analysis. This may be attributed to the fact that determination of the affinity of the clones had reached the limitations of the instrument. However, the quality of the commercially sourced TnI may also introduce non-1:1 binding effects, which at these very slow k_d values caused this variation and the resultant, dramatic apparent improvement in k_d .

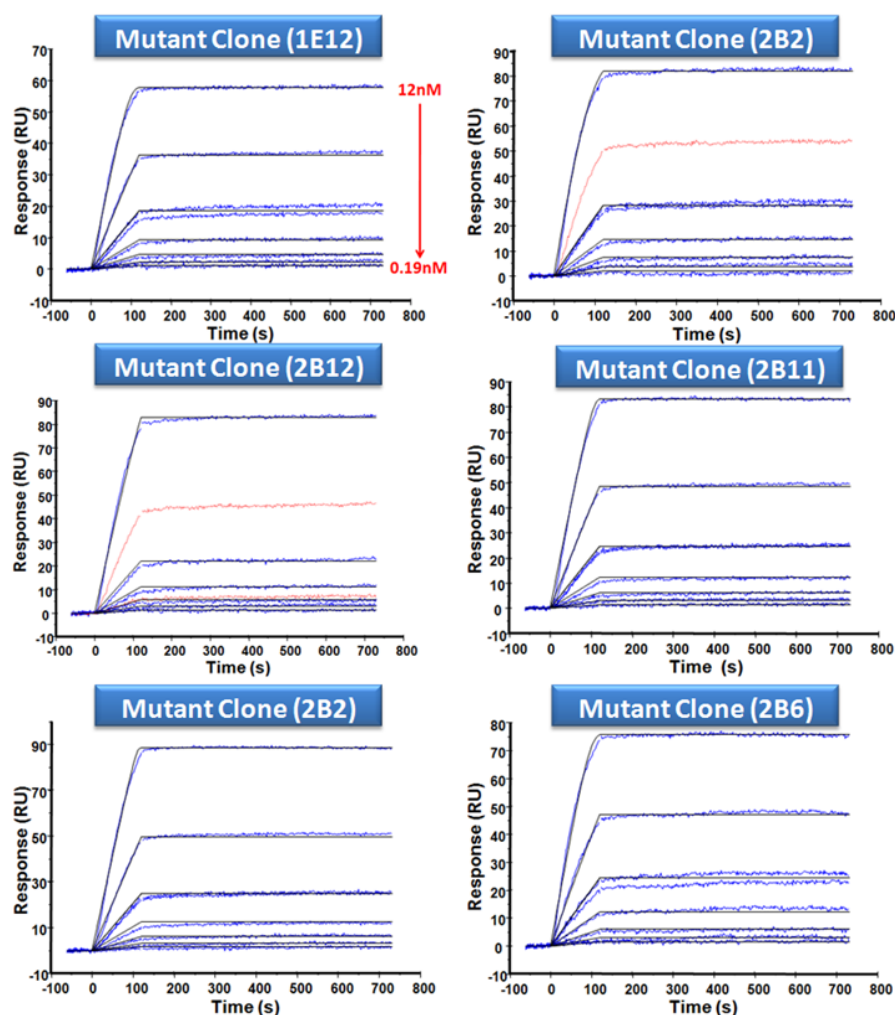


Figure 5.2-35: Full kinetic evaluation of selected scFv mutants on Biacore™ 4000

Clones were analysed over a broad range of serial cTnI concentrations (12→0.19nM). Kinetic fits were applied by the system software with 1:1 Langmuir binding model using local fit option. Blue curves represent the reference subtracted data acquired for each concentration, the black lines represent the fitted association and dissociation curves. Red curves are those rejected by the system software due to the positive slope after the end of the association phase.

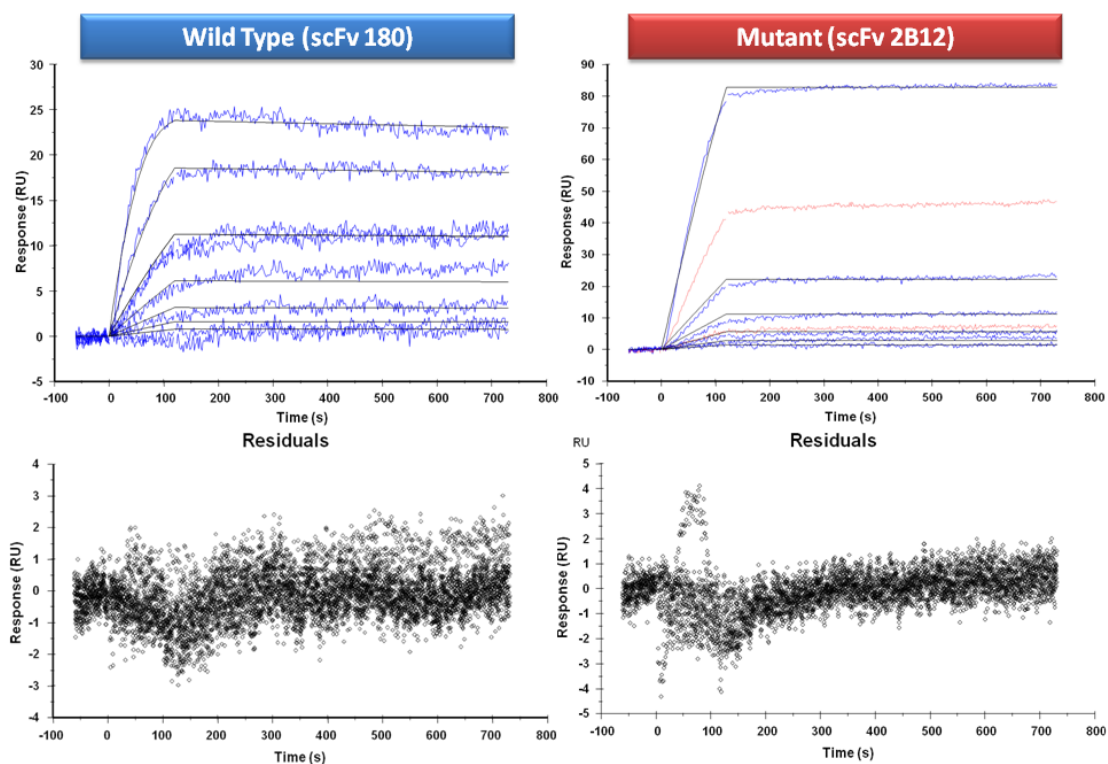


Figure 5.2-36: Kinetic comparison of wild-type and mutant scFv 2B12

Clones were analysed over a broad range of serial cTnI concentrations as in Figure 5.2-35. Kinetic fits were applied by the system software with 1:1 Langmuir binding model using local fit option. Blue curves represent the double referenced data acquired for each concentration, black lines represent the fitted association and dissociation curves. Red curves are those rejected by the system software due to the positive slope after association. The underlying dot plots show the residuals for the data. This allows assessment of bias and represents the ‘goodness’ of the 1:1 model fit. The data points for scFv 180 represent an even spread and indicates no significant bias. The equivalent residual plot for the mutants indicated some bias in the association phase (elliptical trend) suggesting the fit data quality was not truly optimal.

From all the kinetic data acquired throughout the screening campaign and the full comparison, no real conclusion in terms of a ‘hard number’ could be attributed to the MT clones. However, the side-by-side nature of all the analysis ensured that any effects of antigen quality were at least consistent and allowed the conclusion to be drawn that the MT clones selected were certainly improved compared to the WT. A different analysis was required to efficiently rank the clones in a less ambiguous way.

5.2.2.5.2 Inhibition analysis of selected clones

To answer many of the questions left unanswered by the kinetic evaluation, a rigorous inhibition format comparison was undertaken to assess any changes in terms of the half-maximal inhibitory concentration (IC_{50}) value (section 2.3.6). IC_{50} refers to the effective antigen concentration required to decrease antibody binding by 50% at equilibrium.

Lysates were initially titred against cTnI to obtain the optimal working dilution for an inhibition ELISA (Figure 5.2-37-A). Each scFv was incubated with a range of free cTnI concentrations (200→0.39nM) and then converted to a ratio of signal obtained/signal at zero cTnI (A/A₀). Figure 5.2-37-B shows the full complement of selected scFv and their associated inhibition profiles in comparison to the WT scFv. It was apparent that there was a shift towards a lower IC_{50} value for the mutants and as IC_{50} is proportional to K_D this suggests that the clones are indeed of improved affinity. Clones 2B12 and 1E12 were re-analysed with the WT over a more focussed concentration series in the inhibition ELISA. Figure 5.2-37-C reaffirms the previous result showing an improvement in IC_{50} value for clone 2B12 (~6nM) over the WT (~10.5nM).

This encouraging result indicated that clone 2B12 had superior inhibition assay performance compared to the WT, reinforcing the suggested affinity improvement found with the full kinetic analysis. The confirmation of discrete kinetic constants remained a high priority.

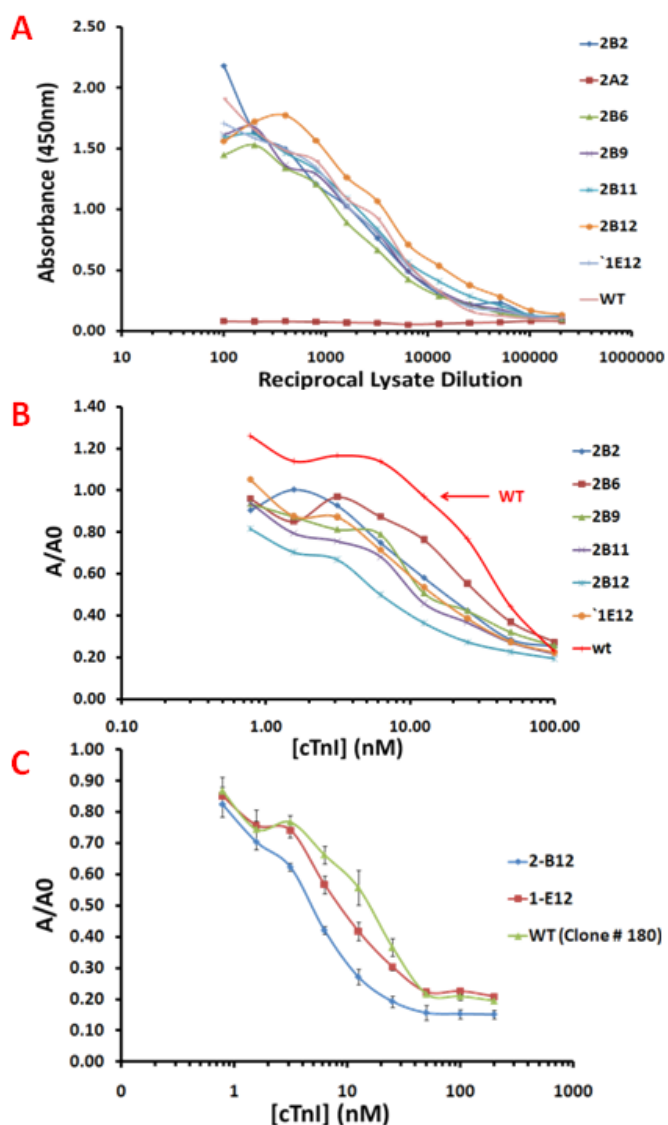


Figure 5.2-37: Titre and competitive analysis of wild-type and mutant scFvs for cTnI and free peptide

- A. Titration of scFvs against cTnI by ELISA: Supernatants were serially diluted in 1% (w/v) PBSTM and applied to individual wells. Bound scFv was detected using anti-HA HRP-labelled secondary antibody. Optimal dilutions of lysate were determined for each clone to give an absorbance of 1.0AU.
- B. Inhibition ELISA for six scFvs and the wild-type: scFv was mixed 1:1 with various concentrations of free cTnI at the optimal scFv dilution derived from A. Post incubation the mix of the various scFvs and free TnI concentrations were applied to the cTnI-coated wells. Unbound scFv was available to bind to the surface-immobilised cTnI. The results here indicated a generalised shift wards lower IC_{50} value compared to the WT.
- C. Two mutants and WT were re-analysed in the inhibition format: IC_{50} for WT ~10.5nM, 1E12 ~10nM and 2B12 ~6nM

From this analysis an improvement in inhibition assay performance was observed and scFv 2B12 was selected as the best clone isolated from the MT screening campaign.

5.2.2.5.3 Purification of scFv from bacterial culture

Both the WT and MT scFv were purified, as described in section 2.3.1.9, using the simplified PBS-based buffers delineated in section 2.1.4.6.2. The scFv were purified by virtue of the 6xHis tag encoded on the pComb3x vector by IMAC. The purification was carried out from 400mL cultures induced overnight (0.5mM IPTG). Both clones expressed well with minimal optimisation of culture conditions (results not shown). It was noted that a significant amount of protein was eluted, especially in the case of the MT scFv (Figure 5.2-38) over the WT (Figure 5.2-39-A), in the washes (W1 and W2). The presence of 0.5% (v/v) Tween®20 may have caused this to occur, whereas the first wash contained many contaminating bands the W2 fraction appeared to be extremely clean. The W2 fraction for 2B12 was concentrated/buffer exchanged alongside the pure fraction. These concentrated samples were re-analysed by SDS-PAGE (Figure 5.2-38-B) and showed a very pure protein preparation. For the analysis of the scFv 180 purification, the W2 fraction was concentrated alongside the pure fraction and run on the SDS-PAGE to ensure maximal recovery of expressed protein (Figure 5.2-39). In this case the loss of protein in the washes was significantly less pronounced, but significant. In both cases the pure fractions eluted (by acidic elution) and concentrated W2 fractions yielded significant quantities of protein of acceptable purity. Protein concentrations were obtained by A_{280} on a ND-1000™ and outlined in Table 5.2-5.

Table 5.2-5: Purified scFv protein determination

	Clone 180 (Pure)	Clone 180 (W2)	Clone 2B12 (Pure)	Clone 2B12 (W2)
Total protein (mg)	1.68mg	0.58mg	1.00mg	0.73mg
µg protein per mL culture	5.7µg/mL		4.3µg/mL	

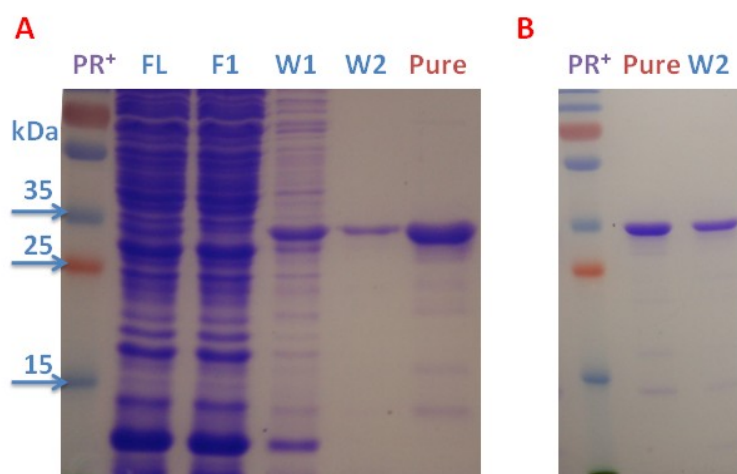


Figure 5.2-38: Purification of 2B12 scFv (mutant) by immobilised metal affinity chromatography (IMAC)

SDS-PAGE analysis of 2B12 scFv purification steps. The lanes are labelled as follows; FL: filtered lysate, F1: flow-through 1, W1: wash 1, W2: wash 2 and pure samples. PR⁺ is the prestained protein ladder.

- A) In the large-scale purification, samples of each step of the process were analysed. A notable amount of protein was washed from the column (W1 and W2) and appeared to be quite pure in the W2 lane. This fraction was concentrated from 5mL to 1mL alongside the eluted pure sample
- B) The concentrated pure and W2 fractions were re-analysed by SDS-PAGE. This showed that a large amount of pure protein was present in the W2 fraction.

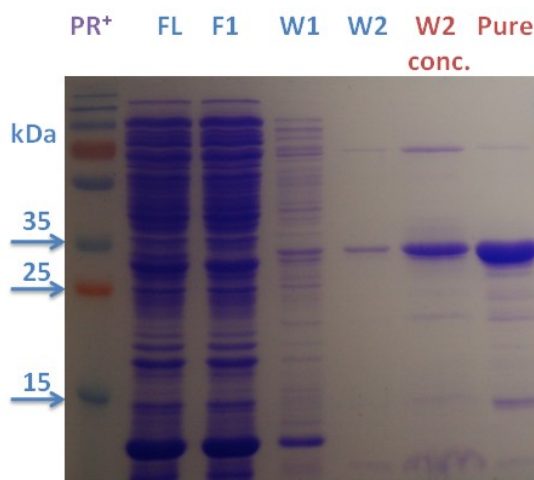


Figure 5.2-39: Purification of scFv 180 (wild-type) by IMAC

SDS-PAGE analysis of 180 scFv purification steps. The lanes are labelled as follows; FL: filtered lysate, F1: flow-through 1, W1: wash 1, W2: wash 2, W2 conc.: concentrated W2 and pure samples. PR⁺ is the prestained protein ladder. As observed in the MT purification (above) specific protein was eluted in the washes (W1 and W2) to a much lesser extent. By concentration of the W2 sample a significant amount of protein was recovered.

5.2.2.5.4 Improved kinetic characterisation using fatty acid binding protein fusion

Kinetic analyses for the WT and MT scFv was carried out using the FABP-P1&2 fusion protein (developed in section 3.2.4) to overcome the unreliability of the kinetic evaluation obtained with the cTnI protein (section 5.2.2.5.1). Kinetics were carried out on the Biacore™ 4000 (section 2.3.7) and permitted each scFv to be analysed on two spots for the full analyte concentration range (25→0.39nM) in a single run. The analyses were carried out on a minimum of three separate occasions with independently prepared analyte samples (total number of independent analysis = 6).

Figure 5.2-40 is an example of the full kinetic profile for scFv 180 and 2B12 using the FABP-P1&2 fusion. Visually the fits are very good with χ^2 values of 0.34 and 0.68, respectively combined with good even residual distribution. In addition, the replicate measurements (3.13nM cTnI) were indistinguishable re-enforcing the reliability of the analysis. Table 5.2-6 outlines fully the kinetic constants obtained. The clones are statistically different from each other in terms of affinity. The scFv 180 was found to have a K_D of 99.2 ± 12.6 pM and scFv 2B12 approximately 27% lower at a K_D of 72.4 ± 11.1 pM. This overall improvement in K_D was attributed to a slowing of the k_d and was somewhat countered by a marginal impairment in k_a . The kinetic constants derived using this ligand indicated a less dramatically improved k_d (Figure 5.2-37), but the data sets were easily modelled and accurate statistical analysis (t-Test: two-sample assuming equal variances) was carried out to give reliable affinities (Table 5.2-6).

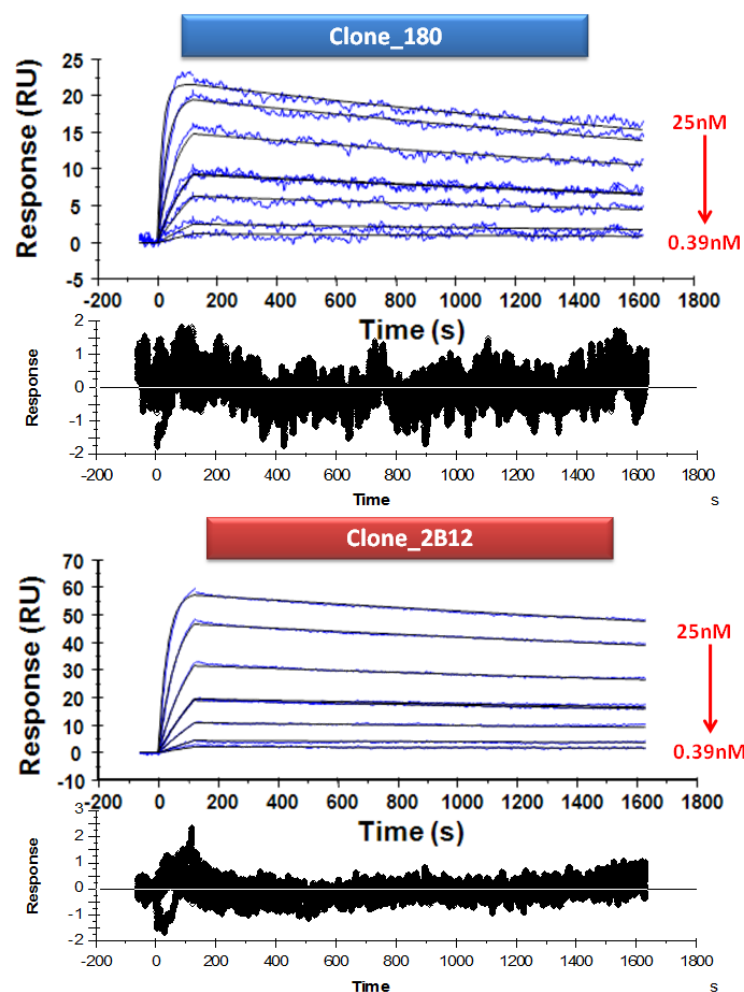


Figure 5.2-40: Full kinetic evaluation of wild-type and mutant scFv with the FABP-peptide fusion

Example of the kinetic profile obtained on Biacore™ 4000 for each scFv using the global fit 1:1 Langmuir binding model. Serially doubling dilutions of FABP-peptide fusions were assayed (25→0.39nM) including one concentration in duplicate (3.13nM) and double referenced against both an equivalently immobilised reference spot and zero antigen concentration. Residuals are indicated for each data point below the kinetic sensorgram indicating the ‘goodness’ of the fit.

Table 5.2-6: Derived kinetic constants for wild-type and mutant scFv using FABP-peptide fusion

	scFv 180	scFv 2B12
k_a ($M^{-1}s^{-1}$)	$2.76 \times 10^6 \pm 5.18 \times 10^5$	$1.70 \times 10^6 \pm 1.06 \times 10^5$
k_d (s^{-1})	$2.70 \times 10^{-4} \pm 3.43 \times 10^{-5}$	$1.22 \times 10^{-4} \pm 1.50 \times 10^{-5}$
K_D (pM)	99.2 ± 12.6	72.4 ± 11.1
n	6	8
Significance (p)	0.001	0.001

5.2.2.5.5 Thermal challenge assay to assess for improved thermostability

To assess how the amino acid changes affected the stability of the proteins, a rapid thermal challenge method was adopted from the literature. High-throughput thermal stability screening has been suggested as a useful tool to isolate stable scFv variants in the area of bispecific and bivalent antibodies. This is especially important in this field as the stability of the scFv is often a limiting factor in its production, quality and yield [91]. In work by Miller and co-workers [92], improved thermally stabilised scFvs were identified by a statistical knowledge-based mutagenesis campaign where single mutations resulted in up to a 14°C difference in melting temperature (T_m). The approach compared scFv variants by a T_{50} binding assay which gave a rapid and useful insight to the thermal characteristics of the scFv variants (section 2.3.9).

This approach was adopted in the characterisation of the WT and MT scFvs as a rapid means to assess the impact of the mutations observed between them. The assay involved heating equivalent protein concentrations over a 30°C temperature range for 90 minutes. Immediately after this, the scFvs were diluted 1 in 2 in 1% (w/v) PBSTM and assayed against cTnI for retained binding. The signals obtained were expressed as a percentage of retained binding activity compared to the non-heat treated samples. Figure 5.2-41 demonstrates the difference in T_{50} binding activity for both WT and MT scFv. A shift of 4°C for the MT was observed (WT: 58°C and MT: 62°C) suggesting improved thermostability.

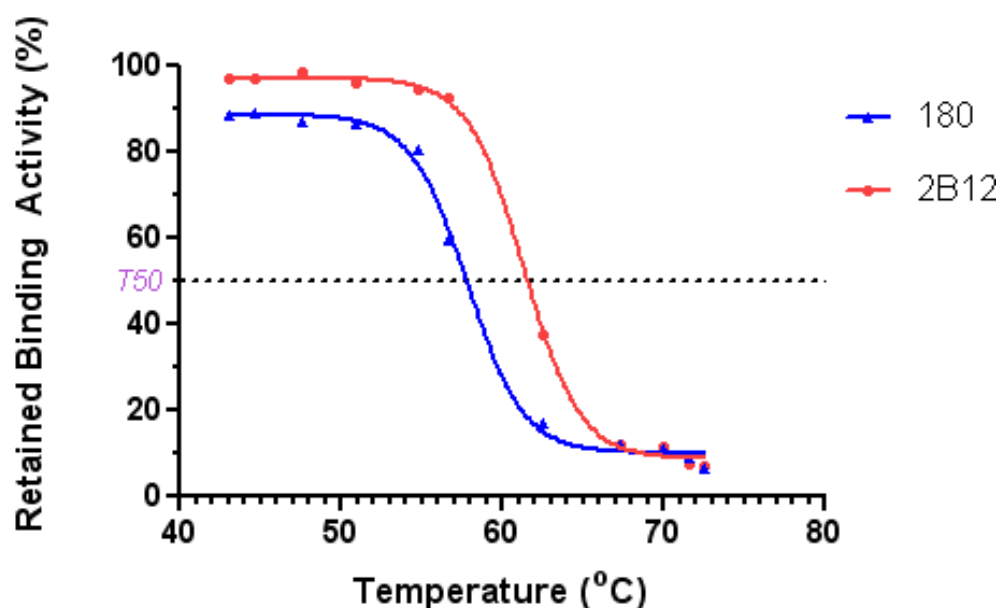


Figure 5.2-41: Comparison of the stability of the scFvs 180 and 2B12 by thermal challenge

Both clones were adjusted to equivalent protein concentrations and their thermal resistance evaluated by thermal challenge assay. Retention of binding activity to cTnI was correlated with temperature and the effect of the mutations introduced by the light chain shuffle appeared to improve the thermo-stability of the mutant.

5.2.2.5.6 Sequence comparison of the two scFvs

To ascertain the structural basis behind the determined improvement in affinity, the scFvs were sequenced by Source BioScience DNA Sequencing, St. James Hospital, Dublin. Sequencing was carried out using the pComb3x sequence primer pair (Table 2.3-4). From the derived sequence the biochemical properties (Table 5.2-7) were estimated using the PROTEIN CALCULATOR v3.3 [296].

Table 5.2-7: Biochemical properties of wild-type and mutant scFv

	ScFv 180	ScFv 2B12
Molecular Weight (kDa)	28.40	28.56
Number of Amino Acids	276	276
Estimated pI	5.97	6.20
Charge at pH7.00	-4.5	-3.5
Extinction Coefficient at 280nm ($M^{-1} cm^{-1}$)	46040	46040

Figure 5.2-42 is the alignment (section 2.3.8.1) of the WT and MT scFv with the CDRs and significant features highlighted as per the caption. Noticeably, no mutations occurred in any of the V_L CDRs, which might have been expected due to the observed affinity improvement. In the light chain there are two mutations in the framework (FR) preceding the CDRL1 (G→E and E→K). Additionally, a PCR introduced mutation in the framework of the V_H preceding CDRH1 was introduced (L→V). These mutations were combined with a change to the linker amino acid structure brought about by use of the published primer sequences [88] which are known to code for the linker GQSSRSSSSGGGSSGGGG in place of the correct primer encoding the linker GGSSRSSSSGGGGSGGGG.

Figure 5.2-42: Sequence alignment of mutant and wild-type antibodies

The effect of the framework mutations was modelled from the sequence information using the online web antibody modelling (WAM) program for the prediction and 3D modelling of antibody Fv structure (section 2.3.8.2). This type of modelling was somewhat limited as the system uses human Fv sequences to predict structure. Such knowledge-based and *ab initio* methods are valuable to assess the changes introduced to the framework region of the mutant library, but apply human antibody structures to the avian antibody.

Figure 5.2-43-A is an overlaid predicted model of the wild-type and mutant clones. The CDRs are coloured for easy visualisation. In the model, the CDR spatial relationships can be observed with the CDRH3 protruding higher than the other CDRs, but angled towards the CDRL3 which can be more clearly observed in the top-down view of the CDR pocket (Figure 5.2-43-B). In the top-down view, the other CDRs can be seen to run around the periphery of the binding pocket with some turns in the loops towards the CDRs L3 and H3. Figure 5.2-43-C shows the CDR view through the heavy and light chains which again highlights the dominant ‘lean’ of CDRH3 towards the LC.

Figure 5.2-44 focuses on the mutated amino acids. The backbone and CDRs are shown with their side chain groups and hydrogen bonds illustrated by the green dashed lines for both the LC and the HC. In the light chain the glycine (GGA) to glutamate (GAA) mutation retained the hydrogen bonds in that area and the second mutation, glutamate (GAG) to lysine (AAG), also showed no change in the hydrogen bond composition of the LC. The HC mutation, leucine (CTG) to valine (GTG), again failed to introduce any new or disrupt any existing hydrogen bonds.

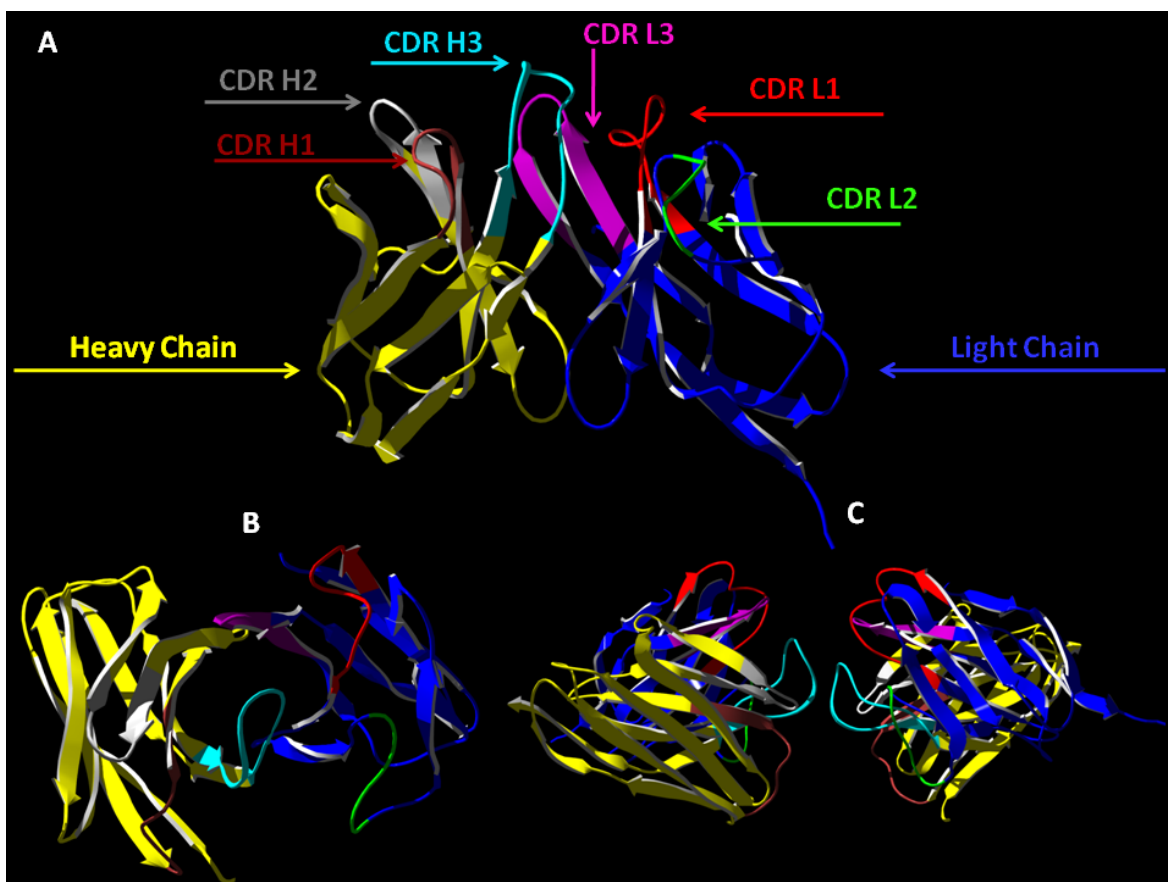


Figure 5.2-43: Predicted hypothetical model of 180 and 2B12 scFvs

- A) Front on view: Heavy and light chain (without linker) illustrating CDR loops/domains. The model was generated using web antibody modelling (WAM - <http://antibody.bath.ac.uk/index.html>) and was visualised using SPDB deep-view and rendered using POV-Ray programs.
- B) Top-down view onto the CDR region: the High CDRH3 loop was the dominant feature of the CDR landscape.
- C) View through heavy and light chains: again the dominant protrusion of CDRH3 can be seen and the twist structure in the CDRL1 is apparent.

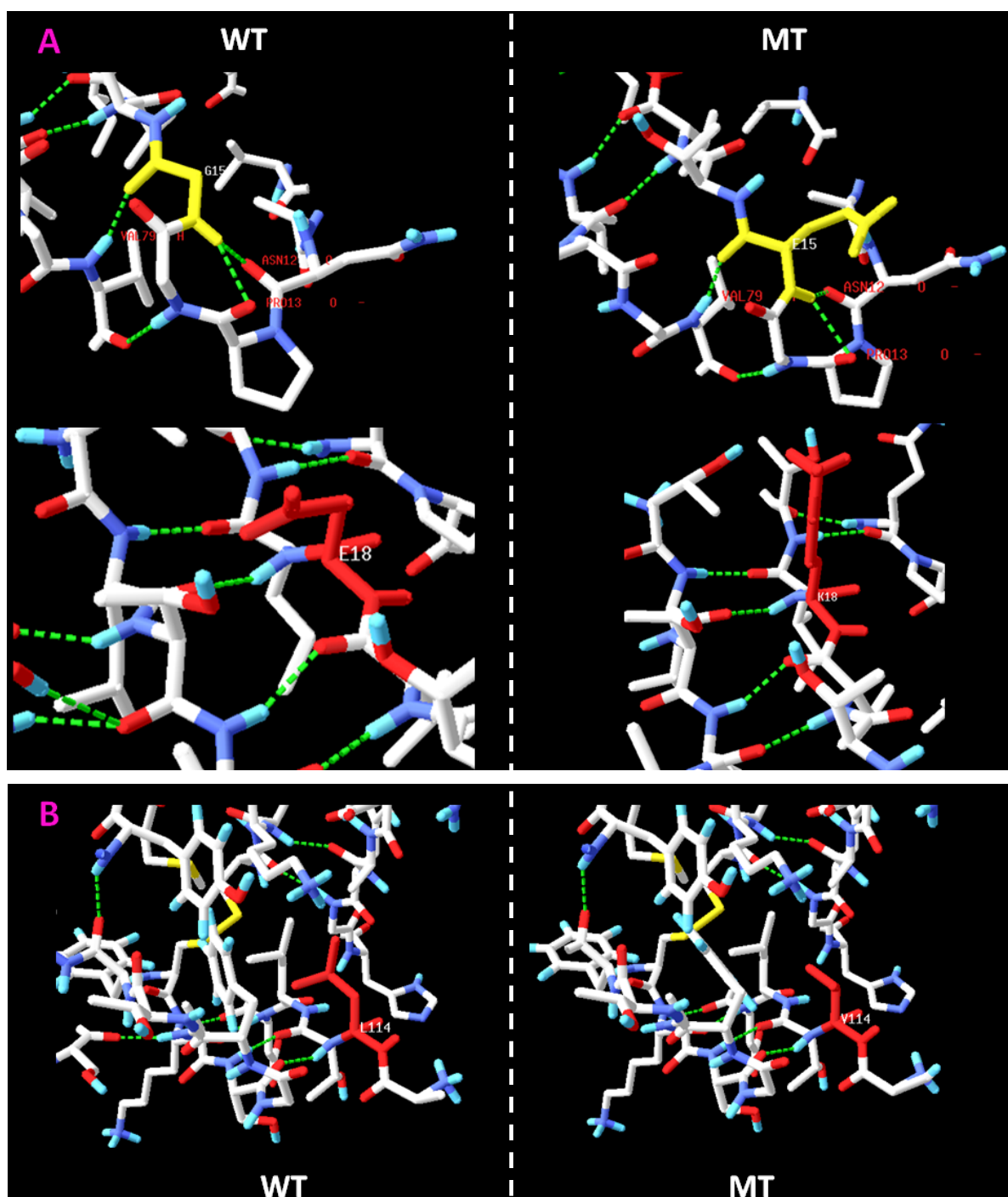


Figure 5.2-44: Modelled mutations for the wild-type and mutant scFvs with displayed side chains

- A) The modelled light chains for the WT (left) and MT (right) scFvs. The hydrogen bond (green dashed lines) landscape was not augmented by the introduced mutations (coloured in yellow).
- B) The modelled heavy chains for the WT (left) and MT (right) scFvs. Again no augmentation in the hydrogen bond (green dashed lines) landscape was observed, by the introduced mutations (coloured in red).

Overall the modelling suggests no change in backbone structure or introduction of new hydrogen bonds. However, the mutations appear to be towards more bulky amino acids with changes from hydrophobic to polar negative (G→E) and polar negative to positive (E→K) resulting in a slight overall effect on the pI of the protein (WT: 5.97 MT: 6.20 at pH 7.0 from Table 5.2-7). This selection of a MT clone with bulkier amino acids may have been facilitated by use of the peptide in the bio-panning procedure. The extraneous parts of the protein were not present (all areas other than epitope one) and the scFv selected did not seem to cause a disadvantageous steric hindrance for binding to cTnI. In fact quite the opposite was suggested, as was observed from the kinetics. The flexible linker was not modelled here, but it is possible that the amino acids within the linker may interact with each other stabilising the scFv differently (Thermal stability, section 5.2.2.5.5) since the linker composition is not equivalent in both scFvs. Linker mutations have previously been demonstrated to impact antibody production, stability and recognition properties [160].

Attempts were made to model the interaction of the cTnI-derived peptide and the scFv using the FlexX program. However, the number of amino acids and areas of the scFv to which the peptide docked were substantial and no one ‘correct’ model could be isolated by *in silico* docking. The same is true in attempts to dock the cTnI molecule using the Patch dock program. As the model of cTnI was based on only one incomplete crystal structure in complex, the scFv were seen to dock in many areas of the protein. In the absence of crystal structure determination the residues involved in mediating antibody-antigen interaction and the possible structural differences between the scFv remains an unknown.

5.2.3 Investigation of crystal structure of recombinant proteins

Understanding protein structure and function is of paramount concern to scientists to understand the interactions between proteins, for example between an antibody and an antigen. Such limitations of *in silico* modelling of the scFv fragments (section 5.2.2.5.6) indicated that our understanding of the antibody 3D structure is limited, and particularly so for those antibodies derived from avian immune repertoires. Searching the PDB with keywords such as “single chain fragment variable” or “scFv” yields 263 and 44 hits, respectively. Of those hits the majority of the structures obtained are 2.0-3.0Å in resolution with few in the 1.5-2.0Å, high-resolution range. Further refining the search to Gallus Gallus (chicken) all the structures relate to avian lysozyme predominantly in complex with many species of antibody (current as of 15 June 2011). Therefore, the fundamental structure of avian derived antibodies would be of benefit to the scientific community and would enhance our combined knowledge of antibody structure. The key to obtaining good quality crystal structures is a pure protein preparation that is homogenous, soluble, mono-dispersed and stable. To achieve this multistep purification protocols are typically required. Given that the scFvs generated in this thesis were stable and soluble proteins they were ideal candidates to carry out initial investigations into crystal structure. The wild-type and mutant scFv were of considerable interest to determine the structural features leading to the demonstrated affinity and assay improvements. However, initial coarse screening conditions did not lend themselves to efficient crystal formation for all constructs as the process of generating protein crystals is ‘trial and error’ rather than a precise science. Due to time constraints it was not possible to investigate all of the protein constructs fully. The wild-type scFv 180 was the only protein optimised further for crystal formation due to the appearance of crystals in coarse screening experiments which allowed for optimisation trials to be setup and some preliminary diffraction data collection. This section describes the work carried out to optimise crystal production for the wild-type 180 scFv in collaboration with Professor James Whisstock’s group at Monash University, Melbourne, Australia.

5.2.3.1 *Crystal structure determination by X-ray crystallography*

Protein structure determination by X-ray crystallography allows the determination of protein structures at the atomic level and has the potential to greatly assist our understanding of protein function. The protein data bank (PDB) houses some 45,000 macromolecular structures largely determined by crystallographic methods [297]. To study atomic structures a crystal is needed as the diffraction of a single molecule would not produce a signal strong enough to be measured. To achieve an ‘amplification’ of the diffraction pattern structural biochemists rely on the formation of ordered, three-dimensional molecular arrays or crystals [298], indeed the bottleneck to obtaining high-resolution structures is the generation of suitable crystals. Proteins can be coerced into forming crystals when placed in the appropriate conditions where the protein undergoes slow precipitation from the aqueous phase. This causes the protein to align into repeating ‘unit cells’ through the adoption of a consistent orientation known as a crystal lattice. The lattice is formed by non-covalent interactions and forms the basis for examination of the atomic structure by X-ray crystallography. For good diffraction the goal of the crystallisation process is to produce well ordered crystals of high purity protein.

5.2.3.1.1 Basic X-ray diffraction instrument setup

X-ray diffraction is a key technology for analysis of the arrangements of atoms within a crystal. Since it is possible to form crystals composed of salts, metals, proteins, peptides and DNA, the technique has become invaluable in the structural biochemists armamentarium and provides fundamental insights into structure for many fields. The basic instrument setup is described in Figure 5.2-45. Essentially a crystal mounted on the goniometer is rotated as it is continuously bombarded with focused X-rays producing a diffraction pattern of spots picked up by a detector (known as reflections). By compiling these various two-dimensional images a three dimensional electron density model can be created. The data set which is built from many different images contains spots relating to the electron density calculated by Fourier transforming the diffraction intensities. The data is indexed (matching electron density variations to spots), merged and scaled (matching

relative strengths of the spots in various images) and combined to give the total electron density (phasing). To achieve these steps powerful computer programs are relied upon to obtain and refine the determined structural information combination with complementary chemical information. The resolution of the images obtained is critical to obtaining precise structural features of the protein. High resolution protein structures are common place in the PDB with resolutions at the sub-atomic level possible. Table 5.2-8 demonstrates the relationship between the resolution (\AA) and the features that can be obtained from diffraction data.

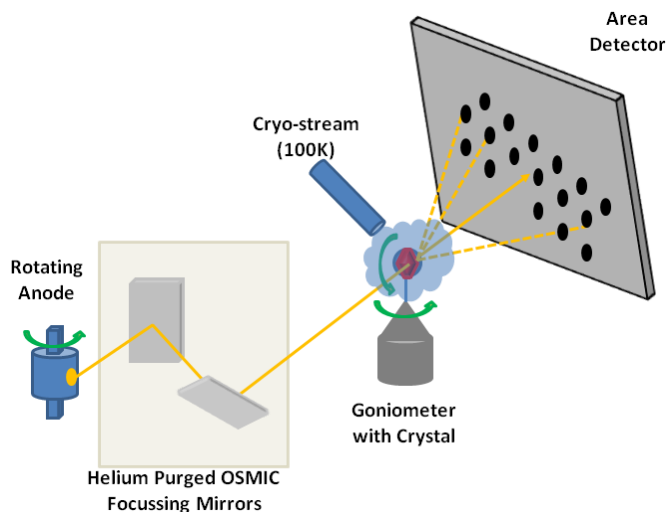


Figure 5.2-45: Instrument setup for collection of X-ray diffraction patterns

Rotating anode X-ray generator produces the primary X-ray beam (yellow line) which is focused onto the crystal mounted on the goniometer by focusing mirrors. The crystal is cooled by the cryo-stream to 100K. The focused beam strikes the cooled crystal and diffracts. The diffraction pattern is detected by an area detector. Green arrows represent rotational abilities of various components. Image was adapted from http://pruffle.mit.edu/atomiccontrol/education/xray/xray_diff.php

Table 5.2-8: Relationship between resolution of X-ray diffraction and the structural features obtained

Resolution (\AA)	Structural features observable on a good map
5.5	Overall shape of the molecule.
3.5	The main chain (ambiguous).
3.0	Partial resolution of side chains.
2.5	Resolution of side chains and plane of peptide bond.
1.5	Atoms located to $\pm 0.1\text{\AA}$.
0.77	Bond lengths.

Table taken from [299].

5.2.3.2 *Results*

5.2.3.2.1 Refinement of protein purity

Typically multistep purification protocols were not undertaken for scFv purification due to the fact that they were readily purified by IMAC. In the literature, protein purity required for the generation of crystal structures is reported from >90% to >98% by SDS-PAGE and so a very high purity is paramount. ScFv 180 purifications were typically of a purity >95% estimated by SDS-PAGE from IMAC (Figure 5.2-39). Accordingly, the scFv (180) was gel filtered using S75 10/30 column on the AKTA Explorer FPLC (GE Healthcare) to ensure that it was mono-dispersed, free from low molecular weight contaminants and further characterised as a single species by matrix-assisted laser-desorption/ionisation (MALDI) time of flight (TOF) mass spectrometry (MS). From the gel filtration chromatogram (Figure 5.2-46) it was seen that the protein, after IMAC purification and storage, contained a mixture of monomer and higher order aggregates. The necessity for the protein to be mono-dispersed and homogenous is critical for high quality crystal lattice formation. Despite storage for numerous days on ice at 4°C post gel filtration the monomeric protein did not revert to aggregated/dimeric forms (data not shown). This gel filtration step also allowed the protein to be buffer exchanged into 1X TBS (with 0.02% (w/v) NaN₃) as phosphate salt crystals from PBS would contaminate any crystal tray setup. Interestingly, in experiments to gauge the state of the protein purified from cytoplasmic versus periplasmic extractions (see appendix Figure 8.1-15 for scFv periplasmic purifications), it was observed that cytoplasmic extractions yielded predominantly dimers and higher order aggregates (data not shown) even in cell-lines such as Rosetta 2 gami that are designed to promote disulfide bond formation in the cytoplasm. The purified monomeric scFv was then analysed by MALDI-TOF MS confirming its purity and accurate determination of the protein molecular weight (28,545Da) as illustrated by the m/z plot in Figure 5.2-47. MALDI-TOF MS is a routine technique to identify proteins, a capability central to life sciences. The use of TOF rather than tandem TOF-TOF or other tandem detectors was the most suitable analysis method for determination of accurate mass in a high-throughput fashion [300]. Now that the protein satisfied the key requirements to generate reliable high quality crystals (homogenous, soluble, mono-dispersed and stable) it was concentrated to approximately 6mg/mL to take forward to coarse screening for crystallisation conditions.

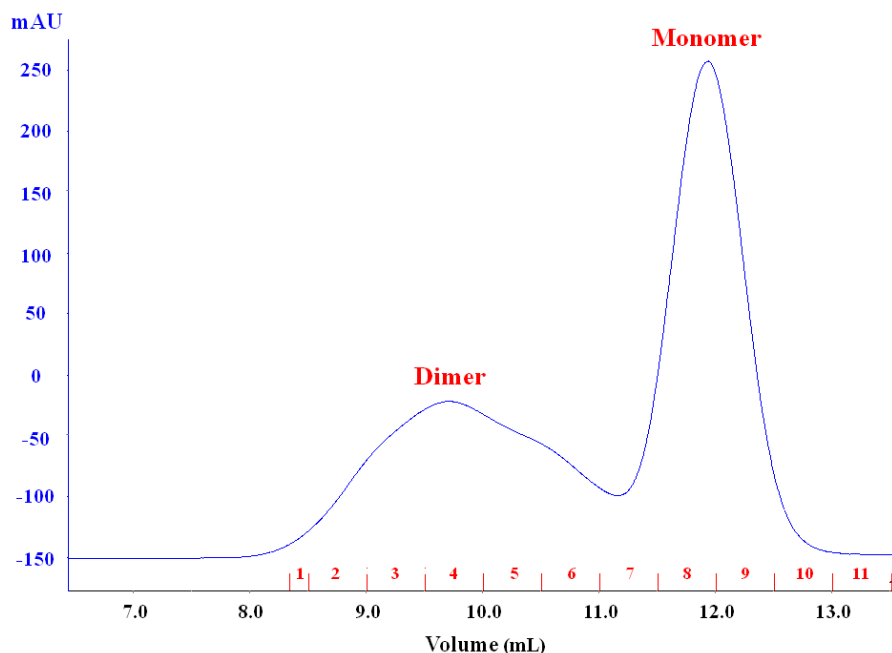


Figure 5.2-46: Gel filtration chromatogram for IMAC-purified scFv 180

Gel filtration profile of scFv 180 after IMAC purification. Protein peaks were observed at 8-11mL for dimer/aggregates and 11.5-13mL for monomeric scFv. Protein was monitored by $A_{280\text{nm}}$. The single monomeric fractions were then pooled and concentrated to approximately 6mg/mL.

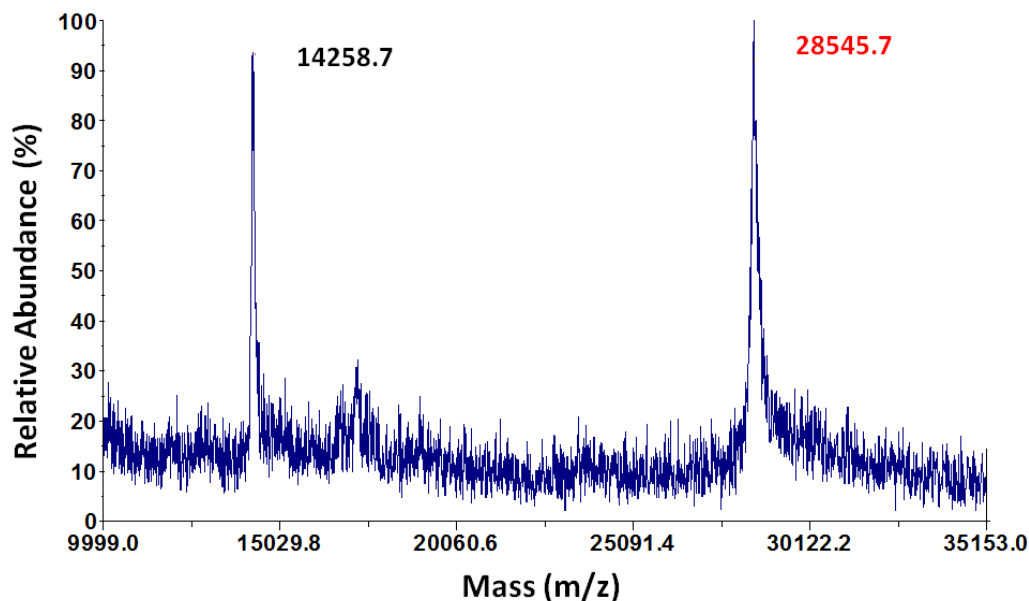


Figure 5.2-47: Mass and purity determination for scFv 180 by MALDI-TOF MS

Species determination was carried out using MALDI-TOF (courtesy of Monash University) to accurately determine the mass of the scFv species in the purified sample. IMAC and gel filtered protein (6mg/mL) in 1X TBS (0.02% (w/v) NaN_3) was used to prepare the spectrum in positive ionisation mode. The spectrum shows typically well resolved peaks representing the $[\text{M}+2\text{H}]^{2+}$ (half mass) and $[\text{M}+\text{H}]^{+1}$ (mass) of the sample. ScFv 180 was observed to be a single species with a mass of 28.54kDa.

5.2.3.2.2 Screening conditions for crystal formation

Manual trays were prepared by the hanging drop method and automated robotic trays by the sitting drop method, as illustrated in Figure 5.2-48. Vapour diffusion occurs when a drop composed of a mixture of sample and reagent is placed in vapour equilibration with a liquid reservoir of reagent (Figure 5.2-48). The lower reagent concentration in the drop causes water vapour to leave the drop to achieve equilibrium and eventually ends up in the reservoir. As water leaves the drop, the sample undergoes an increase in relative supersaturation and both the sample and reagent increase in concentration. Equilibration is reached when the reagent concentration in the drop is approximately the same as that in the reservoir [301]. Typically with this process the success rate is relatively low. Therefore, many conditions are screened and where changes occur, such as precipitation, they can be further altered by adjustment of protein concentrations or precipitant composition. There are a wide range of kits for different types of proteins/complexes to optimise crystallisation experiments. Hampton Research (HR) is the leading provider of these crystallisation screening kits (summarised in appendix, Table 8.1-2). Each kit provides a differing set of crystallants, buffer composition, pH, salts and other additives to comprehensively coarse screen for conditions to promote crystallisation of proteins.

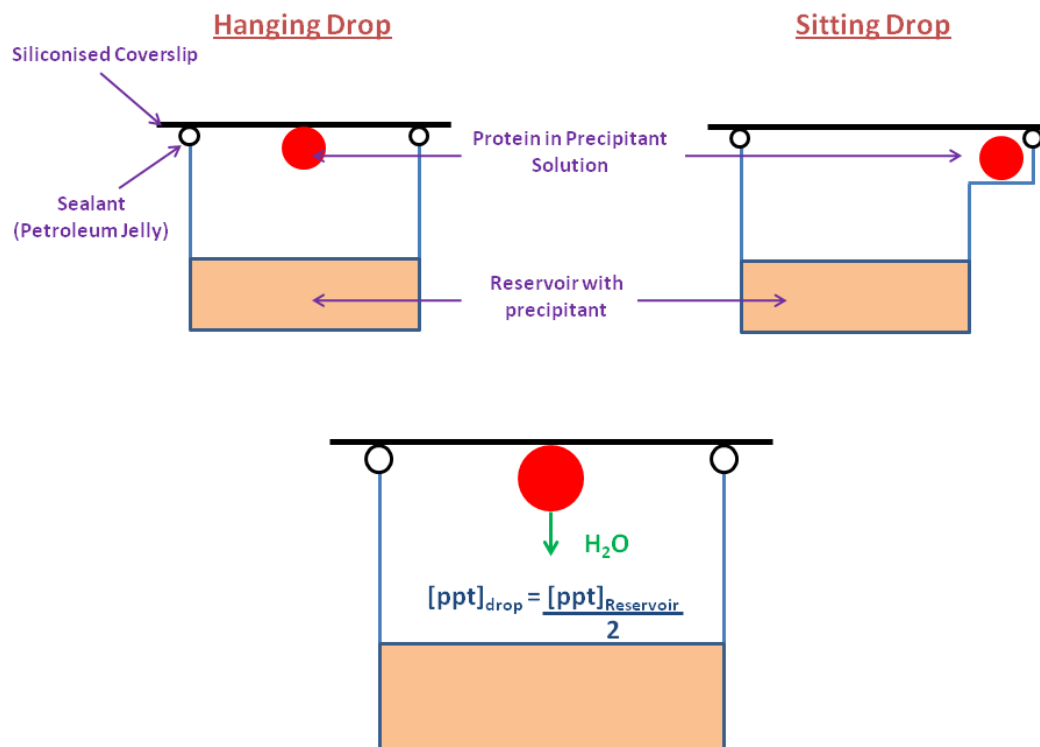


Figure 5.2-48: Drop methods for crystal screening

The hanging drop method involved mixing the antibody solution with precipitant and turning the cover slip over before sealing on the reservoir using petroleum jelly. The sitting drop method was carried out by the automated crystal system depositing 100nL drops of protein and precipitant onto a small well located to the side of the reservoir. Supersaturation occurs as water leaves the drop and the precipitant concentration ([ppt]) moves to equilibrium with the precipitant concentration in the reservoir as described by the equation (inset). This figure was adapted from [301].

5.2.3.2.2.1 Manual tray crystal screening and diffraction

Manual trays were setup in 24-well plates by the hanging drop method (Figure 5.2-48), as described in section 2.3.10.2.1. Each day the trays were manually inspected noting the changes that occurred for example; formation of precipitation, phase contrast and absence of change. After 17 days, a low density of crystals formed in the manual screen for scFv 180 in condition number 40 (0.1M Na-citrate pH 5.6, 20% (v/v) 2-propanol and 20% (w/v) PEG-4000). The crystals were imaged using a light microscope (Figure 5.2-49) and were typical of a protein crystal. However, only two crystals formed in the droplet which was likely to be attributed to the low scFv concentration (6mg/mL). With the protein that remained it was not possible to bring the protein concentration higher without the need to re-express and purify (time limits for the visit). However, fine screen trays were setup around the conditions found as described in section 2.3.10.3. The crystal was extracted from the drop and X-ray diffracted as described in section 2.3.10.4. Figure 5.2-50 shows the generated diffraction pattern collected. The dark spots are the diffraction pattern (or reflections) due to scattering of the X-rays that interact with the atoms in the protein crystal lattice. From this image, rotated through 90°, strong reflections were observed with weaker shadows in an irregular pattern that suggests a somewhat disordered lattice, overlapping second crystal or cracking of the crystal when placed at 100K without a cryo-protectant. In this case fine screening is required to improve a) the lattice order b) the crystal size/number and c) the resolution of the diffraction. The crystallisation conditions were fine screened by varying the pH of the buffer, the 2-propanol and the PEG-4000 percentages as outlined in the plate layout grid described in section 2.3.10.3 (Table 2.3-16). The trays were placed at 20°C and are currently awaiting crystal formation.

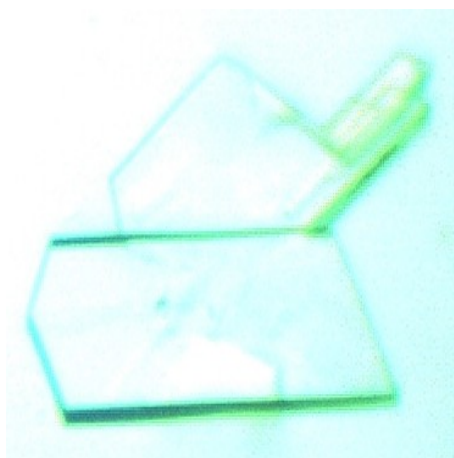


Figure 5.2-49: Formation of a crystal of scFv 180 in a manually prepared screen

The Sigma basic screen condition number 40 (0.1M Na-citrate pH 5.6, 20% (v/v) 2-propanol and 20% (w/v) PEG-4000) gave rise to the formation of the crystals, shown above, after 17 days incubation at 20°C. The two overlapping crystals were promising protein crystals and were allowed to grow further as spikes on the top right are typical of a growing protein crystal.

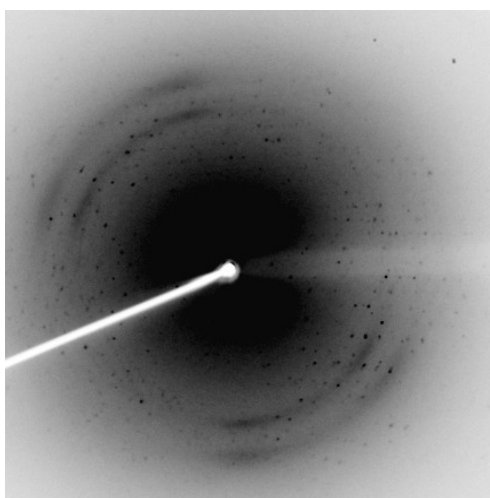


Figure 5.2-50: X-ray diffraction pattern of scFv 180 crystal from the manual tray

X-ray diffraction pattern obtained using the Rigaku *U-3HBR* rotating anode generator with helium purged *OSMIC* focusing mirrors as an X-ray source and the data are collected using an R-AXIS IV++ detector at Monash's X-ray diffraction laboratory. The diffraction pattern confirms the crystal was protein and was of a low resolution at approximately 3.5-4Å.

5.2.3.2.2.2 *Robotic (Crystalmation) crystal screening and diffraction*

Monash University houses an automated crystallography suite which was available to use during the collaborative visit maximising the limited amount of scFv by nano-dispensed spots. The automated suite consists of the Rigaku CrystalMation system which is a fully integrated platform for protein crystallisation. Robotic trays were setup in 96-well plates by the sitting drop method (Figure 5.2-48), as described in section 2.3.10.2.2.

After 3 days, a low density of crystals formed PEG/ION screen position B10 (0.2M Potassium formate and 20% (w/v) PEG-3350) as shown in Figure 5.2-51. The crystals were allowed to grow for a further 12 days which resulted in the formation of a second crystal and were diffracted as described in section 2.3.10.4. In the case of this crystal of 180 scFv the diffraction pattern was much more ordered and the quality of the lattice superior to the previous crystal. Again some smearing of the reflections was observed which was attributed to cracking of the crystal in the cryo-stream or the presence of the second crystal behind the primary one (twinning). In this case the resolution was approximately 3 Å. As for the previous crystal the conditions required modification to yield higher quality crystals and crucially more crystals to carry out numerous diffractions with cryopreservation.

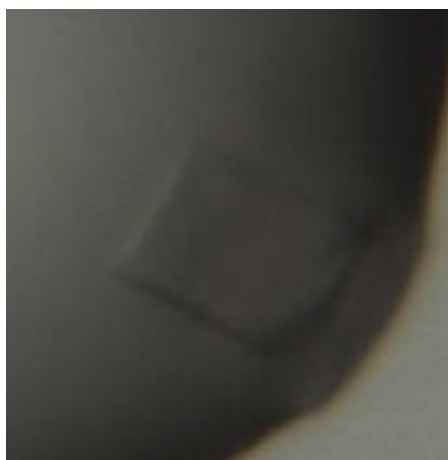


Figure 5.2-51: Formation of a crystal of scFv 180 in position B10 of PEG/ION screen

The PEG/ION condition B10 (0.2M Potassium formate and 20% (w/v) PEG-3350) gave rise to the formation of the crystals, shown above, after 3 days incubation at 20°C.

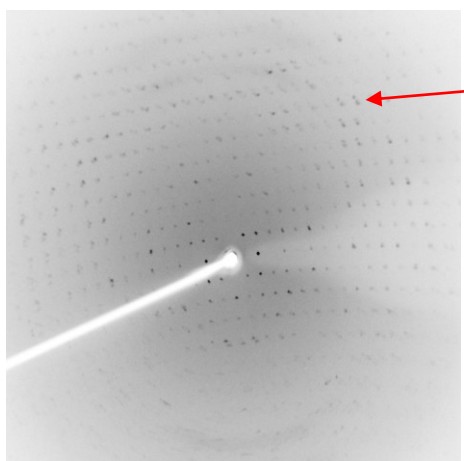


Figure 5.2-52: X-ray diffraction pattern of scFv 180 crystal from condition B10 of PEG/ION screen

X-ray diffraction pattern obtained using the Rigaku *U-3HBR* rotating anode generator with helium purged *OSMIC* focusing mirrors as an X-ray source and the data are collected using an R-AXIS IV++ detector at Monash's X-ray diffraction laboratory. The diffraction pattern confirms the crystal is protein and medium low resolution at approximately 3 Å. Again the slight shadow of the diffraction pattern (red arrow) is indicative of non-uniform lattice or cracking of the crystal

5.2.3.3 *Future work to determine the crystal structure of scFv*

The results outlined for scFv 180 demonstrate successful optimisation of the coarse conditions required to generate protein crystals during a four week period, facilitated by a collaborative visit to Monash University, Melbourne, Australia. In the case of scFv 180, two conditions were found in the coarse screening to support the formation of crystals. In both cases, the abundance of the formed crystals was low presumably due to low protein concentrations and a relatively slow supersaturation process. The 0.2M sodium formate with 20% (w/v) PEG-3350 crystal was the most promising crystal in terms of its ordered X-ray diffraction profile. However, further optimisation of the conditions for efficient crystal formation was required. In the case of the 0.1M Na-citrate pH 5.6, 20% (v/v) isopropanol with 20% (w/v) PEG-4000 crystal, which was larger in size, a less well ordered, but strong diffraction profile was observed under X-ray. In the case of this crystal conditions, at the time of leaving Monash, they were fine screened further and the trays are currently incubating.

The results generated represent a significant advance towards determination of the crystal structure of the scFv 180 and the skills acquired can now be used as a template to examine the other proteins constructs. The work is envisaged to form part of a grant proposal to return to Monash for a significantly longer period of time to investigate and further refine the crystals and to ascertain the conditions required for the remaining proteins.

5.3 Isolation of recombinant antibodies against epitope-3 of cTnI

Early in the lifetime of this work a previously prepared and panned avian scFv immune library was made available by Dr. Stephen Hearty and this library was developed with a cTnI protein-based immunisation protocol and panned against the whole protein molecule. Exhaustive mining of this library yielded a number of scFv-specific for the cTnI protein. As the body of work presented here focussed on particular epitopes crucial to the specificity of the envisaged cardiovascular risk test, initial studies characterised a subset of these scFv against the various epitope regions. This short section focuses on the isolation of the scFv '4G5' and its utility for incorporation into immunoassays as a 'tracer or probe' antibody.

5.3.1 Identification of anti-epitope 3 scFv from the screened library

From a high-throughput robotics-based screening of a scFv library from cTnI protein immunised chicken several clones were identified by IC₅₀ screening. This involved robotic titring of the clones (480) against cTnI (1µg/mL) to determine optimal lysate dilutions for competitive analysis. This was carried out on a custom built Tecan Evo Freedom robot and subsequently, the competitive analysis carried out as normal by the robotic system. A high-throughput Excel macro file was used to tabulate the data into an output of IC₅₀ to rank the clones (Figure 5.3-1). As an initial screen was carried out against the cTnI protein it provided no insight into epitope-specificity.

	Pos/Neg	>5ug/ml	1<X<5ug/ml	500<X<999ng/ml	100<X<499ng/ml	50<X<99ng/ml	5<X<49ng/ml	5000<X<499pg/ml	IC ₅₀	A0 value
A1	ok	—	1<X<5ug/ml	—	—	—	—	—	1.229	0.39
B1	NEGATIVE!	—	—	—	—	—	—	—	0.525	0.02
C1	ok	—	—	—	—	—	—	—	0.000	1.10
D1	NEGATIVE!	—	—	—	—	—	—	—	5.000	0.01
E1	NEGATIVE!	—	—	—	—	—	—	—	5.000	0.14
F1	NEGATIVE!	—	—	—	—	—	—	—	4.400	0.06
G1	NEGATIVE!	—	—	—	—	—	—	—	5.000	0.01
H1	NEGATIVE!	—	—	—	—	—	—	—	5.000	0.01
A2	ok	>5ug/ml	—	—	—	—	—	—	5.000	0.38
B2	ok	—	—	—	—	—	5<X<49ug/ml	—	0.014	0.30
C2	NEGATIVE!	—	—	—	—	—	—	—	0.070	0.05
D2	ok	—	1<X<5ug/ml	—	—	—	—	—	4.782	0.28
E2	NEGATIVE!	—	—	—	—	—	—	—	0.311	0.16
F2	ok	>5ug/ml	—	—	—	—	—	—	5.000	0.25
G2	NEGATIVE!	—	—	—	—	—	—	—	2.686	0.02
H2	ok	>5ug/ml	—	—	—	—	—	—	5.000	0.47
A3	NEGATIVE!	—	—	—	—	—	—	—	0.200	0.01
B3	ok	>5ug/ml	—	—	—	—	—	—	5.000	0.28
C3	NEGATIVE!	—	—	—	—	—	—	—	5.000	0.03
D3	NEGATIVE!	—	—	—	—	—	—	—	5.000	0.01
E3	NEGATIVE!	—	—	—	—	—	—	—	0.458	0.19
F3	ok	—	1<X<5ug/ml	—	—	—	—	—	2.000	0.28
G3	NEGATIVE!	—	—	—	—	—	—	—	5.000	0.00
H3	ok	>5ug/ml	—	—	—	—	—	—	5.000	0.24
A4	ok	—	—	500<X<999ng/ml	100<X<499ng/ml	—	—	—	0.695	0.22
B4	ok	—	—	—	—	—	—	—	0.499	0.21
C4	NEGATIVE!	—	—	—	—	—	—	—	5.000	0.03
D4	ok	—	—	—	—	—	—	—	0.000	0.50
E4	NEGATIVE!	—	—	—	—	—	—	—	5.000	0.09
F4	ok	—	1<X<5ug/ml	—	—	—	—	—	3.560	0.33
G4	NEGATIVE!	—	—	—	—	—	—	—	5.000	0.05
H4	ok	—	—	—	—	—	—	—	1.000	0.40
A5	NEGATIVE!	—	—	—	—	—	—	—	4.830	0.16
B5	ok	—	1<X<5ug/ml	—	—	—	—	—	2.819	0.38
C5	NEGATIVE!	—	—	—	—	—	—	—	3.450	0.19
D5	ok	>5ug/ml	—	—	—	—	—	—	5.000	0.31
E5	ok	—	—	—	—	50<X<99ng/ml	—	—	0.069	0.37
F5	NEGATIVE!	—	—	—	—	—	—	—	0.529	0.14
G5	ok	>5ug/ml	—	—	—	—	—	—	5.000	0.30
H5	ok	—	1<X<5ug/ml	—	—	—	—	—	4.126	0.25
A6	ok	>5ug/ml	—	—	—	—	—	—	5.000	0.30
B6	ok	>5ug/ml	—	—	—	—	—	—	5.000	0.32
C6	ok	>5ug/ml	—	—	—	—	—	—	5.000	0.31
D6	ok	—	1<X<5ug/ml	—	—	—	—	—	3.382	0.27
E6	NEGATIVE!	—	—	—	—	—	—	—	4.879	0.01
F6	ok	>5ug/ml	—	—	—	—	—	—	5.000	0.28
G6	ok	—	1<X<5ug/ml	—	—	—	—	—	4.769	0.28
H6	ok	—	—	—	—	—	—	—	5.000	0.42
A7	NEGATIVE!	—	—	—	—	—	—	—	0.456	0.19
B7	ok	—	—	—	—	50<X<99ng/ml	—	—	0.068	0.27
C7	ok	—	1<X<5ug/ml	—	—	—	—	—	4.801	0.30
D7	ok	>5ug/ml	—	—	—	—	—	—	5.000	0.33
E7	ok	—	1<X<5ug/ml	—	—	—	—	—	1.627	0.56
F7	ok	—	1<X<5ug/ml	—	—	—	—	—	4.818	0.56
G7	ok	—	—	—	100<X<499ng/ml	—	—	—	0.198	0.63
H7	NEGATIVE!	—	—	—	—	—	—	—	0.057	0.01
A8	ok	>5ug/ml	—	—	—	—	—	—	5.000	0.30
B8	ok	>5ug/ml	—	—	—	—	—	—	5.000	0.29
C8	ok	>5ug/ml	—	—	—	—	—	—	5.000	0.29
D8	NEGATIVE!	—	—	—	—	—	—	—	0.000	0.11
E8	ok	—	—	500<X<999ng/ml	—	—	—	—	0.710	0.43
F8	ok	>5ug/ml	—	—	—	—	—	—	5.000	0.27
G8	ok	>5ug/ml	—	—	—	—	—	—	5.000	0.29
H8	NEGATIVE!	—	—	—	—	—	—	—	0.031	0.04
A9	NEGATIVE!	—	—	—	—	—	—	—	5.000	0.04
B9	ok	>5ug/ml	—	—	—	—	—	—	5.000	0.44
C9	ok	—	—	—	—	—	—	—	5.000	0.57
D9	ok	—	1<X<5ug/ml	—	—	—	—	—	4.065	0.37
E9	ok	—	—	—	—	—	—	—	0.000	0.43
F9	ok	—	—	—	—	—	—	—	0.000	0.54
G9	ok	—	—	500<X<999ng/ml	—	—	—	—	0.514	0.49
H9	ok	>5ug/ml	—	—	—	—	—	—	5.000	0.62
A10	ok	—	1<X<5ug/ml	—	—	—	—	—	3.719	0.28
B10	ok	>5ug/ml	—	—	—	—	—	—	5.000	0.53
C10	ok	—	—	—	—	—	5<X<49ug/ml	—	0.046	0.25
D10	NEGATIVE!	—	—	—	—	—	—	—	4.126	0.04
E10	NEGATIVE!	—	—	—	—	—	—	—	4.999	0.16
F10	ok	>5ug/ml	—	—	—	—	—	—	5.000	0.48
G10	ok	—	1<X<5ug/ml	—	—	—	—	—	4.938	0.33
H10	ok	>5ug/ml	—	—	—	—	—	—	5.000	0.39
A11	ok	>5ug/ml	—	—	—	—	—	—	5.000	0.35
B11	ok	>5ug/ml	—	—	—	—	—	—	5.000	0.21
C11	ok	>5ug/ml	—	—	—	—	—	—	5.000	0.24
D11	ok	>5ug/ml	—	—	—	—	—	—	5.000	0.35
E11	ok	>5ug/ml	—	—	—	—	—	—	5.000	0.35
F11	ok	—	—	—	—	50<X<99ng/ml	—	—	0.066	0.39
G11	ok	—	—	—	—	—	5<X<49ug/ml	—	0.049	0.47
H11	ok	—	—	500<X<999ng/ml	—	—	—	—	0.542	0.50
A12	NEGATIVE!	—	—	—	100<X<499ng/ml	—	—	—	5.000	0.03
B12	ok	—	—	—	—	—	—	—	0.107	0.47
C12	NEGATIVE!	—	—	—	—	—	—	—	5.000	0.11
D12	ok	>5ug/ml	—	—	—	—	—	—	5.000	0.53
E12	ok	>5ug/ml	—	—	—	—	—	—	5.000	0.50
F12	ok	>5ug/ml	—	—	—	—	—	—	5.000	0.63
G12	ok	—	—	—	—	—	5<X<49ug/ml	—	0.010	0.58
H12	ok	>5ug/ml	—	—	—	—	—	—	5.000	0.62

Lower IC₅₀ = more sensitive antibody

Figure 5.3-1: Customised macro for anti-epitope-3 scFv ranking experiments

This is an example of a one plate competitive readout from the macro, written by Dr. Paul Leonard. Clones were labelled negative if A0 was < 0.2 and the IC₅₀ values for the clones grouped (central columns) and the actual IC₅₀ value given on the RHS.

The issue of specificity was addressed by employing the custom-designed biotinylated peptides to mine a small subset of the screened library for epitope-specific antibodies. In a direct binding ELISA, the supernatants were diluted and applied in series to wells coated with the peptides. Figure 5.3-2 shows that the clones were either cTnI protein-specific outside of the epitope regions targeted or they were epitope-3-specific. No clones were found to react to either epitopes 1 or 2. Indeed exhaustive mining of this library by others, in a number of formats on the Biacore™ 4000 (when it was acquired), failed to yield any epitope-1 or 2-specific antibodies (data not shown). None-the-less successful identification of an anti-epitope-3 scFv (4G5) was achieved in this analysis. The epitope has utility as a tracer or reporter targeting epitope for specific assay, employing the N-terminal-specific antibodies as capture reagents.

To further analyse the scFv it was compared in an inhibition ELISA format (section 2.3.6.2) in comparison the Hytest equivalent antibody 16A11. Figure 5.3-3 demonstrates the comparable performance in the inhibition format for the isolated scFv 4G5 and for the Hytest mAb 16A11.

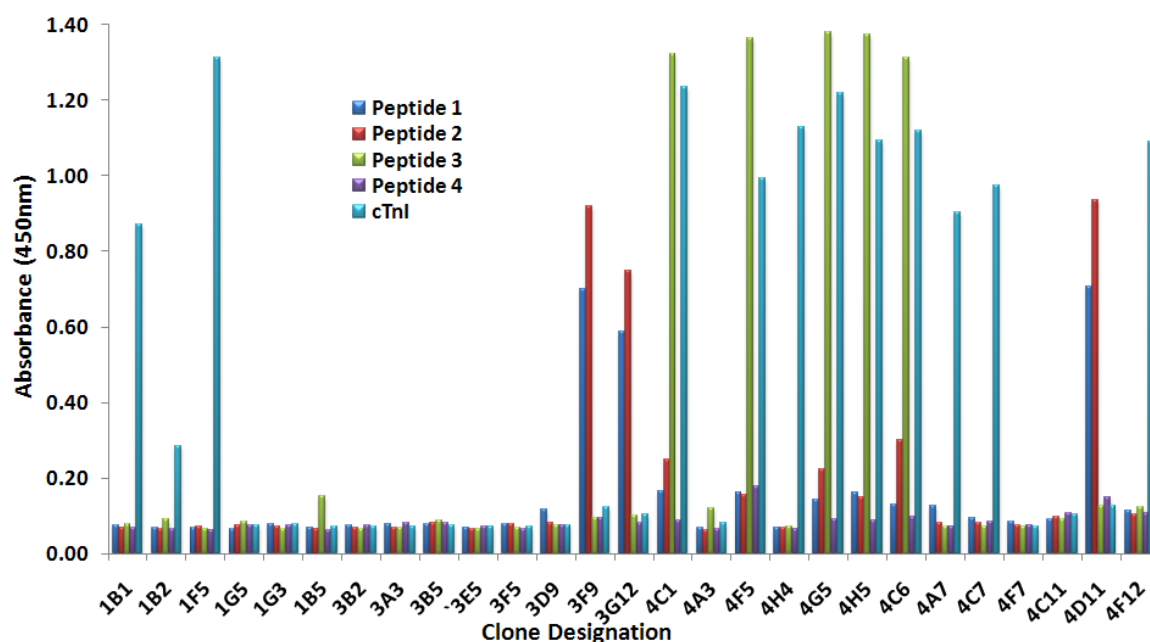


Figure 5.3-2: Epitope-specificity mapping of the scFv isolated from a cTnI protein-based avian library
 Twenty seven clones were analysed against the synthetic biotinylated peptides in a direct binding ELISA format using the neutrAvidin. Each scFv lysate was assayed against all four peptide regions and cTnI. As was observed from the graph a number of false positives were carried through the initial robotic screening, likely caused by suboptimal setup. Additionally, 3 clones reacted with peptide 1 and 2 without reacting to cTnI (3F9, 3G12 and 4D11). As expected quite a few clones reacted to cTnI, but not at the specific epitopes (1B1, 1B2 1F5, 4H4, 4A7, 4C7 and 4F12). A significant number of epitope-3-specific scFv were identified from the analysis (4C1, 4F5, 4G5, 4H5, 4C6).

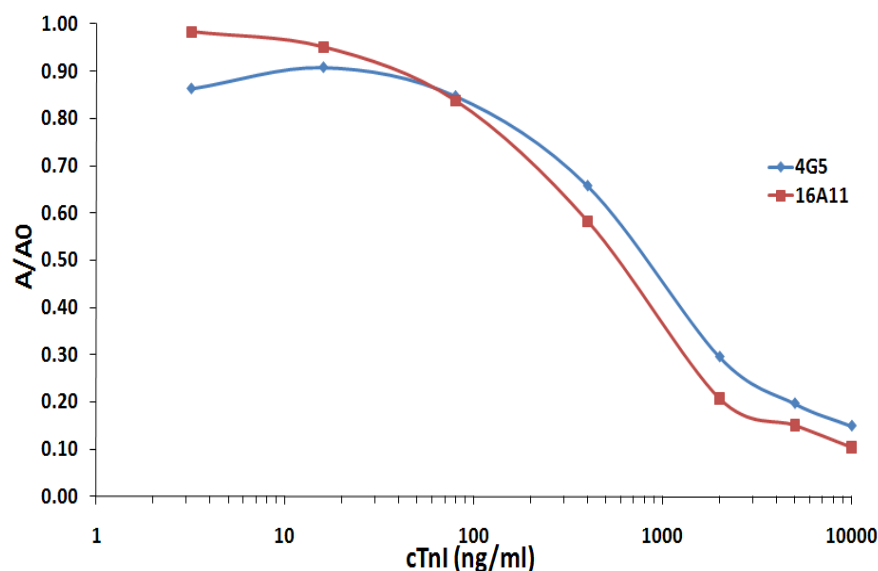


Figure 5.3-3: Inhibition analysis of identified anti-epitope-3-specific clone 4G5
 Comparison of clone 4G5 selected from the immunised library and the equivalent commercial standard antibody 16A11 HRP-labelled mAb. Both clones behave comparably with IC_{50} values approximated at 800ng/mL for 4G5 and 600ng/mL for Hytest 16A11.

5.3.2 Purification of anti-epitope-3 scFv from bacterial culture

From the derived sequence of 4G5 (see appendix Figure 8.1-14) the biochemical properties (Table 5.3-1) were estimated using the PROTEIN CALCULATOR v3.3 [296].

Table 5.3-1: Biochemical properties of the anti-epitope-3 scFv

	4G5
Molecular Weight (kDa)	28.16
Number of Amino Acids	275
Estimated pI	7.12
Charge at pH7.00	0.4
Extinction Coefficient at 280nm ($M^{-1} \text{ cm}^{-1}$)	45450

Purification of the scFv from bacterial expression was carried out (section 2.3.1.9) on a number of occasions, but continuously gave poor yields of functional antibody from IMAC purifications. SDS-PAGE and WB analysis (section 2.3.1.11 and 2.3.1.12) of the purification fractions collected showed successful purification of scFv (data not shown). However, a significant proportion was not retained on the column despite repeated applications of the flow through to the IMAC resin. Typically from a 400mL induced culture only 0.3mg of pure scFv could be obtained (0.75 μ g/mL). Despite numerous expression optimisation experiments and purification modifications the yield of protein remained prohibitively low. The possibility of re-formatting the scFv to scAb (section 2.3.11) was envisaged to help improve the levels of expression by the addition of *skp* chaperone (see appendix, Figure 8.1-7) as yields of scFv were previously shown to be improved by addition of a constant domain [206].

5.4 Chapter conclusions

A synthetic epitope-based immunisation strategy successfully yielded a strong chicken response-specific for the native cTnI protein. A large scFv library was constructed and subjected to stringent selection based on presentation of the cTnI protein. This unique, defined presentation strategy asked several distinct questions of the scFv library i) to bind to a particular epitope of cTnI and ii) to do so in the presence of a second bound antibody. The bio-panned population was screened in a HT-fashion applying percentage left analysis with insights into expression levels in a single run. This data was combined with a novel differential cTnI concentration sandwich assay which provided assessment of each of the clones individual sensitivity to lower cTnI concentrations. Ultimately, the stringently bio-panned and rigorously screened library yielded a single ‘jackpot’ antibody sequence. The WT antibody (scFv 180) was immediately mutated by a conservative light chain shuffle and subjected to in-solution-based bio-panning to mine for higher affinity scFvs. The mutant clones were screened in truly HT-manner assessing kinetic parameters (k_a and k_d) and ranking the stability of the binding events by percentage left analysis at all times in direct comparison to the WT antibody. This information combined with ‘2 over 2’ and full kinetic evaluation led to the isolation of several very high-affinity clones which were superior to the WT in side-by-side analyses. The superior performance of the MT scFvs was further confirmed by inhibition profiling and assignment of definitive affinity values (K_D) to the WT (99.2pM) and selected MT (72.4pM) using the ‘in-house’ recombinantly expressed and purified FABP-P1&2 fusion protein.

In silico modelling sought to determine the structural reasons behind the higher affinity and proven increased thermostability between the WT and selected MT scFvs. These improved properties were not attributed to changes in the protein structure or introduction of stabilising hydrogen bonds, but by subtle modification of protein charge and an increase in the bulk of the amino acids. The nature of these structural differences was of considerable interest and the investigation into the crystal structures of the protein constructs was an exciting avenue to explain the improved cTnI-binding profiles. Despite the crystal structure studies being in their infancy, the fundamental basis behind the structure of avian antibodies, in particular the WT and MT, have the potential to add significantly to our collective knowledge of basic structural biology.

An existing library constructed from a chicken sensitised with the whole cTnI protein was assessed for epitope-specificity using custom designed biotinylated peptides. The spread of epitope-specificity demonstrated in this screening highlighted the challenges to generating epitope-specific antibodies from whole protein-based immunisation regimes. The immunodominance of epitope-3 was apparent and led to poor epitope reactivity for the N-terminal epitopes-1 and -2. The recalcitrance of these crucial epitopes represented a significant challenge to the generation of highly-specific, high-affinity antibodies and these results formed the basis of the rationale behind synthetic epitope-based immunisation protocols. Anti-epitope-3 scFv were successfully isolated and a single clone (4G5) evaluated in comparison to the commercial equivalent. Issues surrounding the purification of the scFv were investigated as the yields were prohibitively low. This was envisaged to be significantly augmented by domain reformatting experiments introducing the chicken constant domain (section 6.2.2).

Demonstrated throughout the generation and isolation of recombinant antibodies was the flexibility of this type of antibody technology. In a relatively small time scale a scFv library was constructed from an avian repertoire of modest serum titre, rigorously bio-panned and immediately taken forward into a mutagenesis strategy to further refine the affinity where one well equalled one antibody. The success of the two bio-panning campaigns for anti-epitope-1 scFv development further validates the synthetic epitope methodology of antibody generation. The successful application of recombinant antibody technology here further supports the decision to move away from monoclonal antibody generation hybridoma technology, albeit a decision forced by the differential responses to cTnI in chicken and mouse-based peptide immunisations. Critical to the success of the subsequent screening campaigns was the rational, well thought-out bio-panning experiments tailored to select for the most optimal antibody pairings for cTnI-diagnostic applications. The selected antibodies exemplify the most desirable outcome from the selection campaigns. The ability to access these high-value and high-affinity reagents was supported by the capability to exhaustively mine large numbers of clones in a HT, assay-relevant manner. The availability of multiplexed, highly-parallel processing power of the Biacore™ 4000 instrument significantly contributed to finding these antibodies. During the screening campaign, multi-parameter data was acquired which was most notably highlighted in the mutant screening campaign.

Chapter 6: Recombinant antibodies – assay development: benefits and pitfalls

6.1 Foreword

Some key parameters exist for the successful exploitation of antibodies in POC-based applications. These include sensitivity, selectivity, stability, immobilisation (i.e. orientation on the surface), labelling and antibody size (impacts on the density of the bio-layer of the POCT test). Recombinant antibodies are an attractive technology to optimise these factors, but chemical modification of scFv fragments can limit their broader utilisation. Some modifications, such as the SNAP-tag offer a methodology to control the site and stoichiometry of modification [302]. Genetic modification facilitates improvements in selectivity, stability, size (sections 5.1.3 and 5.1.4) and, in addition, such novel antibody fragments can aid effective immobilisation [200]. High-throughput screening (section 5.1.10) and display libraries facilitate improvements in sensitivity due to the ability to screen much larger recombinant antibody libraries (Section 5.1.5). The use of coupling chemistries and genetic insertion of tags for immobilisation (section 5.1.9) are valuable in assisting the orientation and immobilisation of such antibodies. The ability to alter properties such as the size and affinity of antibodies has led to the development of novel antibodies which have potential uses in diagnostics (see Table 5.1-3). Commercially available monoclonal antibody-based POC-tests exist, for example in the diagnosis of cardiovascular disease, and include: Abbott's i-STAT® (cTnI) [303], Roche's CARDIAC proBNP assay [304] and those listed in Table 1.3-3. The area of POC-testing for cTnI monitoring is dominated by the use of monoclonal and polyclonal antibodies with no commercially available, approved recombinant examples available. An article published by Ylikotila and co-workers highlights the utility of recombinant Fab fragments, derived from the Hytest® catalogue of mouse monoclonal antibodies, notably for the ability to site-specifically label the fragments [305]. The specificity, and to a large degree the sensitivity, of all these assays is dictated by the biorecognition element [18, 306] and hence, the ability to develop more sensitive and robust systems is reliant on the modification of antibodies to improve these attributes. The capacity to enhance recombinant antibodies with respect to their selection, modification and subsequent applications in biosensors is of critical importance.

6.2 Results

6.2.1 Comparison of wild-type, mutant and Hytest antibodies

The final assessment of the purified scFv was carried out in a ‘side-by-side’ analysis with the Hytest anti-epitope one antibody (19C7) by inhibition analysis (section 2.3.11). All three proteins were titred and optimal concentrations for the inhibition assay identified (Hytest: 1 in 4,000; scFv 180: 1 in 2,000 and scFv 2B12: 1 in 60,000). A serially diluted (doubling) concentration range of cTnI (10,000ng/mL → 0.019ng/mL) was utilised to compare the clones by IC₅₀. The analysis was carried out in duplicate and with three independently prepared antibody and inhibitor preparations. Figure 6.2-1 shows the dramatic superiority of the scFv in this assay format compared to the Hytest standard. The mean IC₅₀ values for the WT and MT clones were 3.2 and 9.0-fold improved, respectively, compared to the mAb. The very conservative light chain shuffle, and the subsequently introduced mutations, led to a 2.7-fold improvement in assay performance between the WT and MT scFv. In addition, the proteins were easily purified in sufficient quantity and purity for analysis. The highly-specific, highly-sensitive reagents generated represent a significant step towards improved cTnI diagnostics and lend themselves readily to incorporation into much higher sensitivity cTnI risk determination platforms. To realise this potential application the limitations of the use of small fragments come into play, for example immobilisation leading to antibody denaturation and labelling of scFv causing loss of binding or blocking the compatible pair interaction. The latter was a phenomenon seen with the amine-coupling of fluorescent dyes to scFv 2B12. The antibody retained its reactivity for cTnI, but the sandwich assay using the mAb 20B3 was compromised. To address these issues reformatting of the scFv was an attractive methodology to increase the molecular surface of the molecule and facilitate site-specific functionalisation.

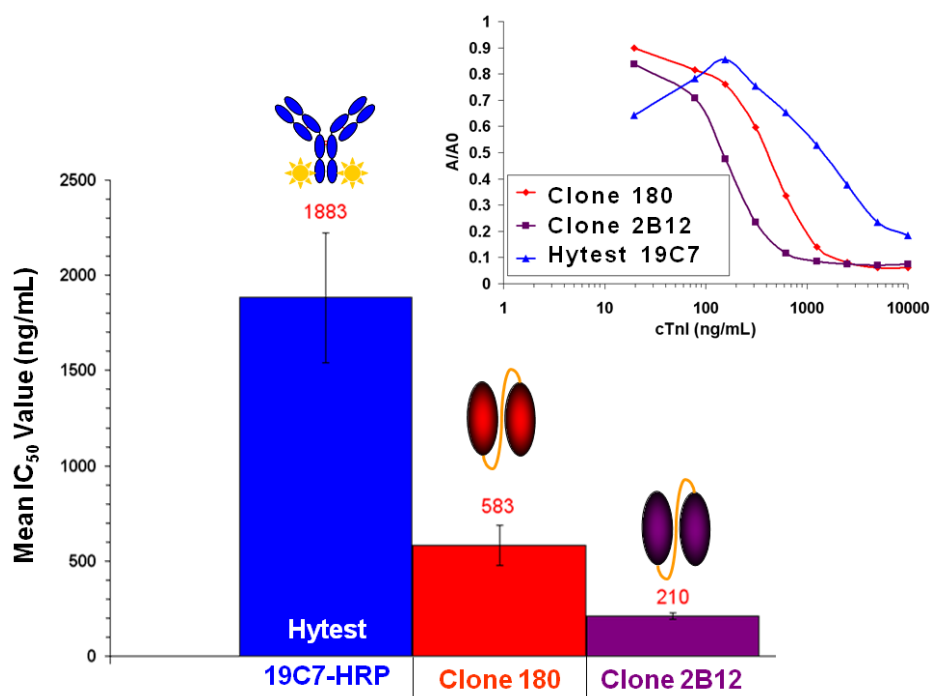


Figure 6.2-1: Comparison of wild-type and mutant scFv to Hytest anti-epitope-1 antibody

IC₅₀ value comparison of WT, MT and commercial antibodies. IC₅₀ values were obtained from three independent analyses (in duplicate) of an optimised inhibition ELISA (inset). Average IC₅₀ values were plotted on a bar chart with standard deviations applied. Hytest mAb (19C7) had a mean IC₅₀ of 1883ng/mL, the WT scFv 180 an IC₅₀ of 583ng/mL and the MT scFv 2B12 an IC₅₀ of 210ng/mL. The analysis shows the clear superiority of the recombinant antibodies generated in the course of this work. The MT scFv shows additional improvement over the WT.

6.2.2 Reformatting recombinant antibodies

Modification of the scFv format to improve potential application in a diagnostic setting was undertaken. Introduction of the C_λ domain from chicken cDNA was of interest to facilitate improved stability and immobilisation or orientation and selective labelling *via* the cysteine residue (Figure 6.2-2). Labelling experiments using commercially available amine coupling kits resulted in a steric hindrance for scFv binding to the antigen in a sandwich assay format (results not shown). With all the substantial effort to develop compatible assay pairings this presented a significant challenge. The ability to specifically label, using the reactive cysteine residue incorporated into the scAb format (Figure 6.2-2), offered a selective method to position the labelling site away from the binding site of the antibody.

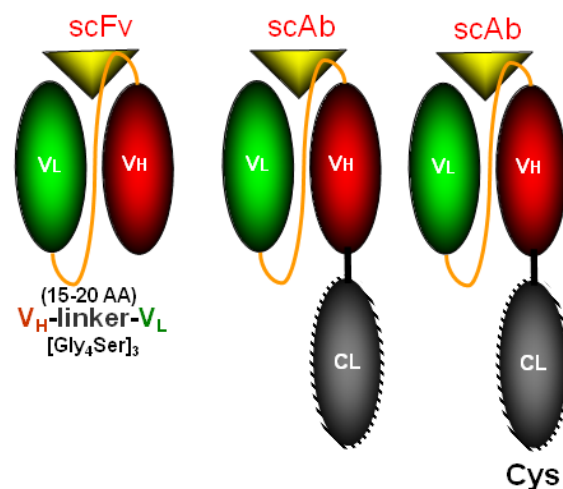


Figure 6.2-2: Reformatting scFv to include chicken constant light domains

Reformatting of the scFv to the scAb format. An additional chicken constant light (CL) domain was added to the V_H of the scFv (V_L-V_H format) by cloning the scFv into the pMopac16 vector with the HuC_κ replaced with chicken C_λ. The co-expression of the periplasmic chaperone *skp* on the pMopac16 vector (Figure 8.1-7) enhanced expression of most clones.

The scFvs 2B12 and 4G5 were reformatted to scAb and scAb-cys as a result of the findings above. The first step to convert the scFv to scAb was switching of the pComb3x *Sfi*I sites to a pMopacC_λ compatible restriction site pair. This was carried out by PCR amplification using primers to ‘switch’ the restriction sites (Table 2.3-18). Figure 6.2-3 shows the successfully amplified PCR products for scFv 2B12 and 4G5 from their pComb3x vectors. The purified products were digested, ligated into the pMopacC_λ vector and transformed as described in sections 2.3.12.1 and 2.3.1.4.

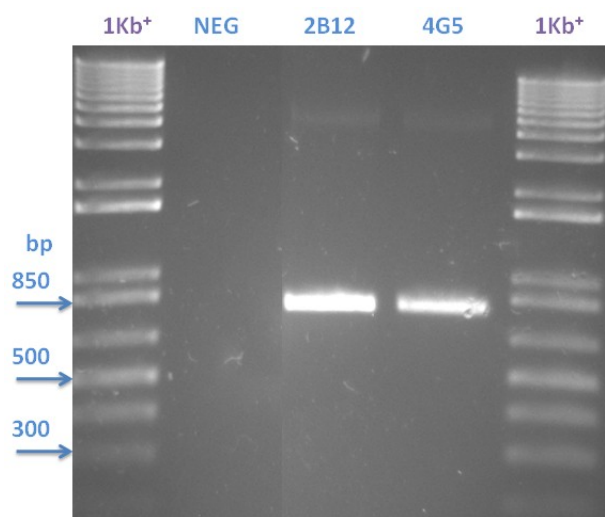


Figure 6.2-3: PCR modification of SfiI sites in 2B12 and 4G5 scFv

Resolution of PCR amplifications from purified plasmid on a 2% (w/v) agarose gel. Discrete bands representing the modified SfiI scFv inserts were observed at approximately 800bp for 2B12 and 4G5. The DNA size was approximated by comparison to 1Kb⁺ DNA ladder. A negative reaction (NEG) ensured no contamination of the reaction components.

Single colonies were isolated for both the scAb constructs and expressed in small-scale to identify functionally active protein expression by ELISA and SDS-PAGE/WB (data not shown). Large-scale expression was undertaken and the protein lysed from *E. coli* cells as described in section 2.3.1.7. The proteins were purified as per the generic protocol in section 2.3.1.9 using the PBS-based buffers prepared as outlined in section 2.1.4.6.2. Figure 6.2-4 shows two significant results. The 2B12_scAb expressed and purified extremely efficiently which was due to the presence of the *SKP* chaperone on the vector. In excess of 12mg of protein was purified from a single 400mL overnight induced culture compared to ~3mg in the same culture volume for the scFv format. The second dramatic result is the comparably sub-optimal expression of the 4G5_scAb construct. Under the same culture conditions it failed to express well (see Figure 6.2-4; FL lane in the WB) and led to very low protein purification yields (comparable to those in scFv format). For comparison purposes the 2B12_scAb-cys was expressed and the purified protein is shown in Figure 6.2-5, illustrating a dramatic decrease in protein expression as can be expected due to the presence of a free cysteine. However, the protein can still be purified better than the 4G5_scAb. Examination of the hydrophobicity plot and amino acid sequence for 4G5 (see appendix Figure 8.1-14) does not reveal any obvious reasons for its low expression.

Attempts to optimise the expression of 4G5_scAb like 4G5 scFv failed to increase the yield of purified protein (data not shown). The issue of rare codon usage was thought to contribute to the sub-optimal expression of the scFv and the scAb formats for 4G5. This was investigated by analysis of the DNA sequence. The 2B12 scFv was found to contain 15 rare codons with 4G5 containing only 12, by comparison. This suggests that the rare codon usage was present, but did not affect the 2B12 scFv. Introduction of the avian C_λ introduced an additional 6 rare codons for *E. coli*, but did not seem to effect the 2B12 construct as dramatically as the 4G5 construct. To overcome any potential limitations of *E. coli* rare codon usage for 4G5 it was transformed into Rosetta2 cells for analysis of expression due to supply of rare codon tRNA by the cell. In this case expression could not be dramatically improved. It may be useful to clone this scFv into a dedicated expression vector, such as pET26b, to tightly control the expression as 4G5 may prove to be toxic to the cells or unstable under the control of the leaky *lac* operon that is present on the pComb3x and pMoPac vectors.

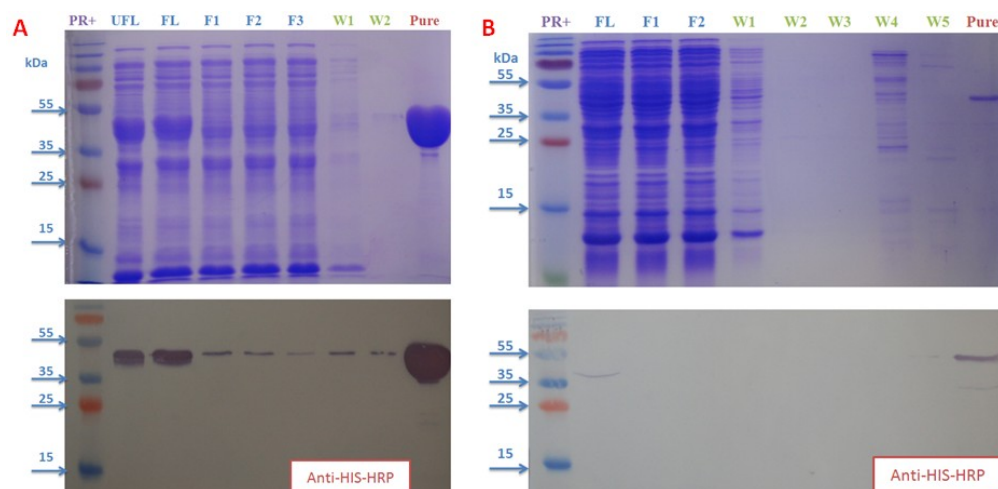


Figure 6.2-4: SDS-PAGE and Western blotting of scAb purification steps

The fractions from each stage of IMAC purification were analysed by SDS-PAGE (top) and WB (bottom). The lanes are labelled as follows; PR⁺: protein ruler, UFL: unfiltered lysate, FL: filtered lysate, F1-3: flow-through, W1-5: wash-steps and pure protein. The WB's were probed with an anti-HIS HRP-labelled antibody.

- The 2B12_scAb protein was purified very successfully as confirmed by the presence of a very large band in the 'pure' lane. When probed with the anti-HIS HRP-labelled antibody in the WB, the protein was seen to express extremely well (UFL lane), was retained on the IMAC resin (F1-3) and little was lost during washing (W1-2).
- The 4G5_scAb, by comparison, purified poorly. This was attributed to low expression levels of the protein as demonstrated by the weak band in the 'FL' lane of the WB.

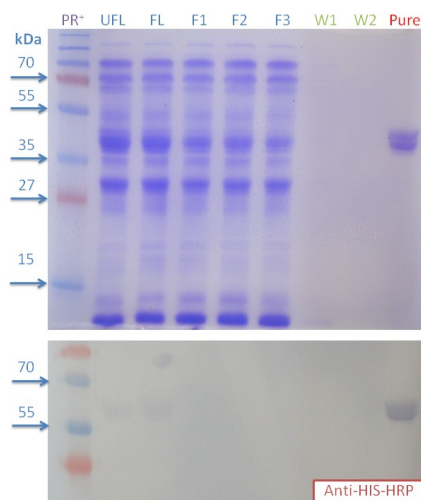


Figure 6.2-5: SDS-PAGE and Western blotting of 2B12_scAb-cys purification steps

The fractions from each stage of IMAC purification were analysed by SDS-PAGE (top) and WB (bottom). The lanes are labelled as follows; PR⁺: protein ruler, UFL: unfiltered lysate, FL: filtered lysate, F1-3: flow-through, W1-5: wash steps and pure protein. The WB was probed with an anti-HIS HRP-labelled antibody. The presence of the free cysteine on the scAb_cys construct resulted in diminished expression. However, the protein was purified in amounts sufficient for characterisation and assay development.

6.2.3 Initial development of plate-based assays

The optimal assay pairings were initially investigated using the 20B3 mAb as the capture reagent. In this case an anti-HA HRP- or anti-HA Cy5-labelled secondary antibodies were employed to remove the need to directly label the scFv format by virtue of targeting the HA-tag. The tests were carried out to assess greatest cTnI sensitivity achievable using the possible pairings available. The available antibodies were paired as follows:

20B3mAb with 2B12 scFv

20B3mAb with 4G5 scFv

20B3mAb with cTnI-specific scFv

Figure 6.2-6 illustrates suboptimal assay sensitivity where the mAb capture was postulated as a potential weakness in developing a highly-sensitive assay format. The high-affinity of the 2B12 scFv made it a very attractive alternative to mAb20B3 as a capture reagent. With its conversion to scAb format it was possible to capture cTnI and probe the available reporter scFv (4G5 or cTnI-specific scFv). From the observed performance of the cTnI-specific scFv (Dr. B. Vijayalakshmi Ayyar.) it was decided to combine it with the 2B12_scAb in a demonstration fluorescent-linked immunosorbent assay (FLISA). Figure 6.2-7 shows the dramatic improvement in sensitivity using the fluorescently labelled anti-HA-Cy5 (Rockland Labs.) and the scAb in a sandwich configuration with the undefined epitope cTnI-specific scFv. This non-optimised assay can detect cTnI down to ~50-100ng/mL. The success of the FLISA was anticipated to be improved further by optimisation of the plate-based assay and use of anti-HA IR®800-labelled antibodies to facilitate *in serum* detection. However, the development of assays was compromised by batch to batch variability in antigen quality.

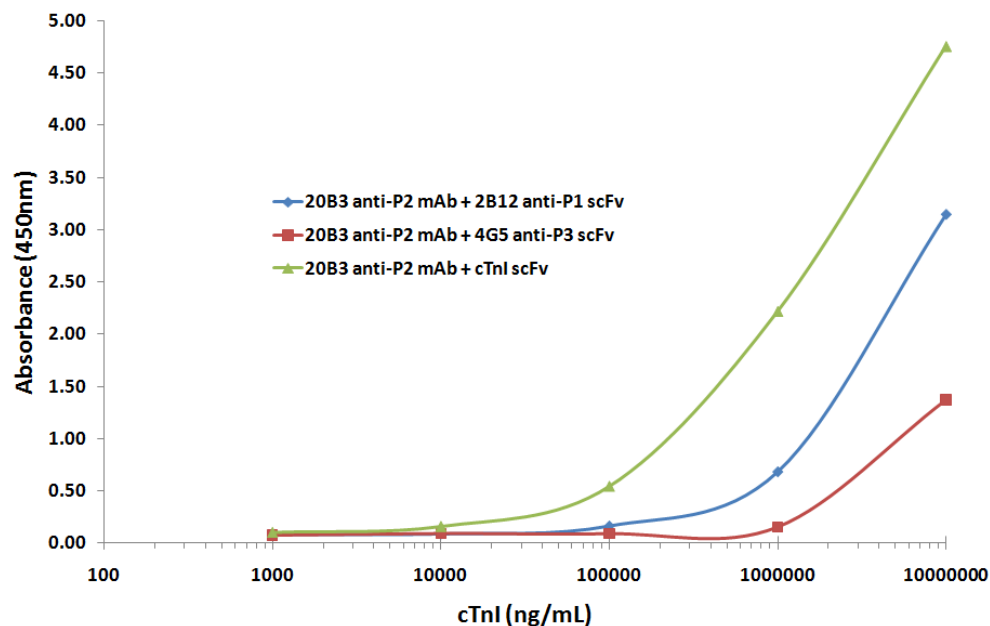


Figure 6.2-6: Optimisation of capture and reporter reagent combinations for a cTnI sandwich assay

20B3 capture and various scFv reporter combinations were assayed to determine the optimal pairing for development of a sensitive sandwich assay. cTnI was captured over a large concentration range and the detected with anti-cTnI-epitope scFv 4G5 (epitope-3) and 2B12 (epitope-1) and the anti-cTnI-specific scFv (undefined epitope). The scFv were detected using an anti-HA HRP-labelled secondary antibody.

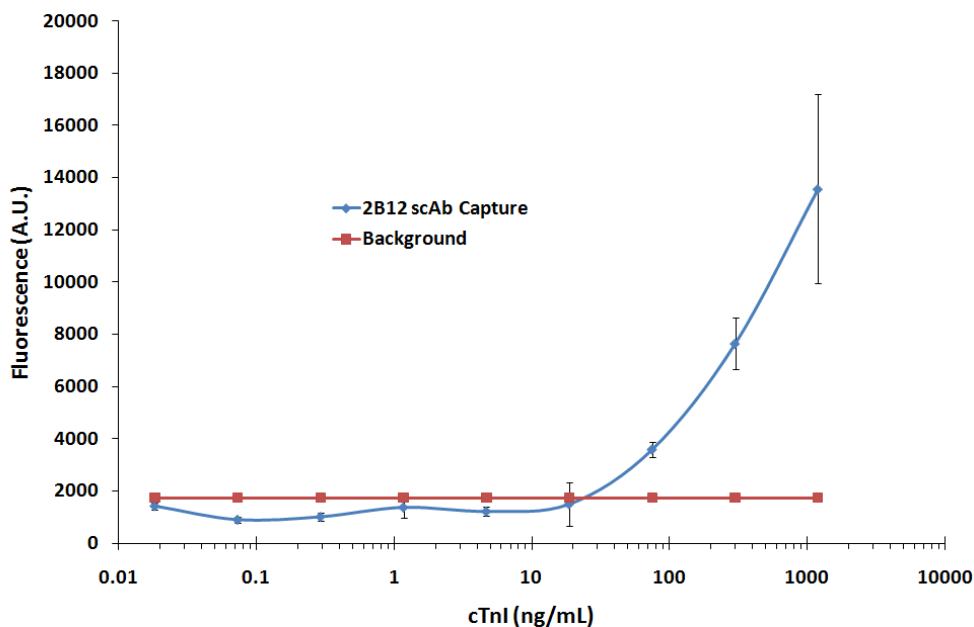


Figure 6.2-7: Demonstration FLISA for a cTnI sandwich assay

Reformatting the 2B12 scFv to scAb facilitated direct immobilisation of the high-affinity anti-epitope-1 antibody to the surface of the FLISA plate. cTnI from 1µg/mL to 0.02ng/mL was captured and detected by anti-cTnI scFv with anti-HA Cy5-labelled reporter antibody. The assay was significantly more sensitive than with the mAb capture and by virtue of using a fluorescence detection system in conjunction with a higher-affinity capture reagent.

6.2.4 Assays compromised by antigen variability

The assays described above were carried out using combinations of the 2B12_scAb with anti-cTnI scFv or 4G5 scFv and mAb 20B3 paired with the 2B12 scFv, 4G5 scFv or cTnI scFv. Initially the coating concentrations of the capture antibodies were investigated. However, no signals were obtained for any analysis pairing despite modification of the coating buffers and concentrations of the reagents (data not shown). To investigate this further a number of test ELISAs using the antibodies in combination with the commercially sourced antibodies as controls were carried out providing an insight into the behaviour of the antibodies with the new batch of antigen. Figure 6.2-8 demonstrates the behaviour of mAb 20B3 and Hytest 228 in comparison to 2B12_scAb. In both cases the capture by anti-epitope-2-specific reagents did not generate a signal, whereas the anti-epitope-1-specific capture worked well with the Hytest mAb 16A11. The only difference between these assays and those carried out previously (in section 6.2.3 and for mAb screening in section 4.2.2 and rAb generation in sections 0) was the cTnI batch from the commercial source. This led to the realisation that the antigen quality was affecting the assay as previously reported in the literature [94]. The cTnI was tested by SDS-PAGE and WB using all the commercial and ‘in-house’ antibodies. In the SDS-PAGE and WB all the antibodies reacted with the antigen (Figure 6.2-9) in much the same pattern as the original batch quality check (Figure 3.2-1). This suggests that the solubilised commercial cTnI antigen had adopted a different conformation which resulted in diminishment of the capacity of the anti-epitope-2 mAbs to bind to it in-solution.

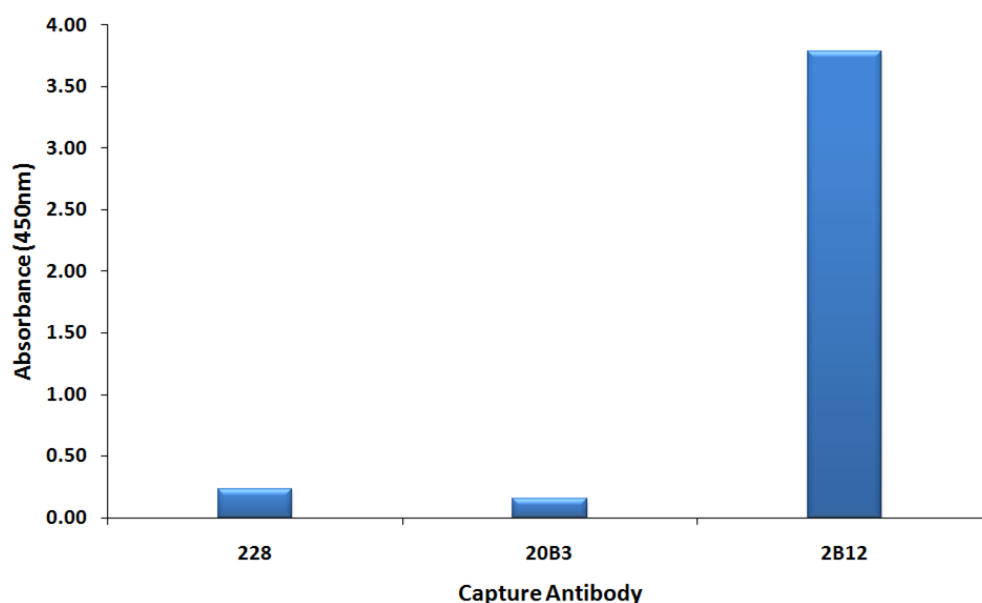


Figure 6.2-8: Test of capture reagents including the positive control mAb 228 with the new batch of cTnI

Analysis of the cTnI batch by sandwich ELISA. MAb20B3, Hytest mAb228 and 2B12_scAb were coated (20µg/mL) onto wells of an ELISA plate and captured 2µg/mL cTnI in 1% (w/v) PBSTM. The captured cTnI was then probed with Hytest 16A11 HRP-labelled mAb. The analysis shows that combinations of anti-epitope-2 mAbs and reporter gave no signal in contrast the anti-epitope-1 scAb and 16A11 combinations which gave a strong signal. This suggests the antigen has adopted a new conformation or has undergone degradation.

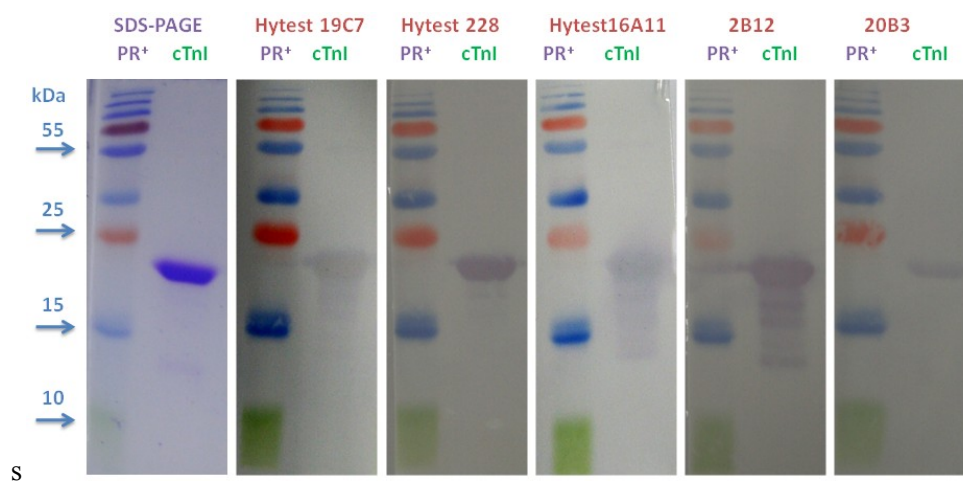


Figure 6.2-9: Test of new cTnI batch by SDS-PAGE and WB

Analysis was carried out using a battery of anti-epitope antibodies. SDS-PAGE (LHS) of cTnI from Life Diagnostics. Multiple transfers of the resolved gel were prepared in series and probed with various antibodies. Hytest control antibodies 19C7 (epitope 1), 228 (epitope 2) and 16A11 (epitope 3), and in-house 20B3 (epitope 2) and 2B12 (epitope 1). 19C7 and 16A11 were both HRP-labelled and were directly detected. MAb 228 and 20B3 were detected using an anti-mouse HRP-labelled secondary antibody and recombinant antibody 2B12 was detected using anti-HA HRP-labelled secondary antibody. PR⁺: Prestained protein ladder

6.3 Chapter conclusions

The developed recombinant anti-epitope-1 scFv were demonstrated to have far superior affinity compared to the industry standard monoclonal antibody from Hytest. The basic light chain shuffled mutant was shown to be further improved over the wild-type in the inhibition ELISA format. The development of truly high-affinity reagents, for deployment in diagnostics test systems was a critical component. However, it is the first stage of ultra-sensitive detection and requires significant support from the assay platform and signal amplification components of the POC format.

Issues relating to the small size, aggregation potential, stability, labelling potential and unsuitability to direct immobilisation of the scFv validates the requirement to reformat the antibodies. Introduction of a single constant domain in the scAb format has the potential to dramatically improve the expression potential and increases the ‘real-estate’ area of the antibody to be exploited without compromising high-affinity binding. The presence of the reactive cysteine residue has applications for ordered immobilisation of the capture reagents and facilitates labelling of the antibody at the C-terminus away from the functionally vital area, the binding pocket. These requirements were highlighted in the experiments carried out to evaluate the effects of directly labelling the scFv. The specific-labelling and immobilisation of the constructs is currently under optimisation, but was successfully applied to the immobilisation of the 2B12_scAb_cys on AFM cantilevers using hetero-bifunctional linkers.

As was observed from the initial antibody pairing experiments, the availability of a number of antibody combinations was valuable in developing the working demonstration assay for cTnI detection. Use of the monoclonal antibody 20B3 in its current form demonstrated lower sensitivity for cTnI than the reformatted 2B12_scAb. It was therefore of considerable importance to isolate the variable domains from the hybridoma and refine the affinity by recombinant antibody-based methodologies.

The promising assay development process centred on the tested pairings and was thwarted by variation in commercially sourced batches of cTnI which was previously reported in the literature as a barrier to standardised cTnI-based cardiovascular assays [94]. The variability in the reactivity of the anti-epitope-2 monoclonal antibodies between the sandwich assay

and the Western blotting analysis suggests that the antigen adopted a different confirmation in-solution and was likely to be causing occlusion of the epitope-2 domain. This was not seen in the previous batch and further highlights the need for a consistent stable and representative antigen or reference standard.

The initial optimisation of the assay pairs and reformatting experiments were undertaken to pre-develop an electro-chemiluminescent (ECL) assay [307]. The development of the ECL assay was an avenue of interest as a novel means to detect ultra-low concentrations of cTnI which was based on results previously obtained using anti-CRP antibodies. The use of ECL has the potential to dramatically increase assay sensitivity by removal of the excitation light source decreasing the background signal. The use of super-critical angle fluorescence (SAF) was a second avenue of assay development which focuses light on a single region of a parabolic chip reducing the bulk fluorescence in the sample and efficiently collecting light for the sample zone even from a single fluorophore [308]. The SAF platform potentially addresses the unmet need for fast and sensitive concentration measurements at low cost and could be useful in POC testing [309]. Both these assay avenues required optimised assay pairings and the introduction of labels-specific to the assay format. The issues highlighted for the labelling and immobilisation of the antibodies were addressed by simple yet novel reformatting experiments. The potential development of these novel assays was compromised by the variance in quality of the antigen. The use and development of a common cTnI assay calibrator has received much attention and rigorous investigation. Harmonisation of different cTnI assays and standards appears to be a complicated process due intractably to the different recognition patterns of different anti-cTnI antibodies used in the assays. Hytest® provides a native cTn ternary complex in liquid form which has received recommendation for use by the American Association for Clinical Chemistry (AACA). Additional rigorous characterisation of this material was developed by the National Institute of Standards and Technology (NIST) as even minor variances in structure of the material can distort the reactivities and hence analytical performance of the material [94]. Despite these barriers the high-affinity antibodies developed are essential for *ultra-sensitive* assay formats, which is the ultimate goal. The relatively simplistic transition of the scFv to both scAb and scAb_cys formats significantly improved stability and orientation while imparting a modular capacity to design and develop highly tailored biorecognition entities for POC testing.

Chapter 7: Concluding remarks and discussion

Acute coronary syndrome is the single greatest killer in the western world placing a massive healthcare and social burden on world economies. The importance of early intervention cannot be emphasised strongly enough in order to provide the patient with an opportunity to change their lifestyle and circumvent the health issues associated with cardiac muscle damage. Due to the massive impact of cardiovascular events, significant research has focussed on the development of reliable methods to detect these events, preferably upstream of irreversible myocardial necrosis. However, many of the potential biomarkers purported to be indicative of future cardiovascular events remain inconclusively proven. The cardiac troponins are the only biomarkers of cardiovascular disease accepted clinically as definitive indicators of a cardiovascular event and the challenges faced by medical practitioners in diagnosing CVD are still substantial.

Cardiac troponin I, a biomarker of myocardial damage, was targeted for the development of highly-specific antibodies for the generation of a low cost point-of-care device. The choice of cTnI as a target, was complicated by its structural and sequence similarity to its skeletal isoform, its existence in complex and modified forms and interferences from serum proteins during analysis. To circumvent these challenges a rational epitope targeting approach was adopted to develop antibodies-specific to the N-terminal cardio-specific region of cTnI.

In Chapter 3, the cTnI antigen was introduced and limitations due to the quality of the antigen available from commercial sources highlighted. The limitations of protein-based immunisation regimes for generating epitope-specific antibodies were discussed, and the principles of the design and use of synthetic peptide-based immunisation regimes were proposed. To overcome the cTnI quality issues, for efficient antibody generation and characterisation, recombinant expression of various forms of the antigen were investigated. The expression and purification of recombinant TnI was complicated by the protein's high-charge. It was successfully expressed, but formed insoluble inclusion bodies and the production strategy was refined to use truncated forms of the protein. The research culminated in the generation of a novel cTnI epitope fusion to fatty acid binding protein which proved to be stable and soluble with the requisite epitopes available for binding in the correct conformations representative of the native antigen. The fusion protein was successfully applied for the characterisation of the recombinant antibodies. This construct has potential as a novel fusion partner for 'difficult-to-express' proteins and peptides. The

use of recombinant protein expression proved to be a multi-faceted process requiring constant adaption in strategy and approach. Given the wealth of structural and genetic information available on many diagnostically-important proteins a rational, knowledge-based approach to antigen design should be undertaken where an antigen is in scarce supply, and also to efficiently support the generation of highly-specific and well characterised antibodies. In any antibody generation project, the quality of the antigen is paramount.

The use of hybridoma technology for the generation of antibodies was an attractive approach due to the patent status of the technology. By not patenting hybridoma technology, Kolher and Milstein ensured that significant and successful applications of the methodology to diagnostics and therapeutics ensued. In Chapter 4, development of the nanomolar affinity IgG_{1κ} monoclonal antibody (20B3) to cTnI was described. It was rigorously evaluated using numerous assay configurations to ensure the optimal assay capture antibody was selected from the hybridoma screening campaign. However, the use of mouse-derived antibodies in diagnostic applications can have potential problems with regard to interferences from circulating human-anti-mouse-antibodies and other activated complement components [93, 291, 292].

The limitations of mouse monoclonal antibodies for human diagnostics favour the development of antibodies from alternative immune repertoires, for example the chicken. The modularity and plasticity of recombinant antibodies was an attractive approach and was introduced in Chapter 5. Recombinant antibody technology surpasses the traditional hybridoma methodology by permitting access to the genes encoding for the antibodies from virtually any species. Chicken in particular have received attention as excellent hosts for diagnostic antibody development [291, 292], twinned with the relative ease at which the simplistic avian genes can be accessed for efficient recombinant antibody development. Chapter 5 outlines the successful development of an anti-epitope-1-specific scFv and its subsequent mutagenesis, resulting in the isolation of an improved mutant derived from genetic engineering approaches. The chapter also exemplifies the benefits of high-throughput systems to screen and affinity rank large numbers of clones from recombinant antibody libraries. Using *in silico* methodologies no structural changes in the antibodies could be discerned and this led into initial studies to ascertain the crystal structure of the parental and mutant scFvs. Recombinant antibodies, such as the scFv, are not without their

limitations for diagnostic-based applications. These include the propensity to aggregate and denature if coated onto surfaces and labelling limitations. However, the modular nature of recombinant antibody formats facilitated their development and tailoring for the intended application.

In chapter 6, the superiority of the developed anti-epitope-1 scFv (WT and MT) in direct comparison to the equivalent industry standard monoclonal antibody was described. The available antibodies and formats were tested for optimal pairing to ensure that the antibody orientation in the assay facilitated the highest sensitivity possible. In light of these results, the limitations of using scFv formats in assays were addressed and initially overcome by re-formatting experiments to introduce constant domains to form the scAb and site-targetable scAb_cys constructs. Such antibody formats could ideally be employed in ECL and SAF-based assays whereby the enhanced signal generation could greatly improve sensitivity.

The research described in the course of this thesis demonstrates the merit in applying a rational design-based approach to antibody generation and antigen targeting. The approach can be applied to any antibody generation campaign and is valid for this particularly complex antigen.

This research was an integral component of a large research effort in the Biomedical Diagnostic Institute (BDI) to optimise all key components of assays for disease markers. This included high-level signal enhancement technologies (e.g. use of high-brightness nanoparticles and specially designed optical detection systems) and novel microfluidics-based surface optimised chips. Due to the high-affinity and modular nature of the antibodies they have major potential as model antibodies to demonstrate the capacity of these technologies to generate ultra-sensitive assays and this process is ongoing with significant industrial inputs. For the development of a low-cost, highly-specific and sensitive point-of-care test for cTnI diagnosis, the issues of affinity and specificity of antibodies have been comprehensively addressed for the platforms currently in development. Accordingly, significant industrial interest in these antibodies has ensued. Advanced licensing agreements for the antibodies and technologies developed in this research are in place with the BDIs industrial partners (Merck Millipore and Biosurfit) and material is currently in the process of transfer.

The comprehensive and integrated approach taken in this research for optimising each element of the antibody generation process is unique. Each stage of antibody development from the design of the antigen to screening and down-stream re-engineering and optimisation of the antibodies was thoroughly and rigorously designed to maximise success. This process is the key reason that the thesis presents some of the highest affinity tailored antibodies generated to date for cTnI.

Chapter 8: Appendices

8.1 Supporting material

Table 8.1-1: Restriction enzymes and recognition sequences

5'→3' cut site is indicated by ^ and complementary 3'→5' by the _ (sequence not shown).

Enzyme	Recognition Sequence
<i>BamHI</i>	G [^] GATC_C
<i>NcoI</i>	C [^] CATG_G
<i>SacI</i>	G_AGCT [^] C
<i>SfiI</i>	GGCCN_NNN [^] NGGCC
<i>NotI</i>	GC [^] GGCC_GC
<i>XhoI</i>	C [^] TCGA_G
<i>XbaI</i>	T [^] CTAG_A
<i>HindIII</i>	A [^] AGCT_T

```

ATGGTGGACGCTTTCCTGGGCACCTGGAAGCTAGTGGACAGCAAGAATTTTCGATGACTAC
  M  V  D  A  F  L  G  T  W  K  L  V  D  S  K  N  F  D  D  Y
ATGAAGTCACTCGGTGTGGGTTTTGCTACCAGGCAGGTGGCCAGCATGACCAAGCCTACC
  M  K  S  L  G  V  G  F  A  T  R  Q  V  A  S  M  T  K  P  T
ACAATCATCGAAAAGAATGGGGACATTCTCACCCTAAAAACACACAGCACCTTCAAGAAC
  T  I  I  E  K  N  G  D  I  L  T  L  K  T  H  S  T  F  K  N
ACAGAGATCAGCTTTAAGTTGGGGGTGGAGTTCGATGAGACAACAGCAGATGACAGGAAG
  T  E  I  S  F  K  L  G  V  E  F  D  E  T  T  A  D  D  R  K
GTCAAGTCCATTGTGACACTGGATGGAGGGAAACTTGTTTCACCTGCAGAAATGGGACGGG
  V  K  S  I  V  T  L  D  G  G  K  L  V  H  L  Q  K  W  D  G
CAAGAGACCACACTTGTGCGGGAGCTAATTGATGGAAAACTCATCCTGACACTCACCAC
  Q  E  T  T  L  V  R  E  L  I  D  G  K  L  I  L  T  L  T  H
GGCACTGCAGTTTGCACTCGCACTTATGAGAAAGAGGCA
  G  T  A  V  C  T  R  T  Y  E  K  E  A

```

Figure 8.1-1: DNA and amino acid sequence of hFABP (Val² to Ala¹³³)

ATGGCGAACTACCGCGCTTATGCCACGGAGCCGCACGCCAAGAAAAAATCTAAGATCTCC
M A N Y R A Y A T E P H A K K K S K I S
 GCCTCGAGAAAATTGCAGCTGAAGACTCTGCTGCTGCAGATTGCAAAGCAAGAGCTGGAG
A S R K L Q L K T L L L Q I A K Q E L E
 CGAGAGGCGGAGGAGCGGCGCGGAGAGAAGGGGCGCGCTCTGAGCACCCGCTGCCAGCCG
R E A E E R R G E K G R A L S T R C Q P
 CTGGAGTTGGCCGGGCTGGGCTTCGCGGAGCTGCAGGACTTGTGCCGACAGCTCCACGCC
L E L A G L G F A E L Q D L C R Q L H A
 CGTGTGGACAAGGTGGATGAAGAGAGATACGACATAGAGGCAAAAGTCACCAAGAACATC
R V D K V D E E R Y D I E A K V T K N I
 ACGGAGATTGCAGATCTGACTCAGAAGATCTTTGACCTTCGAGGCAAGTTTAAGCGGCCC
T E I A D L T Q K I F D L R G K F K R P
 ACCCTGCGGAGAGTGAGGATCTCTGCAGATGCCATGATGCAGGCGCTGCTGGGGGGCCCG
T L R R V R I S A D A M M Q A L L G A R
 GCTAAGGAGTCCCTGGACCTGCGGGCCACCTCAAGCAGGTGAAGAAGGAGGACACCGAG
A K E S L D L R A H L K Q V K K E D T E
 AAGGAAAACCGGGAGGTGGGAGACTGGCGCAAGAACATCGATGCACTGAGTGGAATGGAG
K E N R E V G D W R K N I D A L S G M E
 GGCCGCAAGAAAAAGTTTGAGAGC
G R K K K F E S

Figure 8.1-2: DNA and amino acid sequence of rTnI (Asp²⁵ to Ser²¹⁰)

The pET vectors are sourced from Novagen and the detailed maps were accessed at http://www.merck-chemicals.se/life-science-research/vector-table-novagen-pet-vector-table/c_HdSb.s1O77QAAAEhPqsLdcab?PortalCatalogID=merck4biosciences&CountryName=Ireland

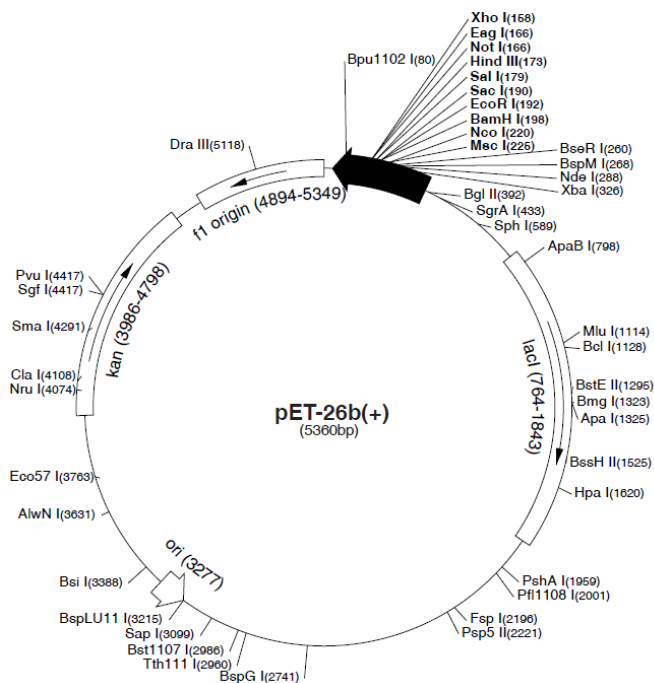


Figure 8.1-3: pET26a-c(+)

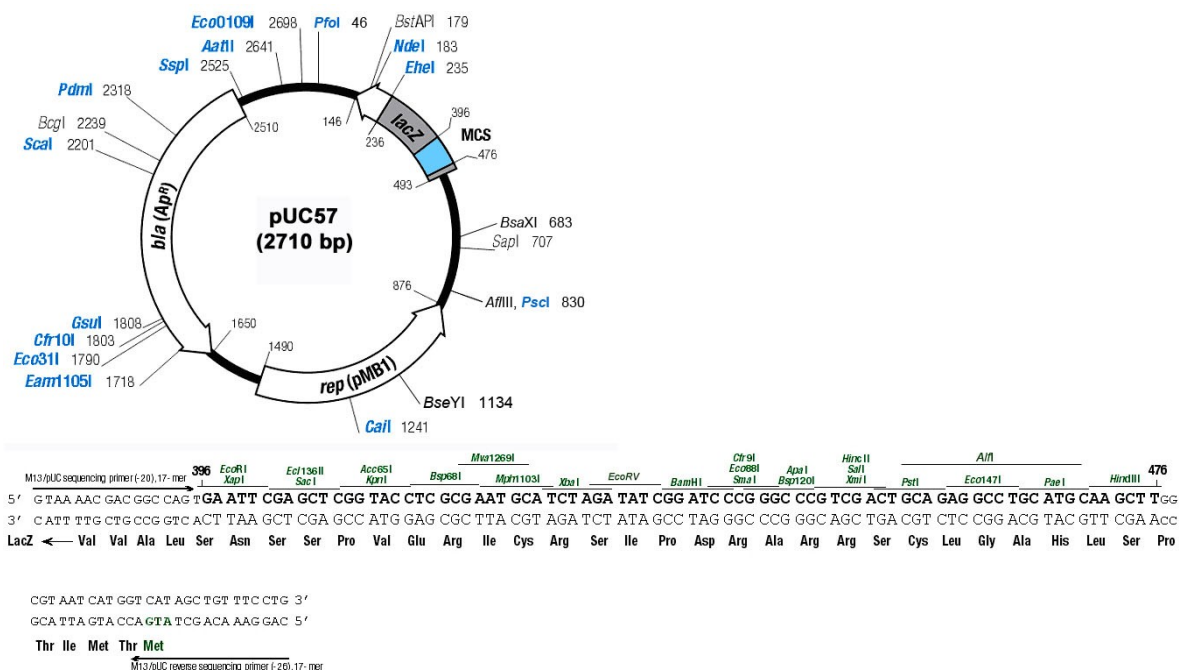


Figure 8.1-6: pUC57

Downloaded from: http://www.genscript.com/site2/document/1400_20060331011034.JPG

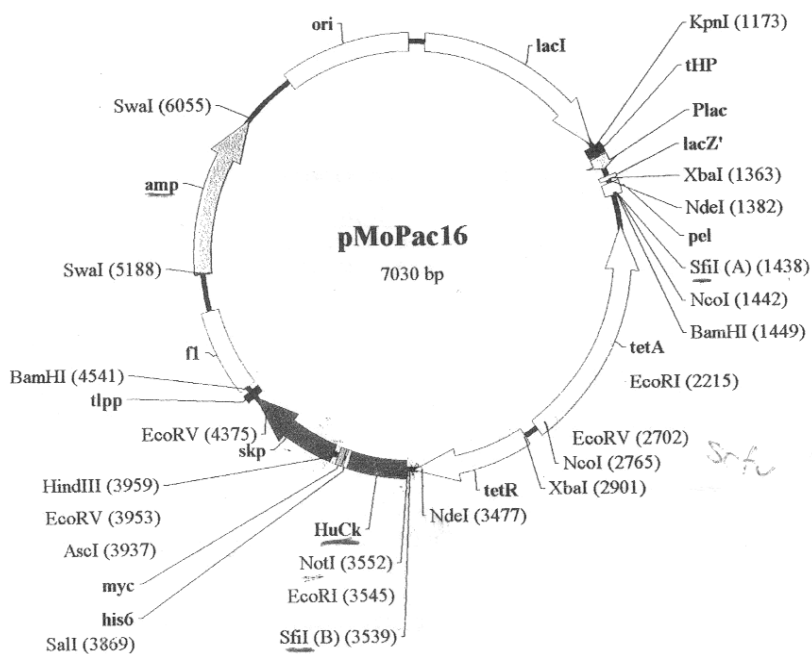


Figure 8.1-7: pMoPac vector

Taken from [206].

Protein A, G, A/G and L are native and recombinant proteins of microbial origin that bind to mammalian immunoglobulins. Binding specificities and affinities of these proteins differ between source species and antibody subclass. Use the following table to select the antibody-binding protein that is best for your application. Consult the Thermo Scientific Pierce Product catalog or web site for more information and a listing of the many available products based on these proteins.

Species	Antibody Class	Protein A	Protein G	Protein A/G	Protein L*
Human	Total IgG	S	S	S	S*
	IgG ₁	S	S	S	S*
	IgG ₂	S	S	S	S*
	IgG ₃	W	S	S	S*
	IgG ₄	S	S	S	S*
	IgM	W	NB	W	S*
	IgD	NB	NB	NB	S*
	IgA	W	NB	W	S*
	Fab	W	W	W	S*
	ScFv	W	NB	W	S*
Mouse	Total IgG	S	S	S	S*
	IgM	NB	NB	NB	S*
	IgG ₁	W	M	M	S*
	IgG _{2a}	S	S	S	S*
	IgG _{2b}	S	S	S	S*
	IgG ₃	S	S	S	S*
Rat	Total IgG	W	M	M	S*
	IgG ₁	W	M	M	S*
	IgG _{2a}	NB	S	S	S*
	IgG _{2b}	NB	W	W	S*
	IgG _{2c}	S	S	S	S*
Cow	Total IgG	W	S	S	NB
	IgG ₁	W	S	S	NB
	IgG ₂	S	S	S	NB
Goat	Total IgG	W	S	S	NB
	IgG ₁	W	S	S	NB
	IgG ₂	S	S	S	NB
Sheep	Total IgG	W	S	S	NB
	IgG ₁	W	S	S	NB
	IgG ₂	S	S	S	NB
Horse	Total IgG	W	S	S	?
	IgG(ab)	W	NB	W	?
	IgG(c)	W	NB	W	?
	IgG(T)	NB	S	S	?
Rabbit	Total IgG	S	S	S	W*
Guinea Pig	Total IgG	S	W	S	?
Pig	Total IgG	S	W	S	S*
Dog	Total IgG	S	W	S	?
Cat	Total IgG	S	W	S	?
Chicken	Total IgY	NB	NB	NB	NB

Legend: W = weak binding M = medium binding NB = no binding
S = strong binding ? = information not available

*Binding to Protein L will occur only if the immunoglobulin has the appropriate kappa light chains. The stated binding affinity refers only to species and subtypes with appropriate kappa light chains. Lambda light chains and some kappa light chains will not bind. For more information, see instructions for Protein L (Product No. 21189).

Figure 8.1-8: Properties of antibody binding proteins A, G and L

Figure taken from Piercenet.com an excellent resource for technical information. Technical document reference number TR0034.3 (www.piercenet.com).

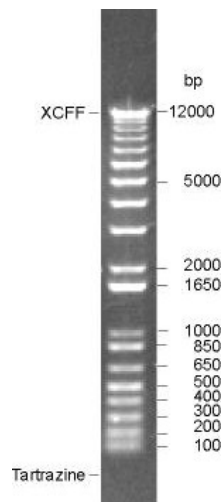


Figure 8.1-9: 1kb plus ladder from Invitrogen.

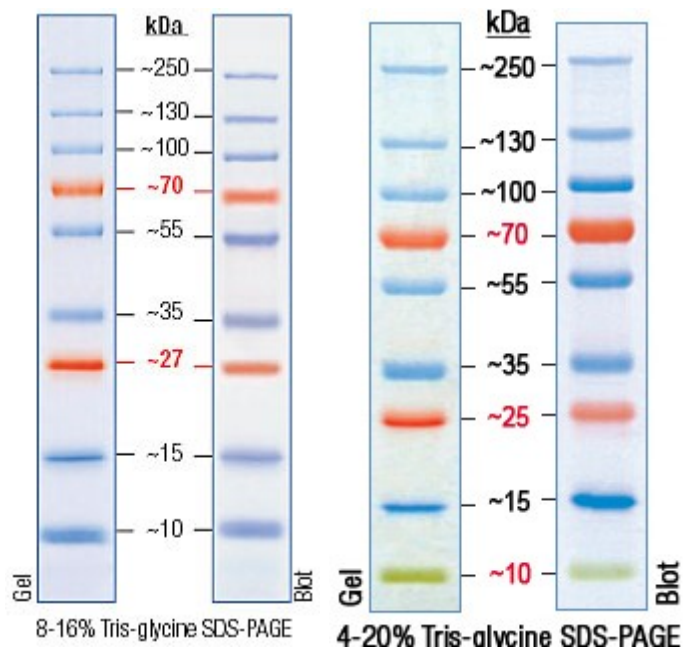


Figure 8.1-10: Fermentas Page-Ruler Plus MW maker.

Left – early maker, right marker modified by company for improved visualisation. Both were utilised in the course of the thesis. The main variation is the 27kDa to 25kDa band change and the green colour applied to 10kDa marker.

Amino Acid: **F L W Y R K** **H I N Q D E C A S T G V P M**

Figure 8.1-11: N-end rule for protein degradation in *E. coli*

Adapted from [107]. Amino acids highlighted in red signify de-stabilising effects on the protein and amino acids in green signify those with stabilising effects on the protein.

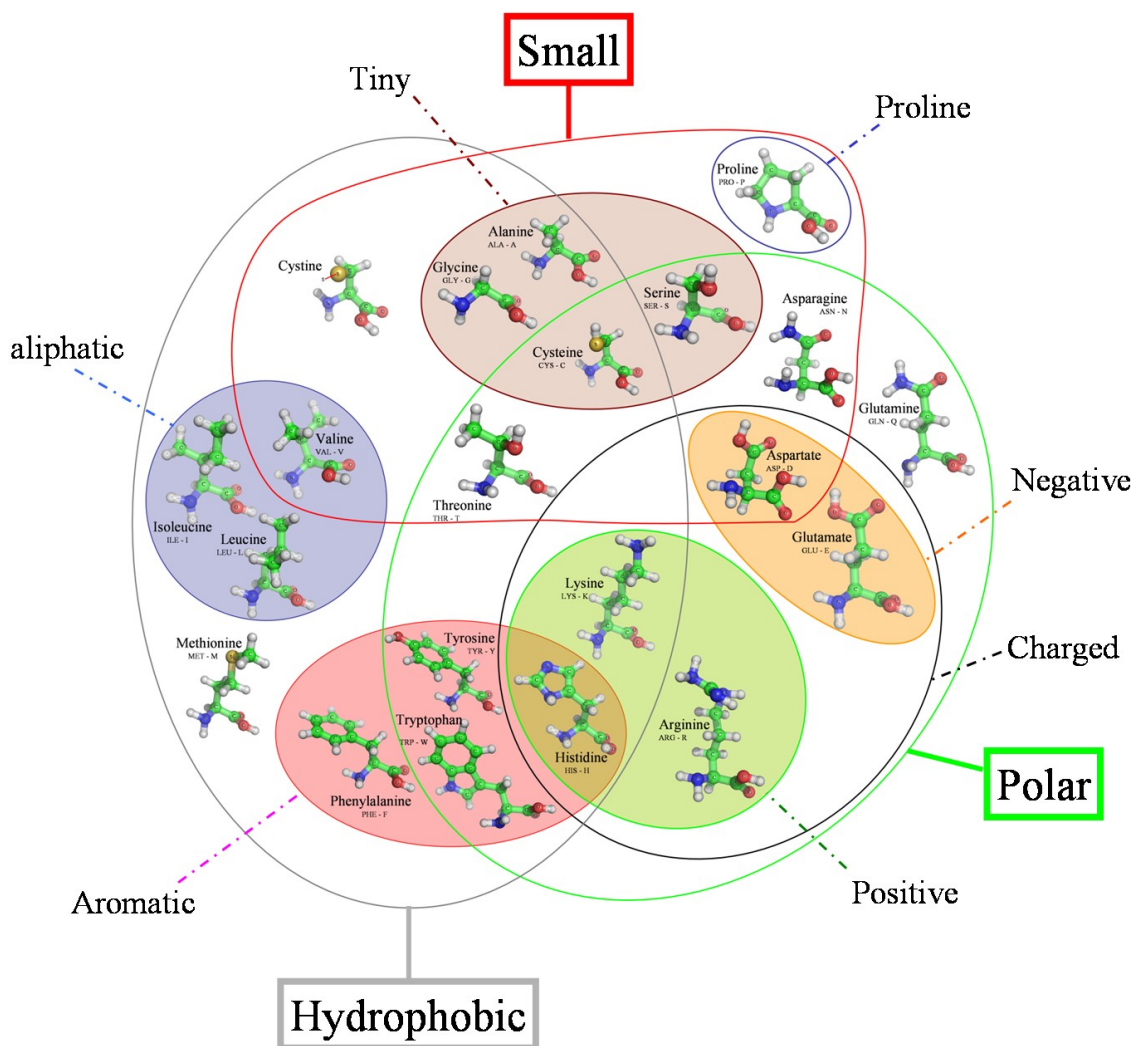


Figure 8.1-12: Venn diagram of amino acid properties

Downloaded from: http://www.dsmb.inserm.fr/~debvern/VENN_DIAGRAM/aa_venn_diagram.png.

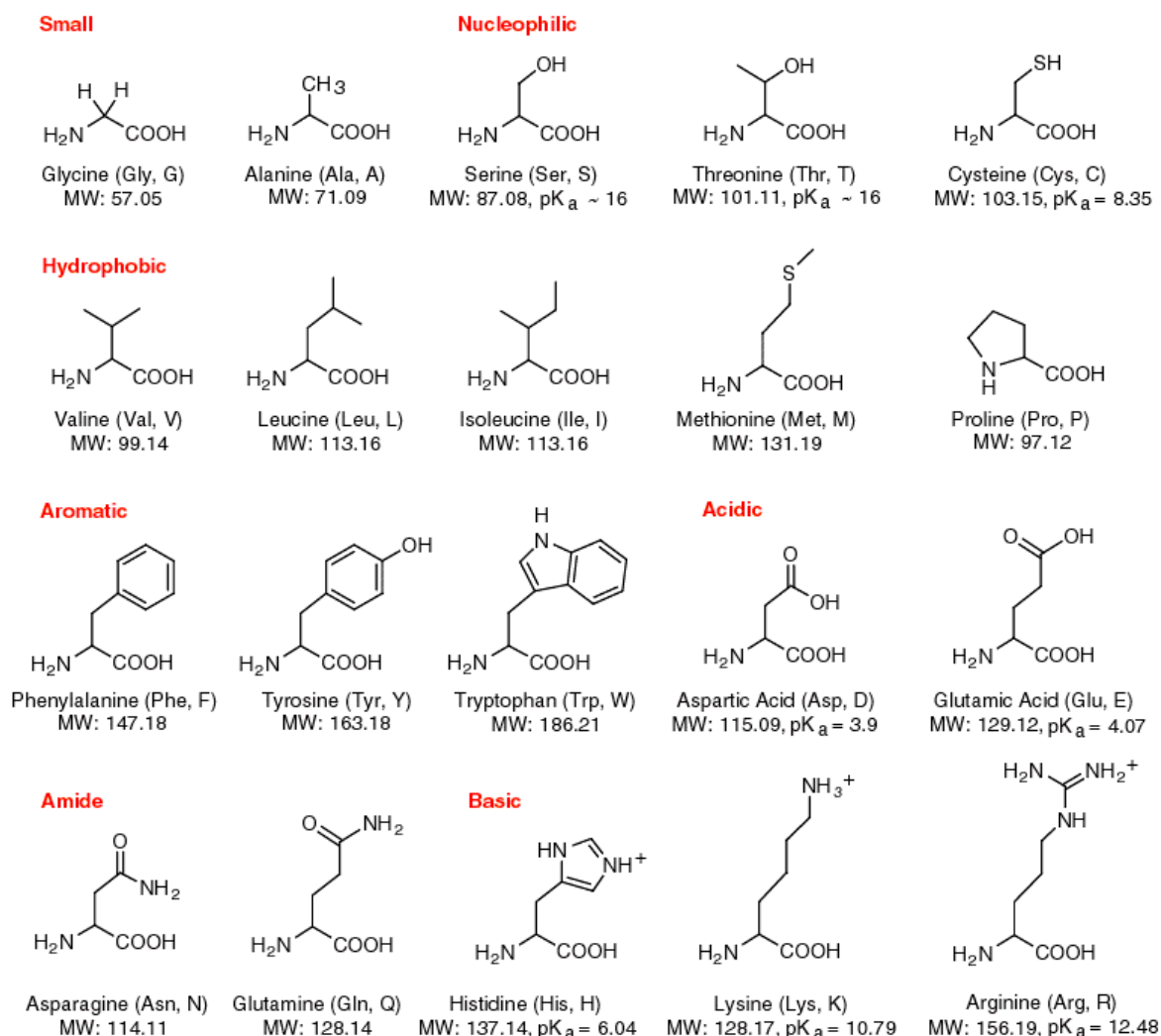


Figure 8.1-13: Amino acid structure and properties

Downloaded from http://www.neb.com/nebecomm/tech_reference/general_data/amino_acid_structures.asp.

Table 8.1-2: Protein crystallisation screening kits

Kit	Crystallisation Screen Type
Crystallisation Basic Kit for Proteins (Sigma)	Primary: Empirical.
Index (HR)	Primary: Diverse reagent.
Crystal Screen (HR)	Primary: Sparse matrix biased.
PEGRx (HR)	Primary/Secondary: pH and polymer.
PEG/ION (HR)	Primary/Secondary: PEG, ion.
Salt Rx (HR)	Primary/Secondary: Salt and pH.
Wizard I, II and III (Emerald)	Primary: Sparse Matrix, pH buffer and salt.

LTQPSSVSAN	PGETVKIACS	GSGGSYGWYQ	QKSPGSAPVT	VIYYNNNRPS	DIPSRFSGSK	60
SGSTATLTIT	GVQAEDEAVY	FCGGWDSSTY	TGIFGAGTTL	TVLGQSSRSS	GGGGSSGGGG	120
SAVTLEESGG	GLQTPGGTSL	LVCKGSGFTF	SSVNMFWVRQ	APGKGLEFVA	GINTGAGSGT	180
NYAPAVKGRA	AISRDNGQST	VRLQLNNLRA	EDTATYFCAK	SSYQCSGDYC	WGHPGTIDAW	240
GRGTEVIVSS	TSGQAGQHHH	HHHGAYPYDV	PDYAS			275

Figure 8.1-14: Amino acid sequence of the avian-derived scFv 4G5

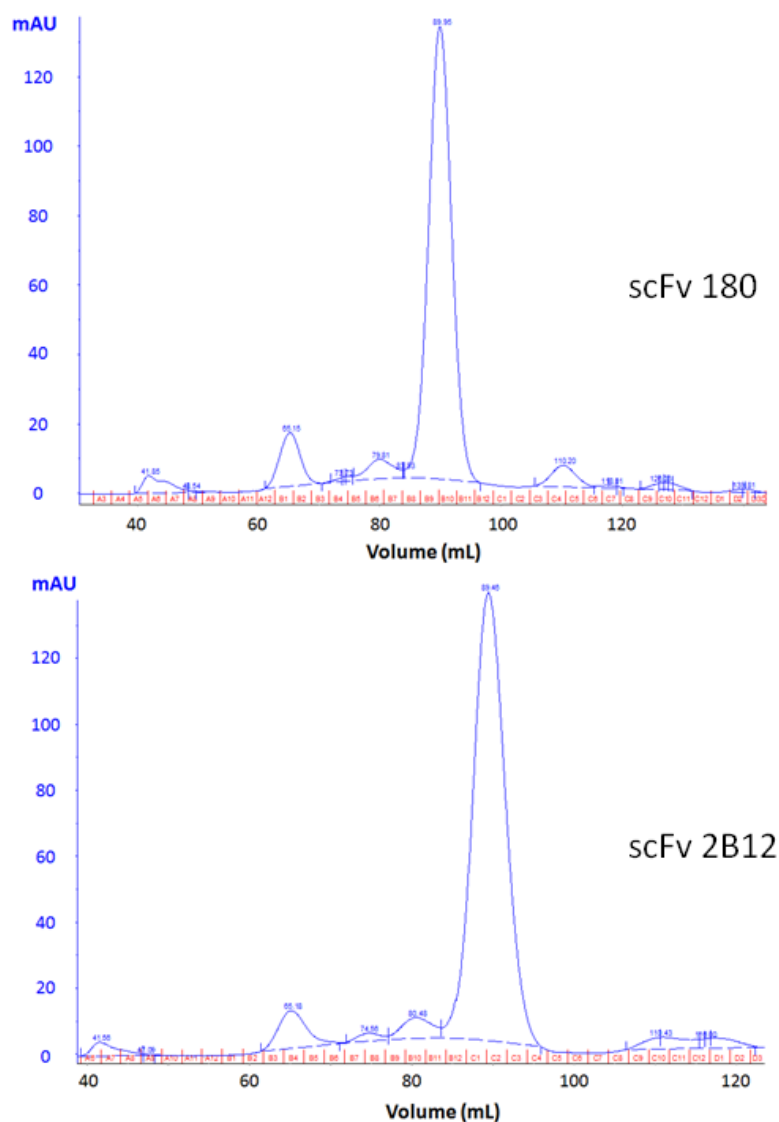


Figure 8.1-15: Gel filtration profiles for the scFvs purified by IMAC from periplasmic extraction

Predominantly monomeric fractions were purified by IMAC as illustrated by the major peak. Higher order fractions or aggregates were much less prominent in comparison to cytoplasmic prepared purifications.

Chapter 9: References

- [1] Harlow, E. and Lane, D., *Antibodies: A Laboratory Manual* vol. I. New York: Cold Spring Harbor Laboratory Press, **1988**.
- [2] McCullough, K. C. and Summerfield, A., "Basic concepts of immune response and defense development," *ILAR J*, vol. 46, pp. 230-40, **2005**.
- [3] Mader, S., *Biology*, 8 ed. New York: McGraw-Hill, **2004**.
- [4] Harlow, E. and Lane, D., *Using Antibodies: A Laboratory Manual*. New York: Cold Spring Harbor Laboratory Press, **1999**.
- [5] Padoa, C. J. and Crowther, J., "Engineered antibodies: A new tool for use in diabetes research," *Diabeties Research and Clinical Practice*, vol. 74S, pp. S51-S62, **2006**.
- [6] Altshuler, E. P., Serebryanaya, D. V., and Katrukha, A. G., "Generation of recombinant antibodies and means for increasing their affinity," *Biochemistry (Mosc)*, vol. 75, pp. 1584-605, **2010**.
- [7] Song, T. (**2009**). *IgG Molecule (Penn State University)*. Available: http://www.bmb.psu.edu/faculty/tan/lab/gallery/igg_ribbon2.jpg
- [8] Ohlin, M. and Zouali, M., "The human antibody repertoire to infectious agents: implications for disease pathogenesis," *Mol Immunol*, vol. 40, pp. 1-11, **2003**.
- [9] Brown, T. A., *Genomes 3*, 3 ed. New York: Garland Science, **2007**.
- [10] Di Noia, J. M. and Neuberger, M. S., "Molecular mechanisms of antibody somatic hypermutation," *Annu Rev Biochem*, vol. 76, pp. 1-22, **2007**.
- [11] Li, Z., Woo, C. J., Iglesias-Ussel, M. D., Ronai, D., and Scharff, M. D., "The generation of antibody diversity through somatic hypermutation and class switch recombination," *Genes Dev*, vol. 18, pp. 1-11, **2004**.
- [12] Lerner, R. A., "Manufacturing immunity to disease in a test tube: the magic bullet realized," *Angew Chem Int Ed Engl*, vol. 45, pp. 8106-25, **2006**.
- [13] Vo-Dinh, T. and Cullum, B., "Biosensors and biochips: advances in biological and medical diagnostics," *Fresenius J Anal Chem*, vol. 366, pp. 540-51, **2000**.
- [14] Hock, B., Seifert, M., and Kramer, K., "Engineering receptors and antibodies for biosensors," *Biosens Bioelectron*, vol. 17, pp. 239-49, **2002**.
- [15] Turner, A. P., Chen, B., and Piletsky, S. A., "In vitro diagnostics in diabetes: meeting the challenge," *Clin Chem*, vol. 45, pp. 1596-601, **1999**.
- [16] D'Orazio, P., "Biosensors in clinical chemistry," *Clin Chim Acta*, vol. 334, pp. 41-69, **2003**.

- [17] Vo-Dinh, T., Tromberg, B. G., Griffin, G. D., Ambrose, K. R., Sepaniak, M. J., and Gardenhire, E. M., "Antibody-based fiberoptics biosensor for the carcinogen Benzo(a)pyrene," *Applied Spectroscopy* vol. 41, pp. 735-738, **1987**.
- [18] Jiang, X., Li, D., Xu, X., Ying, Y., Li, Y., Ye, Z., and Wang, J., "Immunosensors for detection of pesticide residues," *Biosens Bioelectron*, vol. 23, pp. 1577-87, **2008**.
- [19] Patel, P. d., "(Bio)sensors for measurement of analytes implicated in food safety: a review," *Trends in Analytical Chemistry*, vol. 21, pp. 96-115, **2002**.
- [20] Mosiello, L., Laconi, L., Del Gallo, M., Ercole, C., and Lepidi, A., "Development of a monoclonal antibody based potentiometric biosensor for terbuthylazine detection," *Sensors and Actuators B*, vol. 95, pp. 315-320, **2003**.
- [21] Tang, D., Yuan, R., Chai, Y., Zhong, X., Liu, Y., and Dai, J., "Electrochemical detection of hepatitis B surface antigen using colloidal gold nanoparticles modified by a sol-gel network interface," *Clin Biochem*, vol. 39, pp. 309-14, **2006**.
- [22] Tang, D. P. and Ren, J. J., "Direct and rapid detection of diphtherotoxin via potentiometric immunosensor based on nanoparticles mixture and polyvinyl butyral as matrixes," *Electroanalysis*, vol. 17, pp. 2208-2216, **2005**.
- [23] Theegala, C. S., Small, D. D., and Monroe, W. T., "Oxygen electrode-based single antibody amperometric biosensor for qualitative detection of *E. coli* and bacteria in water," *J Environ Sci Health A Tox Hazard Subst Environ Eng*, vol. 43, pp. 478-87, **2008**.
- [24] Zhuo, Y., Yuan, P. X., Yuan, R., Chai, Y. Q., and Hong, C. L., "Nanostructured conductive material containing ferrocenyl for reagentless amperometric immunosensors," *Biomaterials*, vol. 29, pp. 1501-8, **2008**.
- [25] Micheli, L., Grecco, R., Badea, M., Moscone, D., and Palleschi, G., "An electrochemical immunosensor for aflatoxin M1 determination in milk using screen-printed electrodes," *Biosens Bioelectron*, vol. 21, pp. 588-96, **2005**.
- [26] Carralero, V., Gonzalez-Cortes, A., Yanez-Sedeno, P., and Pingarron, J. M., "Nanostructured progesterone immunosensor using a tyrosinase-colloidal gold-graphite-Teflon biosensor as amperometric transducer," *Anal Chim Acta*, vol. 596, pp. 86-91, **2007**.
- [27] Tully, E., Higson, S. P., and Kennedy, R. O., "The development of a 'labelless' immunosensor for the detection of *Listeria monocytogenes* cell surface protein, Internalin B," *Biosensors & Bioelectronics*, vol. 23, pp. 906-912, **2008**.

- [28] Su, X. L. and Li, Y., "A self-assembled monolayer-based piezoelectric immunosensor for rapid detection of *Escherichia coli* O157:H7," *Biosens Bioelectron*, vol. 19, pp. 563-74, **2004**.
- [29] Arce, L., Zougagh, M., Arce, C., Moreno, A., Rios, A., and Valcarcel, M., "Self-assembled monolayer-based piezoelectric flow immunosensor for the determination of canine immunoglobulin," *Biosens Bioelectron*, vol. 22, pp. 3217-23, **2007**.
- [30] Halamek, J., Makower, A., Knosche, K., Skladal, P., and Scheller, F. W., "Piezoelectric affinity sensors for cocaine and cholinesterase inhibitors," *Talanta*, vol. 65, pp. 337-342, **2005**.
- [31] Příbyl, J., Hepel, M., Halánek, J., and Skládal, P., "Development of piezoelectric immunosensors for competitive and direct determination of atrazine," *Sensors and Actuators B*, vol. 91, pp. 333-341, **2003**.
- [32] Campbell, G. A., Delesdernier, D., and Mutharasan, R., "Detection of airborne *Bacillus anthracis* spores by an integrated system of an air sampler and a cantilever immunosensor," *Sensors and Actuators B-Chemical*, vol. 127, pp. 376-382, **2007**.
- [33] Pohanka, M., Pavlis, O., and Skladal, P., "Diagnosis of tularemia using piezoelectric biosensor technology," *Talanta*, vol. 71, pp. 981-985, **2007**.
- [34] Skottrup, P., Hearty, S., Frokiaer, H., Leonard, P., Hejgaard, J., O'Kennedy, R., Nicolaisen, M., and Justesen, A. F., "Detection of fungal spores using a generic surface plasmon resonance immunoassay," *Biosensors & Bioelectronics*, vol. 22, pp. 2724-2729, **2007**.
- [35] Tsutsumi, T., Miyoshi, N., Sasaki, K., and Maitani, T., "Biosensor immunoassay for the screening of dioxin-like polychlorinated biphenyls in retail fish," *Anal Chim Acta*, vol. 617, pp. 177-83, **2008**.
- [36] Bulukin, E., Meucci, V., Minunni, M., Pretti, C., Intorre, L., Soldani, G., and Mascini, M., "An optical immunosensor for rapid vitellogenin detection in plasma from carp (*Cyprinus carpio*)," *Talanta*, vol. 72, pp. 785-790, **2007**.
- [37] Wei, D., Oyarzabal, O. A., Huang, T. S., Balasubramanian, S., Sista, S., and Simoman, A. L., "Development of a surface plasmon resonance biosensor for the identification of *Campylobacter jejuni*," *Journal of Microbiological Methods*, vol. 69, pp. 78-85, **2007**.
- [38] Hearty, S., Leonard, P., Quinn, J., and O'Kennedy, R., "Production, characterisation and potential application of a novel monoclonal antibody for rapid identification of

- virulent *Listeria monocytogenes*," *Journal of Microbiological Methods*, vol. 66, pp. 294-312, **2006**.
- [39] Llamas, N. M., Stewart, L., Fodey, T., Higgins, H. C., Velasco, M. L., Botana, L. M., and Elliott, C. T., "Development of a novel immunobiosensor method for the rapid detection of okadaic acid contamination in shellfish extracts," *Anal Bioanal Chem*, vol. 389, pp. 581-7, **2007**.
- [40] Lathrop, A. A., Jaradat, Z. W., Haley, T., and Bhunia, A. K., "Characterization and application of a *Listeria monocytogenes* reactive monoclonal antibody C11E9 in a resonant mirror biosensor," *J Immunol Methods*, vol. 281, pp. 119-28, **2003**.
- [41] Tschmelak, J., Kumpf, M., Káppel, N., Proll, G., and Gauglitz, G., "Total internal reflectance fluorescence (TIRF) biosensor for environmental monitoring of testosterone with commercially available immunochemistry: Antibody characterization, assay development and real sample measurements," *Talanta*, vol. 69, pp. 343-350, **2006**.
- [42] Engstrom, H. A., Andersson, P. O., and Ohlson, S., "A label-free continuous total-internal-reflection-fluorescence-based immunosensor," *Anal Biochem*, vol. 357, pp. 159-66, **2006**.
- [43] Tschmelak, J., Proll, G., and Gauglitz, G., "Immunosensor for estrone with an equal limit of detection as common analytical methods," *Anal Bioanal Chem*, vol. 378, pp. 744-5, **2004**.
- [44] Nagel, T., Ehrentreich-Forster, E., Singh, M., Schmitt, K., Brandenburg, A., Berka, A., and Bier, F. F., "Direct detection of tuberculosis infection in blood serum using three optical label-free approaches," *Sensors and Actuators B*, vol. 129, pp. 934-940, **2008**.
- [45] Mohrle, B. P., Kohler, K., Jaehrling, J., Brock, R., and Gauglitz, G., "Label-free characterization of cell adhesion using reflectometric interference spectroscopy (RIfS)," *Anal Bioanal Chem*, vol. 384, pp. 407-13, **2006**.
- [46] Szekacs, A., Trummer, N., Adányi, N., Váradi, M., and Szendro, I., "Development of a non-labeled immunosensor for the herbicide trifluralin via optical waveguide lightmode spectroscopic detection," *Analytica Chimica ACTA*, vol. 487, pp. 31-42, **2003**.

- [47] Kim, N., Kim, D. K., and Kim, W. Y., "Sulfamethazine detection with direct-binding optical waveguide lightmode spectroscopy-based immunosensor," *Food Chemistry*, vol. 108, pp. 768-773, **2008**.
- [48] Schipper, E. F., Rauchalles, S., Kooyman, R. P., Hock, B., and Greve, J., "The waveguide Mach-Zender interferometer as atrazine sensor," *Anal Chem*, vol. 70, pp. 1192-7, **1998**.
- [49] Wang, D., Jiang, D., and Yuan, C., "Affinity aspects of HBsAb-HBsAg interaction on the liquid solid interface," *Colloids and Surfaces A: Physiochemical and Engineering Aspects*, vol. 175, pp. 129-134, **2000**.
- [50] Nabok, A. V., Tsargorodskaya, A., Holloway, A., Starodub, N. F., and Gojster, O., "Registration of T-2 mycotoxin with total internal reflection ellipsometry and QCM impedance methods," *Biosens Bioelectron*, vol. 22, pp. 885-90, **2007**.
- [51] Bae, Y. M., Park, K. W., Oh, B. K., Lee, W. H., and Choi, J. W., "Immunosensor for detection of *Salmonella typhimurium* based on imaging ellipsometry," *Colloids and Surfaces a-Physicochemical and Engineering Aspects*, vol. 257-58, pp. 19-23, **2005**.
- [52] Geng, T., Morgan, M. T., and Bhunia, A. K., "Detection of low levels of *Listeria monocytogenes* cells by using a fiber-optic immunosensor," *Applied and Environmental Microbiology*, vol. 70, pp. 6138-6146, **2004**.
- [53] Tims, T. B. and Lim, D. V., "Rapid detection of *Bacillus anthracis* spores directly from powders with an evanescent wave fiber-optic biosensor," *J Microbiol Methods*, vol. 59, pp. 127-30, **2004**.
- [54] Jung, C. C., Saaski, E. W., McCrae, D. A., Lingerfelt, B. M., and Anderson, G. P., "RAPTOR: A fluoroimmunoassay-based fiber optic sensor for detection of biological threats," *Ieee Sensors Journal*, vol. 3, pp. 352-360, **2003**.
- [55] Kendall, L. V., "Making and Using Antibodies: A Laboratory Manual," Howard, G. C. and Kaser, M. R., Eds., ed Florida: CRC Press, **2007**.
- [56] Leenaars, M. and Hendriksen, C. F., "Critical steps in the production of polyclonal and monoclonal antibodies: evaluation and recommendations," *ILAR J*, vol. 46, pp. 269-79, **2005**.
- [57] Sheehan, K. C., "Making and Using Antibodies: A Laboratory Manual," Howard, G. C. and Kaser, M. R., Eds., ed Florida: CRC Press, **2007**.

- [58] Hoogenboom, H. R., "Selecting and screening recombinant antibody libraries," *Nat Biotechnol*, vol. 23, pp. 1105-16, **2005**.
- [59] Daly, S. J., Dillon, P. P., Manning, B. M., Dunne, L., Killard, A., and O'Kennedy, R., "Production and characterization of murine single chain Fv antibodies to aflatoxin B-1 derived from a pre-immunized antibody phage display library system," *Food and Agricultural Immunology*, vol. 14, pp. 255-274, **2002**.
- [60] Yang, Z. and Min Zhou, D., "Cardiac markers and their point-of-care testing for diagnosis of acute myocardial infarction," *Clin Biochem*, vol. 39, pp. 771-80, **2006**.
- [61] Reichlin, T., Hochholzer, W., Bassetti, S., Steuer, S., Stelzig, C., Hartwiger, S., *et al.*, "Early diagnosis of myocardial infarction with sensitive cardiac troponin assays," *N Engl J Med*, vol. 361, pp. 858-67, **2009**.
- [62] Allender, S., Scarborough, P., Peto, V., and Rayner, M., "European cardiovascular disease statistics," *British Heart Foundation Health Promotion Research Group, Department of Public Health* pp. 1-10, **2008**.
- [63] Khan, I. A. and Wattanasuwan, N., "Role of biochemical markers in diagnosis of myocardial infarction," *Int J Cardiol*, vol. 104, pp. 238-40, **2005**.
- [64] Gutstein, D. E. and Fuster, V., "Pathophysiology and clinical significance of atherosclerotic plaque rupture," *Cardiovasc Res*, vol. 41, pp. 323-33, **1999**.
- [65] Lippi, G., Montagnana, M., Salvagno, G. L., and Guidi, G. C., "Potential value for new diagnostic markers in the early recognition of acute coronary syndromes," *CJEM*, vol. 8, pp. 27-31, **2006**.
- [66] McDonnell, B., Hearty, S., Leonard, P., and O'Kennedy, R., "Cardiac biomarkers and the case for point-of-care testing," *Clin Biochem*, vol. 42, pp. 549-61, **2009**.
- [67] Azzazy, H. M. and Christenson, R. H., "Cardiac markers of acute coronary syndromes: is there a case for point-of-care testing?," *Clin Biochem*, vol. 35, pp. 13-27, **2002**.
- [68] Alpert, J. S. and Thygesen, K., "A new global definition of myocardial infarction for the 21st century," *Pol Arch Med Wewn*, vol. 117, pp. 485-6, **2007**.
- [69] Thygesen, K., Alpert, J. S., and White, H. D., "Universal definition of myocardial infarction," *J Am Coll Cardiol*, vol. 50, pp. 2173-95, **2007**.
- [70] Alpert, J. S., Thygesen, K., Antman, E., and Bassand, J. P., "Myocardial infarction redefined--a consensus document of The Joint European Society of

- Cardiology/American College of Cardiology Committee for the redefinition of myocardial infarction," *J Am Coll Cardiol*, vol. 36, pp. 959-69, **2000**.
- [71] Libby, P., Zipes, D., Bonow, R., and Braunwald, E., *Heart Disease: A textbook of cardiovascular medicine*, 7 ed.: Elsevier Saunders, **2005**.
- [72] Calabro, P., Golia, E., and Yeh, E. T., "CRP and the risk of atherosclerotic events," *Semin Immunopathol*, vol. 31, pp. 79-94, **2009**.
- [73] Herrick, J. B., "Landmark article (JAMA 1912). Clinical features of sudden obstruction of the coronary arteries. By James B. Herrick," *JAMA*, vol. 250, pp. 1757-65, **1983**.
- [74] Libby, P., "The molecular mechanisms of the thrombotic complications of atherosclerosis," *J Intern Med*, vol. 263, pp. 517-27, **2008**.
- [75] Sluimer, J. C. and Daemen, M. J., "Novel concepts in atherogenesis: angiogenesis and hypoxia in atherosclerosis," *J Pathol*, vol. 218, pp. 7-29, **2009**.
- [76] Carlson, G. (**2007**). *Carlson Medical and Biological: Atherogenesis*. Available: http://www.gcarlson.com/cellular_atherogenesis.htm
- [77] Jortani, S. A., Prabhu, S. D., and Valdes, R., Jr., "Strategies for developing biomarkers of heart failure," *Clin Chem*, vol. 50, pp. 265-78, **2004**.
- [78] Friess, U. and Stark, M., "Cardiac markers: a clear cause for point-of-care testing," *Anal Bioanal Chem*, vol. 393, pp. 1453-62, **2009**.
- [79] Ladue, J. S., Wroblewski, F., and Karmen, A., "Serum glutamic oxaloacetic transaminase activity in human acute transmural myocardial infarction," *Science*, vol. 120, pp. 497-9, **1954**.
- [80] Kemp, M., Donovan, J., Higham, H., and Hooper, J., "Biochemical markers of myocardial injury," *Br J Anaesth*, vol. 93, pp. 63-73, **2004**.
- [81] Jaffe, A. S., Babuin, L., and Apple, F. S., "Biomarkers in acute cardiac disease: the present and the future," *J Am Coll Cardiol*, vol. 48, pp. 1-11, **2006**.
- [82] Mo, V. Y. and De Lemos, J. A., "Individualizing therapy in acute coronary syndromes: using a multiple biomarker approach for diagnosis, risk stratification, and guidance of therapy," *Curr Cardiol Rep*, vol. 6, pp. 273-8, **2004**.
- [83] Dolci, A. and Panteghini, M., "The exciting story of cardiac biomarkers: from retrospective detection to gold diagnostic standard for acute myocardial infarction and more," *Clin Chim Acta*, vol. 369, pp. 179-87, **2006**.

- [84] Braunwald, E., Antman, E. M., Beasley, J. W., Califf, R. M., Cheitlin, M. D., Hochman, J. S., *et al.*, "ACC/AHA guidelines for the management of patients with unstable angina and non-ST-segment elevation myocardial infarction. A report of the American College of Cardiology/American Heart Association Task Force on Practice Guidelines (Committee on the Management of Patients With Unstable Angina)," *J Am Coll Cardiol*, vol. 36, pp. 970-1062, **2000**.
- [85] Zakynthinos, E. and Pappa, N., "Inflammatory biomarkers in coronary artery disease," *J Cardiol*, vol. 53, pp. 317-33, **2009**.
- [86] Wu, A. H., Apple, F. S., Gibler, W. B., Jesse, R. L., Warshaw, M. M., and Valdes, R., Jr., "National Academy of Clinical Biochemistry Standards of Laboratory Practice: recommendations for the use of cardiac markers in coronary artery diseases," *Clin Chem*, vol. 45, pp. 1104-21, **1999**.
- [87] Apple, F. S., Wu, A. H., Mair, J., Ravkilde, J., Panteghini, M., Tate, J., *et al.*, "Future biomarkers for detection of ischemia and risk stratification in acute coronary syndrome," *Clin Chem*, vol. 51, pp. 810-24, **2005**.
- [88] Andris-Widhopf, J., Rader, C., Steinberger, P., Fuller, R., and Barbas, C. F., 3rd, "Methods for the generation of chicken monoclonal antibody fragments by phage display," *J Immunol Methods*, vol. 242, pp. 159-81, **2000**.
- [89] Barbas, C. F., 3rd, Burton, D. R., Scott, J. K., and Silverman, G. J., *Phage Display: A Laboratory Manual*. New York: Cold Spring Harbor Laboratory Press, **2001**.
- [90] Ayyar, B. V., Hearty, S., and O'Kennedy, R., "Highly sensitive recombinant antibodies capable of reliably differentiating heart-type fatty acid binding protein from noncardiac isoforms," *Anal Biochem*, vol. 407, pp. 165-71, **2010**.
- [91] Michaelson, J. S., Demarest, S. J., Miller, B., Amatucci, A., Snyder, W. B., Wu, X., *et al.*, "Anti-tumor activity of stability-engineered IgG-like bispecific antibodies targeting TRAIL-R2 and LTbetaR," *MAbs*, vol. 1, pp. 128-41, **2009**.
- [92] Miller, B. R., Demarest, S. J., Lugovskoy, A., Huang, F., Wu, X., Snyder, W. B., *et al.*, "Stability engineering of scFvs for the development of bispecific and multivalent antibodies," *Protein Eng Des Sel*, vol. 23, pp. 549-57, **2010**.
- [93] Eriksson, S., Ilva, T., Becker, C., Lund, J., Porela, P., Pulkki, K., Voipio-Pulkki, L. M., and Pettersson, K., "Comparison of cardiac troponin I immunoassays variably affected by circulating autoantibodies," *Clin Chem*, vol. 51, pp. 848-55, **2005**.

- [94] Eriksson, S., Wittfooth, S., and Pettersson, K., "Present and future biochemical markers for detection of acute coronary syndrome," *Crit Rev Clin Lab Sci*, vol. 43, pp. 427-95, **2006**.
- [95] Guex, N. and Peitsch, M. C., "SWISS-MODEL and the Swiss-PdbViewer: an environment for comparative protein modeling," *Electrophoresis*, vol. 18, pp. 2714-23, **1997**.
- [96] Takeda, S., Yamashita, A., Maeda, K., and Maeda, Y., "Structure of the core domain of human cardiac troponin in the Ca^{2+} -saturated form," *Nature*, vol. 424, pp. 35-41, **2003**.
- [97] Baneyx, F., "Recombinant protein expression in *Escherichia coli*," *Curr Opin Biotechnol*, vol. 10, pp. 411-21, **1999**.
- [98] Baneyx, F. and Mujacic, M., "Recombinant protein folding and misfolding in *Escherichia coli*," *Nat Biotechnol*, vol. 22, pp. 1399-408, **2004**.
- [99] Hearty, S., "Production and application of monoclonal antibodies suitable for the specific detection of *Listeria monocytogenes*," Doctorate, School of Biotechnology, Dublin City University, Dublin, **2005**.
- [100] Studier, F. W. and Moffatt, B. A., "Use of bacteriophage T7 RNA polymerase to direct selective high-level expression of cloned genes," *J Mol Biol*, vol. 189, pp. 113-30, **1986**.
- [101] Merck4Biosciences. (2010). Novagen. Available: http://www.emdchemicals.com/life-science-research/novagen/c_YTKb.s1OFbwAAAEjSGVXhFCX
- [102] Novagen. (2011, 11). *pET System Manual*. Available: <http://lifeserv.bgu.ac.il/wb/zarivach/media/protocols/Novagen%20pET%20system%20manual.pdf>
- [103] Orbulescu, J., Micic, M., Ensor, M., Trajkovic, S., Daunert, S., and Leblanc, R. M., "Human cardiac troponin I: a Langmuir monolayer study," *Langmuir*, vol. 26, pp. 3268-74, **2010**.
- [104] Lohmann, K., Westerdorf, B., Maytum, R., Geeves, M. A., and Jaquet, K., "Overexpression of human cardiac troponin in *Escherichia coli*: its purification and characterization," *Protein Expr Purif*, vol. 21, pp. 49-59, **2001**.
- [105] al-Hillawi, E., Minchin, S. D., and Trayer, I. P., "Overexpression of human cardiac troponin-I and troponin-C in *Escherichia coli* and their purification and

- characterisation. Two point mutations allow high-level expression of troponin-I," *Eur J Biochem*, vol. 225, pp. 1195-201, **1994**.
- [106] Yu, Z. B. and Jin, J. P., "Removing the regulatory N-terminal domain of cardiac troponin I diminishes incompatibility during bacterial expression," *Arch Biochem Biophys*, vol. 461, pp. 138-45, **2007**.
- [107] Varshavsky, A., "The N-end rule pathway of protein degradation," *Genes Cells*, vol. 2, pp. 13-28, **1997**.
- [108] Nicol, P. D., Matsueda, G. R., Haber, E., and Khaw, B. A., "Synthetic peptide immunogens for the development of a cardiac myosin light chain-1 specific radioimmunoassay," *J Nucl Med*, vol. 34, pp. 2144-51, **1993**.
- [109] Singh, R., Samant, U., Hyland, S., Chaudhari, P. R., Wels, W. S., and Bandyopadhyay, D., "Target-specific cytotoxic activity of recombinant immunotoxin scFv(MUC1)-ETA on breast carcinoma cells and primary breast tumors," *Mol Cancer Ther*, vol. 6, pp. 562-9, **2007**.
- [110] Fiorentini, S., Marsico, S., Becker, P. D., Iaria, M. L., Bruno, R., Guzman, C. A., and Caruso, A., "Synthetic peptide AT20 coupled to KLH elicits antibodies against a conserved conformational epitope from a major functional area of the HIV-1 matrix protein p17," *Vaccine*, vol. 26, pp. 4758-65, **2008**.
- [111] El-Awady, M. K., Tabll, A. A., Yousif, H., El-Abd, Y., Reda, M., Khalil, S. B., El-Zayadi, A. R., Shaker, M. H., and Bader El Din, N. G., "Murine neutralizing antibody response and toxicity to synthetic peptides derived from E1 and E2 proteins of hepatitis C virus," *Vaccine*, vol. 28, pp. 8338-44, **2010**.
- [112] Mahajan, B., Berzofsky, J. A., Boykins, R. A., Majam, V., Zheng, H., Chattopadhyay, R., *et al.*, "Multiple antigen peptide vaccines against *Plasmodium falciparum* malaria," *Infect Immun*, vol. 78, pp. 4613-24, **2010**.
- [113] Kohler, G. and Milstein, C., "Continuous cultures of fused cells secreting antibody of predefined specificity," *Nature*, vol. 256, pp. 495-7, **1975**.
- [114] Shulman, M., Wilde, C. D., and Kohler, G., "A better cell line for making hybridomas secreting specific antibodies," *Nature*, vol. 276, pp. 269-70, **1978**.
- [115] Kearney, J. F., Radbruch, A., Liesegang, B., and Rajewsky, K., "A new mouse myeloma cell line that has lost immunoglobulin expression but permits the construction of antibody-secreting hybrid cell lines," *J Immunol*, vol. 123, pp. 1548-50, **1979**.

- [116] Lane, R. D., "A short-duration polyethylene glycol fusion technique for increasing production of monoclonal antibody-secreting hybridomas," *J Immunol Methods*, vol. 81, pp. 223-8, **1985**.
- [117] Campbell, A. M., *Monoclonal Antibody Technology* vol. 13: Elsevier, **1984**.
- [118] Zandstra, P. W., "Pairing cells to enhance fusion," *Nat Methods*, vol. 6, pp. 123-4, **2009**.
- [119] Skelley, A. M., Kirak, O., Suh, H., Jaenisch, R., and Voldman, J., "Microfluidic control of cell pairing and fusion," *Nat Methods*, vol. 6, pp. 147-52, **2009**.
- [120] Bartal, A. H. and Hirshaut, Y., Eds., *Selection and isolation of stable antibody-producing murine hybridomas*. The Humana Press, **1987**, p.^pp. Pages.
- [121] Safsten, P., Klakamp, S. L., Drake, A. W., Karlsson, R., and Myszka, D. G., "Screening antibody-antigen interactions in parallel using Biacore A100," *Anal Biochem*, vol. 353, pp. 181-90, **2006**.
- [122] Moller, I., Marcus, S. E., Haeger, A., Verhertbruggen, Y., Verhoef, R., Schols, H., *et al.*, "High-throughput screening of monoclonal antibodies against plant cell wall glycans by hierarchical clustering of their carbohydrate microarray binding profiles," *Glycoconj J*, vol. 25, pp. 37-48, **2008**.
- [123] Rieger, M., Cervino, C., Saucedo, J. C., Niessner, R., and Knopp, D., "Efficient hybridoma screening technique using capture antibody based microarrays," *Anal Chem*, vol. 81, pp. 2373-7, **2009**.
- [124] De Masi, F., Chiarella, P., Wilhelm, H., Massimi, M., Bullard, B., Ansorge, W., and Sawyer, A., "High throughput production of mouse monoclonal antibodies using antigen microarrays," *Proteomics*, vol. 5, pp. 4070-81, **2005**.
- [125] Abdulhalim, I., Zourob, M., and Lakhtakia, A., "Surface plasmon resonance for biosensing: A mini-review," *Electromagnetics*, vol. 28, pp. 214-242, **2008**.
- [126] Abbas, A., Linman, M. J., and Cheng, Q., "New trends in instrumental design for surface plasmon resonance-based biosensors," *Biosens Bioelectron*, vol. 26, pp. 1815-24, **2011**.
- [127] Hearty, S., Conroy, P. J., Ayyar, B. V., Byrne, B., and O'Kennedy, R., "Surface plasmon resonance for vaccine design and efficacy studies: recent applications and future trends," *Expert Rev Vaccines*, vol. 9, pp. 645-64, **2010**.

- [128] Harriman, W. D., Collarini, E. J., Sperinde, G. V., Strandh, M., Fathollahi, M. M., Dutta, A., *et al.*, "Antibody discovery via multiplexed single cell characterization," *J Immunol Methods*, vol. 341, pp. 135-45, **2009**.
- [129] Darcy, E., Leonard, P., Fitzgerald, J., Danaher, M., and O'Kennedy, R., "Purification of antibodies using affinity chromatography," *Methods Mol Biol*, vol. 681, pp. 369-82, **2011**.
- [130] James, S., Flodin, M., Johnston, N., Lindahl, B., and Venge, P., "The antibody configurations of cardiac troponin I assays may determine their clinical performance," *Clinical Chemistry*, vol. 52, pp. 832-837, **2006**.
- [131] ResearchInternational. (2009). *Raptor(TM) Bioassay Detection System*. Available: <http://www.resrchintl.com/raptor-detection-system.html>
- [132] Lim, D. V., "Detection of microorganisms and toxins with evanescent wave fiber-optic biosensors," *Proceedings of the Ieee*, vol. 91, pp. 902-907, **2003**.
- [133] Lim, D. V., Simpson, J. M., Kearns, E. A., and Kramer, M. F., "Current and developing technologies for monitoring agents of bioterrorism and biowarfare," *Clin Microbiol Rev*, vol. 18, pp. 583-607, **2005**.
- [134] Healy, D. A., Hayes, C. J., Leonard, P., McKenna, L., and O'Kennedy, R., "Biosensor developments: application to prostate-specific antigen detection," *Trends Biotechnol*, vol. 25, pp. 125-31, **2007**.
- [135] Encarnacao, J. M., Rosa, L., Rodrigues, R., Pedro, L., da Silva, F. A., Goncalves, J., and Ferreira, G. N., "Piezoelectric biosensors for biorecognition analysis: application to the kinetic study of HIV-1 Vif protein binding to recombinant antibodies," *J Biotechnol*, vol. 132, pp. 142-8, **2007**.
- [136] Nanduri, V., Bhunia, A. K., Tu, S. I., Paoli, G. C., and Brewster, J. D., "SPR biosensor for the detection of *L. monocytogenes* using phage-displayed antibody," *Biosens Bioelectron*, vol. 23, pp. 248-52, **2007**.
- [137] Benhar, I., Eshkenazi, I., Neufeld, T., Opatowsky, J., Shaky, S., and Rishpon, J., "Recombinant single chain antibodies in bioelectrochemical sensors," *Talanta*, vol. 55, pp. 899-907, **2001**.
- [138] Qi, C., Duan, J., Wang, Z., Chen, Y., Zhang, P., Zhan, L., Yan, X., Cao, W., and Jin, G., "Investigation of interaction between two neutralizing monoclonal antibodies and SARS virus using biosensor based on imaging ellipsometry " *Biomed Microdevices*, vol. 8, **2006**.

- [139] Hu, W. G., Thompson, H. G., Alvi, A. Z., Nagata, L. P., Suresh, M. R., and Fulton, R. E., "Development of immunofiltration assay by light addressable potentiometric sensor with genetically biotinylated recombinant antibody for rapid identification of Venezuelan equine encephalitis virus," *J Immunol Methods*, vol. 289, pp. 27-35, **2004**.
- [140] Love, T. E., Redmond, C., and Mayers, C. N., "Real time detection of anthrax spores using highly specific anti-EA1 recombinant antibodies produced by competitive panning," *J Immunol Methods*, vol. 334, pp. 1-10, **2008**.
- [141] Dillon, P. P., Manning, B. M., Daly, S. J., Killard, A. J., and O'Kennedy, R., "Production of a recombinant anti-morphine-3-glucuronide single-chain variable fragment (scFv) antibody for the development of a "real-time" biosensor-based immunoassay," *J Immunol Methods*, vol. 276, pp. 151-61, **2003**.
- [142] Dunne, L., Daly, S., Baxter, A., Haughey, S., and O'Kennedy, R., "Surface plasmon resonance-based immunoassay for the detection of aflatoxin B1 using single-chain antibody fragments," *Spectroscopy Letters*, vol. 38, pp. 229-245, **2005**.
- [143] Horacek, J., Garrett, S. D., Skladal, P., and Morgan, M. R. A., "Characterization of the interactions between immobilized parathion and the corresponding recombinant scFv antibody using a piezoelectric biosensor," *Food and Agricultural Immunology*, vol. 10, pp. 363-374, **1998**.
- [144] Grennan, K., Strachan, G., Porter, A. J., Killard, A. J., and Smyth, M. R., "Atrazine analysis using an amperometric immunosensor based on single-chain antibody fragments and regeneration-free multi-calibrant measurement," *Analytica Chimica Acta*, vol. 500, **2003**.
- [145] Pluckthun, A. and Skerra, A., "Expression of functional antibody Fv and Fab fragments in *Escherichia coli*," *Methods Enzymol*, vol. 178, pp. 497-515, **1989**.
- [146] Skerra, A. and Pluckthun, A., "Assembly of a functional immunoglobulin Fv fragment in *Escherichia coli*," *Science*, vol. 240, pp. 1038-41, **1988**.
- [147] Racher, A. J., Moreira, J. L., Alves, P. M., Wirth, M., Weidle, U. H., Hauser, H., Carrondo, M. J., and Griffiths, J. B., "Expression of recombinant antibody and secreted alkaline phosphatase in mammalian cells. Influence of cell line and culture system upon production kinetics," *Appl Microbiol Biotechnol*, vol. 40, pp. 851-6, **1994**.

- [148] Dorai, H., McCartney, J. E., Hudziak, R. M., Tai, M. S., Laminet, A. A., Houston, L. L., Huston, J. S., and Oppermann, H., "Mammalian cell expression of single-chain Fv (sFv) antibody proteins and their C-terminal fusions with interleukin-2 and other effector domains," *Biotechnology (N Y)*, vol. 12, pp. 890-7, **1994**.
- [149] Reavy, B., Ziegler, A., Diplexcito, J., Macintosh, S. M., Torrance, L., and Mayo, M., "Expression of functional recombinant antibody molecules in insect cell expression systems," *Protein Expr Purif*, vol. 18, pp. 221-8, **2000**.
- [150] Edelman, L., Margaritte, C., Chaabihi, H., Monchatre, E., Blanchard, D., Cardona, A., *et al.*, "Obtaining a functional recombinant anti-rhesus (D) antibody using the baculovirus-insect cell expression system," *Immunology*, vol. 91, pp. 13-9, **1997**.
- [151] Boder, E. T. and Wittrup, K. D., "Yeast surface display for screening combinatorial polypeptide libraries," *Nat Biotechnol*, vol. 15, pp. 553-7, **1997**.
- [152] Whitelam, G. C., Cockburn, W., and Owen, M. R., "Antibody production in transgenic plants," *Biochem Soc Trans*, vol. 22, pp. 940-4, **1994**.
- [153] Hanes, J. and Pluckthun, A., "*In vitro* selection and evolution of functional proteins by using ribosome display," *Proc Natl Acad Sci U S A*, vol. 94, pp. 4937-42, **1997**.
- [154] Verma, R., Boleti, E., and George, A. J., "Antibody engineering: comparison of bacterial, yeast, insect and mammalian expression systems," *J Immunol Methods*, vol. 216, pp. 165-81, **1998**.
- [155] Griffiths, A. D. and Duncan, A. R., "Strategies for selection of antibodies by phage display," *Curr Opin Biotechnol*, vol. 9, pp. 102-8, **1998**.
- [156] Azzazy, H. M. and Highsmith, W. E., Jr., "Phage display technology: clinical applications and recent innovations," *Clin Biochem*, vol. 35, pp. 425-45, **2002**.
- [157] Krebber, A., Bornhauser, S., Burmester, J., Honegger, A., Willuda, J., Bosshard, H. R., and Pluckthun, A., "Reliable cloning of functional antibody variable domains from hybridomas and spleen cell repertoires employing a reengineered phage display system," *J Immunol Methods*, vol. 201, pp. 35-55, **1997**.
- [158] Bird, R. E., Hardman, K. D., Jacobson, J. W., Johnson, S., Kaufman, B. M., Lee, S. M., *et al.*, "Single-chain antigen-binding proteins," *Science*, vol. 242, pp. 423-6, **1988**.
- [159] Glockshuber, R., Malia, M., Pfitzinger, I., and Pluckthun, A., "A comparison of strategies to stabilize immunoglobulin Fv-fragments," *Biochemistry*, vol. 29, pp. 1362-7, **1990**.

- [160] Tang, Y., Jiang, N., Parakh, C., and Hilvert, D., "Selection of linkers for a catalytic single-chain antibody using phage display technology," *J Biol Chem*, vol. 271, pp. 15682-6, **1996**.
- [161] Atwell, J. L., Breheney, K. A., Lawrence, L. J., McCoy, A. J., Kortt, A. A., and Hudson, P. J., "scFv multimers of the anti-neuraminidase antibody NC10: length of the linker between VH and VL domains dictates precisely the transition between diabodies and triabodies," *Protein Eng*, vol. 12, pp. 597-604, **1999**.
- [162] Muller, B. H., Chevrier, D., Boulain, J. C., and Guesdon, J. L., "Recombinant single-chain Fv antibody fragment-alkaline phosphatase conjugate for one-step immunodetection in molecular hybridization," *J Immunol Methods*, vol. 227, pp. 177-85, **1999**.
- [163] Mousli, M., Turki, I., Kharmachi, H., Saadi, M., and Dellagi, K., "Recombinant single-chain Fv antibody fragment-alkaline phosphatase conjugate: a novel in vitro tool to estimate rabies viral glycoprotein antigen in vaccine manufacture," *J Virol Methods*, vol. 146, pp. 246-56, **2007**.
- [164] Liu, M., Wang, X., Yin, C., Zhang, Z., Lin, Q., Zhen, Y., and Huang, H., "A novel bivalent single-chain variable fragment (scFV) inhibits the action of tumour necrosis factor alpha," *Biotechnol Appl Biochem*, vol. 50, pp. 173-9, **2008**.
- [165] Lindner, P., Bauer, K., Krebber, A., Nieba, L., Kremmer, E., Krebber, C., *et al.*, "Specific detection of his-tagged proteins with recombinant anti-His tag scFv-phosphatase or scFv-phage fusions," *Biotechniques*, vol. 22, pp. 140-9, **1997**.
- [166] de Wildt, R. M., Mundy, C. R., Gorick, B. D., and Tomlinson, I. M., "Antibody arrays for high-throughput screening of antibody-antigen interactions," *Nat Biotechnol*, vol. 18, pp. 989-94, **2000**.
- [167] Leonard, P., Safsten, P., Hearty, S., McDonnell, B., Finlay, W., and O'Kennedy, R., "High throughput ranking of recombinant avian scFv antibody fragments from crude lysates using the Biacore A100," *J Immunol Methods*, vol. 323, pp. 172-9, **2007**.
- [168] Ling, M. M., "Large antibody display libraries for isolation of high-affinity antibodies," *Comb Chem High Throughput Screen*, vol. 6, pp. 421-32, **2003**.
- [169] Rader, C. and Barbas, C. F., 3rd, "Phage display of combinatorial antibody libraries," *Curr Opin Biotechnol*, vol. 8, pp. 503-8, **1997**.

- [170] He, M. and Taussig, M. J., "Antibody-ribosome-mRNA (ARM) complexes as efficient selection particles for *in vitro* display and evolution of antibody combining sites," *Nucleic Acids Res*, vol. 25, pp. 5132-4, **1997**.
- [171] He, M. and Taussig, M. J., "Handbook of Therapeutic Antibodies," in *Emerging Developments*. vol. 2, Dubel, S., Ed., ed: Wiley-VCH, **2007**.
- [172] Griffiths, A. D., Williams, S. C., Hartley, O., Tomlinson, I. M., Waterhouse, P., Crosby, W. L., *et al.*, "Isolation of high affinity human antibodies directly from large synthetic repertoires," *EMBO J*, vol. 13, pp. 3245-60, **1994**.
- [173] Irving, R. A., Coia, G., Roberts, A., Nuttall, S. D., and Hudson, P. J., "Ribosome display and affinity maturation: from antibodies to single V-domains and steps towards cancer therapeutics," *J Immunol Methods*, vol. 248, pp. 31-45, **2001**.
- [174] Schier, R., McCall, A., Adams, G. P., Marshall, K. W., Merritt, H., Yim, M., *et al.*, "Isolation of picomolar affinity anti-c-erbB-2 single-chain Fv by molecular evolution of the complementarity determining regions in the center of the antibody binding site," *J Mol Biol*, vol. 263, pp. 551-67, **1996**.
- [175] Zahnd, C., Spinelli, S., Luginbuhl, B., Amstutz, P., Cambillau, C., and Pluckthun, A., "Directed *in vitro* evolution and crystallographic analysis of a peptide-binding single chain antibody fragment (scFv) with low picomolar affinity," *J Biol Chem*, vol. 279, pp. 18870-7, **2004**.
- [176] Mondon, P., Dubreuil, O., Bouayadi, K., and Kharrat, H., "Human antibody libraries: a race to engineer and explore a larger diversity," *Front Biosci*, vol. 13, pp. 1117-29, **2008**.
- [177] Razai, A., Garcia-Rodriguez, C., Lou, J., Geren, I. N., Forsyth, C. M., Robles, Y., *et al.*, "Molecular evolution of antibody affinity for sensitive detection of botulinum neurotoxin type A," *J Mol Biol*, vol. 351, pp. 158-69, **2005**.
- [178] Stahl, S. and Uhlen, M., "Bacterial surface display: trends and progress," *Trends Biotechnol*, vol. 15, pp. 185-92, **1997**.
- [179] Lipovsek, D. and Pluckthun, A., "In-vitro protein evolution by ribosome display and mRNA display," *J Immunol Methods*, vol. 290, pp. 51-67, **2004**.
- [180] Xu, L., Aha, P., Gu, K., Kuimelis, R. G., Kurz, M., Lam, T., *et al.*, "Directed evolution of high-affinity antibody mimics using mRNA display," *Chem Biol*, vol. 9, pp. 933-42, **2002**.

- [181] Rader, C., "Antibody libraries in drug and target discovery," *Drug Discov Today*, vol. 6, pp. 36-43, **2001**.
- [182] Liguori, M. J., Hoff-Velk, J. A., and Ostrow, D. H., "Recombinant human interleukin-6 enhances the immunoglobulin secretion of a rabbit-rabbit hybridoma," *Hybridoma*, vol. 20, pp. 189-98, **2001**.
- [183] Saini, S. S., Kaushik, A., Basrur, P. K., and Yamashiro, S., "Ultrastructural and immunologic characteristics of mouse x cattle xenogeneic hybridomas originating from bovine leukemia virus-infected cattle," *Vet Pathol*, vol. 40, pp. 460-4, **2003**.
- [184] Matsuda, H., Mitsuda, H., Nakamura, N., Furusawa, S., Mohri, S., and Kitamoto, T., "A chicken monoclonal antibody with specificity for the N-terminal of human prion protein," *FEMS Immunol Med Microbiol*, vol. 23, pp. 189-94, **1999**.
- [185] Yu, X., McGraw, P. A., House, F. S., and Crowe, J. E., Jr., "An optimized electrofusion-based protocol for generating virus-specific human monoclonal antibodies," *J Immunol Methods*, vol. 336, pp. 142-51, **2008**.
- [186] Barbas, C. F., 3rd, Amberg, W., Simoncsits, A., Jones, T. M., and Lerner, R. A., "Selection of human anti-hapten antibodies from semisynthetic libraries," *Gene*, vol. 137, pp. 57-62, **1993**.
- [187] Clackson, T., Hoogenboom, H. R., Griffiths, A. D., and Winter, G., "Making antibody fragments using phage display libraries," *Nature*, vol. 352, pp. 624-8, **1991**.
- [188] Yamanaka, H. I., Inoue, T., and Ikeda-Tanaka, O., "Chicken monoclonal antibody isolated by a phage display system," *J Immunol*, vol. 157, pp. 1156-62, **1996**.
- [189] Ridder, R., Schmitz, R., Legay, F., and Gram, H., "Generation of rabbit monoclonal antibody fragments from a combinatorial phage display library and their production in the yeast *Pichia pastoris*," *Biotechnology (N Y)*, vol. 13, pp. 255-60, **1995**.
- [190] Lang, I. M., Barbas, C. F., 3rd, and Schleef, R. R., "Recombinant rabbit Fab with binding activity to type-1 plasminogen activator inhibitor derived from a phage-display library against human alpha-granules," *Gene*, vol. 172, pp. 295-8, **1996**.
- [191] Alvarez-Rueda, N., Behar, G., Ferre, V., Pugniere, M., Roquet, F., Gastinel, L., *et al.*, "Generation of llama single-domain antibodies against methotrexate, a prototypical hapten," *Mol Immunol*, vol. 44, pp. 1680-90, **2007**.

- [192] Liu, J. L., Anderson, G. P., and Goldman, E. R., "Isolation of anti-toxin single domain antibodies from a semi-synthetic spiny dogfish shark display library," *BMC Biotechnol*, vol. 7, p. 78, **2007**.
- [193] Kim, Y. J., Lebreton, F., Kaiser, C., Cruciere, C., and Remond, M., "Isolation of foot-and-mouth disease virus specific bovine antibody fragments from phage display libraries," *J Immunol Methods*, vol. 286, pp. 155-66, **2004**.
- [194] Li, Y., Kilpatrick, J., and Whitelam, G. C., "Sheep monoclonal antibody fragments generated using a phage display system," *J Immunol Methods*, vol. 236, pp. 133-46, **2000**.
- [195] Park, S. G., Jeong, Y. J., Lee, Y. Y., Kim, I. J., Seo, S. K., Kim, E. J., *et al.*, "Hepatitis B virus-neutralizing anti-pre-S1 human antibody fragments from large naive antibody phage library," *Antiviral Res*, vol. 68, pp. 109-15, **2005**.
- [196] Masson, J. F., Battaglia, T. M., Khairallah, P., Beaudoin, S., and Booksh, K. S., "Quantitative measurement of cardiac markers in undiluted serum," *Anal Chem*, vol. 79, pp. 612-9, **2007**.
- [197] McDonnell, B., Hearty, S., Finlay, W. J., and O'Kennedy, R., "A high-affinity recombinant antibody permits rapid and sensitive direct detection of myeloperoxidase," *Anal Biochem*, vol. 410, pp. 1-6, **2011**.
- [198] Ylikotila, J., Valimaa, L., Vehniainen, M., Takalo, H., Lovgren, T., and Pettersson, K., "A sensitive TSH assay in spot-coated microwells utilizing recombinant antibody fragments," *J Immunol Methods*, vol. 306, pp. 104-14, **2005**.
- [199] Charlton, K., Harris, W. J., and Porter, A. J., "The isolation of super-sensitive anti-hapten antibodies from combinatorial antibody libraries derived from sheep," *Biosens Bioelectron*, vol. 16, pp. 639-46, **2001**.
- [200] Townsend, S., Finlay, W. J., Hearty, S., and O'Kennedy, R., "Optimizing recombinant antibody function in SPR immunosensing. The influence of antibody structural format and chip surface chemistry on assay sensitivity," *Biosens Bioelectron*, vol. 22, pp. 268-74, **2006**.
- [201] Brennan, J., Dillon, P., and O'Kennedy, R., "Production, purification and characterisation of genetically derived scFv and bifunctional antibody fragments capable of detecting illicit drug residues," *J Chromatogr B Analyt Technol Biomed Life Sci*, vol. 786, pp. 327-42, **2003**.

- [202] Foord, A. J., Muller, J. D., Yu, M., Wang, L. F., and Heine, H. G., "Production and application of recombinant antibodies to foot-and-mouth disease virus non-structural protein 3ABC," *J Immunol Methods*, vol. 321, pp. 142-51, **2007**.
- [203] Muller, J. D., Wilkins, M., Foord, A. J., Dolezal, O., Yu, M., Heine, H. G., and Wang, L. F., "Improvement of a recombinant antibody-based serological assay for foot-and-mouth disease virus," *J Immunol Methods*, vol. 352, pp. 81-8, **2010**.
- [204] Welbeck, K., Leonard, P., Gilmartin, N., Byrne, B., Viguier, C., Arora, S., and O'Kennedy, R., "Generation of an anti-NAGase single chain antibody and its application in a biosensor-based assay for the detection of NAGase in milk," *J Immunol Methods*, vol. 364, pp. 14-20, **2011**.
- [205] Bhatia, S., Gangil, R., Gupta, D. S., Sood, R., Pradhan, H. K., and Dubey, S. C., "Single-chain fragment variable antibody against the capsid protein of bovine immunodeficiency virus and its use in ELISA," *J Virol Methods*, vol. 167, pp. 68-73, **2010**.
- [206] Hayhurst, A., Happe, S., Mabry, R., Koch, Z., Iverson, B. L., and Georgiou, G., "Isolation and expression of recombinant antibody fragments to the biological warfare pathogen *Brucella melitensis*," *J Immunol Methods*, vol. 276, pp. 185-96, **2003**.
- [207] Rangnoi, K., Jaruseranee, N., O'Kennedy, R., Pansri, P., and Yamabhai, M., "One-Step Detection of Aflatoxin-B(1) Using scFv-Alkaline Phosphatase-Fusion Selected from Human Phage Display Antibody Library," *Mol Biotechnol*, **2011**.
- [208] Fitzgerald, J., Leonard, P., Darcy, E., Danaher, M., and O'Kennedy, R., "Light-chain shuffling from an antigen-biased phage pool allows 185-fold improvement of an anti-halofuginone single-chain variable fragment," *Anal Biochem*, vol. 410, pp. 27-33, **2011**.
- [209] Meyer, T., Stratmann-Selke, J., Meens, J., Schirrmann, T., Gerlach, G. F., Frank, R., Dubel, S., Strutzberg-Minder, K., and Hust, M., "Isolation of scFv fragments specific to OmpD of *Salmonella Typhimurium*," *Vet Microbiol*, vol. 147, pp. 162-9, **2011**.
- [210] Smith, G. P., "Filamentous fusion phage: novel expression vectors that display cloned antigens on the virion surface," *Science*, vol. 228, pp. 1315-7, **1985**.
- [211] Huse, W. D., Sastry, L., Iverson, S. A., Kang, A. S., Altling-Mees, M., Burton, D. R., Benkovic, S. J., and Lerner, R. A., "Generation of a large combinatorial library

- of the immunoglobulin repertoire in phage lambda," *Science*, vol. 246, pp. 1275-81, **1989**.
- [212] McCafferty, J., Griffiths, A. D., Winter, G., and Chiswell, D. J., "Phage antibodies: filamentous phage displaying antibody variable domains," *Nature*, vol. 348, pp. 552-4, **1990**.
- [213] Kehoe, J. W. and Kay, B. K., "Filamentous phage display in the new millennium," *Chem Rev*, vol. 105, pp. 4056-72, **2005**.
- [214] Barbas, C. F., 3rd, Kang, A. S., Lerner, R. A., and Benkovic, S. J., "Assembly of combinatorial antibody libraries on phage surfaces: the gene III site," *Proc Natl Acad Sci U S A*, vol. 88, pp. 7978-82, **1991**.
- [215] Schier, R., Bye, J., Apell, G., McCall, A., Adams, G. P., Malmqvist, M., Weiner, L. M., and Marks, J. D., "Isolation of high-affinity monomeric human anti-c-erbB-2 single chain Fv using affinity-driven selection," *J Mol Biol*, vol. 255, pp. 28-43, **1996**.
- [216] Nagumo, Y., Oguri, H., Tsumoto, K., Shindo, Y., Hiram, M., Tsumuraya, T., *et al.*, "Phage-display selection of antibodies to the left end of CTX3C using synthetic fragments," *J Immunol Methods*, vol. 289, pp. 137-46, **2004**.
- [217] Gao, X., Huang, Y., and Zhu, S., "Construction of murine phage antibody library and selection of ricin-specific single-chain antibodies," *IUBMB Life*, vol. 48, pp. 513-7, **1999**.
- [218] Wassaf, D., Kuang, G., Kopacz, K., Wu, Q. L., Nguyen, Q., Toews, M., *et al.*, "High-throughput affinity ranking of antibodies using surface plasmon resonance microarrays," *Anal Biochem*, vol. 351, pp. 241-53, **2006**.
- [219] Malmborg, A. C., Duenas, M., Ohlin, M., Soderlind, E., and Borrebaeck, C. A., "Selection of binders from phage displayed antibody libraries using the BIAcore biosensor," *J Immunol Methods*, vol. 198, pp. 51-7, **1996**.
- [220] Schier, R. and Marks, J. D., "Efficient *in vitro* affinity maturation of phage antibodies using BIAcore guided selections," *Hum Antibodies Hybridomas*, vol. 7, pp. 97-105, **1996**.
- [221] Figini, M., Obici, L., Mezzanzanica, D., Griffiths, A., Colnaghi, M. I., Winter, G., and Canevari, S., "Panning phage antibody libraries on cells: isolation of human Fab fragments against ovarian carcinoma using guided selection," *Cancer Res*, vol. 58, pp. 991-6, **1998**.

- [222] Hoogenboom, H. R., Lutgerink, J. T., Pelsers, M. M., Rousch, M. J., Coote, J., Van Neer, N., *et al.*, "Selection-dominant and nonaccessible epitopes on cell-surface receptors revealed by cell-panning with a large phage antibody library," *Eur J Biochem*, vol. 260, pp. 774-84, **1999**.
- [223] Mutuberria, R., Hoogenboom, H. R., van der Linden, E., de Bruine, A. P., and Roovers, R. C., "Model systems to study the parameters determining the success of phage antibody selections on complex antigens," *J Immunol Methods*, vol. 231, pp. 65-81, **1999**.
- [224] Pasqualini, R. and Ruoslahti, E., "Organ targeting in vivo using phage display peptide libraries," *Nature*, vol. 380, pp. 364-6, **1996**.
- [225] Paschke, M., "Phage display systems and their applications," *Appl Microbiol Biotechnol*, vol. 70, pp. 2-11, **2006**.
- [226] Iannolo, G., Minenkova, O., Petruzzelli, R., and Cesareni, G., "Modifying filamentous phage capsid: limits in the size of the major capsid protein," *J Mol Biol*, vol. 248, pp. 835-44, **1995**.
- [227] Carmen, S. and Jermutus, L., "Concepts in antibody phage display," *Brief Funct Genomic Proteomic*, vol. 1, pp. 189-203, **2002**.
- [228] Hoogenboom, H. R., Griffiths, A. D., Johnson, K. S., Chiswell, D. J., Hudson, P., and Winter, G., "Multi-subunit proteins on the surface of filamentous phage: methodologies for displaying antibody (Fab) heavy and light chains," *Nucleic Acids Res*, vol. 19, pp. 4133-7, **1991**.
- [229] Hoogenboom, H. R., de Bruine, A. P., Hufton, S. E., Hoet, R. M., Arends, J. W., and Roovers, R. C., "Antibody phage display technology and its applications," *Immunotechnology*, vol. 4, pp. 1-20, **1998**.
- [230] Sidhu, S. S., Fairbrother, W. J., and Deshayes, K., "Exploring protein-protein interactions with phage display," *Chembiochem*, vol. 4, pp. 14-25, **2003**.
- [231] Bradbury, A. R. and Marks, J. D., "Antibodies from phage antibody libraries," *J Immunol Methods*, vol. 290, pp. 29-49, **2004**.
- [232] de Bruin, R., Spelt, K., Mol, J., Koes, R., and Quattrocchio, F., "Selection of high-affinity phage antibodies from phage display libraries," *Nat Biotechnol*, vol. 17, pp. 397-9, **1999**.
- [233] Lou, J., Marzari, R., Verzillo, V., Ferrero, F., Pak, D., Sheng, M., Yang, C., Sblattero, D., and Bradbury, A., "Antibodies in haystacks: how selection strategy

- influences the outcome of selection from molecular diversity libraries," *J Immunol Methods*, vol. 253, pp. 233-42, **2001**.
- [234] Lo, B. K., *Antibody Engineering: Methods and Protocols*, 1 ed. vol. 248: Humana, **2004**.
- [235] Roberts, B. L., Markland, W., Siranosian, K., Saxena, M. J., Guterman, S. K., and Ladner, R. C., "Protease inhibitor display M13 phage: selection of high-affinity neutrophil elastase inhibitors," *Gene*, vol. 121, pp. 9-15, **1992**.
- [236] Kang, A. S., Barbas, C. F., Janda, K. D., Benkovic, S. J., and Lerner, R. A., "Linkage of recognition and replication functions by assembling combinatorial antibody Fab libraries along phage surfaces," *Proc Natl Acad Sci U S A*, vol. 88, pp. 4363-6, **1991**.
- [237] Wind, T., Stausbol-Gron, B., Kjaer, S., Kahns, L., Jensen, K. H., and Clark, B. F., "Retrieval of phage displayed scFv fragments using direct bacterial elution," *J Immunol Methods*, vol. 209, pp. 75-83, **1997**.
- [238] Engberg, J., Andersen, P. S., Nielsen, L. K., Dziegiel, M., Johansen, L. K., and Albrechtsen, B., "Phage-display libraries of murine and human antibody Fab fragments," *Mol Biotechnol*, vol. 6, pp. 287-310, **1996**.
- [239] Ward, R. L., Clark, M. A., Lees, J., and Hawkins, N. J., "Retrieval of human antibodies from phage-display libraries using enzymatic cleavage," *J Immunol Methods*, vol. 189, pp. 73-82, **1996**.
- [240] Cendron, A. C., Wines, B. D., Brownlee, R. T., Ramsland, P. A., Pietersz, G. A., and Hogarth, P. M., "An FcγRIIa-binding peptide that mimics the interaction between FcγRIIa and IgG," *Mol Immunol*, vol. 45, pp. 307-19, **2008**.
- [241] Santala, V. and Saviranta, P., "Affinity-independent elution of antibody-displaying phages using cleavable DNA linker containing streptavidin beads," *J Immunol Methods*, vol. 284, pp. 159-63, **2004**.
- [242] Jermutus, L., Ryabova, L. A., and Pluckthun, A., "Recent advances in producing and selecting functional proteins by using cell-free translation," *Curr Opin Biotechnol*, vol. 9, pp. 534-48, **1998**.
- [243] Jermutus, L., Honegger, A., Schwesinger, F., Hanes, J., and Pluckthun, A., "Tailoring *in vitro* evolution for protein affinity or stability," *Proc Natl Acad Sci U S A*, vol. 98, pp. 75-80, **2001**.

- [244] Amstutz, P., Pluckthun, A., and Zahnd, C., *Ribosome Display: In Vitro Selection of Protein-Protein Interactions*, 3 ed. vol. 1: Elsevier Academic Press, **2006**.
- [245] Villemagne, D., Jackson, R., and Douthwaite, J. A., "Highly efficient ribosome display selection by use of purified components for *in vitro* translation," *J Immunol Methods*, vol. 313, pp. 140-8, **2006**.
- [246] Zahnd, C., Amstutz, P., and Pluckthun, A., "Ribosome display: selecting and evolving proteins *in vitro* that specifically bind to a target," *Nat Methods*, vol. 4, pp. 269-79, **2007**.
- [247] He, M. and Taussig, M. J., "Ribosome display: cell-free protein display technology," *Brief Funct Genomic Proteomic*, vol. 1, pp. 204-12, **2002**.
- [248] Nicholls, P. J., Johnson, V. G., Andrew, S. M., Hoogenboom, H. R., Raus, J. C., and Youle, R. J., "Characterization of single-chain antibody (sFv)-toxin fusion proteins produced *in vitro* in rabbit reticulocyte lysate," *J Biol Chem*, vol. 268, pp. 5302-8, **1993**.
- [249] Fedorov, A. N. and Baldwin, T. O., "Contribution of cotranslational folding to the rate of formation of native protein structure," *Proc Natl Acad Sci U S A*, vol. 92, pp. 1227-31, **1995**.
- [250] He, M. and Taussig, M. J., "Ribosome display of antibodies: expression, specificity and recovery in a eukaryotic system," *J Immunol Methods*, vol. 297, pp. 73-82, **2005**.
- [251] Coia, G., Pontes-Braz, L., Nuttall, S. D., Hudson, P. J., and Irving, R. A., "Panning and selection of proteins using ribosome display," *J Immunol Methods*, vol. 254, pp. 191-7, **2001**.
- [252] Hanes, J., Jermutus, L., Weber-Bornhauser, S., Bosshard, H. R., and Pluckthun, A., "Ribosome display efficiently selects and evolves high-affinity antibodies *in vitro* from immune libraries," *Proc Natl Acad Sci U S A*, vol. 95, pp. 14130-5, **1998**.
- [253] Hanes, J., Jermutus, L., and Pluckthun, A., "Selecting and evolving functional proteins *in vitro* by ribosome display," *Methods Enzymol*, vol. 328, pp. 404-30, **2000**.
- [254] Schaffitzel, C., Zahnd, C., Amstutz, P., Luginbühl, B., and Plückthun, A., *In Vitro Selection and Evolution of Protein-Ligand Interactions by Ribosome Display*, 2 ed. vol. 548. New York: Cold Spring Harbor Laboratory Press, **2001**.

- [255] Schaffitzel, C., Hanes, J., Jermutus, L., and Pluckthun, A., "Ribosome display: an *in vitro* method for selection and evolution of antibodies from libraries," *J Immunol Methods*, vol. 231, pp. 119-35, **1999**.
- [256] Pluckthun, A., Schaffitzel, C., Hanes, J., and Jermutus, L., "*In vitro* selection and evolution of proteins," *Adv Protein Chem*, vol. 55, pp. 367-403, **2000**.
- [257] Hanes, J., Jermutus, L., Schaffitzel, C., and Pluckthun, A., "Comparison of *Escherichia coli* and rabbit reticulocyte ribosome display systems," *FEBS Lett*, vol. 450, pp. 105-10, **1999**.
- [258] Mössner, E. and Pluckthun, A., "Directed Evolution with Fast and Efficient Selection Technologies," *Chimia*, vol. 55, pp. 324-328, **2001**.
- [259] Brizzard, B., "Epitope tagging," *Biotechniques*, vol. 44, pp. 693-5, **2008**.
- [260] Graslund, S., Nordlund, P., Weigelt, J., Hallberg, B. M., Bray, J., Gileadi, O., *et al.*, "Protein production and purification," *Nat Methods*, vol. 5, pp. 135-46, **2008**.
- [261] Scibek, J. J., Evergren, E., Zahn, S., Canziani, G. A., Van Ryk, D., and Chaiken, I. M., "Biosensor analysis of dynamics of interleukin 5 receptor subunit beta(c) interaction with IL5:IL5R(alpha) complexes," *Anal Biochem*, vol. 307, pp. 258-65, **2002**.
- [262] Lori, J. A., Morrin, A., Killard, A. J., and Smyth, M. R., "Development and characterization of nickel-NTA-polyaniline modified electrodes," *Electroanalysis*, vol. 18, pp. 77-81, **2006**.
- [263] Mersich, C. and Jungbauer, A., "Generic method for quantification of FLAG-tagged fusion proteins by a real time biosensor," *Journal of Biochemical and Biophysical Methods*, vol. 70, pp. 555-563, **2007**.
- [264] Gaj, T., Meyer, S. C., and Ghosh, I., "The AviD-tag, a NeutrAvidin/avidin specific peptide affinity tag for the immobilization and purification of recombinant proteins," *Protein Expression and Purification*, vol. 56, pp. 54-61, **2007**.
- [265] Helali, S., Fredj, H. B., Cherif, K., Abdelghani, A., Martelet, C., and Jaffrezic-Renault, N., "Surface plasmon resonance and impedance spectroscopy on gold electrode for biosensor application," *Materials Science and Engineering: C*, vol. 28, pp. 588-593, **2008**.
- [266] Cui, X. Q., Pei, R. J., Wang, X. Z., Yang, F., Ma, Y., Dong, S. J., and Yang, X. R., "Layer-by-layer assembly of multilayer films composed of avidin and biotin-labeled

- antibody for immunosensing," *Biosensors & Bioelectronics*, vol. 18, pp. 59-67, **2003**.
- [267] Dutra, R. F. and Kubota, L. T., "An SPR immunosensor for human cardiac troponin T using specific binding avidin to biotin at carboxymethyl-dextran-modified gold chip," *Clin Chim Acta*, vol. 376, pp. 114-20, **2007**.
- [268] Keefe, A. D., Wilson, D. S., Seelig, B., and Szostak, J. W., "One-step purification of recombinant proteins using a nanomolar-affinity streptavidin-binding peptide, the SBP-Tag," *Protein Expr Purif*, vol. 23, pp. 440-6, **2001**.
- [269] Li, Y. J., Bi, L. J., Zhang, X. E., Zhou, Y. F., Zhang, J. B., Chen, Y. Y., Li, W., and Zhang, Z. P., "Reversible immobilization of proteins with streptavidin affinity tags on a surface plasmon resonance biosensor chip," *Analytical and Bioanalytical Chemistry*, vol. 386, pp. 1321-1326, **2006**.
- [270] Piervincenzi, R. T., Reichert, W. M., and Hellinga, H. W., "Genetic engineering of a single-chain antibody fragment for surface immobilization in an optical biosensor," *Biosens Bioelectron*, vol. 13, pp. 305-12, **1998**.
- [271] Hofer, T., Thomas, J. D., Burke, T. R., Jr., and Rader, C., "An engineered selenocysteine defines a unique class of antibody derivatives," *Proc Natl Acad Sci U S A*, vol. 105, pp. 12451-6, **2008**.
- [272] Conroy, P. J., Hearty, S., Leonard, P., and O'Kennedy, R. J., "Antibody production, design and use for biosensor-based applications," *Semin Cell Dev Biol*, vol. 20, pp. 10-26, **2009**.
- [273] Bravman, T., Bronner, V., Lavie, K., Notcovich, A., Papalia, G. A., and Myszka, D. G., "Exploring "one-shot" kinetics and small molecule analysis using the ProteOn XPR36 array biosensor," *Anal Biochem*, vol. 358, pp. 281-8, **2006**.
- [274] Abdiche, Y., Malashock, D., Pinkerton, A., and Pons, J., "Determining kinetics and affinities of protein interactions using a parallel real-time label-free biosensor, the Octet," *Anal Biochem*, vol. 377, pp. 209-17, **2008**.
- [275] Abdiche, Y. N., Malashock, D. S., and Pons, J., "Probing the binding mechanism and affinity of tanezumab, a recombinant humanized anti-NGF monoclonal antibody, using a repertoire of biosensors," *Protein Sci*, vol. 17, pp. 1326-35, **2008**.
- [276] Luong, J. H., Male, K. B., and Glennon, J. D., "Biosensor technology: technology push versus market pull," *Biotechnol Adv*, vol. 26, pp. 492-500, **2008**.

- [277] Havard, J., Gillock, N., Martin, A., and Quinn, J., "An automated surface plasmon resonance-based system," *American Biotechnology Laboratory*, vol. 27, pp. 24-25, **2009**.
- [278] Boozer, C., Kim, G., Cong, S., Guan, H., and Londergan, T., "Looking towards label-free biomolecular interaction analysis in a high-throughput format: a review of new surface plasmon resonance technologies," *Curr Opin Biotechnol*, vol. 17, pp. 400-5, **2006**.
- [279] Abdiche, Y. N., Malashock, D. S., Pinkerton, A., and Pons, J., "Exploring blocking assays using Octet, ProteOn, and Biacore biosensors," *Anal Biochem*, vol. 386, pp. 172-80, **2009**.
- [280] Rich, R. L., Papalia, G. A., Flynn, P. J., Furneisen, J., Quinn, J., Klein, J. S., *et al.*, "A global benchmark study using affinity-based biosensors," *Anal Biochem*, vol. 386, pp. 194-216, **2009**.
- [281] Narat, M., "Production of Antibodies in Chickens," *Food Technol. Biotechnol*, vol. 41, pp. 259-267, **2003**.
- [282] Davidson, F., Kaspers, B., and Schat, K. A., *Avian Immunology*: Academic Press, **2008**.
- [283] Kovacs-Nolan, J. and Mine, T., "Avian egg antibodies: basic and potential applications," *Avian and Poultry Biology Reviews*, vol. 15, pp. 25-46, **2004**.
- [284] GallusImmunotech. (2010). Available: http://www.gallusimmunotech.com/Comparison_of_IgG_IgE_IgY_and_IgY_deltaFc
- [285] Michael, N., Accavitti, M. A., Masteller, E., and Thompson, C. B., "The antigen-binding characteristics of mAbs derived from *in vivo* priming of avian B cells," *Proc Natl Acad Sci U S A*, vol. 95, pp. 1166-71, **1998**.
- [286] Finlay, W. J., Shaw, I., Reilly, J. P., and Kane, M., "Generation of high-affinity chicken single-chain Fv antibody fragments for measurement of the *Pseudonitzschia pungens* toxin domoic acid," *Appl Environ Microbiol*, vol. 72, pp. 3343-9, **2006**.
- [287] Finlay, W. J., deVore, N. C., Dobrovolskaia, E. N., Gam, A., Goodyear, C. S., and Slater, J. E., "Exploiting the avian immunoglobulin system to simplify the generation of recombinant antibodies to allergenic proteins," *Clin Exp Allergy*, vol. 35, pp. 1040-8, **2005**.

- [288] Sayegh, C. E., Demaries, S. L., Pike, K. A., Friedman, J. E., and Ratcliffe, M. J., "The chicken B-cell receptor complex and its role in avian B-cell development," *Immunol Rev*, vol. 175, pp. 187-200, **2000**.
- [289] Hof, D., Hoeke, M. O., and Raats, J. M., "Multiple-antigen immunization of chickens facilitates the generation of recombinant antibodies to autoantigens," *Clin Exp Immunol*, vol. 151, pp. 367-77, **2008**.
- [290] Wu, T. T., Johnson, G., and Kabat, E. A., "Length distribution of CDRH3 in antibodies," *Proteins*, vol. 16, pp. 1-7, **1993**.
- [291] Carlander, D. and Larsson, A., "Avian antibodies can eliminate interference due to complement activation in ELISA," *Uppsala Journal of Medical Sciences*, vol. 106, pp. 189-195, **2001**.
- [292] Greunke, K., Braren, I., Alpers, I., Blank, S., Sodenkamp, J., Bredehorst, R., and Spillner, E., "Recombinant IgY for improvement of immunoglobulin-based analytical applications," *Clinical Biochemistry*, vol. 41, pp. 1237-1244, **2008**.
- [293] Daigo, K., Sugita, S., Mochizuki, Y., Iwanari, H., Hiraishi, K., Miyano, K., Kodama, T., and Hamakubo, T., "A simple hybridoma screening method for high-affinity monoclonal antibodies using the signal ratio obtained from time-resolved fluorescence assay," *Anal Biochem*, vol. 351, pp. 219-28, **2006**.
- [294] Birtalan, S., Zhang, Y., Fellouse, F. A., Shao, L., Schaefer, G., and Sidhu, S. S., "The intrinsic contributions of tyrosine, serine, glycine and arginine to the affinity and specificity of antibodies," *J Mol Biol*, vol. 377, pp. 1518-28, **2008**.
- [295] Lou, J., Geren, I., Garcia-Rodriguez, C., Forsyth, C. M., Wen, W., Knopp, K., *et al.*, "Affinity maturation of human botulinum neurotoxin antibodies by light chain shuffling via yeast mating," *Protein Eng Des Sel*, vol. 23, pp. 311-9, **2010**.
- [296] Putnam, C. (**2011**). *The Protein Calculator V3.3*. Available: <http://www.scripps.edu/~cdputnam/protcalc.html>
- [297] Wlodawer, A., Minor, W., Dauter, Z., and Jaskolski, M., "Protein crystallography for non-crystallographers, or how to get the best (but not more) from published macromolecular structures," *FEBS J*, vol. 275, pp. 1-21, **2008**.
- [298] Lawson, D. (**2011**). *A Brief Introduction to Protein Crystallography*. Available: <http://www.jic.ac.uk/staff/david-lawson/xtallog/summary.htm>

- [299] Little, J. W. (2010). *Relationship between resolution of an x-ray structure and information available in the structure*. Available: <http://www.biochem.arizona.edu/classes/bioc568/resolution.htm>
- [300] Domon, B. and Aebersold, R., "Mass spectrometry and protein analysis," *Science*, vol. 312, pp. 212-7, **2006**.
- [301] HamptonResearch. (2011). *Crystal Growth 101*. Available: http://hamptonresearch.com/documents/growth_101/4.pdf
- [302] Kampmeier, F., Ribbert, M., Nachreiner, T., Dembski, S., Beaufls, F., Brecht, A., and Barth, S., "Site-specific, covalent labeling of recombinant antibody fragments via fusion to an engineered version of 6-O-alkylguanine DNA alkyltransferase," *Bioconjug Chem*, vol. 20, pp. 1010-5, **2009**.
- [303] Abbott. (2009). *i-STAT(R) Precision*. Available: <http://www.abbottpointofcare.com/istat/www/products/index.htm>
- [304] Roche. (2009). *Cardiac proBNP Assay*. Available: http://www.roche.com/home/products/prod_diag_roche-cardiac.htm
- [305] Ylikotila, J., Hellstrom, J. L., Eriksson, S., Vehniainen, M., Valimaa, L., Takalo, H., Bereznikova, A., and Pettersson, K., "Utilization of recombinant Fab fragments in a cTnI immunoassay conducted in spot wells," *Clin Biochem*, vol. 39, pp. 843-50, **2006**.
- [306] Lippa, P. B., Sokoll, L. J., and Chan, D. W., "Immunosensors--principles and applications to clinical chemistry," *Clin Chim Acta*, vol. 314, pp. 1-26, **2001**.
- [307] Dennany, L., O'Reilly, E. J., Innis, P. C., Wallace, G. G., and Forster, R. J., "Solid state photochemistry of novel composites containing luminescent metal centers and poly(2-methoxyaniline-5-sulfonic acid)," *J Phys Chem B*, vol. 113, pp. 7443-8, **2009**.
- [308] Kurzbuch, D., Bakker, J., Melin, J., Jönsson, C., Ruckstuhl, T., and MacCraith, B. D., "A biochip reader using super critical angle fluorescence," *Sensors and Actuators B: Chemical*, vol. 137, pp. 1-6, **2008**.
- [309] Ruckstuhl, T., Winterflood, C. M., and Seeger, S., "Supercritical angle fluorescence immunoassay platform," *Anal Chem*, vol. 83, pp. 2345-50, **2011**.